

1-1-1986

Spectroscopic characterization of the microstructure of polybutadiene based polyurethane elastomers/

Steven E. Molis

University of Massachusetts Amherst

Follow this and additional works at: https://scholarworks.umass.edu/dissertations_1

Recommended Citation

Molis, Steven E., "Spectroscopic characterization of the microstructure of polybutadiene based polyurethane elastomers/" (1986).
Doctoral Dissertations 1896 - February 2014. 713.
https://scholarworks.umass.edu/dissertations_1/713

This Open Access Dissertation is brought to you for free and open access by ScholarWorks@UMass Amherst. It has been accepted for inclusion in Doctoral Dissertations 1896 - February 2014 by an authorized administrator of ScholarWorks@UMass Amherst. For more information, please contact scholarworks@library.umass.edu.

UMASS/AMHERST



312066 0006 1009 3

SPECTROSCOPIC CHARACTERIZATION OF THE MICROSTRUCTURE
OF POLYBUTADIENE BASED POLYURETHANE ELASTOMERS

A Dissertation Presented

By

Steven Earle Molis

Submitted to the Graduate School of the
University of Massachusetts in partial fulfillment
of the requirements for the degree of

DOCTOR OF PHILOSOPHY

September 1986

Department of Polymer Science and Engineering

Steven Earle Molis

©

All Rights Reserved

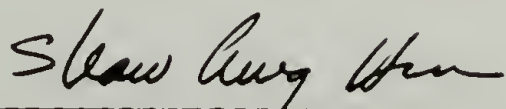
SPECTROSCOPIC CHARACTERIZATION OF THE MICROSTRUCTURE
OF POLYBUTADIENE BASED POLYURETHANE ELASTOMERS

A Dissertation Presented

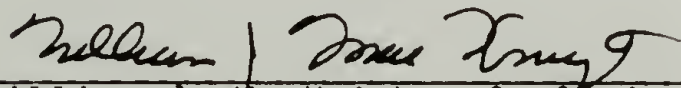
By

Steven Earle Molis

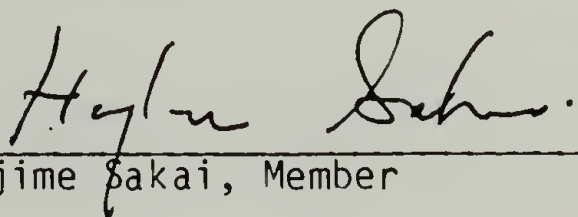
Approved as to style and content by:



Shaw Ling Hsu, Co-Chairperson of Committee



William J. MacKnight, Co-Chairperson of Committee



Hajime Sakai, Member

Edwin L. Thomas
Department of Polymer Science
and Engineering

To my parents.

ACKNOWLEDGEMENTS

I wish to acknowledge the guidance and encouragement given to me by my advisors, Professors Shaw Ling Hsu and William J. MacKnight, throughout my graduate education. I would also like to thank Professor Hajime Sakai for serving on my dissertation committee and for his helpful comments during the writing of my dissertation.

I would like to thank my fellow graduate students for their companionship and discussions over the past five years. My sincere appreciation is extended to Bruce Bengston and Bernie Fu for the preparation of samples characterized in this work. Don Burchell and Jim Lasch were of tremendous help in the laboratory as well as being great friends.

Special thanks are extended to Marilyn Putnam. The assistance which she has given during the preparation of this manuscript, and in general over the past four years, has been a tremendous help to me.

Finally, I would like to thank Jaye, for her love and understanding during the writing of this dissertation.

ABSTRACT

Spectroscopic Characterization of the Microstructure of Polybutadiene Based Polyurethane Elastomers

(September 1986)

Steven E. Molis, B.S. University of New Hampshire

Ph.D., University of Massachusetts

Directed by Professors Shaw Ling Hsu and William J. MacKnight

Segmental orientation response for macroscopic deformations and hard segment microstructural ordering in model polyurethane elastomers have been characterized using Fourier transform infrared spectroscopy. These systems are highly phase separated linear polyurethanes having a polybutadiene soft segment and toluene diisocyanate (TDI)-butanediol hard segment. A sample prepared with TDI that is a mixture of the 2,4 and 2,6 isomers exhibits microstructural ordering in the hard segment which has been characterized by frequency shifts in infrared absorptions characteristic to this phase. The absorption component corresponding to the ordered structure is present only in samples cast from tetrahydrofuran solution. It has been attributed to the ordering of hard segments involving consecutive runs of the 2,6 TDI isomer which results from the kinetics of the polymerization process. Using polarized infrared spectroscopy it has been observed that the ordered component becomes highly oriented as the sample is deformed, indicating

an extended anisotropic structure. When this sample is heated to a temperature of 170°C or higher it loses the ability to develop this ordered structure. It is proposed that above this temperature urethane interchange reactions result in the disruption of the crystallizable 2,6 TDI sequences. This is supported by Monte Carlo simulation studies of the "as polymerized" structure and "randomized" structure of the heat treated sample. Infrared dichroism has been used to characterize the dynamics of segmental orientation for a model butadiene based elastomer with an amorphous monodisperse hard segment. A new time resolved infrared method has been developed to characterize dynamic segmental orientation during polymer deformation. This technique is unique in that it utilizes a separate microprocessor programmed in Pascal to control and monitor the synchronization of the deformation event to the interferometer. The extent of orientation and rate of relaxation of both the hard and soft segments have been characterized as a function of temperature. Soft segment orientation closely follows the strain profile while hard segment orientation is non-existent. The soft segment orientation relaxation rate is greater at room temperature while the magnitude of the orientation is greater at -20°C. A model has been developed to account for these properties.

TABLE OF CONTENTS

ACKNOWLEDGMENTS.....	v
ABSTRACT.....	vi
LIST OF TABLES.....	xi
LIST OF FIGURES.....	xii

Chapter

I. INTRODUCTION.....	1
Overview of Dissertation.....	1
Introduction to Linear Segmented Polyurethanes.....	2
Polyurethane Chemical Structure.....	3
Polyurethane Characterization.....	8
Characterization of Microphase Separation.....	8
Infrared Characterization of Hydrogen Bonding.....	10
Segmental Orientation Studies by Infrared Spectroscopy.....	12
Research Objectives of this Investigation.....	14
References.....	19
II. INVESTIGATIONS OF MOLECULAR ORIENTATION BY THE METHOD OF INFRARED DICHROISM.....	24
Introduction.....	24
Theory of Infrared Orientation Measurements.....	27
The Relationship Between Segmental Orientation and Polymer Strain.....	32
Experimental.....	35
Data Collection.....	35
Synthesis of N-Phenyl Urethane.....	36
Sample Preparation.....	39
Preparation of Polyurethane Elastomer for Uniaxial Deformation Study.....	42
Results and Discussion.....	45
Molecular Orientation of N-Phenyl Urethane with Spherulitic Structure.....	45
Characterization of Segmented Orientation of a Uniaxially Strained Polyurethane Elastomer.....	51
Calculation of Random Links in Polybutadiene Soft Segment.....	63
References.....	70

III. INFRARED CHARACTERIZATION OF MICROSTRUCTURAL ORDERING IN A POLYBUTADIENE BASED POLYURETHANE PEPAED WITH MIXED ISOMER TOLUENE DIISOCYANATE.....	75
Introduction.....	75
Experimental.....	78
Preparation of Samples.....	78
Infrared Characterization.....	81
Results and Discussion.....	82
The Effect of Hydrogen Bonding on Infrared Absorption Intensities.....	92
The Dependence of Hard Segment Order on Sample Preparation and Thermal History.....	98
Solvent Induced Crystallization.....	112
Orientation of Ordered Hard Segment.....	116
Hard Segment Length Redistribution by Urethane Interchange Reactions.....	121
References.....	126
IV. CARLO SIMULATION OF POLYURETHANE HARD SEGMENT SEQUENCE DISTRIBUTION.....	130
Introduction.....	130
Simulation Program.....	133
Polymerization Simulation.....	134
Determination of Sequence Distributions.....	139
Determination of Standard Deviations.....	140
Results and Discussion.....	140
References.....	160
V. TECHNIQUE DEVELOPMENT OF SOFTWARE SYNCHRONIZED TIME RESOLVED INFRARED SPECTROSCOPY.....	162
Introduction.....	162
Technique Development.....	164
Experimental.....	165
Continuous Sinusoidal Event.....	167
Periodic Squarewave Event.....	175
Results and Discussion.....	182
References.....	206
VI. THE DYNAMICS OF SEGMENTAL RESPONSE DURING DEFORMATION OF A POLYURETHANE ELASTOMER.....	208
Introduction.....	208
Experimental.....	209
Materials.....	209
Methods.....	215

Results and Discussion.....	218
Dynamics of Segmental Relaxation.....	222
Evaluation of Noise in TRS Spectra.....	229
Comparison of Ambient and Subambient Orientation Behavior.....	239
References.....	248
 VII. GENERAL RESULTS AND RECOMMENDATIONS FOR FUTURE WORK.....	251
General Results.....	251
Microstructural Ordering in Polyurethane Hard Segments.....	251
Characterization of Segmental Orientation.....	253
Investigations of Hardsegment Microstructural Ordering.....	256
Segmental Orientation Investigations.....	258

APPENDIX

A. PASCAL PROGRAM FOR INTEGRATION OF INFRARED ABSORPTIONS..	260
 B. PASCAL PROGRAMS FOR A MONTE CARLO SIMULATION OF HARD SEGMENT LENGTH DISTRIBUTIONS.....	266
 C. SYNCHRONIZATION AND SORTING PROGRAM FOR TIME RESOLVED INFRARED SPECTROSCOPY.....	284
 D. INTERFACE AND DRIVER ELECTRONICS FOR TIME RESOLVED METHOD.....	296

LIST OF TABLES

	<u>Page</u>
2.1 Band Assignments for Urethane Linkage of NPU	50
4.1 Polymerization Simulation Parameters.....	144
5.1 The Experimental Conditions Used to Test the Operation of the Time-Resolved Infrared Spectroscopic Equipment.....	183
5.2 The Experimental Conditions Used for the Poly(butylene terephthalate) Experiment.....	202
6.1 Experimental Conditions Used for the Time-Resolved Deformation Collection at 20°C.....	219
6.2 Experimental Conditions Used for the Time-Resolved Deformation Collection at -20°C.....	220

LIST OF FIGURES

	<u>Page</u>
1.1 Schematic of segmented polyurethane copolymer and phase separated microstructure.....	5
1.2 Molecular structure of polybutadiene based polyurethane.....	17
2.1 Schematic representation of relationship between transition moment and molecular axis. a. Perfectly ordered sample.....	30
b. With distribution of chain axis orientations.....	31
2.2 Molecular structure of N-phenyl urethane NPU.....	38
2.3 Schematic of NPU between KBr plates. a. Nucleated spherulitic crystal, b. positioning of window for infrared collection.....	41
2.4 Structure of monodispersed polyurethane T5MD.....	44
2.5 Infrared spectrum of NPU a. 3600 - 2600 cm^{-1}	47
b. 1800 - 1000 cm^{-1}	48
c. 1000 - 400 cm^{-1}	49
2.6 Orientation of NPU relative to crystalline growth axis.....	53
2.7 Infrared survey spectrum of T5MD.....	55
2.8 Dichroic ratio of T4MD as a function of sample strain. a. Soft segment absorptions.....	58
b. Hard Segment absorptions.....	59
2.9 Model of 1,2 vinyl butadiene linkage showing steric hinderance to rotation. a. Photograph of space filling model, b. schematic representation.....	61
2.10 Ratio of equation 2.6, Q(s) plotted as a function of strain for T5MD.....	65
2.11 Dichroic ratio fo 1,2 vinyl absorption as a function of estimated soft segment strain.....	69

3.1	Two step reaction sequence used in the synthesis of segmented polyurethane elastomers.....	80
3.2	Survey spectrum of T3MI prepared by a) solution casting from THF..... b) prepared by melt pressing at 140°C.....	84 85
3.3	Expanded scale spectrum of N-H stretching region of T3MI. a) solution cast from THF; b) melt pressed at 140°C; c) difference spectrum of a-b.....	88
3.4	Expanded scale spectrum of carbonyl region of T3MI; a) solution cast from THF, b) melt pressed at 140°C, c) difference spectrum of a-b.....	90
3.5	The carbonyl stretching absorption of amorphous T3MI plotted as a function of temperature.....	95
3.6	Total integrated peak areas of N-H and carbonyl absorptions plotted as a function of temperature.....	97
3.7	ATR spectrum of carbonyl region for T3MI prepared by solution casting on release paper.....	101
3.8	Carbonyl region of an annealed sample of polyurethane with a hard segment containing 2,6 TDI.....	104
3.9	Comparison of subtraction spectra corresponding to ordered component. a) T3MI, b) sample with pure 2,6 TDI hard segments.....	106
3.10	Infrared spectra of carbonyl absorption of solution cast T3MI are plotted as a function of thermal history.....	109
3.11	Integrated area of the ordered component of the carbonyl absorption plotted as a function of thermal history.....	111
3.12	Integrated area of ordered component of carbonyl absorption for solvent vapor treated T3MI as a function of thermal history.....	114
3.13	Polarized spectra for N-H region of T3MI which has been deformed 20%.....	118

3.14	Deformation model of ordered hard segment domains. Hard segment chain axes orient perpendicular to the deformation axis.....	120
3.15	Comparison of infrared spectra of BTB model compound, BTB after vacuum heating at 180°C and 2,4 TDI/BDO model polymer.....	125
4.1	Indexing array for ortho and para NCO groups of the 2,4 and 2,6 TDI molecules.	
	a. Before randomization showing partitioning of NCO types.....	137
	b. After randomization.....	138
4.2	Most probable distribution of hard segment lengths for TDI/soft segment mole ratio of 3.3.....	146
4.3	Standard deviation for segment of one TDI unit plotted as a function of the size of the ensemble.....	148
4.4	Unreacted fraction of NCO units as a function of total groups reacted.	
	a. Para/ortho reactivity ratio = 1.....	151
	b. Para/ortho reactivity ratio = 12.....	152
	c. Para/ortho reactivity ratio = 1000.....	153
4.5	Comparison of the distribution for the most probable case with that generated by Monte Carlo method for para/ortho reactivity ratio of 12/1.....	156
4.6	Distributions of weight fractions of consecutive 2,6 TDI sequences.....	159
5.1:	The schematic diagram of a time resolved experiment.....	170
5.2:	Flow diagram of computer control program for continuous deformation experiment.....	172
5.3:	Scheme showing the phase relationship between the interferometer movement and the external event for a continuous deformation cycle. A separate interferogram file is collected for each of n clock values, where $n = \text{event period} / \text{time resolution}$	174
5.4	a. During the data collection the phase relationship between the interferogram and the external event is varied in a systematic manner. Here the interferogram is shown segmented to depict how it is divided for the sorting procedure.....	177
	b. After sorting, each interferogram corresponds to a specific segment of time.....	178

5.5	Scheme showing phase relationship between the interferometer movement and the external event for a squarewave event cycle. The computer output array contains the waveform of the external event.....	181
5.6	The interferogram obtained which shows a low frequency modulation related to absorbance change as a function of the external event.....	185
5.7	The modulation manifests itself as a sawtooth pattern in the sorted interferogram.....	188
5.8	The Fourier transformed spectrum of the interferograms containing low frequency modulation can show an artifact in the form of evenly spaced spikes.....	190
5.9	Interferogram containing computer simulated sawtooth function. a. as collected..... b. after computer modification.....	192 193
5.10	When the modified interferogram is transformed the resulting ratioed spectrum exhibits a distinct derivative-like artifact.....	195
5.11	Change in CH rocking intensity as a function of angle between polarizer and film orientation direction.....	198
5.12	Characteristic CH ₂ rocking vibration in PBT associated with the α , β , and amorphous phase.....	201
5.13	A measure of the α - β phase transformation in poly(butylene terephthalate). Integrated absorbance change as a function of strain amplitude.....	205
6.1	Solenoid driven polymer deformation apparatus.....	212
6.2	Phase relationship between interferogram files and squarewave strain event. a. as collected, b. after sorting.....	214
6.3	Dichroic ratio of 1,2 vinyl absorption as a function of time for 40% static deformation.....	217

6.4	Relationship between stress relaxation and squarewave strain function.....	224
6.5	Time resolved dichroic ratios as a function of time at ambient temperature.	
	a. 1,2 vinyl C-H deformation.....	226
	b. 1,4 trans C-H deformation.....	227
	c. N-H stretching vibration.....	228
6.6	Time resolved dichroic ratios as a function of time at -20°C.....	231
6.7	Noise level spectra and corresponding absorbance spectrum, a. static collection mode, b. time resolved mode, c. absorbance spectrum.....	235
6.8	Time resolved spectra of 1,2 vinyl C-H deformation region. Lower trace: first clock period (0-19 msec), upper trace: second clock period (19-37 msec).....	238
6.9	Temperature dependence of stress relaxation for 40% squarewave deformation.....	242
6.10	Schematic representation of hard segment positioning in hard segment domain; a. traverses domain center, b. on domain surface.....	246
D.1	Wiring diagram for interface of CCS micro-processor, infrared digital driver board, and stretcher solenoid driver board.....	298
D.2	Circuit diagram of stretcher solenoid driver.....	300

C H A P T E R I

INTRODUCTION

Overview of Dissertation

The focus of this investigation is the microstructural characterization of polyurethane elastomers. Since macroscopic properties of a polymeric system may be correlated to the chemical structure of the polymer chain and subsequent levels of microstructural organization, it is clear that characterization at the molecular level is of fundamental importance. One of the most powerful techniques for molecular level characterization is Fourier transform infrared spectroscopy (FTIR). In this study FTIR is used as a direct probe for characterizing microstructural ordering of polyurethane hard segments. The segmental orientation response for a macroscopic deformation is also characterized using infrared spectroscopy and lends additional insight into the nature of the polyurethane microstructure. The polyurethane systems investigated in this study were chosen as they are model systems with well defined chemical and physical structures.

This dissertation is presented in seven chapters. This first chapter introduces the basic concepts of polyurethane elastomeric systems. Included in this chapter are: the basic chemical components and synthetic techniques, the concept of a phase separated microstructure and methods of characterizing phase separation, infrared orientation studies of polyurethane deformation, as well as a description of the

polyurethane systems characterized in this investigation. The second chapter presents the method of infrared dichroism along with models which are used to explain the way polymers of differing microstructural composition respond to a macroscopic deformation. In Chapter III the extent of hard segment microstructural ordering is characterized by monitoring changes in the frequency and intensity of infrared absorptions which are characteristic of substituents involved in hydrogen bond interactions. The extent of order is determined as a function of the method of sample preparation as well as thermal history. A Monte Carlo simulation of the polymerization process of this polyurethane system is presented in Chapter IV. Particular emphasis is placed on the effects of monomer reactivity on the resulting fraction and distribution of crystallizable hard segment sequences. A new method of time resolved Fourier transform infrared spectroscopy has been developed to monitor the segmental dynamics of polymer deformation and is detailed in Chapter V. In Chapter VI the time resolved technique is utilized for characterizing dynamic chain orientation response during the deformation of a model polyurethane elastomer. This study utilizes the method of infrared dichroism to determine the segmental orientation and orientation relaxation rate as a function of sample temperature. The final chapter summarizes the results of the previous chapters and proposes work for future studies.

Introduction to Linear Segmented Polyurethanes

Linear segmented polyurethanes are copolymers which consist of

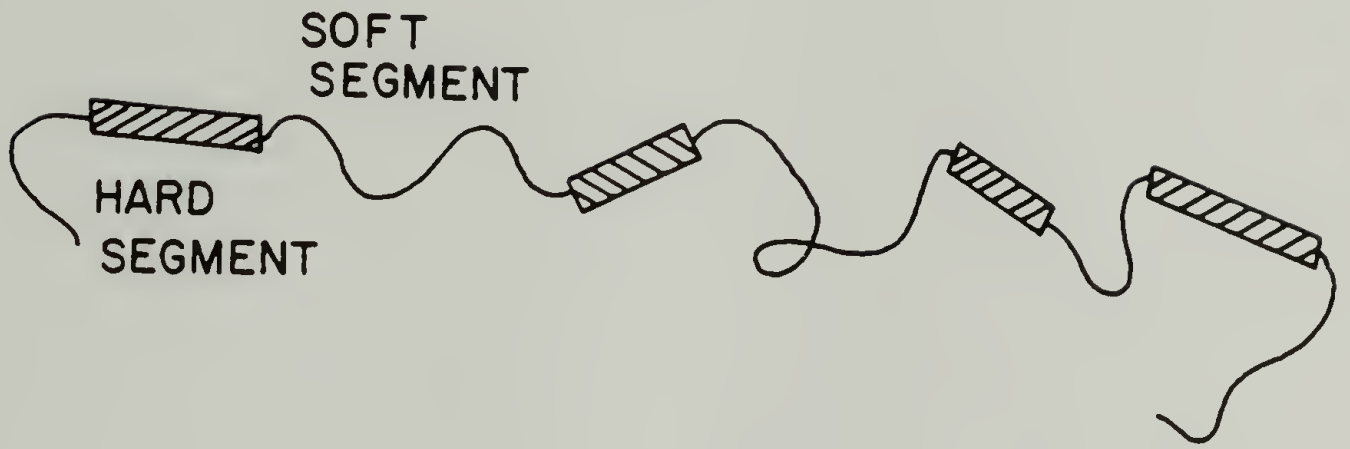
alternating hard and soft segment units. These two segment types are thermodynamically incompatible, resulting in a phase separated morphology of hard segment rich domains and soft segment rich domains (Figure 1.1). At low hard segment content the hard segment domains act as physical crosslinks for the elastomeric matrix giving the polymer properties which are similar to those of a crosslinked rubber, but without having primary valance crosslinking. Since the polymer is a linear chain it may be processed using conventional processing methods that are less energy intensive than methods required for rubber processing. The low energy processing coupled with the desirable mechanical properties of toughness, flexibility, and abrasion resistance have led to the use of these polymers in a wide variety of industrial and consumer applications. This has resulted in an abundance of research investigating correlations between the macroscopic polymer properties and component microstructure in an effort to develop superior polyurethane systems. Due to the complexity of these materials, a comprehensive understanding of these relationships has not been developed. This is partly due to the wide variety of polyurethane chemical structures which result from a multitude of precursory materials.

Polyurethane Chemical Structure

Polyurethane elastomers are prepared from the addition reaction of a diisocyanate with a hydroxy terminated oligomeric elastomer and low molecular weight diol. This is a high yield reaction which produces no low molecular weight by-products. This reaction is based on the diiso-

FIGURE 1.1: Schematic of segmented polyurethane copolymer and phase separated microstructure.

SEGMENTED BLOCK COPOLYMER



MICROPHASE SEPARATION

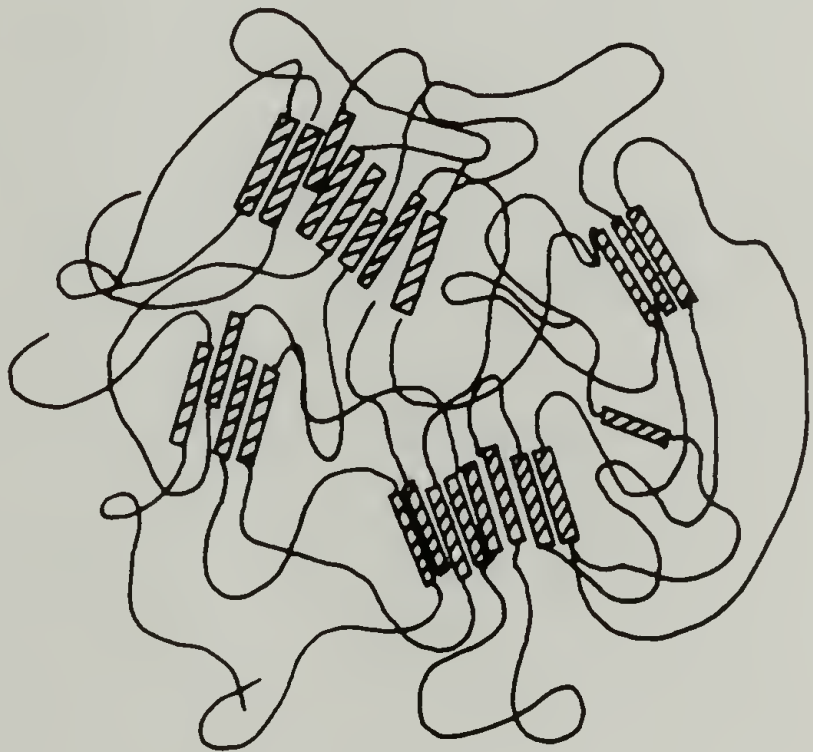


FIGURE 1.1

cyanate polyaddition process developed in 1937 by O. Bayer and coworkers (1). The use of this reaction for elastomeric systems was introduced in 1958 by Schollenburger (2,3). The soft segment macrodiol used in these systems is typically a polyester or polyether oligomer having a molecular weight between 500 and 5000. Poly(ethylene adipate) is often used for the polyester type soft segment while poly(tetramethylene oxide) or poly(propylene oxide) are the common polyether soft segments. The hard segment units are most often aromatic diisocyanates coupled with a low molecular weight diol. A majority of polyurethane systems are prepared with either 4,4'-diphenylmethane diisocyanate (MDI) or toluene diisocyanate (TDI) chain extended with butanediol.

The chemical structure of the hard segments plays an important role in the nature of hard segment microstructural ordering. Hard segments with symmetric diisocyanate residues such as those prepared from MDI or 2,6 TDI have the potential to form semicrystalline structures while those made with asymmetrically substituted diisocyanates such as 2,4 TDI have amorphous hard segment domains (4,5). The ability of the hard segments to form semicrystalline domains and the potential of specific intersegmental interactions (such as hydrogen bonding) occurring between the hard and soft segments are controlling factors in the development of microphase separation. When hydrogen bonding can occur between the soft and hard segments, as is known for the systems with polyester and polyether soft segments, the thermodynamic driving force for phase separation is reduced. This results in systems with enhanced segmental mixing and an interphase region between hard and soft domains which makes modeling the structure-property relationship

more complex.

Several systems have been investigated where the interphase region has been minimized by utilizing soft segments which have no potential for hydrogen bonding with the hard segments. The soft segments in these systems are oligomeric glycols of polybutadiene, its hydrogenated derivative, and polyisobutylene. These soft segments are less polar than the polyester and polyether types, thus decreasing their compatibility with the urethane hard segments. Polyurethanes based on these soft segments tend to be more completely phase separated than those based on the ester or ether oligomers (6-9). Increasing phase separation is generally thought to improve mechanical properties (10), however, polyurethanes having polybutadiene soft segments have been found to have inferior mechanical properties in comparison to more conventional polyurethane systems (11). An advantage of these systems, however, is that they exhibit improved hydrolytic stability over the polyester or polyether based polyurethanes (12,13).

Another aspect of the polyurethane chain structure which adds to the complexity of these systems is that there is a distribution of the lengths of the hard component segments. The distribution of the lengths of the soft segment results from the method of synthesis of the hydroxy terminated soft segment oligomer. The distribution of the lengths of the hard segments results from the step growth nature of the polyurethane polymerization process. In the ideal case this would be the most probable distribution and has been shown by Flory (14) to be

$$w_x = x(1 - p)^2 p^{x-1} \quad (1.1)$$

where w_x is the weight fraction of hard segments of length x and P is a probability term which is equal to the mole ratio of chain extender residues to soft segment residues. In actual polyurethane systems, the hard segment distribution deviates from the ideal case due to inhomogeneous reaction mixtures which result from the thermodynamic incompatibility of the component molecules in the reaction as well as the unequal reactivities of the monomer functional groups. Several investigators have eliminated the complexity of hard segment length distribution by synthesizing and characterizing polyurethanes which have hard segments that are monodisperse in length (15-19). In general, the synthetic procedures required for these model systems is quite tedious and results in low yields which restrict their use to laboratory investigations. However, the study of these materials has proven to be very useful in developing an understanding of fundamental structure-property correlations.

Polyurethane Characterization

Characterization of Microphase Separation

The concept of microphase separation occurring in polyurethane elastomers was first proposed by Cooper and Tobolsky in 1966 (20). This was based on experimental studies characterizing the modulus-time and modulus-temperature behavior of polyurethane elastomers. The work suggested the interpretation of the system as being a block copolymer with each block having its own glass transition temperature T_g . This

led to investigations at a number of laboratories to characterize polyurethane phase separation since the physical properties of these systems may be directly related to the presence of a two phase microstructure. These characterization methods include: dynamic mechanical analysis (DMA), differential scanning calorimetry (DSC), electron microscopy, x-ray scattering, and infrared spectroscopy. Each of these methods may be used to characterize particular aspects of polyurethane microstructure. The details of all of these techniques are not within the scope of this work and the reader should consult the appropriate review articles.

Of particular interest, and the focus of this investigation, is the characterization of polyurethane microstructure using infrared spectroscopy. Infrared spectroscopy is a powerful technique for molecular level characterization because each of the vibrational absorptions are characteristic of a specific unit of the molecular structure. This is particularly useful when characterizing segmented polyurethanes because it allows one to probe the microstructure of the hard segment and soft segment domains independently. Infrared spectroscopy is useful for characterizing intermolecular interactions of the component segments as well as the segmental orientation which occurs when the sample is deformed macroscopically. Both of these aspects of infrared characterization have contributed to the development of a comprehensive understanding of the relationship between polymer microstructure and mechanical properties.

Infrared Characterization of Hydrogen Bonding

Infrared spectroscopy has been widely used for investigating molecular interaction in polyurethane elastomers. These studies have focused on the extent and specificity of hydrogen bonding as a means of evaluating microphase separation of the hard and soft segments in segmented polyurethanes (4,5,21-26). Vibrational absorptions of the carbonyl and N-H groups exhibit perturbations in their frequencies and intensities when hydrogen bonding interactions occur. When the N-H group participates in hydrogen bonding, the frequency of the stretching vibration is decreased and its intensity increases. Typically, the frequency of the non-bonded group is about 3450 cm^{-1} , shifting to around 3320 cm^{-1} as it becomes hydrogen bonded (27). Detailed analysis of the infrared spectrum can thus be extremely useful in the characterization of the specific nature of hydrogen bonding.

N-phenyl urethane is a low molecular weight compound which has been used as a model for the urethane linkage and has been characterized using infrared spectroscopy in two investigations (21,28). In both of these studies the extent of hydrogen bonding of this compound was determined at several concentrations in solution as well as the specificity of its interaction with several proton accepting groups. The frequency shift of the N-H stretching vibration was found to be a good indication of the strength of the hydrogen bond interaction. These considerations have been applied to intersegmental hydrogen bond interactions in polyurethane-urea elastomers (22,29). In

this type of system the inter-urea hydrogen bonds were found to be more specific and of greater strength than hydrogen bond interactions between the hard segment and polyester carbonyl groups. It was found that the mechanical properties of these systems could be correlated quite well to the extent of intermolecular interaction.

Several investigators have reported quantitative studies of the extent of hydrogen bonding as a function of temperature. By evaluating the equilibrium of free and associated N-H groups at several temperatures the enthalpy of the hydrogen bond interactions were calculated (4,5,25,26,30). These calculations, however, were based on absorbance maxima and did not take into account the existence of a distribution of hydrogen bond lengths and the effect of this on absorption intensity. Tsubomura has reported that the N-H absorption intensity has a strong dependence on the hydrogen bond length (31). Quantitative interpretation of the extent and specificity of hydrogen bonding is only possible when this dependence is taken into account. Recent work by Coleman and Painter has shown that the fraction of N-H groups which are hydrogen bonded in a polyamide system is relatively independent of temperature. The distribution of hydrogen bond lengths, however, varies significantly, thus changing the bandshape of the N-H absorption. In consideration of these studies, it is clear that with careful spectral interpretation, infrared spectroscopy is a useful technique for characterizing phase separation and domain microstructure in segmented polyurethane elastomers.

Segmental Orientation Studies by Infrared Spectroscopy

When polyurethane elastomers are strained macroscopically, the individual hard and soft segment domains orient and deform in a manner which is dependent on the domain microstructure. Characterization of this process is essential for understanding the mechanisms of the deformation and also lends insight as to the nature of the initial component microstructure. The determination of chain orientation using the method of infrared dichroism has been applied to a variety of polymeric systems and is well suited to characterizing segmental orientation in polyurethane elastomers. The specificity of infrared absorptions enables one to characterize the orientation of each of the component segment types independently. The application of the method of infrared dichroism to polymer orientation studies has been reviewed by several authors (33-36). This technique has been used extensively for characterizing microstructural orientation in several polyurethane systems (22,33,35,37,38).

Considerable attention in the characterization of polyurethane segmental orientation has focused on systems having polyester or polyether type soft segments with hard segments of p,p' diphenylmethane diisocyanate, chain extended with butanediol. In an early investigation of this system, Cooper et al. (39) found that as the sample was deformed macroscopically the soft segments readily oriented in the direction of the applied stress and returned to an unoriented state when the stress was removed. The urethane domains oriented to an extent similar to the soft segments but remained partially oriented

after removal of stress. This behavior was attributed to plastic deformation of the hard segment domains. In a subsequent investigation, segmental orientation was monitored systematically for a series of polyurethane elastomers as a function of hard segment content (40). As the hard segment content was increased, a distinct change in the mechanism of hard segment orientation occurred which was interpreted as a crossover from isolated to interconnected hard segment domains.

The preparation method and thermal history of some samples was controlled to introduce microcrystallinity into the hard segment domains. When these samples were deformed, the hard segment chains oriented transverse to the deformation axis at low strain then rotating into the deformation axis at strains above 150%. This was consistent with earlier studies of Bonart, who used wide angle x-ray scattering to characterize hard segment orientation as a function of strain (41). The hard segment orientation behavior in these studies was interpreted as a transition from the orientation of crystallites as a whole at small elongations to the orientation of molecular chains at large elongations. This is a result of stress induced crystalline restructuring changing from the lamellar structure initially to a fibrillar structure in the deformed state.

The transverse orientation behavior is a general phenomenon occurring in semicrystalline polyurethanes as well as in poly(urethane-ureas) (22). In the poly(urethane-urea) systems, intermolecular crystalline bonding is stronger than for the polyurethane elastomers and results in transverse orientation which lasts up to strains as high as 300%.

Polyurethane elastomers have been utilized in many applications due to their viscoelastic nature. However, there have been no investigations of the dynamics of the molecular orientation mechanisms responsible for this behavior. The major focus of the orientation studies in this current investigation is on the dynamics of segmental orientation for a model polyurethane system during uniaxial deformation.

Research Objectives of This Investigation

The objectives of this investigation are two-fold. The first focus of this study is to characterize the extent and specificity of hard segment microstructural ordering in a polyurethane having partially crystallizable hard segments. The dependence of the extent of hard segment ordering on the method of sample preparation and thermal history is investigated by monitoring hydrogen bonding interaction which are determined using infrared spectroscopy. The second focus of this study is to characterize the dynamics of segmental orientation response for a polyurethane elastomer subjected to uniaxial deformation. The method of infrared dichroism is used to determine the orientation of the component segments of the polyurethane. This orientation study includes the development and implementation of a time resolved infrared technique to make possible the collection of infrared spectra in the time scale of milliseconds with a signal to noise ratio sufficient for calculating dichroic ratios of characteristic absorptions.

In both the microstructural ordering and chain orientation studies it is desirable to characterize systems which are well defined and have a simple morphological structure. For this reason, a polyurethane system with a polybutadiene soft segment and hard segment of toluene diisocyanate (TDI) chain extended with butanediol was selected (Figure 1.2). This type of system has been chosen as a model polyurethane as it has been characterized in several investigations and has been found to be highly phase separated (6-9,16,30,42). This is due to the facts that the hard and soft segments are thermodynamically incompatible and hydrogen bonding is restricted to hard segment interactions. This is in contrast to many commercial systems where hydrogen bonding may occur between hard and soft segments, thus promoting segmental mixing which adds to the complexity of the polyurethane microstructure. While the basic components of the polyurethanes investigated in the hard segment ordering and dynamic orientation studies are the same, they differ in the isomeric structure of the hard segments. The sample characterized in the microstructural ordering study has a hard segment component which is prepared with a mixture of 2,4 and 2,6 toluene diisocyanate using solution polymerization. The 2,4 and 2,6 isomers are present in a ratio of 80:20 respectively, which is the same ratio found in most commercial grade TDI. Correlations between the hard segment microstructural ordering found in this system and factors such as the method of sample preparation, i.e. solution casting and melt pressing, as well as the thermal history, aid in developing an understanding of the distribution of sequences of the 2,4 and 2,6 TDI residues. Specific interest is in determining if sequences with consecutive

FIGURE 1.2: Molecular structure of polybutadiene based polyurethane.

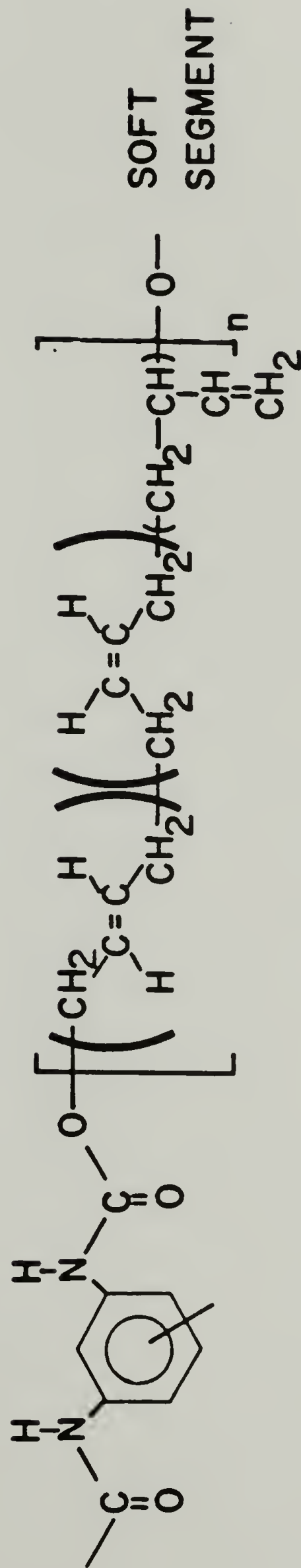


Figure 1.2

placement of the symmetric 2,6 isomer are sufficient to account completely for hard segment ordering. Computer modeling of the polymerization process will be utilized for determining the effects of the reaction kinetics of the two TDI isomers on the sequence distributions of these isomers in the hard segments. This simulation is intended to complement the experimental determinations of hard segment ordering using infrared spectroscopy.

The sample characterized in the investigation of segmental orientation dynamics has a hard segment which is monodispersed in length and contains five residues of 2,4 TDI. The monodispersed hard segment exhibits no permanent set during deformation; a necessary criterion for a sample being characterized in time resolved infrared deformation studies. The objective of this study is to correlate the response of polymer microstructure, such as segmental orientation with macroscopic properties such as stress in the uniaxially deformed sample. The dependence of the rate and amplitude of microstructural changes during deformation on the temperature of the system will help in developing a model of the deformation process.

References

1. O. Bayer, H. Rinke, W. Siefken, L. Orthner, and H. Schile, DRP 728981, 31.11, 1937.
2. C.S. Schollenberger, H. Scott, and G.R. Moore, "PUVC a Virtually Crosslinked Elastomer", *Rubber World*, 137, 549 (1958).
3. C.S. Schollenberger, U.S. Pat. 2,871,218 (Jan. 27, 1959).
4. C.S. Paik Sung and N.S. Schneider, "Temperature Dependence of Hydrogen Bonding in Toluene Diisocyanate Based Polyurethanes", *Macromolecules*, 10, 452 (1977).
5. N.S. Schneider and C.S. Paik Sung, "Transition Behavior and Phase Segregation in TDI Polyurethanes", *Polym. Eng. Sci.*, 17, 73 (1977).
6. N.S. Schneider and W. Matton, "Thermal Transition Behavior of Polybutadiene Containing Polyurethanes", *Polym. Eng. Sci.*, 19, 1122 (1979).
7. C.M. Brunette, S.L. Hsu, W.J. MacKnight, and N.S. Schneider, "Structure and Mechanical Properties of Polybutadiene-Containing Polyurethanes", *Polym. Eng. Sci.*, 21, 163 (1981).
8. C.M. Brunette, S.L. Hsu, M. Rossman, W.J. MacKnight, and N.S. Schneider, "Thermal and Mechanical Properties of Linear Segmented Polyurethanes with Butadiene Soft Segments", *Polym. Eng. Sci.*, 21, 668 (1981).
9. B.H. Bengston, "Structure-Property Relationships in Linear Polyurethanes", Ph.D. Dissertation, University of Massachusetts, 1985.

10. A. Lilaonitkul and S.L. Cooper, Advances in Urethane Science and Technology, Vol. 7, p. 163, K.C. Frisch and S.L. Reegen, Eds., Tecnominc Publ. Co., 1979.
11. C.Z. Yang, K.K.S. Hwang, and S.L. Cooper, "Morphology and Properties of Polybutadiene and Polyether-Polyurethane Zwitteronomers", Makromol. Chemie, 184, 651 (1983).
12. C.J. Arnold, Jr., "Development and Characterization of EN7: A Ferric Accetylacetonate Catalyzed Polybutadiene Based Elastomer", J. Elast. Plast., 6, 238 (1974).
13. V.S.C. Chang and J.P. Kennedy, "Optimizing Urethane Synthesis by Studying the Kinetics of Reactions Between A Model Alcohol and Isocyanates in Various Solvents", Polym. Bull, 8, 69 (1983).
14. P.J. Flory, Principles of Polymer Chemistry, Cornell University Press, Ithaca, NY, 1953.
15. G.M. Estes, S.L. Cooper, and A.V. Tobolsky, "Block Polymers and Related Heterophase Elastomers", J. Macromol. Sci., B3(2), 337 (1969).
16. B. Fu, "Synthesis, Characterization, and Properties of Segmented Polyurethanes Containing Monodisperse Hard Segments", Ph.D. Dissertation, University of Massachusetts, 1985.
17. L.L. Harrell, Jr., "Segmented Polyurethane Properties as a Function of Segment Size and Distribution", Macromolecules, 2, 607 (1969).
18. C. Christianson, private communication.

19. H.N. Ng, A.E. Allegrezza, R.W. Seymour, and S.L. Cooper, "Effect of Segment Size and Polydispersity on the Properties of Polyurethane Block Polymers", *Polymer* 14, 225 (1973).
20. S.L. Cooper and A.V. Tobolsky, "Properties of Linear Elastomeric Polyurethanes", *J. Appl. Polym. Sci.*, 10, 1837 (1966).
21. T. Tanaka, T. Yokayama, and Y. Yamaguchi, "Quantitative Study on Hydrogen Bonding Between Urethane Compound and Ethers by Infrared Spectroscopy", *J. Polym. Sci., A-1*, 6, 2137 (1968).
22. H. Ishihara, I. Kimura, K. Saito, and H. Ono, "Infrared Studies on Segmented Polyurethane-Urea Elastomers," *J. Macromol. Sci.-Phys.*, B10(4), 591 (1974).
23. R. Seymour and S.L. Cooper, "Thermal Analysis of Polyurethane Block Polymers", *Macromolecules*, 6, 48 (1973).
24. T. Tanaka, T. Yokayama, and Y. Yamaguchi, "Effects of Methyl Sidegroup on the Extent of Hydrogen Bonding and Modulus of Polyurethane Elastomers", *J. Polym. Sci., A-1*, 6, 2153 (1968).
25. W.J. MacKnight and M. Yang, "Property-Structure Relationships in Polyurethanes: Infrared Studies", *J. Polym. Sci., Part C*, 42, 817 (1973).
26. G.A. Senich and W.J. MacKnight, "Fourier Transform Infrared Thermal Analysis of a Segmented Polyurethane", *Macromolecules*, 13, 106 (1980).
27. G.C. Pimentel and A.L. McClellan, The Hydrogen Bond, W.H. Freeman and Co., San Francisco, 1960.

28. Y.M. Boyarchuk, L.Y. Rappoport, V.N. Nikitin, and N.P. Apukhtina, "Study of Hydrogen Bonding in Urethane Elastomers by Infrared Spectroscopy", *Polym. Sci. U.S.S.R.*, 7, 859 (1965).
29. G.S. Kitukhina and V.V. Zharkov, "Features of Self-Association of Urea Groups in Polyester Urethane Ureas", *Polym. Sci.-U.S.S.R.*, 23, 2446 (1981).
30. C.M. Brunette, "Structure-Property Relationships in Polybutadiene Polyurethanes", Ph.D. Dissertation, University of Massachusetts, 1982.
31. H. Stubomura, "Nature of the Hydrogen Bond. III. The Measurement of the Infrared Absorption Intensities of Free and Hydrogen-Bonded OH Bands. Theory of the Increase of the Intensity Due to the Hydrogen Bond", *J. Chem. Phys.*, 245, 927 (1956).
32. P. Painter and M. Coleman, private communication.
33. G.M. Estes, R.W. Seymour, and S.L. Cooper, "Infrared Dichroism of Segmented Polyurethane Elastomers", *Amer. Chem. Soc., Polym. Preprints*, 11(2), 516 (1970).
34. B. Jasse and J.L. Koenig, "Orientation Measurements in Polymers Using Vibrational Spectroscopy", *J. Macromol. Sci.-Rev. Macromol. Chem.*, C17(1), 61 (1979).
35. G.L. Wilkes, "Rheo-Optical Methods and Their Application to Polymeric Solids", *J. Macromol. Sci.-Revs. Macromol. Chem.*, C10(2), 149 (1974).
36. A. Garton, D.J. Carlsson, and D.M. Wiles, "Molecular Orientation Measurements in Polymers by Infrared Spectral Subtraction", *Appl. Spectrosc.*, 35, 432 (1981).

37. H.W. Siesler, "Rheo-Optical Fourier Transform IR Spectroscopy of Polyurethane Elastomers, 1. Principle of the Method and Measurement at Ambient Temperature", *Polym. Bull.*, 9, 382 (1983).
38. V.N. Vatulev, S.V. Laptii, R.L. Garduk, and Yu.Yu. Kercha, "On the Inversion of IR Dichroism in Segmented Polyurethane Elastomers", *Polym. Sci. U.S.S.R.*, 23, 2679 (1981).
39. G.M. Estes, R.W. Seymour, and S.L. Cooper, "Infrared Studies of Segmented Polyurethane Elastomers. II. Infrared Dichroism", *Macromol.*, 4, 452 (1971).
40. R.W. Seymour, A.E. Allegrezza, Jr., and S.L. Cooper, "Segmental Orientation Studies of Block Polymers. I. Hydrogen-Bonded Polyurethanes", *Macromolecules*, 6, 846 (1973).
41. R. Bonart, "X-Ray Investigations Concerning the Physical Structure of Crosslinking in Segmented Urethane Elastomers", *J. Macromol. Sci.-Phys.*, 2, 115 (1968).
42. C. Chen-Tsai, "Morphology Studies on Amorphous Segmented Polyurethanes", Ph.D. Dissertation, University of Massachusetts.

C H A P T E R I I

INVESTIGATIONS OF MOLECULAR ORIENTATION BY THE METHOD OF INFRARED DICHROISM

Introduction

A variety of properties of polymeric materials depend on the orientation of the component microstructure. From a commercial standpoint there is particular interest in the effect of molecular orientation on the mechanical properties of polymers. This has led to extensive research in characterizing various aspects of polymeric structure and the mechanisms by which the systems respond to a macroscopic deformation. Depending on the chemical nature and processing history of the material, structural organization may occur over a wide range of spatial scales; ranging from local chain conformations with a length scale of a few angstroms to macroscopic superstructures of several microns in size as in spherulitic crystalline polymers. In characterizing polymer deformation it is important to evaluate how both the micro and superstructure respond during the deformation process.

Several characterization techniques are available for determining orientation at different levels of structural organization (1). Deformation of spherulitic superstructures in semicrystalline polymers may be characterized using the techniques of small angle light scattering (2,3). Changes in the scattering patterns using polarized laser

light results from elongation of the spherulitic structures during deformation (4). A technique which may be used to determine the orientation of the individual crystalline lamellae is wide angle x-ray scattering (WAXS) (5). The intensities of reflections specific to geometric spacings of atoms in a crystalline lattice are used to determine orientation of the crystalline component. Another method for determining orientation in polymeric systems is the birefringence technique. While WAXS may only be used to determine the orientation of the crystalline component, the measured birefringence Δ results from several contributions of the oriented microstructure (1). As indicated in Equation 2.1

$$\Delta = \phi_{cr}\Delta_{cr} + (1-\phi_{cr})\Delta_{am} + \Delta_{form} \quad (2.1)$$

these terms are additive with ϕ_{cr} being the weight fraction of the crystalline phase and Δ_{cr} and Δ_{am} the birefringence of the crystalline and amorphous phases, respectively. The last term Δ_{form} , the form birefringence, is due to distortion of the electric field of the lightwave at the phase boundary (6). Often the birefringence method is used to determine the orientation of the amorphous phase after the contribution from the crystalline phase has been determined from WAXS measurements (1).

Infrared and Raman spectroscopy are two methods which have an advantage in that they may be used to directly determine the segmental orientation for specific phases of the polymer microstructure through the characterization of vibrational transitions. Studies of molecular

orientation using polarized Raman scattering have appeared in recent years (7-9), while investigations by the use of the method of infrared dichroism have been reported over the past four decades (1,5,9-18). Although both may be used for quantitative determinations of molecular orientation, the infrared method has been most widely used due to two factors: an availability of instrumentation and a simplified theoretical approach. In the present investigation the method of infrared dichroism has been used exclusively. It is particularly well suited to the characterization of segmented polyurethane elastomers as vibrations characteristic to the soft segment and hard segment may be used for the determination of molecular orientation in each phase.

In a uniaxially deformed sample the alignment of polymer chains is never perfect but corresponds to a distribution of angles between the molecular axis of a segment and the deformation axis. All of the methods, infrared dichroism, Raman scattering, and WAXS, yield an average value which is some moment of the distribution. The method of infrared dichroism results in an orientation value which corresponds to the average of the cosine squared of the angle between the chain axis and the deformation axis taken over all chains, known as the second moment of the distribution. Polarized Raman scattering gives the second and fourth moments while WAXS can be used to determine the complete orientation distribution.

A second moment orientation function, f , is used to characterize the distribution of angles, θ , between the deformation axis and chain axes. A common way of expressing this is the Hermans' orientation

function

$$f = \frac{3\langle \cos^2\theta \rangle - 1}{2} \quad (2.2)$$

where $\langle \cos^2\theta \rangle$ is the average of the cosine squared of over all chains (20). This function has a value of 1 for perfect parallel orientation, 0 for isotropic, and $-1/2$ for perfect perpendicular chain orientation. The quantity f may be experimentally determined from infrared absorption measurements using linearly polarized radiation.

Theory of Infrared Orientation Measurements

Infrared activity in organic molecules occurs when a vibrational mode produces a changing electric dipole moment \underline{M} . Absorption occurs when the electric field vector of the incident radiation, \underline{E} , has a component parallel to the direction of \underline{M} (1). The infrared absorption is expressed in terms of the absorbance A defined by

$$A = -\log_{10} \frac{I}{I_0} \quad (2.3)$$

where I_0 is the incident intensity and I is the transmitted intensity. The ratio I/I_0 is often called the transmittance and is proportional to $(\underline{M} \cdot \underline{E})^2$. If the angle between \underline{M} and \underline{E} is β , then the strength of the absorption is proportional to $\cos^2\beta$. For unpolarized radiation, the absorption of a specific transition \underline{M} is independent of its orientation in the sample plane. However, the electric field vector of the incident radiation may be linearly polarized and the resulting absorption will indeed have a dependence on the angle between the transition

moment vector and electric field vector. For the method of infrared dichroism, the absorbance of a specific vibrational mode is determined once with the incident electric field vector polarized parallel to a preferred axis of the sample such as the deformation axis, A_{\parallel} , then with perpendicular polarization A_{\perp} . The dichroic ratio D , defined as

$$D = A_{\parallel} / A_{\perp} \quad (2.4)$$

determines the average orientation of a characteristic absorption.

While bond orientation in molecular systems may be specific relative to three cartesian coordinates, of particular interest in polymer deformation studies is the case of uniaxial orientation. Here, orientation is isotropic in a plane perpendicular to a preferred sample axis, being the axis of deformation. The relationship between transition moment, chain axis, and deformation axis will be discussed for a uniaxial system. This model is discussed in terms of a characteristic transition moment which forms an angle α to the chain axis. If all chains are perfectly aligned and the transition moments distributed symmetrically about this axis as is depicted in Figure 2.1a, then the dichroic ratio of this transition is given by the following equation (9,10)

$$D_0 = 2 \cot^2 \alpha \quad (2.5)$$

Using this equation it would be possible to calculate the transition moment angle α for an absorption of a perfectly oriented sample given the dichroic ratio of this absorption. However, in general orientation is only partial and a more complex model is necessary. The chain axis

FIGURE 2.1: Schematic representation of relationship between transition moment and molecular axis.
a. Perfectly ordered sample.
b. With distribution of chain axis orientations.

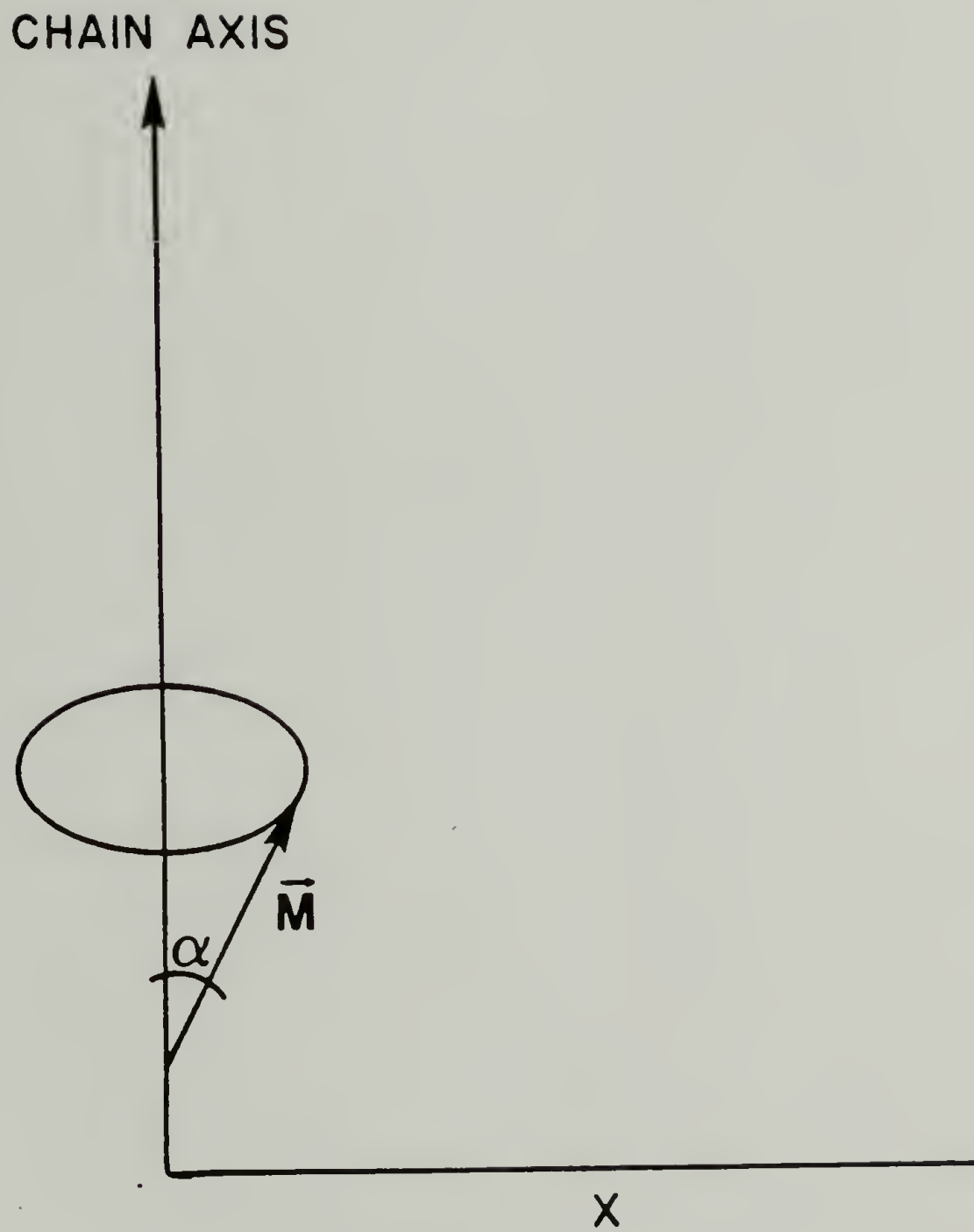


Figure 2.1a

STRETCHING
DIRECTION

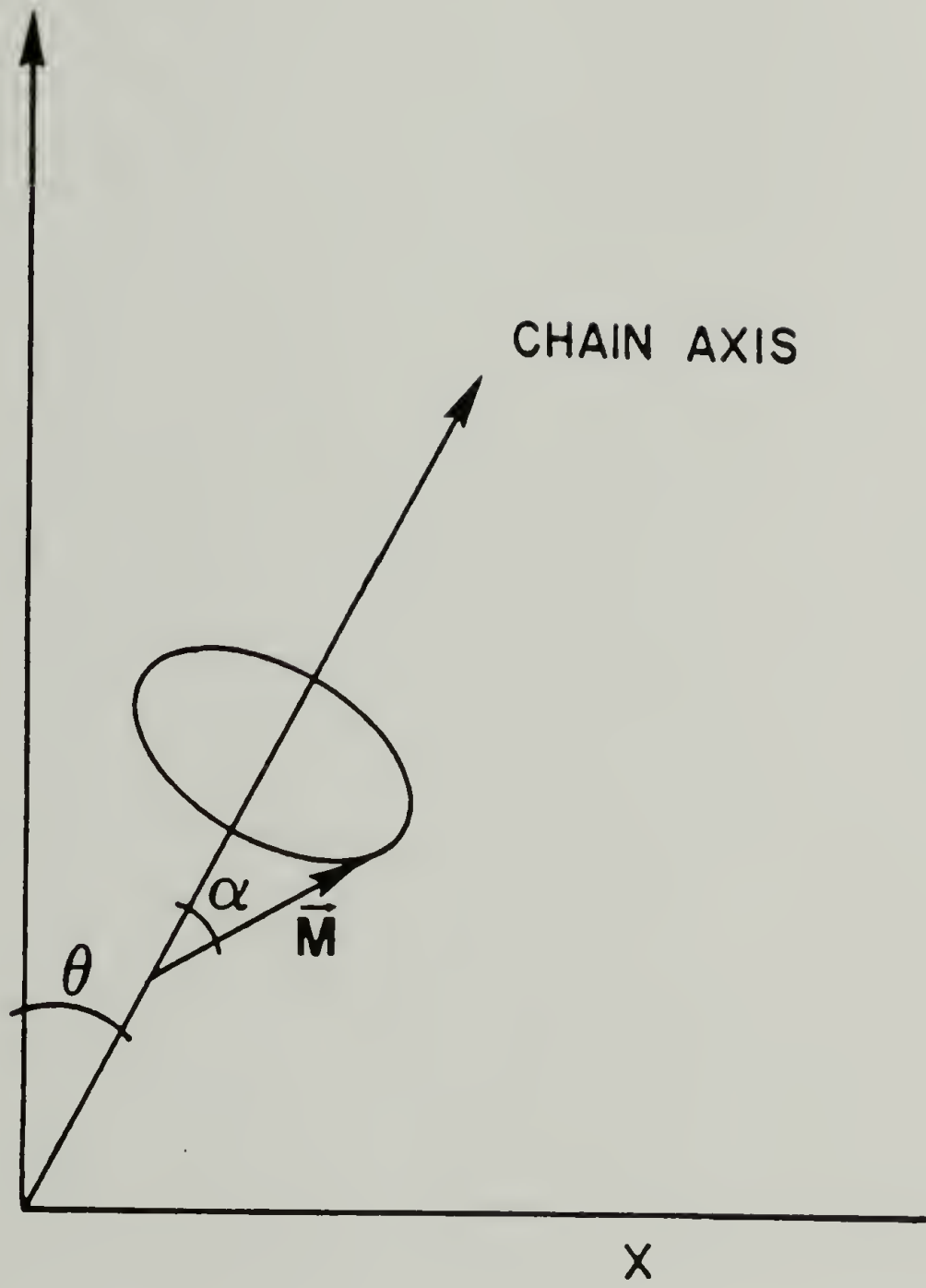


Figure 2.1b

is misaligned from the deformation axis by an angle θ (Figure 2.1b). This angle is not unique and there would be a distribution of angles between the deformation axis and the chain axis. If both the dichroic ratio and the transition moment angle are known for a specific vibration, then the second moment orientation function, f , of Equation 2.2 may be determined using Equation 2.6 (9).

$$f = \frac{D_0+2}{D_0-1} \cdot \frac{D-1}{D+2} \quad (2.6)$$

Conversely, if f is determined by independent means, then the transition moment angle of a vibration may be calculated from its dichroic ratio. Therefore, if two different vibrational modes are both characteristic of a chain segment the dichroic ratios may be used to calculate the angle of one of the transitions given the angle of the other.

The Relationship Between Segmental Orientation and Polymer Strain

The orientation of polymer chains in response to a macroscopic deformation may occur by several mechanisms which depend on the chain flexibility and microstructural organization. Macroscopic strain may result in the elongation of polymer chains occurring by either plastic deformation or rubber-like deformation. Several theories have been developed for these different mechanisms to relate chain orientation and infrared dichroism to polymer strain (21-23).

Two general approaches are taken in modelling segmental orientation in deformed polymers. A pseudo affine deformation model was introduced by Kratky where orientation is treated as occurring with the

angular rotation of a microstructural element behaving the same as a line having end coordinates which separate in the same ratio as the external dimensions of the sample (22). The resulting second moment orientation function is given by

$$f = \frac{3\lambda^3}{2(\lambda^2-1)} \left(1 - \frac{\tan^{-1}(\lambda^3-1)^{1/2}}{(\lambda^3-1)^{1/2}} \right) - 1/2 \quad (2.7)$$

where λ is the elongation ratio, L/L_0 with L_0 being the initial sample length and L being the strained sample length. This model is particularly useful in predicting crystalline orientation where the crystallites may be considered as rigid bodies of high axial ratio floating in a homogeneous matrix (24). This model has been used by Stein in predicting the orientation behavior of ethylene crystallites in ethylene propylene copolymers (25) and by Cunningham in modelling the orientation of poly(ethylene terephthalate) at high draw ratios (26).

A different approach has been taken in modelling the orientation behavior of a rubber-like network. For elongation of a polymer system of this nature, the crosslink points of the network are modelled as deforming in an affine manner, with the network chains treated as flexible gaussian coils (27,28). In this model the flexibility of the chain is interpreted by the number of random links between crosslink points. Partitioning of a chain into links, each having an orientation independent of the previous one, has been a useful concept in characterizing elastomers and was first described by Kuhn and Grun (23). The length of a link is related to the stiffness of a polymer chain and is

a measure of the rotational freedom both within the repeat unit and between repeat units. Roe and Krigbaum considered the uniaxial deformation of a crosslinked rubber and derived the following relationship

$$\langle \cos^2 \theta \rangle = \frac{1}{3} + \frac{2}{15N} \left(\lambda^2 - \frac{1}{\lambda} \right) + \left(\frac{2}{75N^2} \right) \left(\lambda^4 + \frac{\lambda}{3} + \frac{4}{3\lambda^2} \right) + \left(\frac{2}{105N^3} \right) \left(\lambda^6 + \frac{3\lambda^2}{5} - \frac{8}{5\lambda^3} \right) \quad (2.8)$$

where N is the number of random links and λ is the elongation ratio (21).

This may be interpreted in terms of the orientation function as

$$f = \frac{1}{5N} \left(\lambda^2 - \frac{1}{\lambda} \right) \text{ plus higher order terms.} \quad (2.9)$$

Using this equation, the number of random links may be calculated from the orientation function and elongation ratio. This relationship is best suited for modelling network deformation at low elongation, i.e. $\lambda < N^{1/2}$ (29). It has been successfully used by Cunningham et al. for modelling the orientation behavior of amorphous poly(ethylene-terephthalate) at elongation ratios of up to 4 (26). This is quite surprising as the number of random links was calculated to be 5, making it fall well outside of the $N^{1/2}$ limit. This orientation theory has recently been extended by Nobbs and Bower for application to deformations where $\lambda > N^{1/2}$ (29).

Another approach to the relationship between elongation ratio and infrared dichroism is that of Marrinan (30). The derivation of this relationship is not within the scope of this work, however, the resulting equation which relates the dichroic ratio to the elongation ratio is

$$D = \frac{Z + \frac{2}{5}(\cos^2\alpha - \frac{1}{2} \sin^2\alpha)(\lambda^2 - \frac{1}{\lambda})}{Z - \frac{1}{5}(\cos^2\alpha - \frac{1}{2} \sin^2\alpha)(\lambda^2 - \frac{1}{\lambda})} \quad (2.10)$$

where Z is the number of random links and α is the transition moment angle. It is a generalization of the derivation of Stein which was specific to transitions having an angle of 90° to the chain axis (13).

In this chapter the method of infrared dichroism is used to characterize orientation in a crystalline urethane model compound and in a deformed model polyurethane elastomer. The model compound is *N*-phenyl urethane which crystallizes from the melt into a highly oriented spherulitic structure. Characterization of vibrational absorptions of two hydrogen bonded substituents is used to determine the relative orientation of their transition moment angles. The polyurethane elastomer has a monodispersed hard segment and a polybutadiene soft segment. Infrared dichroism is used to determine the transition moment angle of the 1,2 vinyl substituent of the soft segment as this has not been previously reported. The number of random links in the soft segment domain has been determined using the relationship of Marrinan.

Experimental

Data Collection

Infrared spectra were collected on an International Business Machine model IR-98 Fourier transform infrared spectrometer. The

spectral resolution used in these studies is 2 cm^{-1} and the spectral range is from 4000 cm^{-1} to 400 cm^{-1} . Each spectrum is the average of 100 co-added interferograms. The interferogram is Fourier transformed, ratioed with a background spectrum, and stored as absorbance units on a magnetic disc. The source light was polarized using a Perkin Elmer wire grid polarizer with a AgBr substrate. A computer controlled polarizer rotating device developed in this laboratory was used to automatically position the polarizer at angles of 0° and 90° relative to the sample deformation axis. Computer programs written in Pascal have been developed to facilitate the calculation of relative peak areas and dichroic ratios for each pair of spectra in the deformation series. These are listed in Appendix A.

Synthesis of N-Phenyl Urethane

The model compound N-phenylurethane (NPU) (Figure 2.2) was prepared by a one step solution synthesis involving the reaction of phenylisocyanate with ethanol. The apparatus used was a 100 ml three neck round bottom flask fitted with a condenser, nitrogen inlet tube, and magnetic stirrer. To the purged flask were added 50 mls of absolute ethanol and 5 g (0.042 moles) of phenyl isocyanate.

The reaction mixture was stirred and heated to reflux for 2 hours. Completion of the reaction was determined using infrared spectroscopy to monitor the disappearance of the NCO band at 2267 cm^{-1} . The excess methanol was removed with a rotary evaporator. After standing at room temperature for 2 hours the compound crystallized and the yield was

FIGURE 2.2: Molecular structure of N-phenyl urethane NPU.

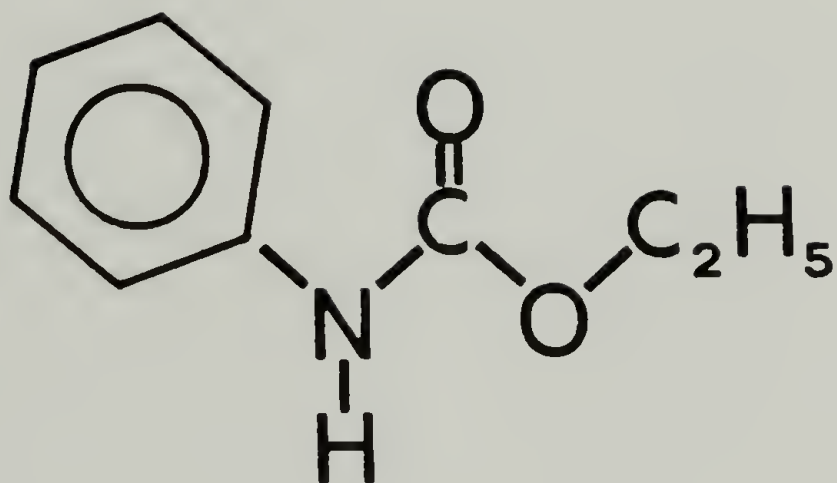


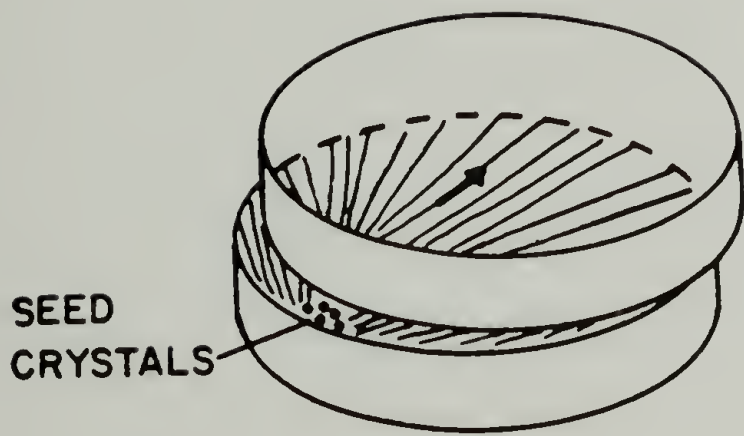
Figure 2.2

determined to be 100%. The compound had a slight yellowish color and was purified by vacuum distillation at 230°C, 10 mm. The purified NPU had a melting point of 53°C.

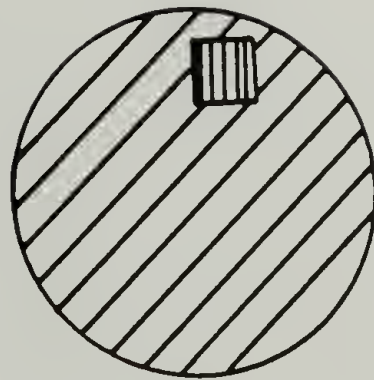
Sample Preparation

The NPU sample used for infrared spectroscopy was prepared in a manner so as to create a highly oriented crystalline structure. Several milligrams of NPU were placed between two polished KBr windows. This was then heated to 75°C to melt the compound. The NPU flowed between the plates to create a meniscus with a thickness of approximately 8 μm . The sample was then cooled slowly on an aluminum block with the temperature being monitored by a copper-constantin thermocouple. As the temperature reached 53°C (the melting point of the compound) several crystals of NPU were placed in contact with the melt to seed nucleation. The NPU began to crystallize with radial growth from the seed point. Growth occurred at a constant rate of 2 mm/minute. Since spontaneous nucleation did not occur at other locations in the sample, the result was a single truncated spherulite with a radius of 2.3 cm (Figure 2.3a). So that polarized infrared spectra could be collected from a region of specific orientation, the sample was masked with aluminum foil with a 2 mm window left at the outer edge of the spherulite (Figure 2.3b). Infrared spectra of the window region were collected with the radiation polarized both parallel and perpendicular to the radial growth vector.

FIGURE 2.3: Schematic of NPU between KBr plates.
a. Nucleated spherulitic crystal.
b. Positioning of window for infrared collection.



A



B

WINDOW REGION IN FOIL MASK

Figure 2.3

Preparation of Polyurethane Elastomer for Uniaxial Deformation Study

The polyurethane elastomer used for the uniaxial orientation study had a polybutadiene soft segment and a hard segment of 2,4-toluene diisocyanate chain extended with butanediol. The polybutadiene prepolymer had a molecular weight of 2200 and a polydispersity of 1.2. The hard segment was monodispersed and contained 5 TDI units and 4 butanediol units (Figure 2.4). The synthesis of the hard segments was by sequential blocking-deblocking reactions described in a recent publication (31). The film used in the deformation experiment was prepared by solvent casting from a 10% tetrahydrofuran (THF) solution onto urethane grade release paper (Brown paper Co. #5337). Approximately 0.5 mls of solution was placed near the edge of the release paper. A glass rod was used to spread the solution with spacers holding the rod at a constant height of 0.15 mm. The solvent was allowed to evaporate in air for 20 minutes and the sample was then vacuum dried at ambient temperature for 24 hours. Removal of the film is facilitated using a tagboard retaining frame to maintain the initial sample geometry. The retaining frame is necessary to prevent damage to the sample during handling and mounting in the deformation apparatus. The mechanical stretcher used in this experiment is manually operated and was designed so as to symmetrically deform the sample about the central position of the infrared beam. Polarized infrared spectra were collected after each strain increment of 10%.

The instrumentation, data collection parameters, and film casting procedure described previously are also applicable to the investiga-

FIGURE 2.4: Structure of monodispersed polyurethane T5MD.

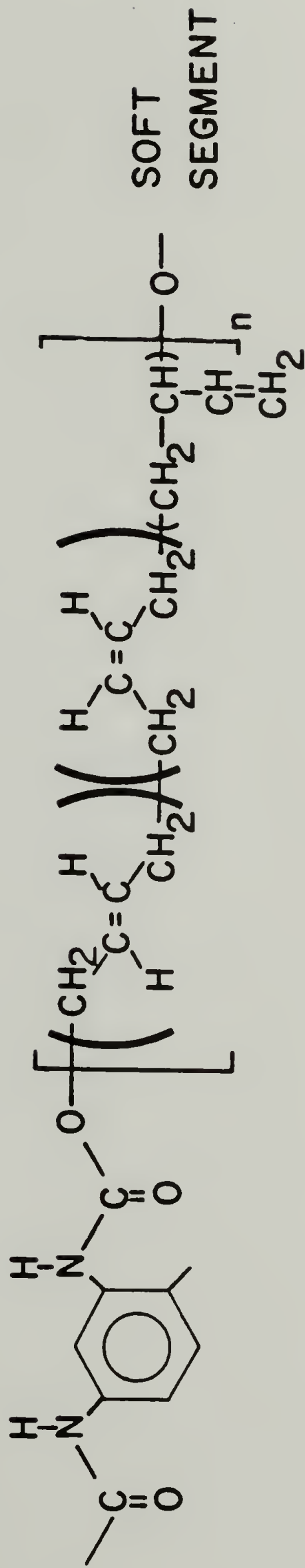


Figure 2.4

tions of Chapters III and VI. The details are presented in this chapter only so as to avoid redundancy throughout the manuscript.

Results and Discussion

Molecular Orientation of N-Phenyl Urethane with Spherulitic Structure

Polarized infrared spectra of N-phenyl urethane (NPU) collected through the window region depicted in Figure 2.3 are shown in Figures 2.5a-c. Most of the absorption bands in this spectrum exhibit strong dichroism, indicating a highly oriented structure. Several absorptions which are characteristic of the urethane linkage are listed in Table 2.1.

For the characterization of molecular orientation it is necessary to choose vibrations which are well characterized and are of known geometry. The N-H and carbonyl stretching vibrations are two modes which have been used extensively in the characterization of hard segment orientation for segmented polyurethane elastomers. These absorptions will be utilized in the hard segment orientation studies of subsequent chapters.

The dichroic ratios (Table 2.1) of both the N-H and carbonyl vibrations indicate that the transition moments of these vibrations are parallel to the crystal growth axis. These vibrations are both shifted to a lower frequency than the fundamental, indicating that they are hydrogen bonded (32,22). It has been reported in the literature that NPU exists with the urethane linkage in the trans conformation (34).

FIGURE 2.5: Infrared spectrum of NPU
a. 3600 - 2600 cm^{-1}
b. 1800 - 1000 cm^{-1}
c. 1000 - 400 cm^{-1}

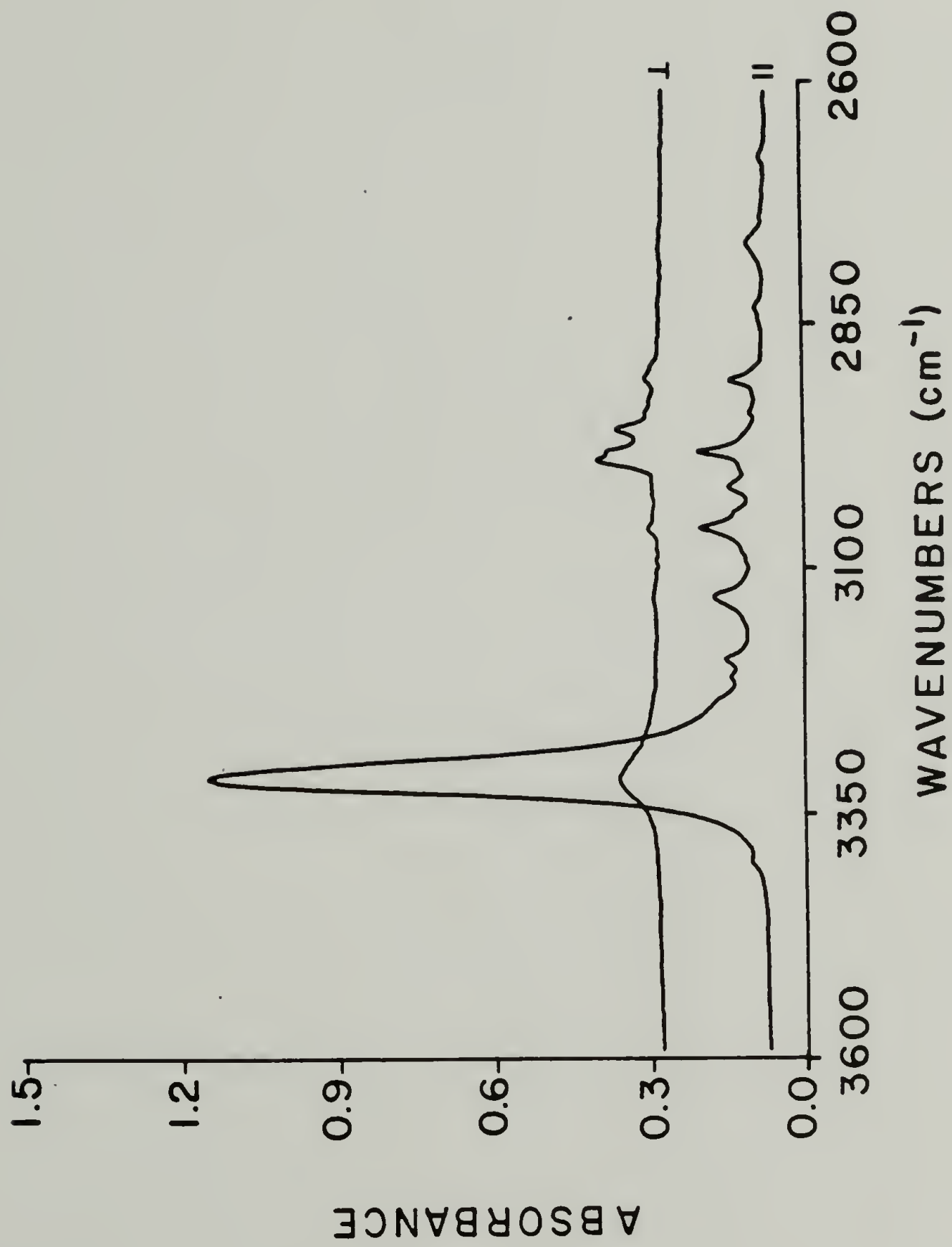


Figure 2.5a

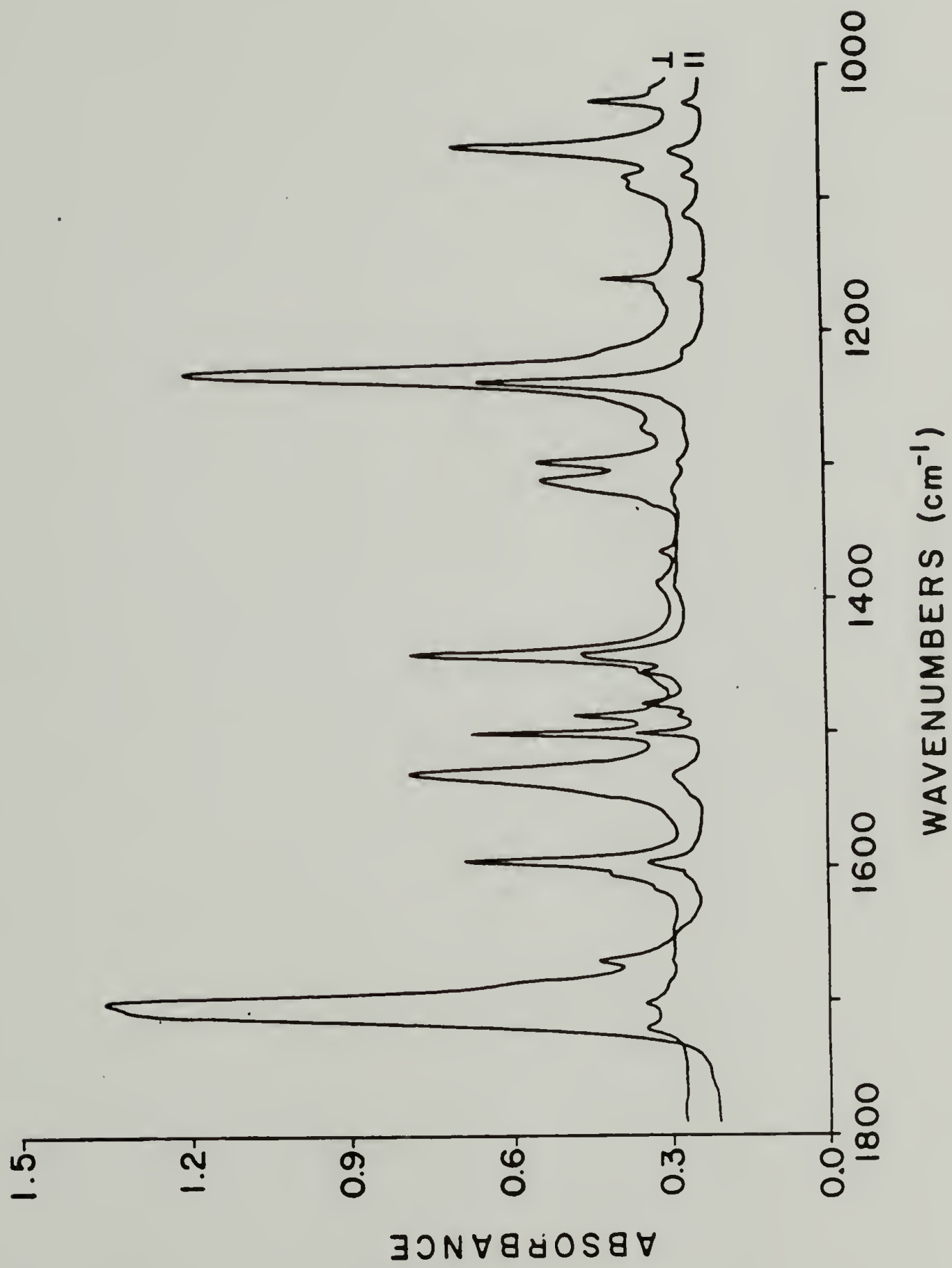


Figure 2.5b

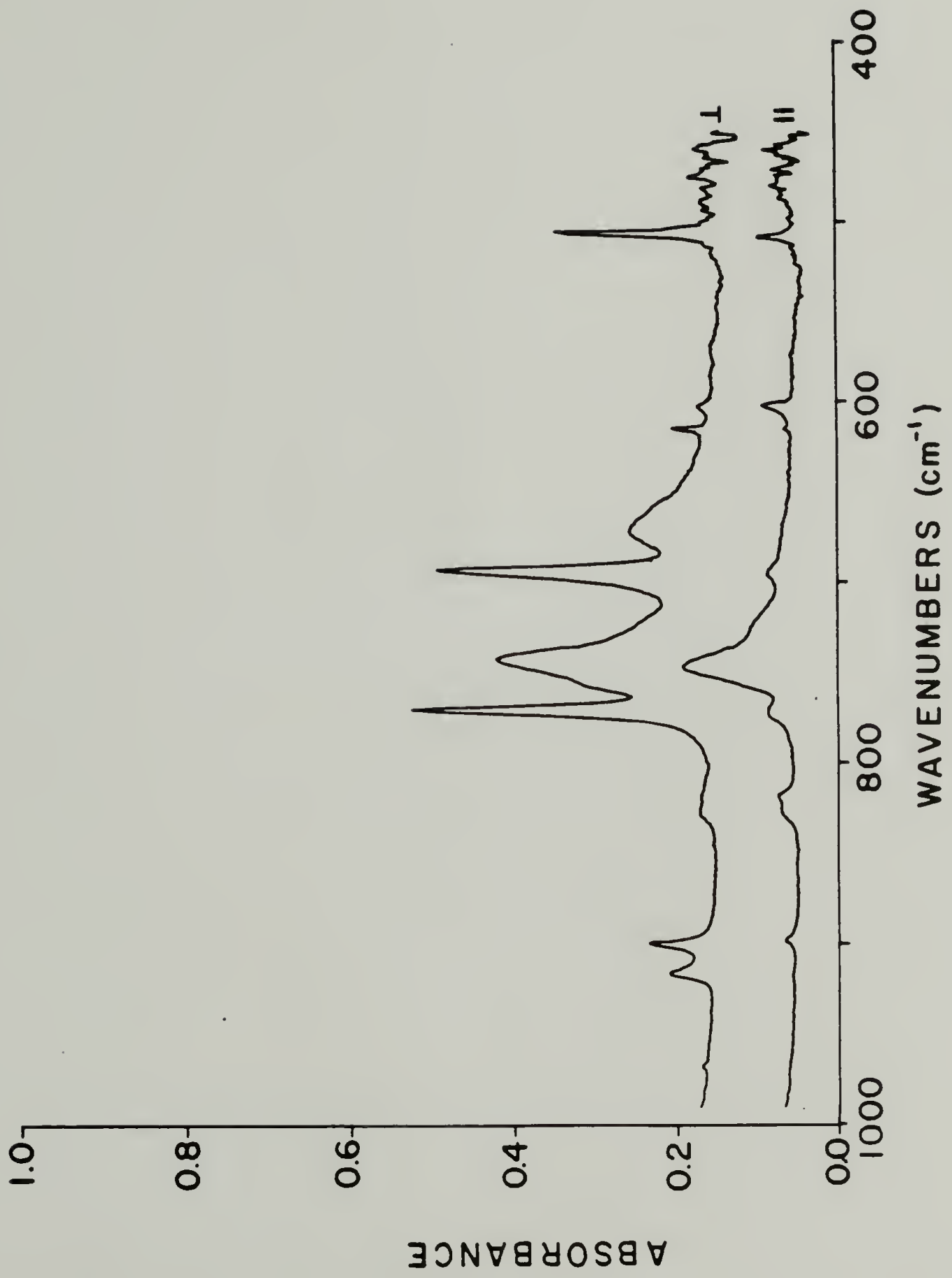


Figure 2.5c

TABLE 2.1

Band Assignments for Urethane Linkage of NPU

Frequency	Assignment ^a	Dichroic Ratio
3398	$\nu(\text{N-H})$ free	—
3316	$\nu(\text{N-H})$ H-bonded	17
1703	$\nu(\text{C=O})$ H-bonded	18
1533	$\sigma(\text{N-H}) + \nu(\text{C-N})$	0.11
1237	$\sigma(\text{N-H}) + \nu(\text{C-N})$	—
1066	$\nu(\text{C-O-C})$ in $\begin{array}{c} \text{C} \\ \parallel \\ \text{C-O-C} \end{array}$	0.15
772	$\lambda(-\overset{\text{C}}{\parallel}\text{C}-\text{O})$	0.053

^a ν = stretching

σ = in plane bending

λ = out of plane bending

In consideration of this it is likely that molecular organization in the crystalline phase is similar to the model depicted in Figure 2.6. This would allow both the N-H and carbonyl groups to be hydrogen bonded while maintaining the trans conformation.

The dichroic ratios of the N-H and carbonyl vibrations, 17 and 18 respectively, are considerably less than the infinite value that would be expected for a perfectly oriented sample if the transition moment angles are at zero degrees with respect to the crystalline growth axis. This indicates that either orientation is not perfect or the transition moment angles are greater than zero degrees. A maximum value for the transition moment angles may be calculated using Equation 2.3 and the perfect orientation assumption. This results in a value of 18.9° for the N-H vibration and 18.4° for the carbonyl. From this example the limitation of only knowing the second moment of an orientation distribution is demonstrated. A more complete characterization of the orientation distribution is necessary to determine if imperfect orientation or non zero transition moment angles are responsible for the low value of the dichroic ratio.

Characterization of Segmented Orientation of a Uniaxially Strained Polyurethane Elastomer

The unpolarized infrared spectrum of the polyurethane investigated in this section is shown in Figure 2.7. Several absorptions have been found to be useful for characterizing segmental orientation in this system. The N-H stretching and carbonyl absorptions at 3320 cm^{-1} and

FIGURE 2.6: Orientation of NPU relative to crystalline growth axis.

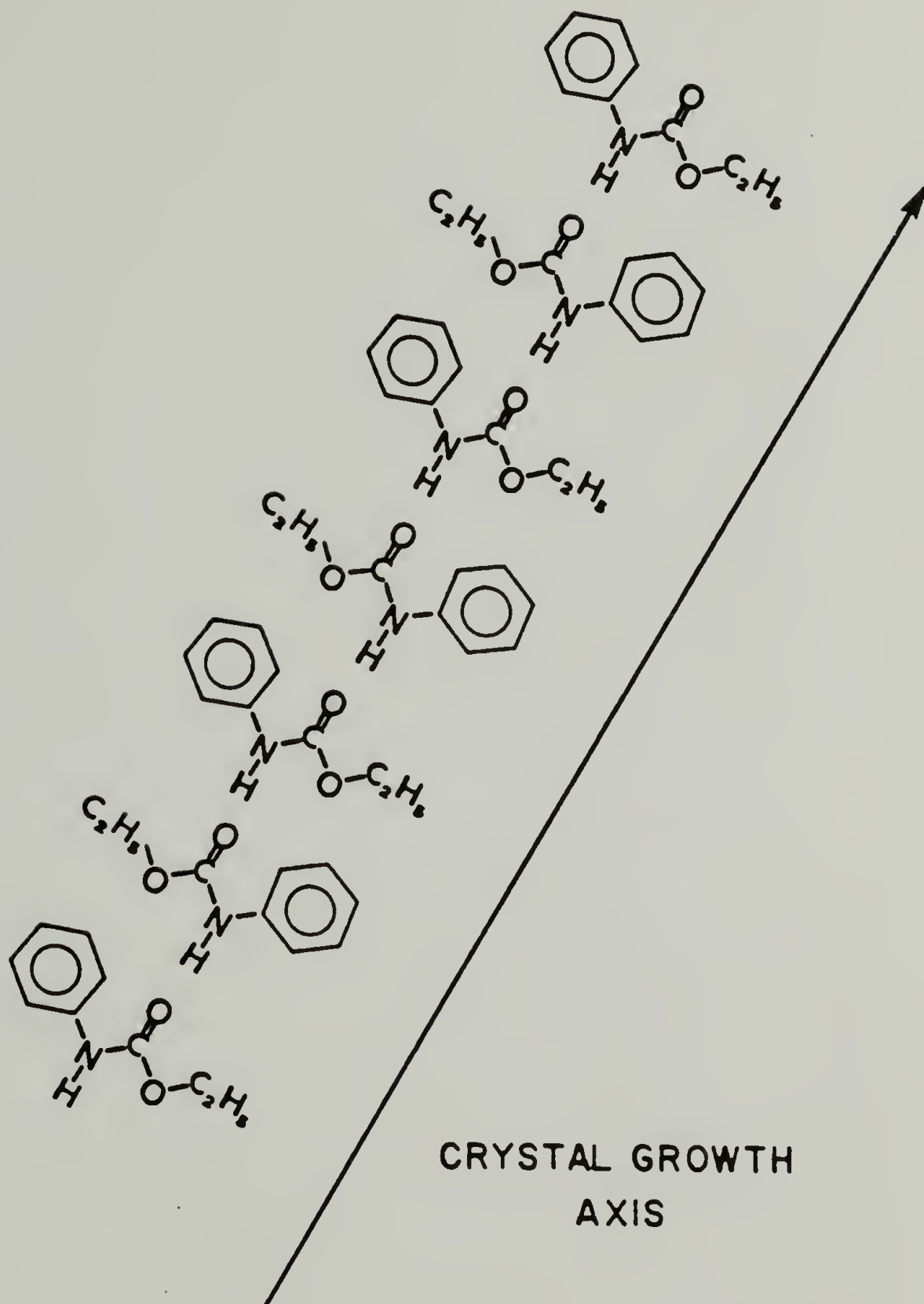


Figure 2.6

FIGURE 2.7: Infrared survey spectrum of T5MD.

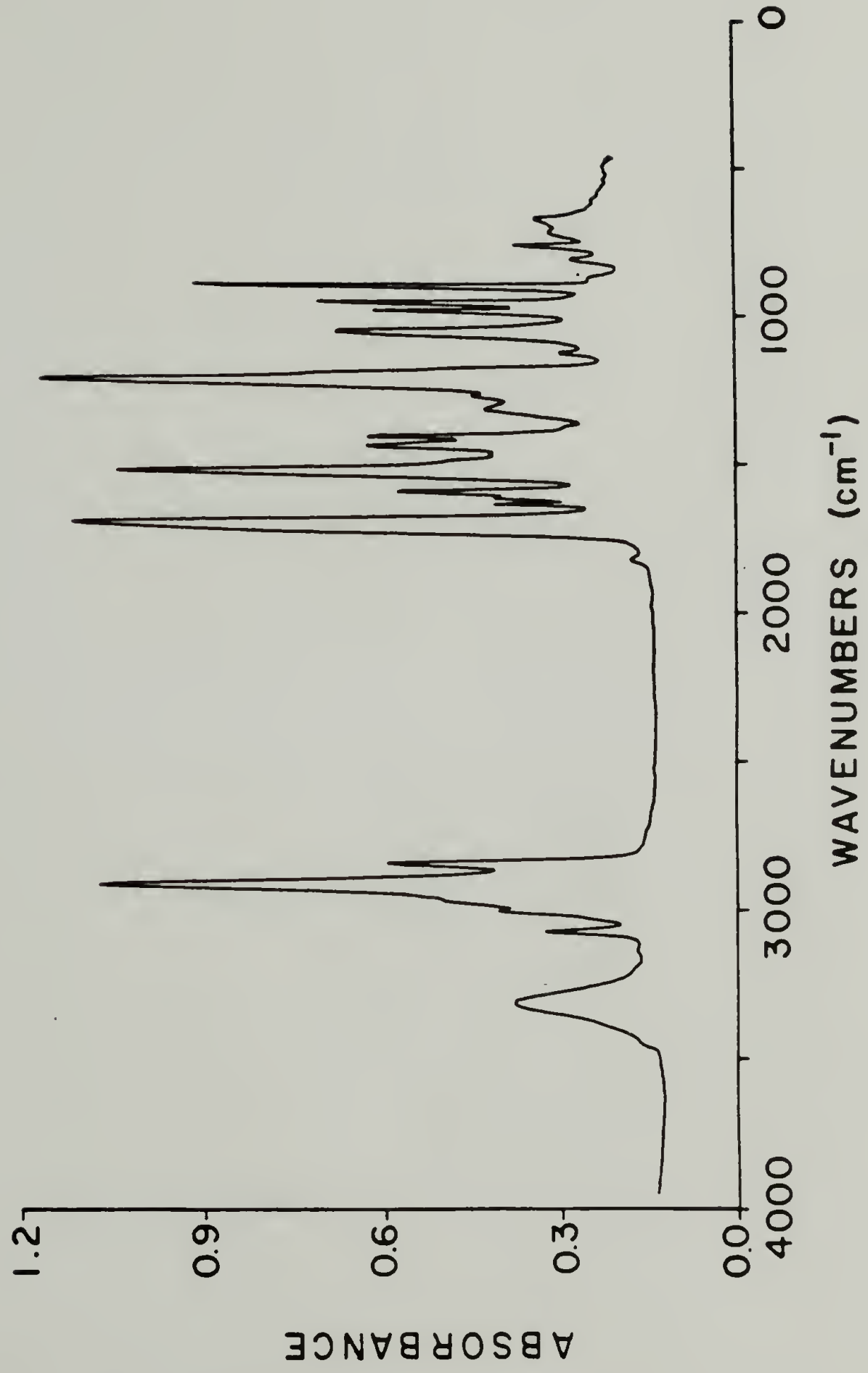


Figure 2.7

1710 cm^{-1} respectively are characteristic of the TDI-BDO hard segment and the 1,4 trans and 1,2 vinyl C-H out of plane deformations at 965 cm^{-1} and 910 cm^{-1} are characteristic of the polybutadiene soft segment. Although these two polybutadiene vibrations have been previously used to calculate isomer fractions, the author is unaware of any reports where they have been used to calculate segmental orientation functions.

The dichroic ratios of these characteristic vibrations are shown in Figure 2.8a and 2.8b as a function of sample strain. The vibrations corresponding to the soft segment have a dichroic ratio that is dependent on strain while those corresponding to the hard segment are relatively independent of applied strain. This is consistent with the fact that the sample has no permanent set (plastic deformation) at strains up to 100%. The dichroic ratio of the 1,2 vinyl band increases as a function of strain and has a transition moment in the parallel direction relative to the chain axis while that of the 1,4 trans deformation decreases as a function of strain indicating that it is a perpendicular vibration. The 1,2 vinyl group is a pendant group on the butadiene chain making it an unlikely substituent for characterizing chain orientation. One might expect that rotational freedom would result in a transition moment that is not well defined. However, examination of a space filling model of this structure determined that the rotation of the vinyl substituent is sterically hindered by the adjacent hydrogen atoms. A photograph of this model along with the schematic representation is shown in Figure 2.9. Steric interference of the adjacent atoms causes the vinyl group to be

FIGURE 2.8: Dichroic ratio of T4MD as a function of sample strain
a. Soft segment absorptions (\square : 1,2 vinyl; Δ : 1,4 trans)
b. Hard Segment absorptions (\square : carbonyl; *: N-H stretching)

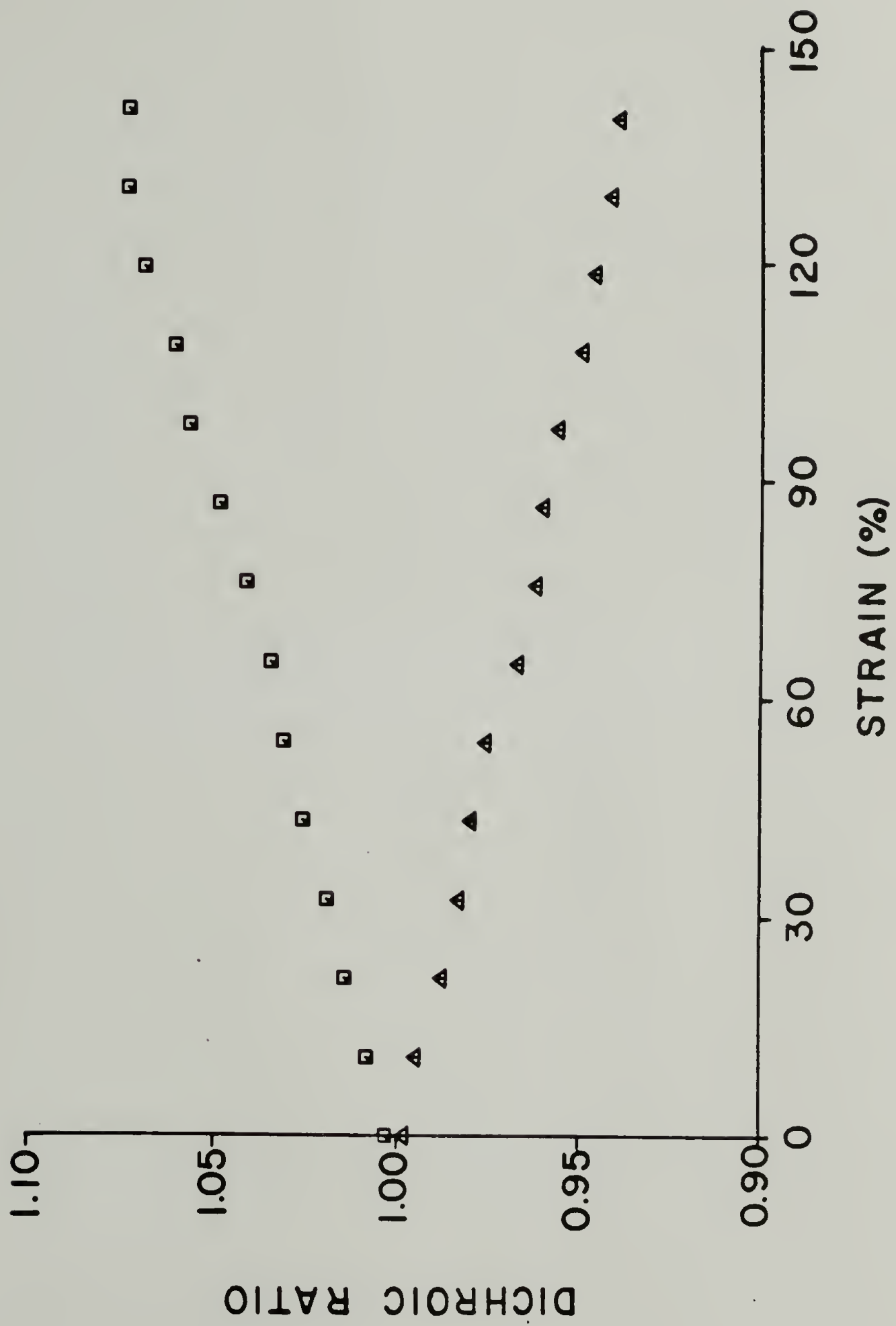


Figure 2.8a

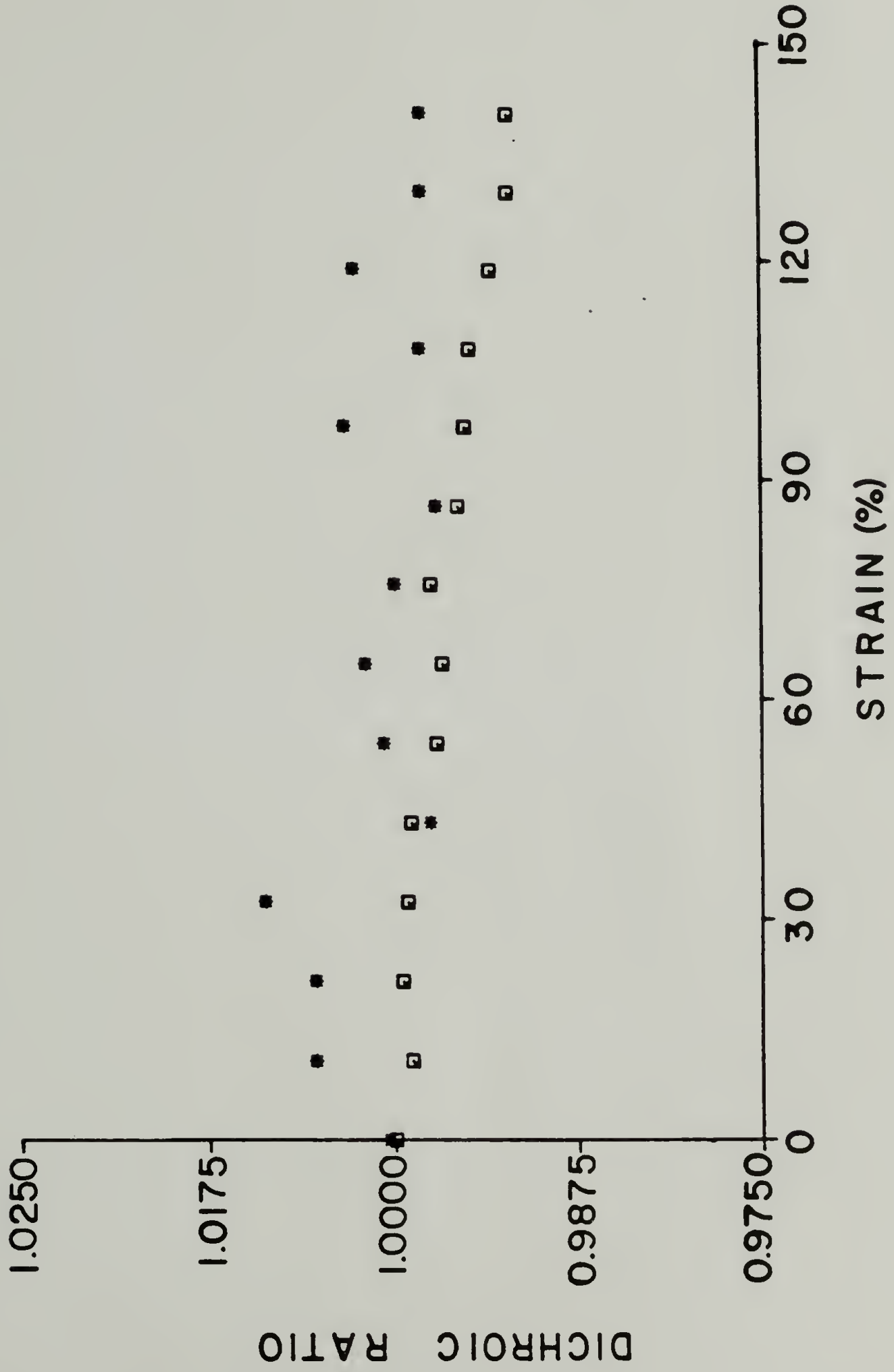


Figure 2.8b

FIGURE 2.9: Model of 1,2 vinyl butadiene linkage showing steric hindrance to rotation.
a. Photograph of space filling model.
b. Schematic representation.

A)



B)

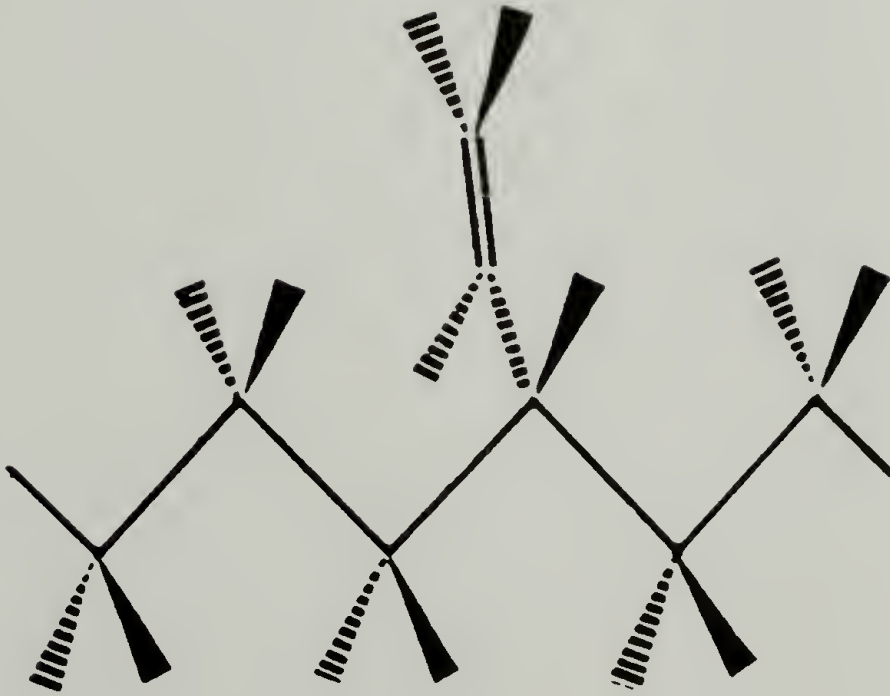


Figure 2.9

locked in one of two rotational isomeric states. In each of these potential minima the 1,2 vinyl C-H out of plane deformation has a parallel transition moment with respect to the chain axis.

A value for the transition moment angle of the 1,2 vinyl group may be determined using the transition moment of the 1,4 trans vibration which may be directly interpreted from the geometry of this group. Since the transition moment of the vinyl group is dependent on intramolecular interaction it is of particular interest to determine if this value is effected by strain induced conformational changes. In the 1,4 trans configuration the carbon-carbon double bond is part of the chain backbone. Assuming the chain axis lies in the plane of this olefinic linkage it is possible to assign the C-H out of plane vibration as having a transition moment angle of 90° . This is possible by comparing the dichroic ratios of the two vibrations as a function of strain. The value of the chain orientation as defined by Equation 2.2 is determined as the cosine squared average of the angle between the chain axis and deformation axis. This value should depend only on the sample strain. Therefore, orientation functions calculated using Equation 2.3 should be the same using the 1,2 vinyl data or the 1,4 trans data. This leads to the equality of Equation 2.11,

$$\frac{D_{OV+2}}{D_{OV-1}} \cdot \frac{D_V(S)-1}{D_T(S)+2} = \frac{D_{OT+2}}{D_{OT-1}} \cdot \frac{D_T(S)-1}{D_T(S)+2} \quad (2.11)$$

which may be arranged to give

$$\frac{D_V(S)-1}{D_T(S)+2} \cdot \frac{D_T(S)-1}{D_T(S)+2} = \frac{D_{OT+2}}{D_{OT-1}} \cdot \frac{D_{OV+2}}{D_{OV-1}} \quad (2.12)$$

where the subscripts V and T refer to values associated with the 1,2

vinyl or 1,4 trans configurations and S is the strain of the sample. As can be seen from the right side of Equation 2.12, this relationship is a constant value and is independent of strain. The quotient on the left is designated as $Q(S)$ and is plotted as a function of strain in Figure 2.10. This quotient is independent of strain and has a value of -1.15. The scattered points at low values of strain are due to division of values that are close to zero. Using Equation 2.5 and a value of 90° for the transition moment angle of the 1,4 trans vibration, it is possible to calculate a value for the transition moment of the vinyl group. This angle is calculated to be 31° with respect to the backbone axis of the chain. It represents an average value as the pendant group has limited rotational freedom.

Calculation of Random Links in Polybutadiene Soft Segment

The flexibility of the polybutadiene soft segment may be interpreted in terms of the number of random links, Z , using the relationship of Marrinan (Equation 2.10)

$$D = \frac{Z + \frac{2}{5}(\cos^2\alpha - \frac{1}{2} \sin^2\alpha)(\lambda^2 - \frac{1}{\lambda})}{Z - \frac{1}{5}(\cos^2\alpha - \frac{1}{2} \sin^2\alpha)(\lambda^2 - \frac{1}{\lambda})}$$

The number of random links may be determined if it is the only adjustable parameter in plotting a curve of the dichroic ratio as a function of the elongation ratio λ . However, the values used for λ must correspond to the strain of the soft segment phase rather than the

FIGURE 2.10: Ratio of equation 2.6, $Q(s)$ plotted as a function of strain for T5MD.

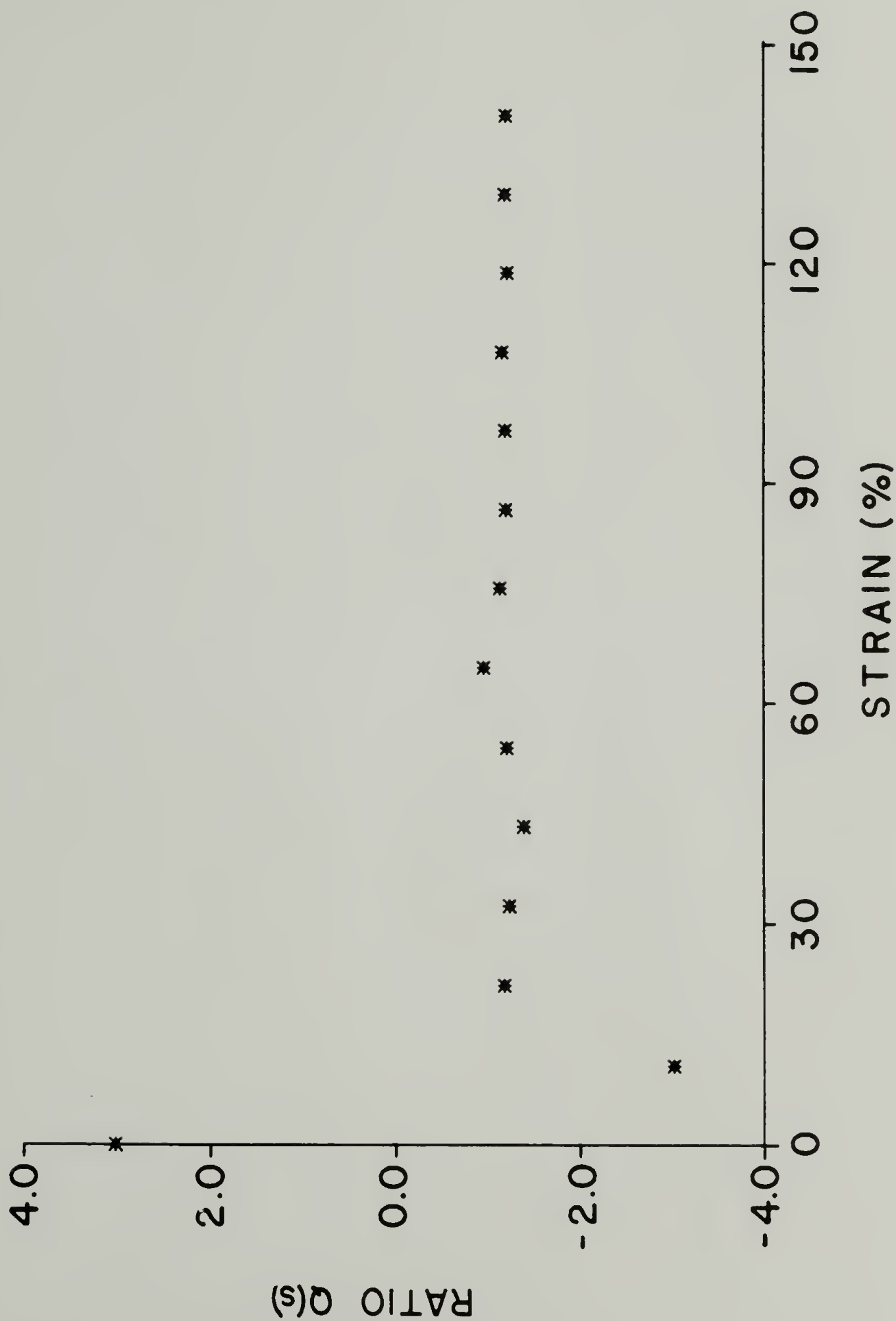


Figure 2.10

measured sample strain. A corrected elongation ratio may be calculated for the soft segment by considering the hard segment domains as spherical filler particles. As indicated in Figure 2.8, the hard segment phase shows no orientation, indicating that these domains are unaffected by sample strain. Also, in previous studies of this system, electron micrographs indicate a hard segment phase that has an elongated spherical morphology (35).

Smallwood has calculated that for systems with spherical filler particles at low concentrations the matrix strain ϵ may be interpreted in terms of the sample strain ϵ_0 by Equation 2.13,

$$\epsilon = \epsilon_0(1 + 2.5c) \quad (2.13)$$

where c is the volume fraction of filler (36). However, this equation is only valid for values of c below 0.1. Although no account was taken for interaction between neighboring filler particles in this equation, an extension by Guth and Gold included this, resulting in Equation 2.14 (37)

$$\epsilon = \epsilon_0(1 + 2.5c + 14.1c^2) \quad (2.14)$$

Guth found that this equation held true for systems filled to a volume fraction of 0.3. The polyurethane system investigated in this chapter has a hard segment volume fraction of 0.28. While several assumptions must be made in the applicability of this equation, it should result in calculated values for the soft segment strain that are closer to the true value than if no correction was made.

In Figure 2.11 the dichroic ratio of the 1,2 vinyl band is plotted as a function of the corrected elongation ratio. The continuous line is the theoretical value as determined by Equation 2.4 with a value for α_{vinyl} of 31° and Z equal to 19. The polybutadiene prepolymer used in the preparation of this polymer has a molecular weight of 2200. This corresponds to 40 butadiene units. Considering that 65% of the butadiene units are in the 1,2 vinyl configuration, the number of chain atoms between hard segments is ~ 110 . Therefore, the number of carbon atoms in a random link is 6. This agrees quite well with the value of 7 that was calculated by Kuhn for polyethylene.

FIGURE 2.11: Dichroic ratio for 1,2 vinyl absorption as a function of estimated soft segment strain. (*: experimental values; —: using theory of Marrinan with $Z=19$).

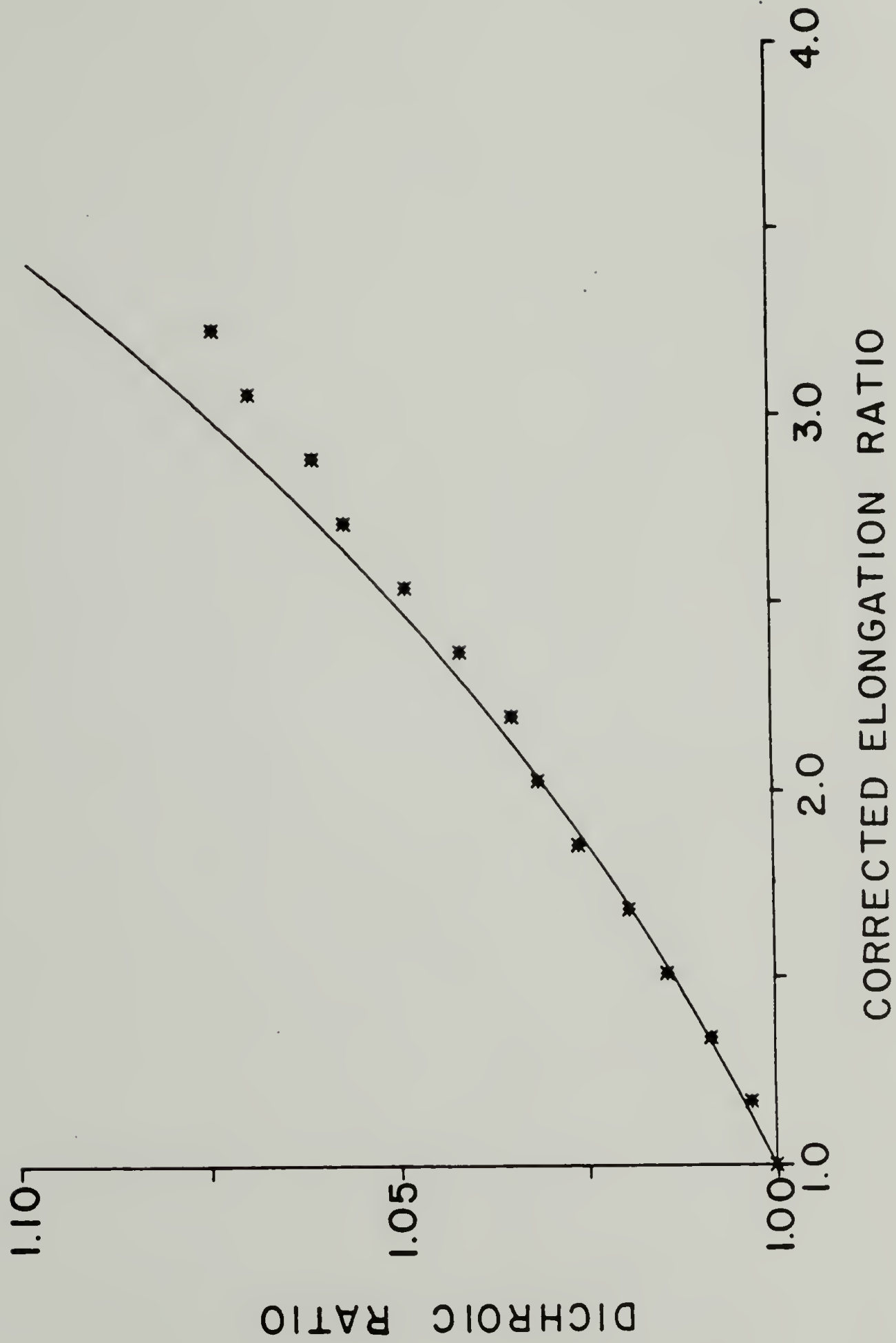


Figure 2.11

References

1. G.L. Wilkes, "Rheo-Optical Methods and Their Application to Polymeric Solids", J. Macromol. Sci.-Revs. Macromol. Chem., C10(2), 149 (1974).
2. R.S. Stein, M.B. Rhodes, P.R. Wilson, and S.N. Stidham, "Optical Studies of the Morphological Changes in Deforming Polyolefins", Pure Appl. Chem., 4, 219 (1962).
3. R.S. Stein, "The Scattering of Light by Heterogeneities in Crystalline Polymeric Solids", reprinted from I.C.E.S., Pergamon Press, 5, 439 (1963).
4. R.S. Stein and M.B. Rhodes, "Photographic Light Scattering by Polyethylene Films, J. Appl. Phys., 31, 1873 (1960).
5. R.S. Stein, "The X-Ray Diffraction, Birefringence, and Infrared Dichroism of Stretched Polyethylene. II. Generalized Uniaxial Crystal Orientation", J. Polym. Sci., 31, 327 (1958).
6. B. Cviki, D. Moroi, and W. Frankin, "Form Birefringence of Some Smectic Liquid Crystals", Mol. Cryst. and Liq. Cryst., 12, 267 (1971).
7. J. Purris and D.I. Bower, "Molecular Orientation in Poly(ethylene Terephthalate) by Means of Laser-Raman Spectroscopy", J. Polym. Sci., Polym. Phys. Ed., 14, 1461 (1976).
8. M.E. Robinson, D.I. Bower, and W.F. Maddams, "Molecular Orientation in Poly(vinyl chloride) Studied by Raman Spectroscopy and Birefringence Measurements", J. Polym. Sci., Polym. Phys. Ed., 16, 2115 (1978).

9. B. Jasse and J.L. Koenig, "Orientation Measurements in Polymers Using Vibrational Spectroscopy", *J. Macromol. Sci.-Rev. Macromol. Chem.*, C17(1), 61 (1979).
10. R.D.B. Fraser, "The Interpretation of Infrared Dichroism in Fibrous Protein Structures", *J. Chem. Phys.*, 21(9), 1511 (1953).
11. R.D.B. Fraser, "Interpretation of Infrared Dichroism in Fibrous Proteins in the 2 μ m Region", *J. Chem. Phys.*, 24(1), 89 (1956).
12. R.D.B. Fraser, "Interpretation of Infrared Dichroism in Axially Oriented Polymers", *J. Chem. Phys.*, 28,(6),1113 (1958).
13. R.S. Stein, "Determination of the Stiffness of the Chain of a Rubber Like Polymer", *J. Polym. Sci.*, 28, 83 (1958).
14. S. Onogi and T. Asada, "Rheo-Optical Studies of High Polymers. IX. A Study of Deformation Process of Low Density Polyethylene by Simultaneous Measurements of Stress, Strain, and Infrared Absorption", *J. Polym. Sci., Part C*, 16, 1445 (1967).
15. B.E. Read and D.A. Hughes, "Stress-Dichroism Studies of the 4.92 μ m Band of Amorphous Crosslinked Polyethylene," *Polymer*, 13, 495 (1972).
16. R.W. Seymour, A.E. Allegrezza, and S.L. Cooper, "Segmental Orientation Studies of Block Polymers. I. Hydrogen-Bonded Polyurethanes", *Macromol.*, 6(6), 896 (1973).
17. R.J. Samuels, "Infrared Dichroism, Molecular Structure, and Deformation Mechanisms of Isotactic Polypropylene", *Die Makromol. Chemie, Supp.* 4, 241 (1981).

18. H.W. Siesler, "Rheo-Optical Fourier Transform Infrared Spectroscopy of Polyurethane Elastomers. 1. Principle of the Method and Measurements at Ambient Temperatures", *Polym. Bull.*, 9, 382 (1983).
19. D.J. Burchell, J.E. Lasch, E. Dobrovolny, N. Page, J. Domian, R.J. Farris, and S.L. Hsu, "Deformation Studies of Polymers by Fourier Transform Infrared Spectroscopy II: Mechanical Stretcher and its Interface to the Spectrometer", *Appl. Spectr.* 38, 343 (1984).
20. P.H. Hermans and P. Platzek, "The Deformation Mechanism and Fine Structure of Hydrate Cellulose IX. The Theoretical Relation Between Anisotropy and the Characteristic Double Refraction of Oriented Polymers", *Kolloid Z.*, 88, 69 (1939).
21. R.J. Roe and W.R. Krigbaum, "Orientation Distribution Function of Statistical Segments in Deformed Polymer Networks", *J. Appl. Phys.*, 35, 2215 (1964).
22. O. Kratky, "Deformation Mechanism of Fibrous Substances", *Kolloid Z.*, 64, 21 (1933).
23. W. Kuhn and F. Grun, "Single Chain Molecules and Statistical Behavior of Assemblies Consisting of Chain Molecules", *Kolloid Z.*, 101, 248 (1942).
24. I.M. Ward, Mechanical Properties of Solid Polymers, Wiley, London (1971).
25. K. Baba and R.S. Stein, "Rheo-Optical and Mechanical Studies of the Crystallization and Orientation of Ethylene-Propylene Copolymers", to be published.

26. A. Cunningham, I.M. Ward, H.A. Willis, and Veronica Zichy, "An Infrared Spectroscopic Study of Molecular Orientation and Conformational Changes in Poly(ethylene terephthalate)", *Polymer* 15, 749 (1974).
27. P.J. Flory, "Statistical Thermodynamics of Random Networks", *Proc. R. Soc. Lond. A* 351, 351 (1976).
28. H.M. James, "Statistical Properties of Networks of Flexible Chains", *J. Chem. Phys.*, 15(9), 651 (1947).
29. J.H. Nobbs and D.I. Bower, "Orientation Averages for Drawn Rubber Networks", *Polymer*, 19, 1100 (1978).
30. H.J. Marrinan, "The Infrared Dichroism of a Stretched Polymer. Part I. The Theoretical Treatment of Rubberlike Polymers", *J. Polym. Sci.*, 39, 461 (1959).
31. B. Fu, C. Feger, and W.J. MacKnight, "Synthesis and Properties of Monodisperse Hydroxy-Terminated Oligomers of 1,4-Butanediol and 2,4-Toluene Diisocyanate", *Polym. Sci. and Eng.*, in press.
32. Y.M. Boyarchuk, L.Y. Rappoport, V.N. Nikitin, and N.P. Apukhtina, "A Study in Hydrogen Bonding in Urethane Elastomers by Infrared Spectroscopy", *Vysokomol. Soyed.*, 7(5), 778 (1965).
33. T. Tanaka, T. Yokoyama, and Y. Yamaguchi, "Quantitative Study of Hydrogen Bonding Between Urethane Compound and Ethers by Infrared Spectroscopy", *J. Polym Sci.*, A-1, 6, 2137 (1968).
34. C.N. Rao, K.G. Rao, A. Goel, and D. Balasubramanian, "Configuration of Secondary Amides and Thioamides: Spectroscopic and Theoretical Studies," *J. Chem. Soc. (A)*, 3077 (1971).

35. C. Chen-Tsai, "Morphology Studies on Amorphous Segmented Polyurethanes", Ph.D. Dissertation, University of Massachusetts, 1984.
36. H.M. Smallwood, "Limiting Law of the Reinforcement of Rubber", J. Appl. Phys., 15, 758 (1944).
37. E. Guth, "Theory of Filler Reinforcement", J. Appl. Phys., 16, 20 (1945).

C H A P T E R I I I

INFRARED CHARACTERIZATION OF MICROSTRUCTURAL ORDERING IN A POLYBUTADIENE BASED POLYURETHANE PREPARED WITH MIXED ISOMER TOLUENE DIISOCYANATE

Introduction

It is well known that segmented polyurethane elastomers have an extended rubbery plateau in their modulus-temperature curve which is due to the physical crosslinking of the hard segment phase. The integrity of the hard segment phase and corresponding strength of the physical crosslinking is a function of several aspects of the polymer microstructure. The degree of phase separation and extent of microstructural ordering of the hard phase play an important role in the development of superior mechanical properties. Phase separation is controlled by the thermodynamic incompatibility of the hard and soft segments as well as segmental length and length distribution. The extent of hard segment microstructural ordering is dependent on specific intersegmental interactions and the symmetry of the hard segment structural units (1,2). The hard segment microstructural ordering is of particular importance as semicrystalline hard segment domains tend to have greater integrity and thus superior physical crosslinking as compared to the corresponding amorphous domain (1,3,4). In light of this it is clear that hard segment microstructural characterization is of great importance for developing a concise understanding of polyurethane structure-property correlations.

Fourier transform infrared spectroscopy was chosen as the characterization method for the present investigation of hard segment microstructural ordering as it is a sensitive technique for analyzing intermolecular interactions. Numerous infrared investigations at several laboratories have resulted in the accumulation of an extensive data base for a variety of polyurethanes and model compounds. This facilitates the interpretation of infrared spectroscopic data (5-12). Much of this interest has centered on the analysis of absorption bands corresponding to molecular substituents which are involved in hydrogen bond interactions. In particular are bands corresponding to the vibrational modes of the N-H and carbonyl groups of the urethane linkage of the hard segment and the carbonyl and ether groups of polyester or polyether soft segments. Several changes occur in the N-H and carbonyl stretching vibrations as these substituents become involved in hydrogen bond interactions. The absorption shifts to a lower frequency with a corresponding increase in the half width and intensity. Hydrogen bonding in a crystalline hard segment phase results in frequency shifts that are even greater in magnitude due to the strength of the interaction. An infrared spectroscopic investigation of a model polyurethane system which has a spectrum exhibiting frequency shifts that correspond to an ordered hard segment structure is the focus of this chapter.

The polyurethane is well defined with respect to its chemical structure so as to minimize ambiguities in microstructural interpretations. This system is a polybutadiene based polyurethane with a hard

segment of toluene diisocyanate (TDI), chain extended with butanediol. It is one of a series of polybutadiene polyurethanes synthesized in this laboratory by a solution polymerization process (13). Solution polymerization was chosen because the reaction kinetics in a homogeneous medium result in a polymer system which has a statistical distribution of the lengths of the hard segment sequences. This is in contrast to previous work involving a similar system prepared by the bulk polymerization technique (14). During the bulk polymerization, partial phase separation occurred prior to reaction due to the incompatibility of the reactants, resulting in a bimodal distribution of hard segment sequences (15). The TDI used in the system for this current investigation is a mixture of the 2,4 and 2,6 isomers and is similar to commercial grade TDI used in the manufacturing of polyurethane foams. Previous investigations have shown that polyurethanes prepared with the purified, symmetric 2,6-TDI isomer can have highly crystalline hard segment domains, while those prepared with the 2,4 isomer are completely amorphous (1,2). In consideration of this, the development of an understanding of the crystallization behavior of a system prepared with the mixed isomer TDI is of fundamental and commercial importance.

The objective of this study is to quantitatively characterize the extent of hard segment microstructural ordering in a polyurethane prepared with mixed isomer TDI using infrared spectroscopy. Incorporated in this study is a determination of the effect of the method of sample preparation and thermal history on the extent of order, as well as the influence of solvent plasticization on the ordering process.

Experimental

The sample characterized in this investigation is one of a series of solution polymerized polyurethanes with a polybutadiene soft segment. The hard segment contains TDI (which is a mixture of the 2,4 and 2,6 isomers having an 80:20 mole ratio) chain extended with butanediol. The mole ratio of the 2,4 and 2,6 isomers was determined by infrared spectroscopy using a modification of the method of Corbett (16). The polymerization of this material is done in two steps (Figure 3.1). First the hydroxy terminated polybutadiene prepolymer is reacted in THF with the mixed isomer TDI. After this reaction is complete, butanediol is added as a chain extender to yield the high molecular weight polymer. The mole ratio of polybutadiene:TDI:BD0 is 1:3.3:2.3. This mixed isomer system is referred to as T3MI throughout this chapter. The details of the polymerization of this elastomer have been studied by Bengston (13).

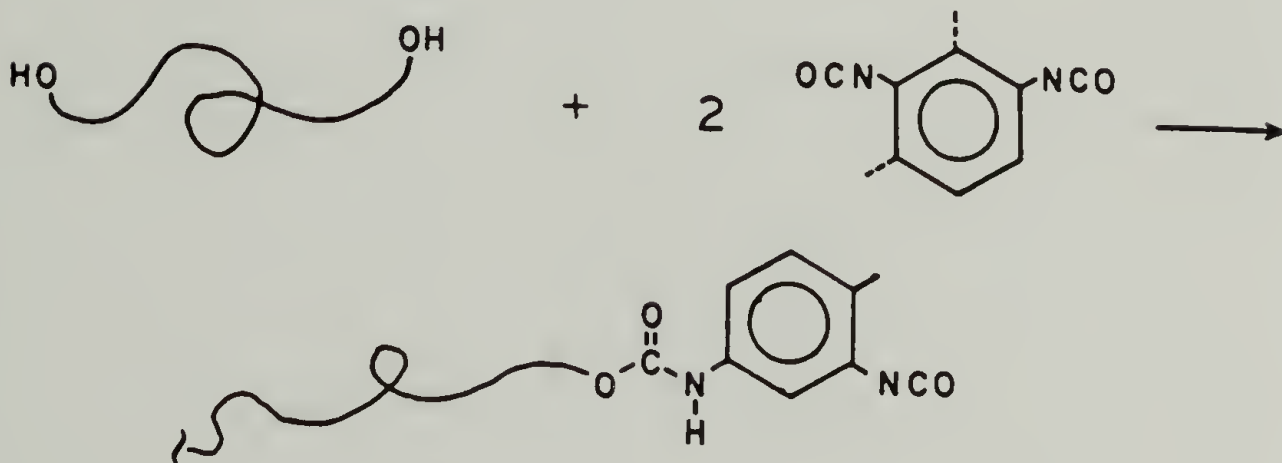
Preparation of Samples

Samples characterized by infrared spectroscopy were prepared as films by casting from a 10% solution in THF. Samples used in the infrared-thermal characterization studies were cast on KBr disks while those used for infrared-deformation and surface characterization were cast on polyurethane grade release paper purchased from Brown Paper Co. (#5337). The solution cast sample was allowed to dry in air at

FIGURE 3.1: Two step reaction sequence used in the synthesis of segmented polyurethane elastomers.

TWO STEP POLYMERIZATION

I. ENDCAPPING OF SOFT SEGMENT



2. CHAIN EXTENSION

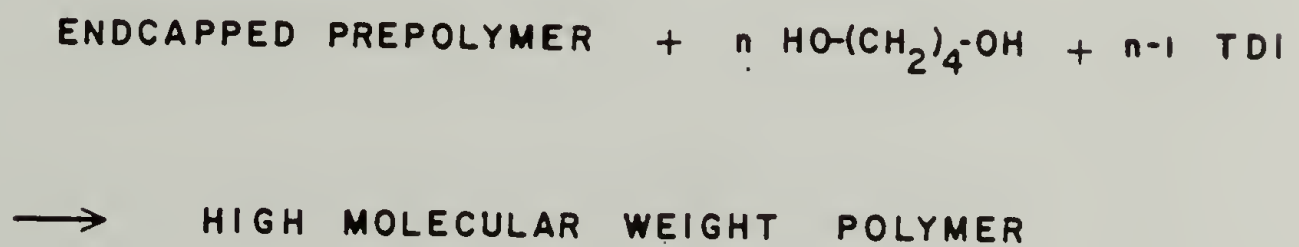


Figure 3.1

ambient temperature for 5 hours, then under vacuum at 25°C for 24 hours. Several samples were prepared under slow evaporation conditions to allow better control of the development of hard segment microstructural ordering. This was accomplished by saturating the atmosphere surrounding the polyurethane solution with THF vapor. The THF was allowed to dissipate slowly and exhausted into a fume hood. After one day the evaporation was complete and the samples were vacuum dried.

Films of the polyurethane copolymer prepared with 2,4 TDI as well as the model hard segment homopolymer prepared with 2,4 TDI were solution cast from THF and vacuum dried. The model hard segment homopolymer prepared with 2,6 TDI was cast from dimethylformamide, DMF, due to the lack of solubility of this polymer in THF. A model compound consisting of one 2,4 TDI residue capped with butanediol at each end was synthesized in a previous investigation and is designated as BTB (17). A film of the low molecular weight model compound was prepared by melting BTB crystals on a KBr disk at 130°C. The liquid was then spread to form a thin film using a heated razor knife.

Infrared Characterization

Infrared characterization was accomplished using an International Business Machines model IR98. Data collection parameters and accessories for collecting polarized spectra of deformed samples have been detailed in the previous chapter. Infrared surface spectra were

collected using a Harrick attenuated total reflectance (ATR) apparatus with a germanium trapezoidal prism. Infrared thermal analysis was facilitated using a variable temperature cell developed in this laboratory. Nitrogen gas of the appropriate temperature passes through a copper cell which is machined to fit a 15 mm KBr disc. The nitrogen gas is first cooled by passing through a copper coil which is submerged in liquid nitrogen. It is then heated to the appropriate temperature with a resistance heating coil which is powered by a Wattlow model 800 temperature controller with a copper-constantin thermocouple feedback system. The thermocouple junction is inserted in a 0.2 mm hole that has been drilled in the KBr disc. This system has a maximum heating rate of 30°C per minute and a maximum cooling rate of 25°C per minute.

Results and Discussion

The infrared spectra of the polybutadiene based polyurethane, T3MI, prepared with TDI which is a mixture of the 2,4 and 2,6 isomers have features which are dependent on the procedure by which the film is prepared. Survey spectra are shown in Figures 3.2 a and b for a sample cast from THF solution and a sample prepared by melt pressing. Distinct differences may be noted in several absorption bands that are characteristic of the TDI-BDO urethane linkage. The greatest difference may be noted in the N-H stretching vibration at 3350 cm^{-1} while more subtle differences may also be noted in the Amide I stretching vibration at 1712 cm^{-1} , the amide II band at 1525 cm^{-1} , and the amide III band at 1227 cm^{-1} . These vibrational absorptions are all sensitive

FIGURE 3.2: Survey spectrum of T3MI. a) prepared by solution casting from THF, b) prepared by melt pressing at 140°C.

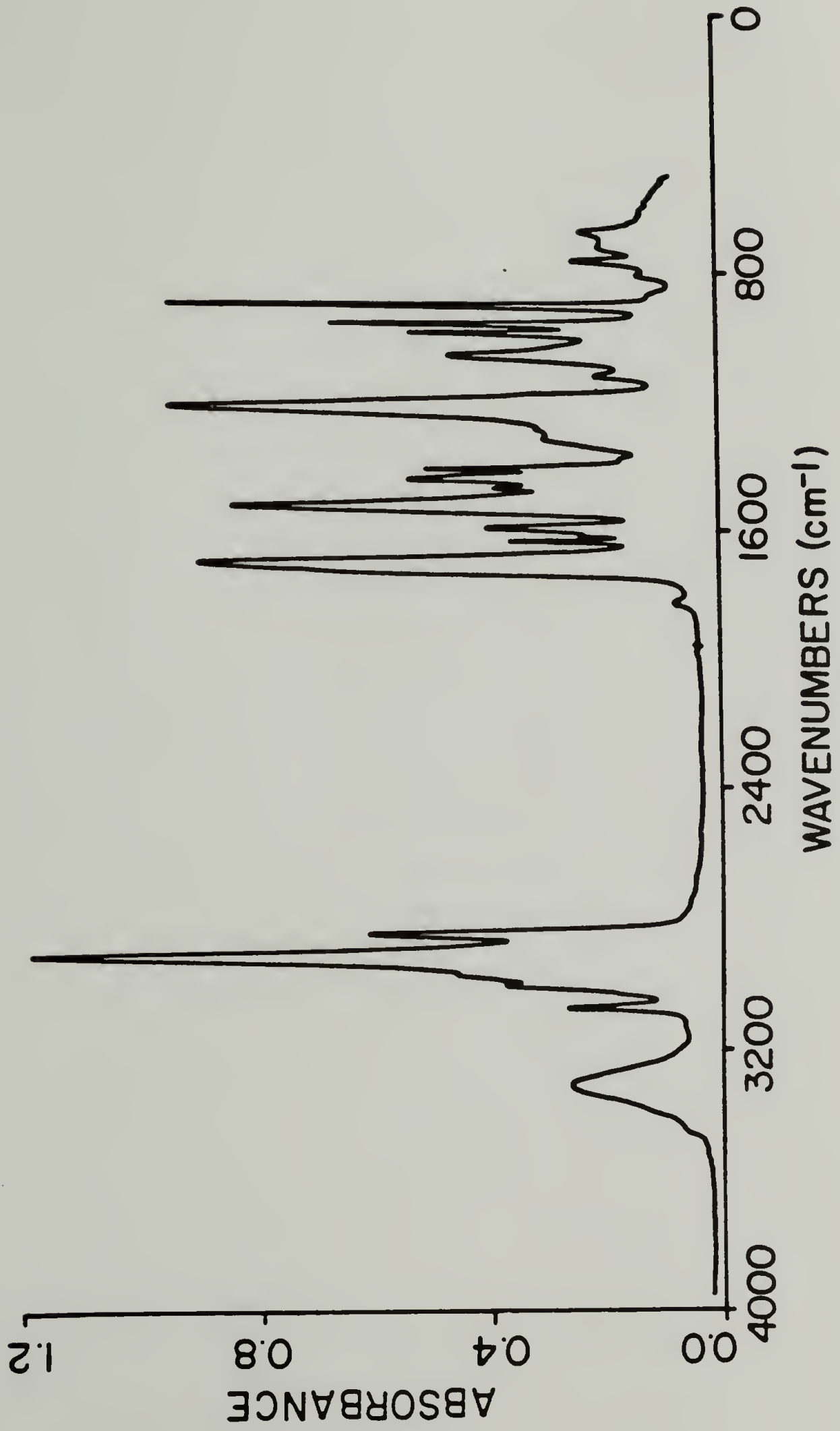


Figure 3.2a

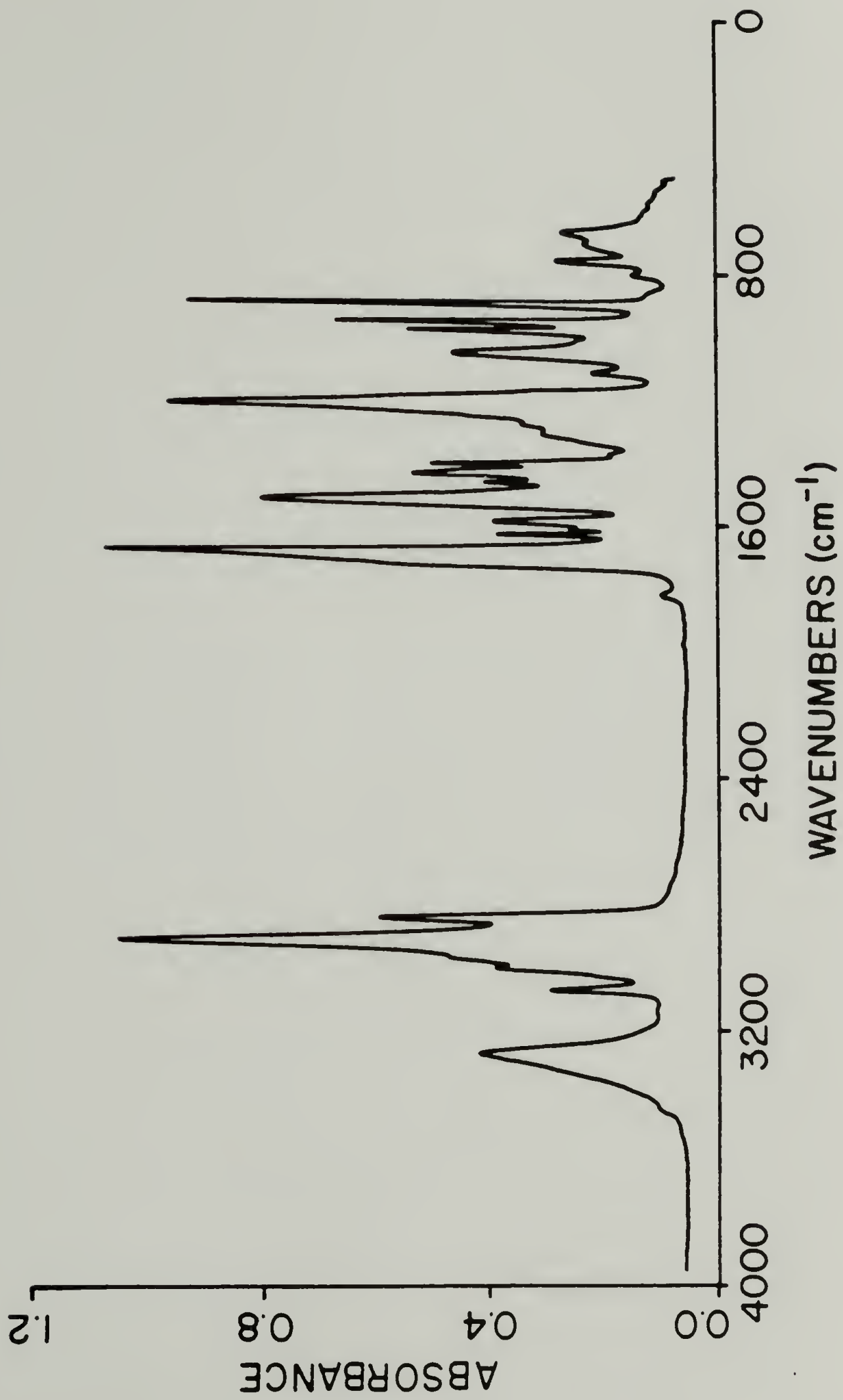


Figure 3.2b

to the intermolecular interactions of the urethane linkage and are well known to show changes in their frequency, intensity, and width that are dependent on the extent and specificity of hydrogen bonding. The N-H and carbonyl stretching vibrations are the absorptions that have been reported most often in the literature as being useful for quantitative investigations of hydrogen bonding (1,4,5,11). This is because these absorptions are characteristic of single vibrational modes while most of the other absorptions of the urethane linkage are due to coupled vibrational modes (18).

Expanded scale spectra of the N-H and carbonyl stretching regions for the two sample preparation methods are shown in Figures 3.3 and 3.4. These two absorptions both exhibit vibrational components which are characteristic of a hydrogen bonded system. Since the components of these two vibrations are similar in magnitude and origin, they will be discussed only in terms of the N-H stretching vibration. The spectra of both the solution cast and melt pressed samples have N-H stretching components at 3450 cm^{-1} and 3330 cm^{-1} . The component at 3450 cm^{-1} appears as a small shoulder on the high frequency side of the main absorption and corresponds to the N-H stretching fundamental. When the N-H proton becomes hydrogen bonded the vibration is perturbed and shifts to a lower frequency. The broad peak which is the dominant feature of this multiplet is due to the hydrogen bonded N-H of the amorphous hard segment phase. The strength of the hydrogen bond interaction determines how large a shift occurs in the N-H stretching vibration (19). The length of the hydrogen bond reflects the strength

FIGURE 3.3: Expanded scale spectrum of N-H stretching region of T3MI. a) solution cast from THF, b) melt pressed at 140°C, c) difference spectrum of a-b.

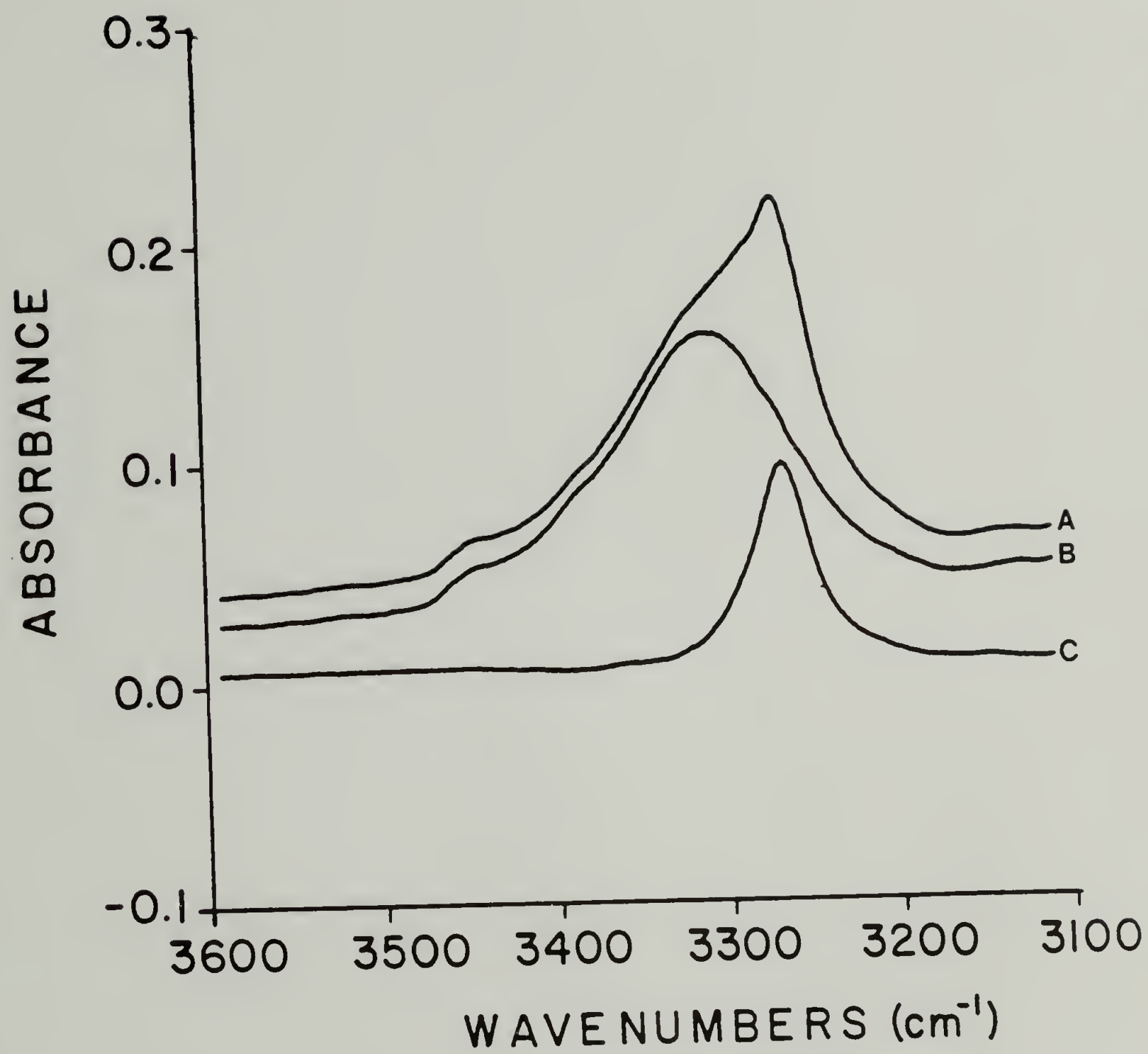


Figure 3.3

FIGURE 3.4: Expanded scale spectrum of carbonyl region of T3MI.
a) solution cast from THF, b) melt pressed at 140°C,
c) difference spectrum of a-b.

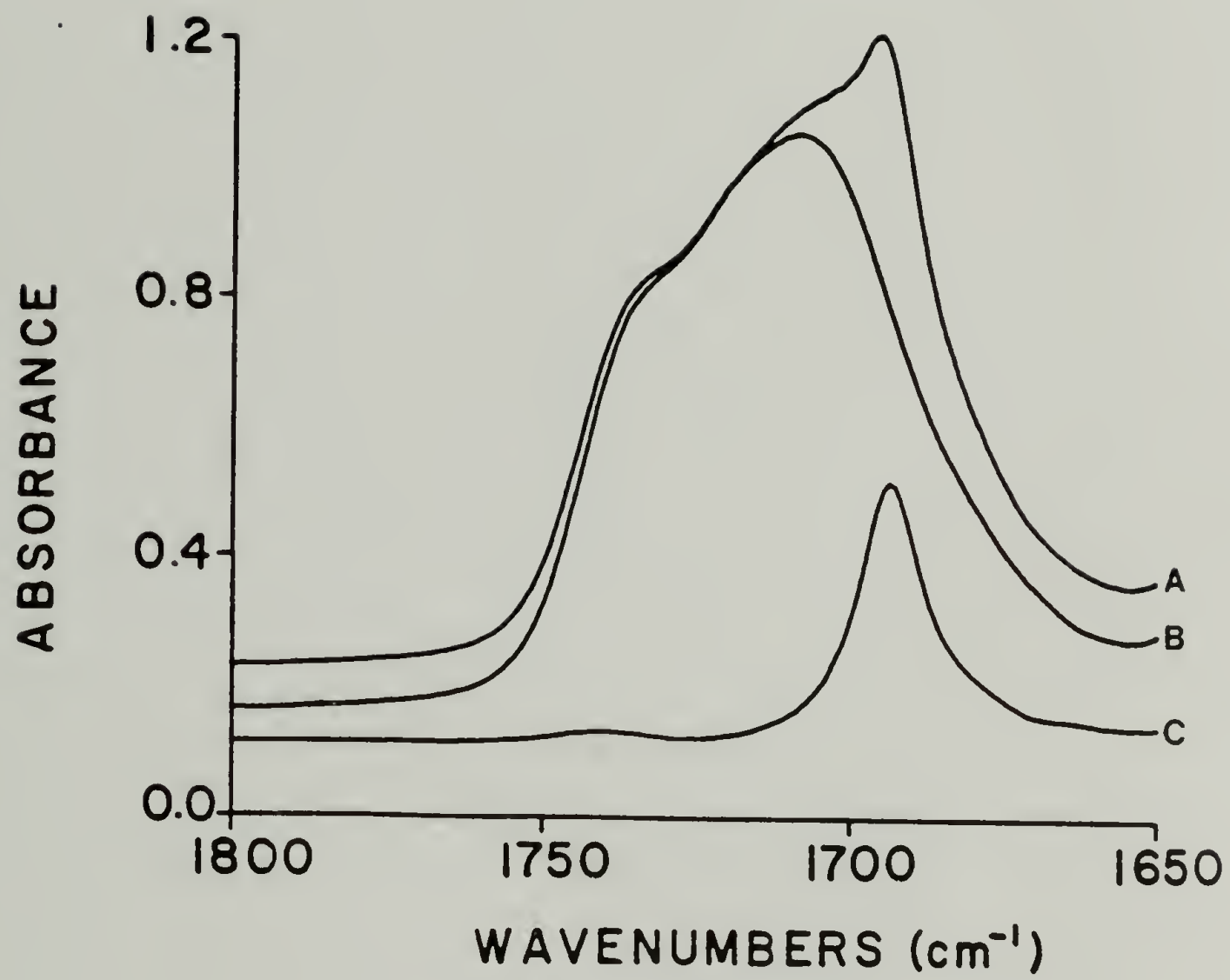


Figure 3.4

of this interaction. In the amorphous hard segment phase there is a distribution in the hydrogen bond lengths. This results in a distribution of frequency shifts, thus broadening the absorption band corresponding to the hydrogen bonded N-H groups. A third component of the N-H absorption can be seen in the spectrum of the sample that is solution cast. It is shifted to an even lower frequency, resulting in an asymmetric shape of the N-H absorption peak. This peak may be seen more clearly by subtracting the spectrum of the melt pressed sample from that of the solution cast sample. The three spectra in both Figures 3.3 and 3.4 are offset on the vertical axes for the reader's clarity. This component of the N-H vibration corresponds to a fraction of the urethane groups which are more strongly hydrogen bonded. The narrow halfwidth indicates greater specificity in the hydrogen bond interaction. This component of the N-H and carbonyl stretching vibrations corresponds to the ordered hard segment fraction and is used throughout this chapter for determining the extent of hard segment ordering.

While similar components are present in both the N-H and the carbonyl region, a difference in the nature of these two absorptions is the relative intensity of the subtracted peak in comparison to the total absorption for the solvent cast sample. Peak areas for both regions have been determined by a computer integration routine (see Appendix A), and it was found that the subtracted peak is 23% of the total absorption for the N-H vibration but only 13% of the total for the carbonyl absorption. Since a quantitative determination of the

volume fraction of the ordered component is desirable, it is first necessary to develop an understanding of the nature of the absorption intensities for these two vibrations and how they are affected by hydrogen bonding.

The Effect of Hydrogen Bonding on Infrared Absorption Intensities

One way to investigate the effect of the hydrogen bond interaction on the intrinsic intensity of the infrared absorptions is by analyzing the infrared spectra as a function of the extent of hydrogen bonding. The hydrogen bond has an interaction enthalpy of approximately 5 to 7 Kcal/mole (19). It is possible to change the distribution of the hydrogen bond interaction by varying the temperature of the system. Investigations of hydrogen bonding in polyurethanes as a function of temperature using infrared spectroscopy have been reported by a number of authors (1,2,8,10,11). These studies were usually aimed at determining a transition temperature corresponding to the onset of hydrogen bond dissociation. The authors considered the substituent groups involved as existing in only the hydrogen bonded or non-hydrogen bonded state. The extinction coefficient of the infrared absorptions was treated as having one value in the bonded state and another in the non-bonded state. Coleman and Painter have shown that as the temperature of a polyamide system is increased, there is a gradual redistribution of the hydrogen bonded fraction with a corresponding frequency shift of the band envelope for the hydrogen bonded group (20). They found that there was very little change in

the absorption for the non-bonded fraction.

In the present study, infrared intensities for the polyurethane elastomer were investigated by analyzing spectra as a function of temperature. The carbonyl region is shown as a function of temperature in Figure 3.5. The band corresponding to the hydrogen bonded components shifts steadily to higher frequencies as the temperature is increased until degradation begins to occur. The total integrated peak areas are shown as a function of temperature in Figure 3.6. The integrated area of the N-H band decreases by a factor of two as the temperature is increased from -90 to 180°C, however, the area of the carbonyl vibration decreases only slightly. This change in intensity as a function of frequency can be interpreted in terms of infrared intensity theory (21,22,23). In general, the intensity, I , is proportional to the square of the change in the dipole moment, μ , with respect to the normal coordinate, Q :

$$I \propto z \left(\frac{\partial \mu}{\partial Q} \right)^2 \quad (3.1)$$

The dipole moment is the product of the effective charge, q , and the bond length, r :

$$\mu = q \cdot r \quad (3.2)$$

This relationship is more complicated in hydrogen bonded systems. The charge transfer moment, $\frac{\partial \mu}{\partial Q}$ of a hydrogen bonded N-H group is several times larger than that of the non-hydrogen bonded system (23). However, it is very unlikely that the properties of the N-H group such as charge distribution and equilibrium bond length change enough during

FIGURE 3.5: The carbonyl stretching absorption of amorphous T3MI plotted as a function of temperature.

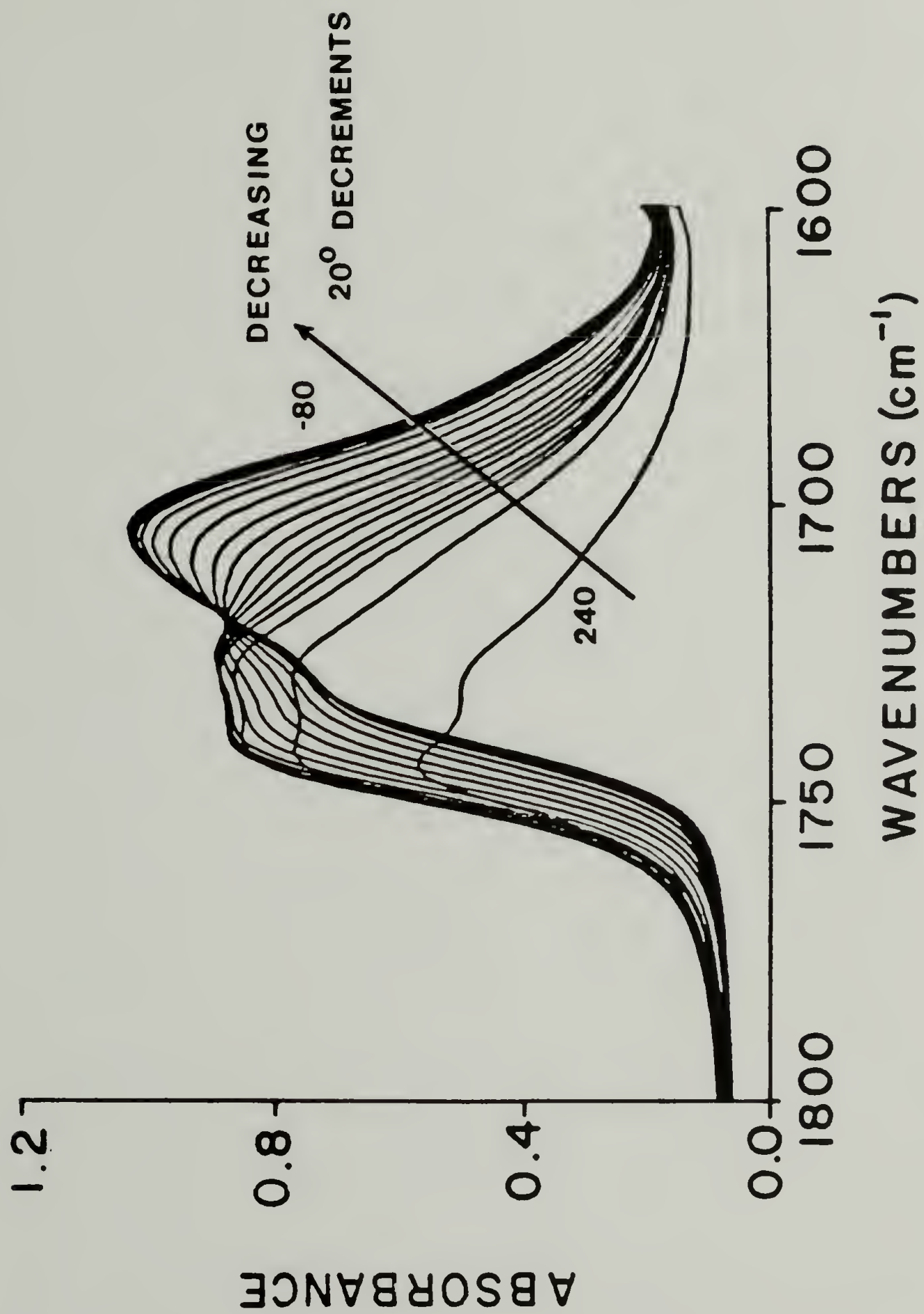


Figure 3.5

FIGURE 3.6: Total integrated peak areas of N-H and carbonyl absorptions plotted as a function of temperature (Δ : N-H stretch; * - carbonyl stretch).

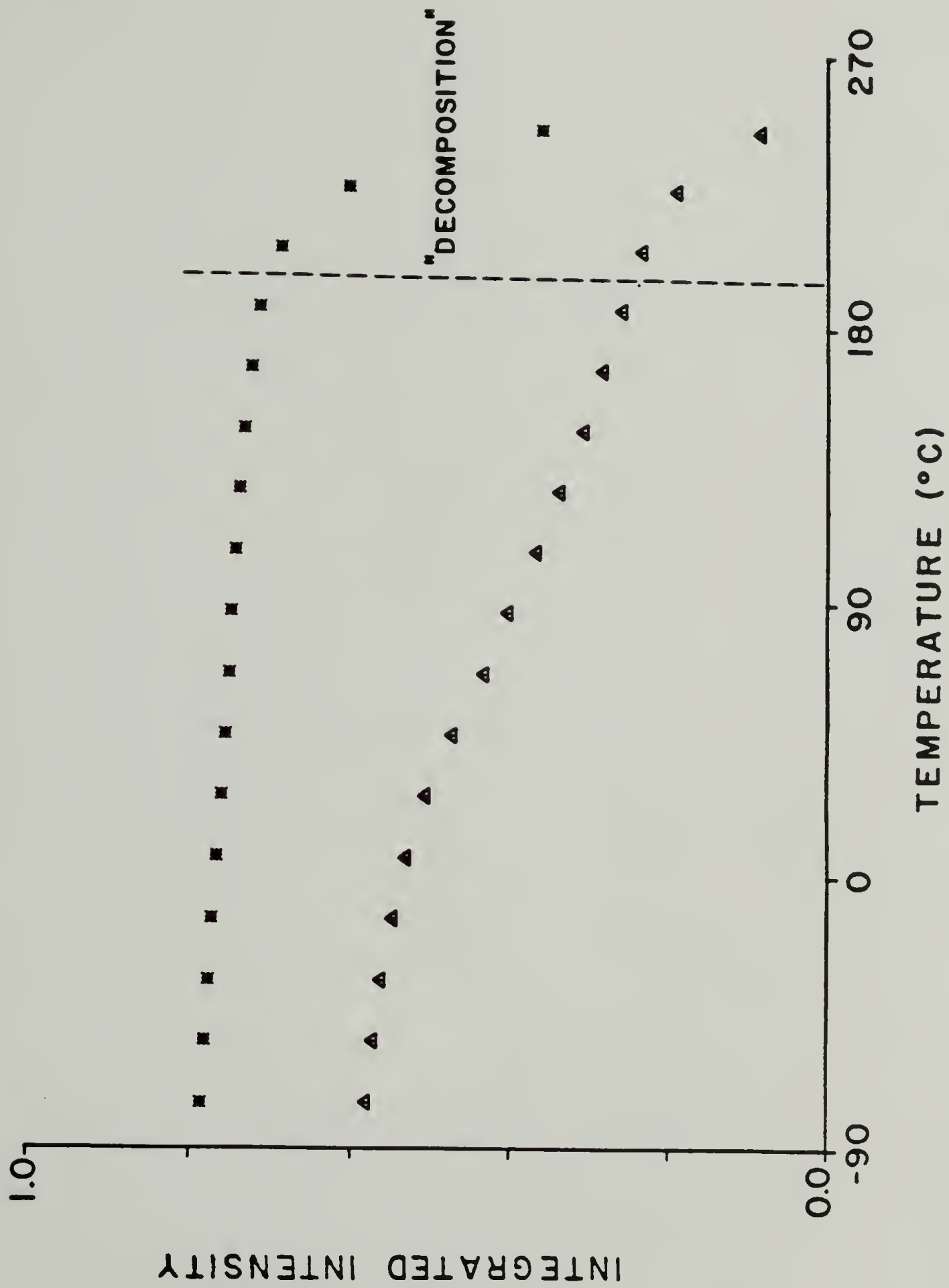


Figure 3.6

hydrogen bonding to account for this as the energy of the hydrogen bond is small compared to the N-H bond energy. It is more likely that resonance and charge transfer is the most important factor in determining the increase in $\partial\mu/\partial Q$. Thus, in consideration of Equation 3.1 it is clear that the N-H stretching absorption has a strong dependence on the degree of hydrogen bonding.

The Dependence of Hard Segment Order on Sample Preparation and Thermal History

From the evaluation of infrared intensities as a function of hydrogen bond strength, it is clear that the carbonyl absorption band is the best choice for quantitative studies of hard segment ordering. Analysis of the carbonyl peak corresponding to the ordered fraction by spectral subtraction for solvent cast samples prepared with controlled evaporation rates indicated that the ordered structure developed more readily when the solvent was evaporated slowly.

Since evaporation occurs from one surface when casting on a substrate, it was believed that the hard segment ordering would not be uniform through a cross section of the film. This was investigated utilizing the infrared surface characterization technique of attenuated total reflectance spectroscopy, ATR. Spectra which are collected using the ATR technique will have absorption intensities that are wavelength dependent. In this study ATR was used only for qualitative purposes and no corrections were made for this dependency. A sample of $\sim 10 \mu\text{m}$ thickness was cast on release paper and removed so

that both surfaces could be characterized. The ATR spectrum of the carbonyl region of the outer surface along with the subtraction spectrum of the inner surface minus the outer surface are shown in Figure 3.7. The positive component on the low frequency side of the subtraction spectrum indicates that there is greater hard segment order at the surface that was in contact with the substrate than at the surface where evaporation occurred. The mobility of the hard segments at the surface that was in contact with the substrate was enhanced due to plasticization by solvent molecules. This increased mobility allowed for a greater degree of order to be achieved than at the surface where evaporation took place. The concentration of solvent molecules near the surface where evaporation occurs is less than in the bulk material. This decreases the plasticization effect to the point where conformations are frozen in before hard segment ordering can occur.

In most semicrystalline polymer systems heat treating a sample at temperatures between the glass transition and crystalline melting point results in an annealing process which increases the extent of crystalline order. Previous investigations of polybutadiene based polyurethanes prepared with pure 2,6 TDI have indicated that these samples are semicrystalline and that annealing the sample at temperatures above the glass transition of the hard segment (90°C) results in a significant increase in the extent of crystallinity as determined by differential scanning calorimetry, DSC (18). This crystalline nature is also apparent in the infrared spectrum (18). The carbonyl region for an annealed sample of a polybutadiene based

FIGURE 3.7: ATR spectrum of carbonyl region for T3MI prepared by solution casting on release paper (—: outer surface of film; ----: inner surface minus outer surface).

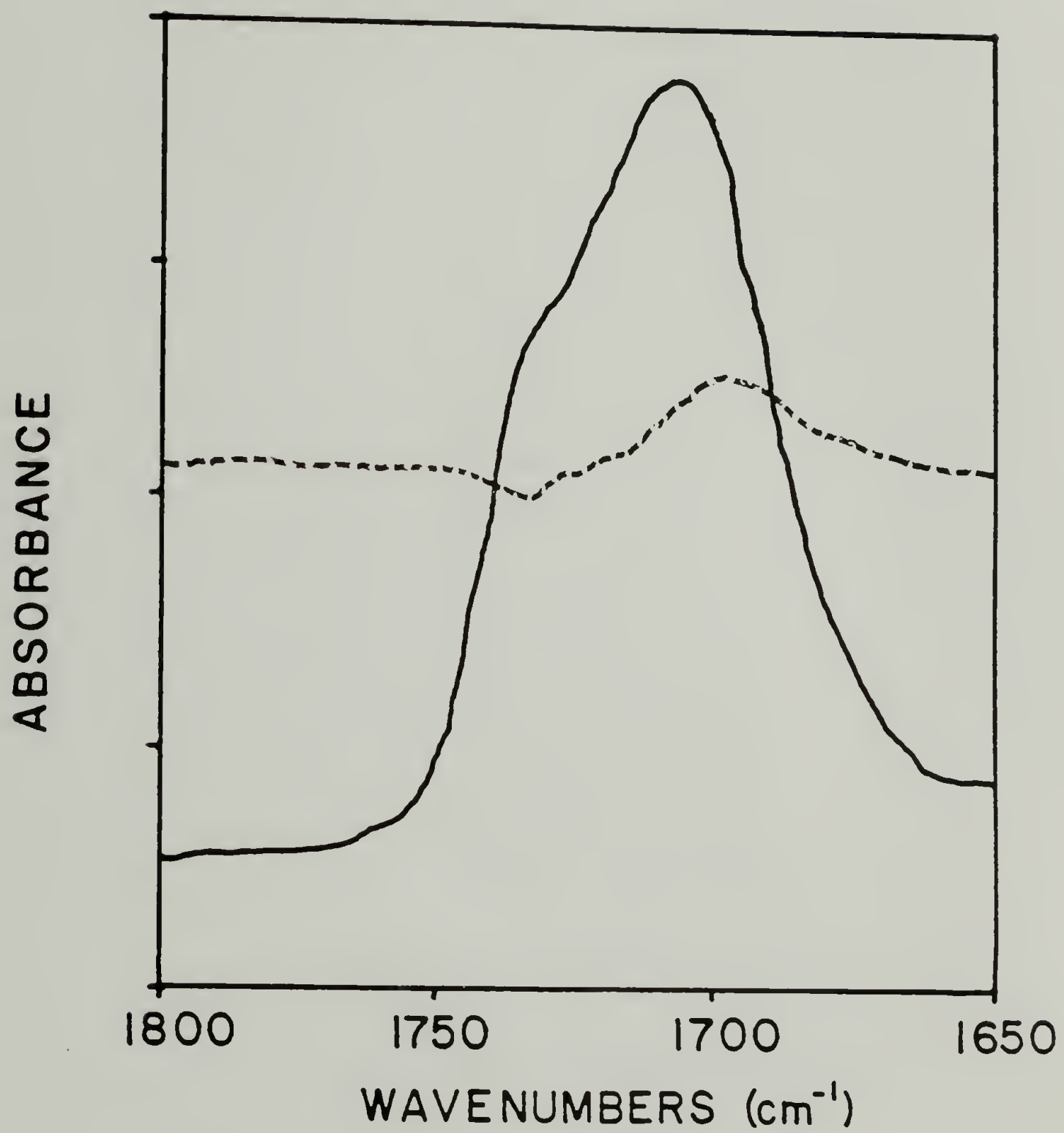


Figure 3.7

polyurethane having a 2,6-TDI/BDO hard segment and TDI:BDO:polybutadiene mole ratio of 3.2:2.2:1 is shown in Figure 3.8. The component on the low frequency side of the band is considerably stronger than for the sample of the same mole ratio of reactants but using mixed isomer TDI. The amorphous component for the carbonyl region for each of these samples is subtracted away as described previously. The resulting spectra corresponding to the ordered fractions are compared in Figure 3.9. The intensity of the bands are normalized using a multiplication factor so that peak shape may be more closely compared. It can be seen that both frequency and width are virtually the same and strongly indicate that the ordered component in the sample prepared with mixed isomer TDI is of similar origin as that of the sample prepared with pure 2,6 TDI. It is likely that this is due to ordering of consecutive sequences of 2,6 TDI in the mixed isomer system.

Unlike the sample prepared with pure 2,6 TDI, it is interesting to note that annealing the polyurethane prepared with mixed isomer TDI does not result in any increase in the extent of hard segment ordering. In fact, heat treatment of these samples only results in a decrease of the ordered hard segment phase. The amount of ordered phase remaining after heat treating is dependent only on the highest temperature in the thermal history of these samples. Heating to 160°C results in complete loss of the peak corresponding to the ordered fraction. When the sample is cooled to room temperature, the ordered phase does not reform even at cooling rates of 5° per hour.

To develop a better understanding of this disordering phenomenon a thermal cycling infrared study was used. All spectra were collected at

FIGURE 3.8: Carbonyl region of an annealed sample of the polyurethane having a 2,6 TDI/BDO hard segment.

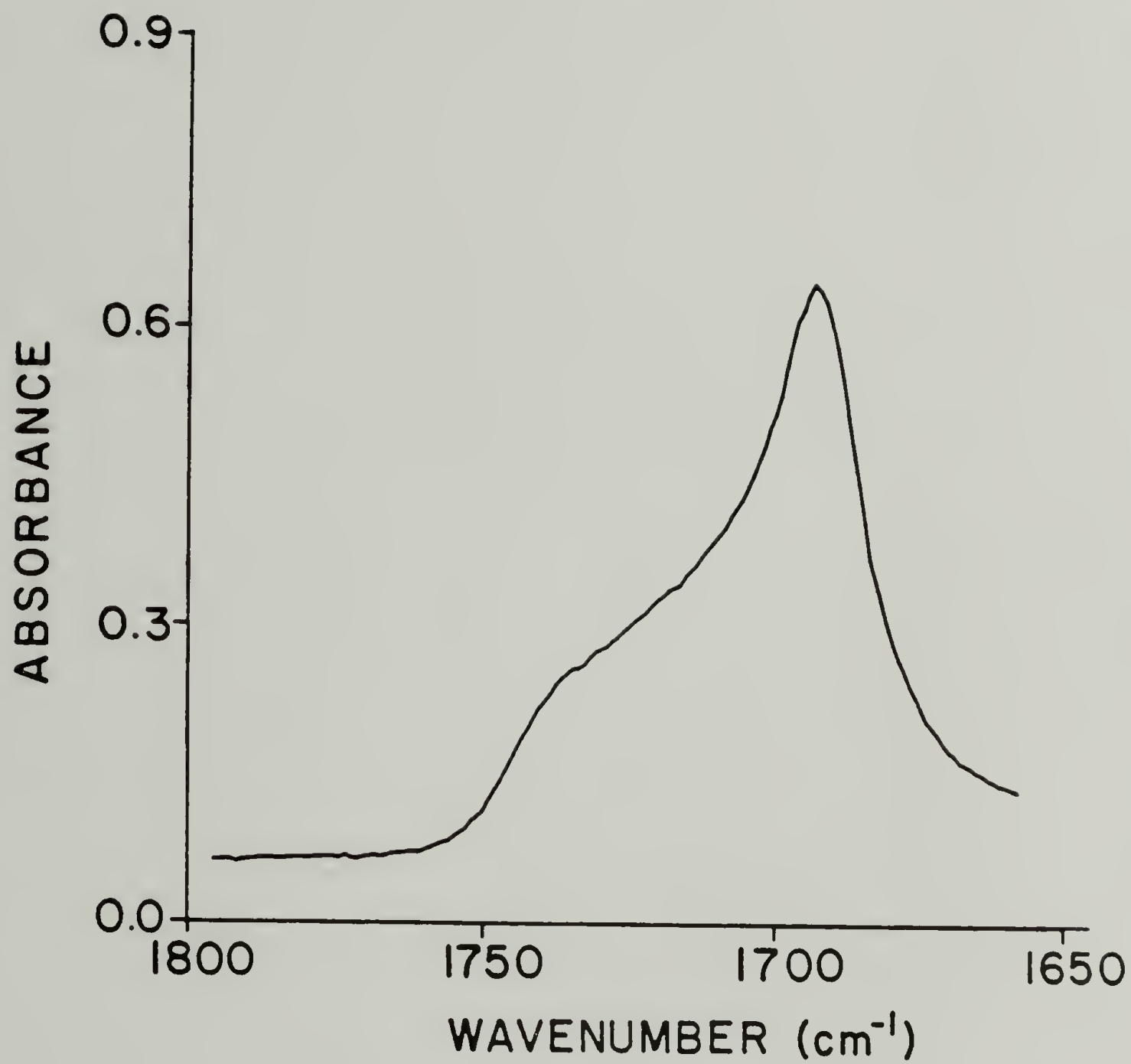


Figure 3.8

FIGURE 3.9: Comparison of subtraction spectra corresponding to ordered component. a) T3MI, b) sample with pure 2,6 TDI hard segment.

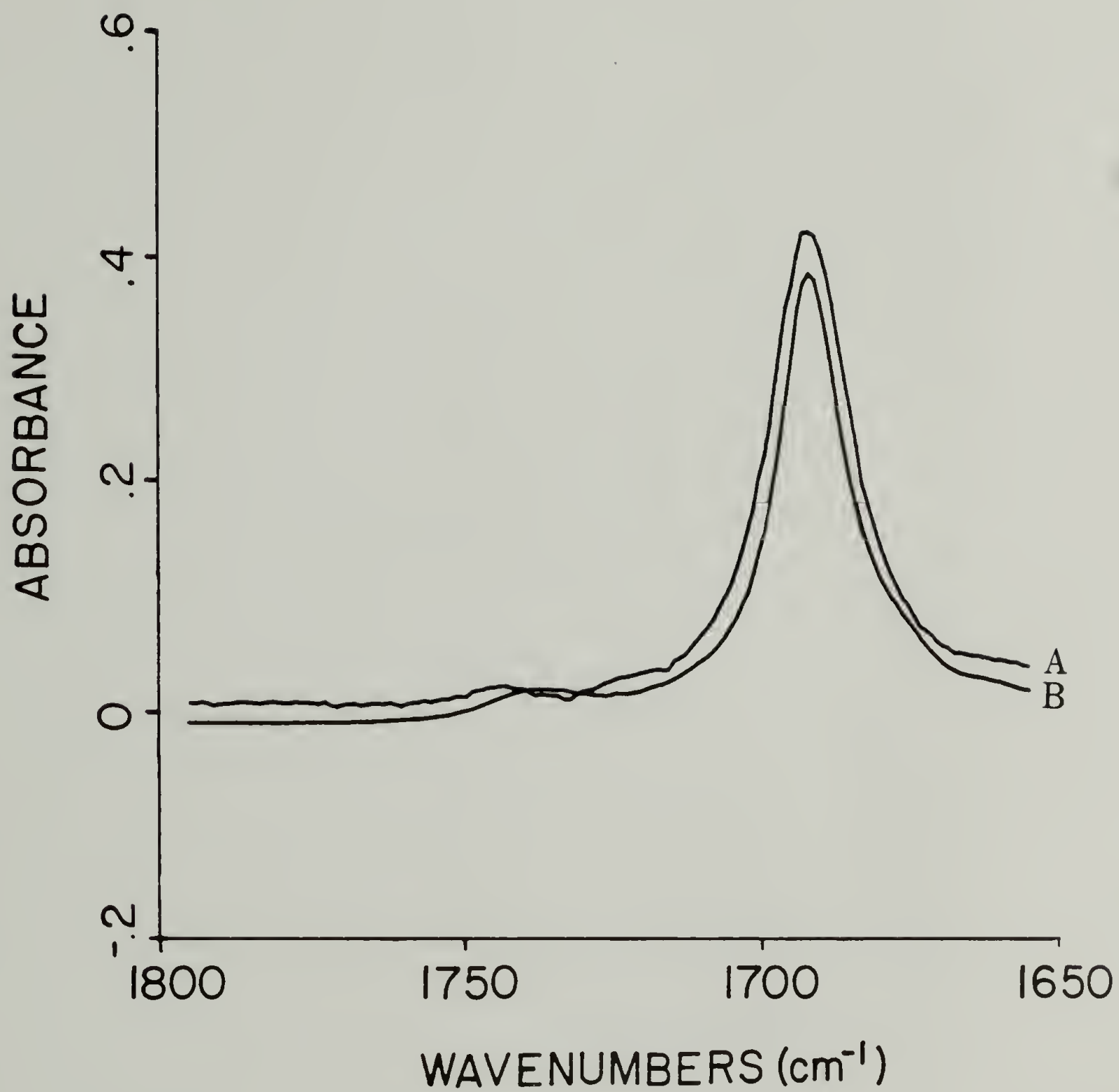


Figure 3.9

a constant reference temperature with the sample being heated to successively higher temperatures between each collection. It is assumed that no change in the ordered structure occurred during the cooling cycle of this study. The infrared spectra of the carbonyl region collected at ambient temperature are shown as a function of temperature history in Figure 3.10. The fraction of hard segment phase having a high degree of order was monitored using the carbonyl region by integration of the peak in the subtracted spectra corresponding to the ordered phase. In Figure 3.11 the integrated area of this peak for a solution cast sample is shown as a function of the thermal history. From this plot it may be inferred that there is a broad distribution of disordering temperatures. That disordering occurs over a range of temperatures could result from the existence of ordered domains having a distribution in size and degree of order due to the polydispersity in the length of the consecutive 2,6 TDI sequences. Attempts to characterize this transition using differential scanning calorimetry (DSC) have been unsuccessful. This may be due to the low weight fraction of the ordered phase having a distribution of disordering temperatures. Therefore, no sharp endotherm would be present in the DSC thermogram. The weight fraction of the ordered hard segment phase can be interpreted from the integrated intensity of the component of the carbonyl absorption corresponding to the ordered phase in comparison to the integrated intensity of the entire carbonyl absorption. The investigation of infrared intensity in the preceding section demonstrated there was only a slight change in the integrated intensity of the carbonyl absorption while there was a large shift in

FIGURE 3.10: Infrared spectra of carbonyl absorption of solution cast T3MI are plotted as a function of thermal history.

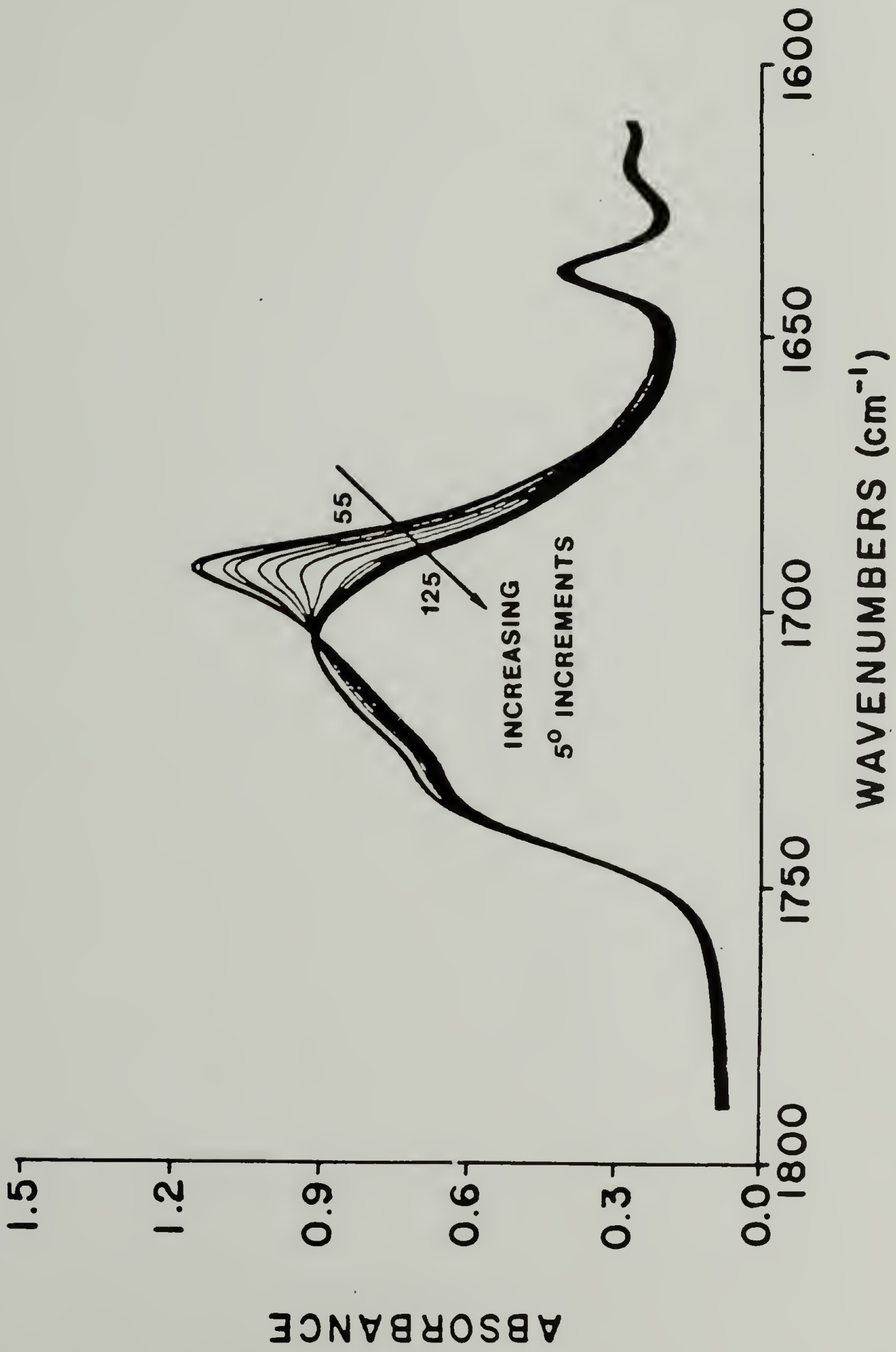


Figure 3.10

FIGURE 3.11: Integrated area of the ordered component of the carbonyl absorption plotted as a function of thermal history.

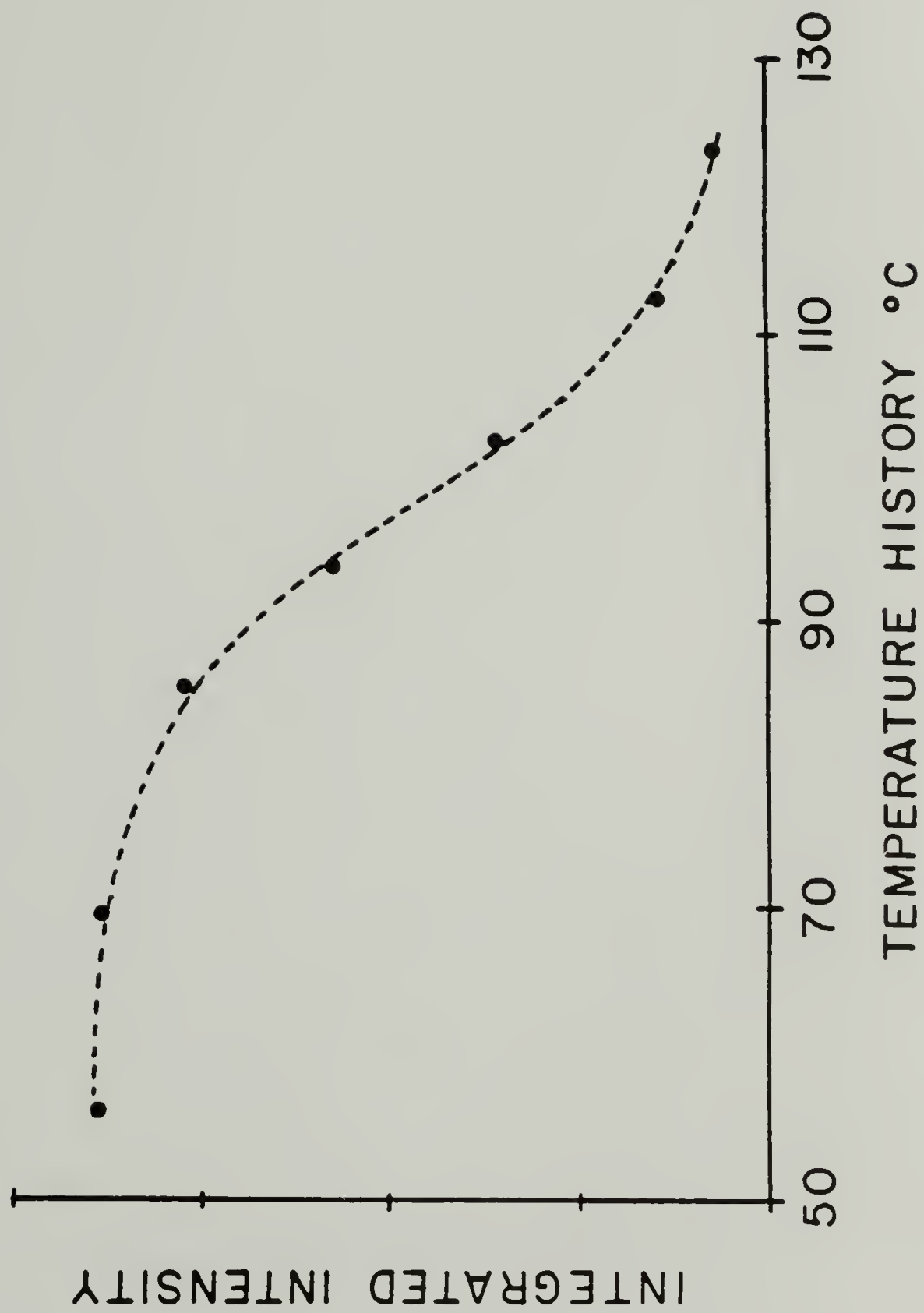


Figure 3.11

vibrational frequency. This indicates that a reasonable first order approximation of the weight fraction of the ordered phase may be determined from the relative intensity of the component of the carbonyl absorption corresponding to this fraction. For the solution cast sample this fraction is 13% of the total hard segment content. Since this is only 3.5% of the total sample weight, and considering that there is a distribution of disordering temperatures, it is likely that any thermal transition in the DSC thermogram is obscured in baseline drift.

Solvent Induced Crystallization

As mentioned previously, attempts to increase the extent of hard segment microstructural order by annealing the samples at temperatures below that where disordering occurs were unsuccessful. However, when these samples were exposed to either THF or toluene vapor, the extent of microstructural order was increased. In fact, the vapor treatment method was successful in regenerating the ordered structure in samples which had been heated above the temperature where all of the initially ordered structure was disassociated. The solvent vapor treatment involved exposing samples cast on KBr plates to saturated solvent vapor for two hours followed by vacuum drying at ambient temperature. The infrared thermal cycling experiment discussed previously was then carried out for each of these samples and the results are shown in Figure 3.12. The distribution of disordering temperatures for the THF treated sample is narrower and occurs at a higher temperature than

FIGURE 3.12: Integrated area of ordered component of carbonyl absorption for solvent vapor treated T3MI as a function of thermal history (●: treated with THF vapor; o: toluene vapor).

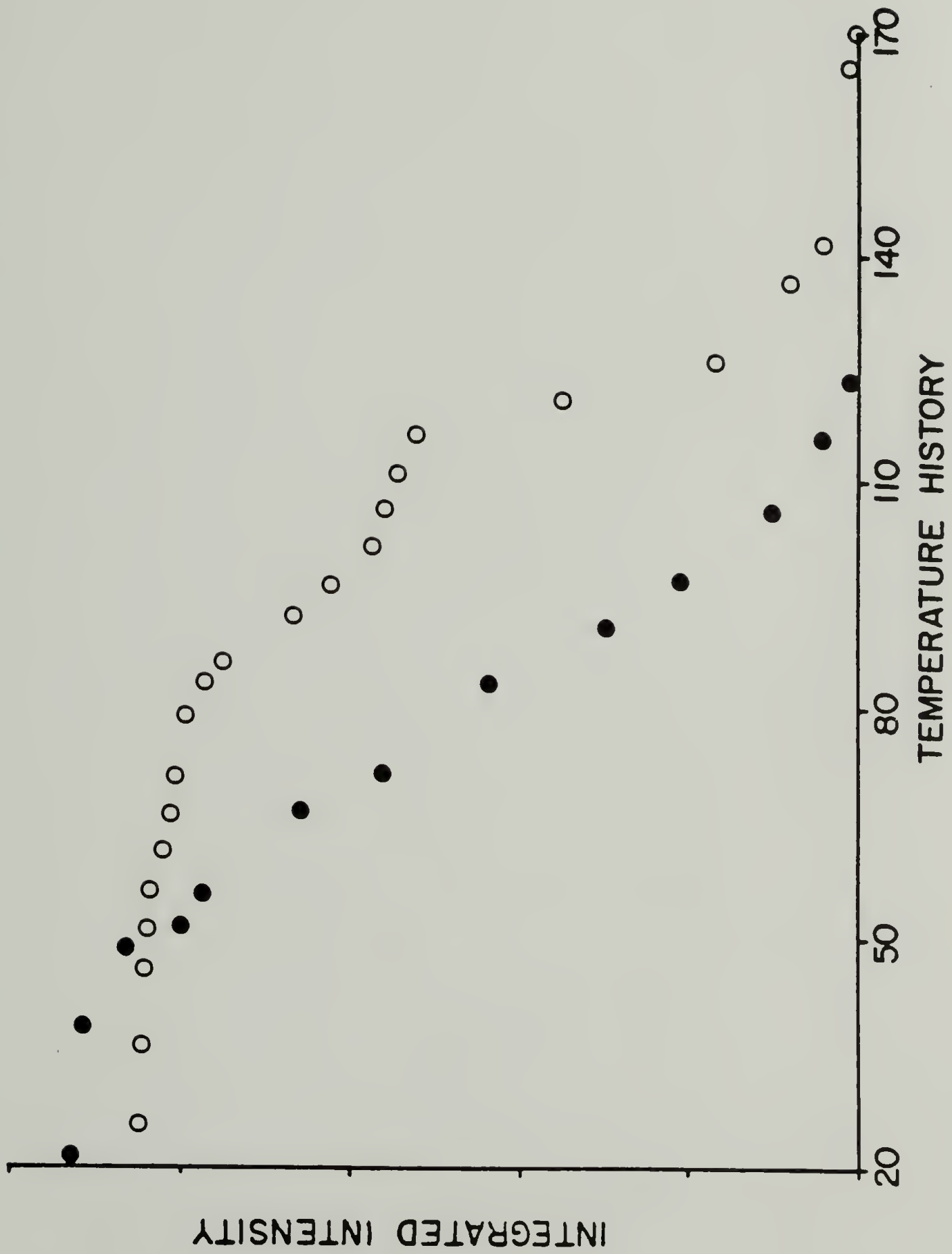


Figure 3.12

that of the solvent case sample shown in Figure 3.11. This is most likely due to the fact that hard segment mobility occurs for a longer period of time than during solvent casting and thus more perfect ordering results. The sample which was treated with toluene vapor has a much broader distribution of disordering temperatures. Since toluene is not a solvent for the hard segment phase, the domains are not plasticized to the extent as with THF resulting in lower segmental mobility and ordering which is less perfect.

This phenomenon of solvent induced crystallization has been reviewed by several authors (24,25,26). Of particular interest is the case of bisphenyl A polycarbonate, which does not crystallize through annealing yet is readily crystallized when exposed to acetone (27,28). This results from a T_g depression mechanism (27). It has been suggested that this is a general phenomenon for polymers which have glass transitions and thermal melting points at similar temperatures (29).

In the current study of polyurethanes with hard segments of mixed isomer TDI, the 2,6 TDI component has the potential to crystallize while the 2,4 component does not. The 2,4 TDI units in hard segment sequences do contribute to the elevated glass transition of the hard segment, however the driving force for crystallization is due only to the sequences of consecutive 2,6 TDI units. This results in the hard segment phase having a T_g and T_m of similar magnitude, thus creating a system where hard segment order is not increased by thermal annealing, yet exhibits a significant increase with solvent plasticization.

Orientation of Ordered Hard Segment

Polarized infrared characterization can yield important information on the nature of segmental microstructure. In Chapter II it was used to investigate the orientation of a crystalline model compound NPU and soft segment orientation of the polyurethane (with monodispersed hard segment) T5MD. Polarized infrared spectra of the N-H stretching region for T3MI which has been deformed 20% are shown in Figure 3.13. The ordered component of the absorption is more pronounced in the spectrum with radiation polarized parallel to the stretching direction than in the spectrum with perpendicular polarization. The subtraction of the parallel spectrum minus the perpendicular spectrum is also shown in Figure 3.13 with all three of the spectra being offset for clarity. This shows that the ordered component is strongly polarized. It is of particular interest that this subtraction indicates that the ordered fraction of the N-H groups is oriented in the direction of deformation. Since the N-H groups are perpendicular to the hard segment axis, this indicates that the hard segment chain axes of the ordered fraction are oriented perpendicular to the deformation axis. This type of hard segment orientation has been reported previously for polyurethanes with semicrystalline hard segment domains (4,9). It can be explained in terms of the orientation model depicted in Figure 3.14. Long range order develops in semi-crystalline hard segment domains. The width of the crystallite is limited by the hard segment length and crystalline growth occurs perpendicular to the chain axis. This is a similar situation as for crystallization of the n-phenyl

FIGURE 3.13: Polarized spectra for N-H region of T3MI which has been deformed 20% (upper trace is with parallel polarization, middle trace is with perpendicular polarization, lower trace is the difference spectrum).

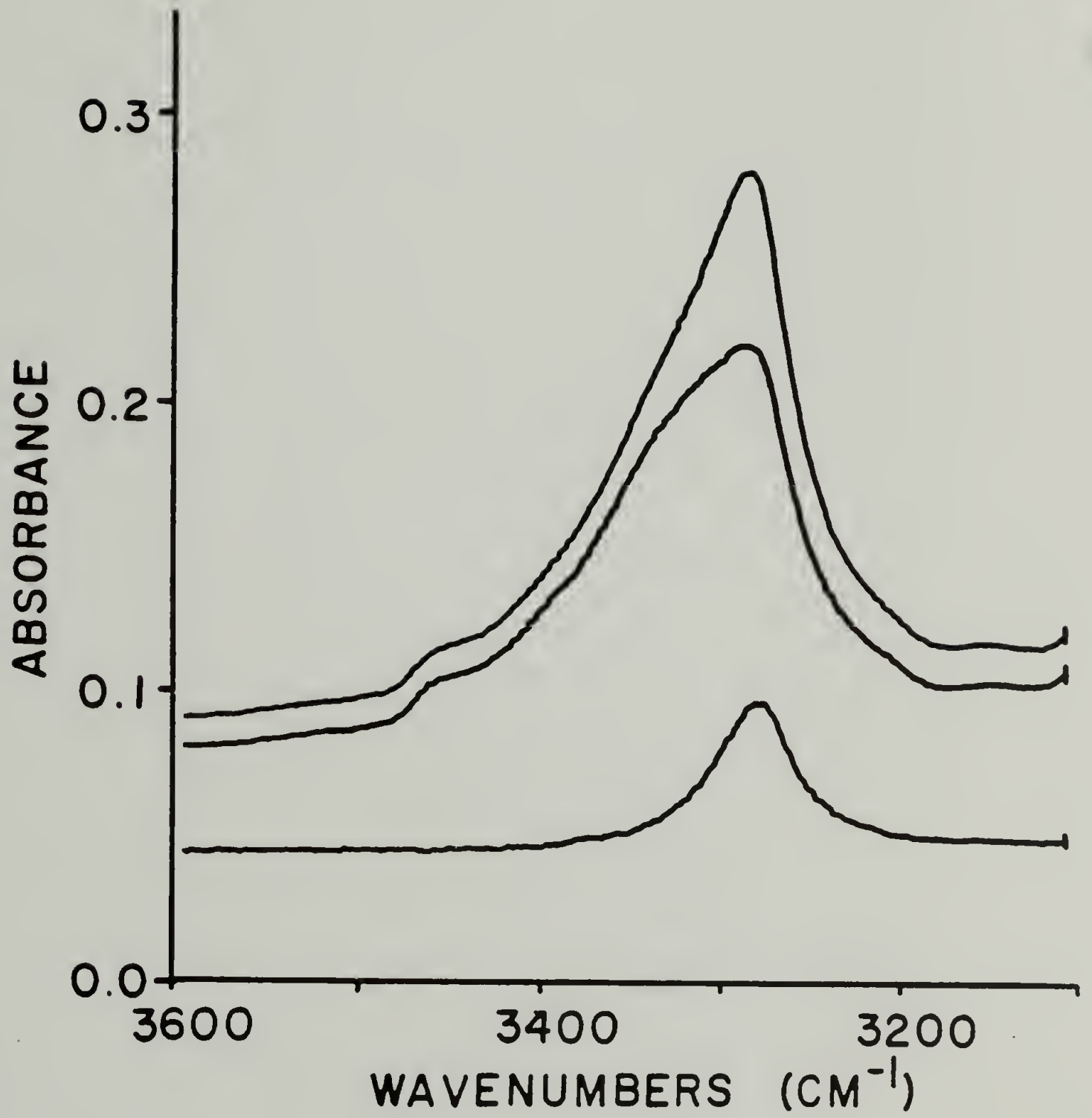


Figure 3.13

FIGURE 3:14: Deformation model of ordered hard segment domains. Hard segment chain axes orient perpendicular to the deformation axis.

ORIENTATION OF LAMELLAR MICROSTRUCTURE

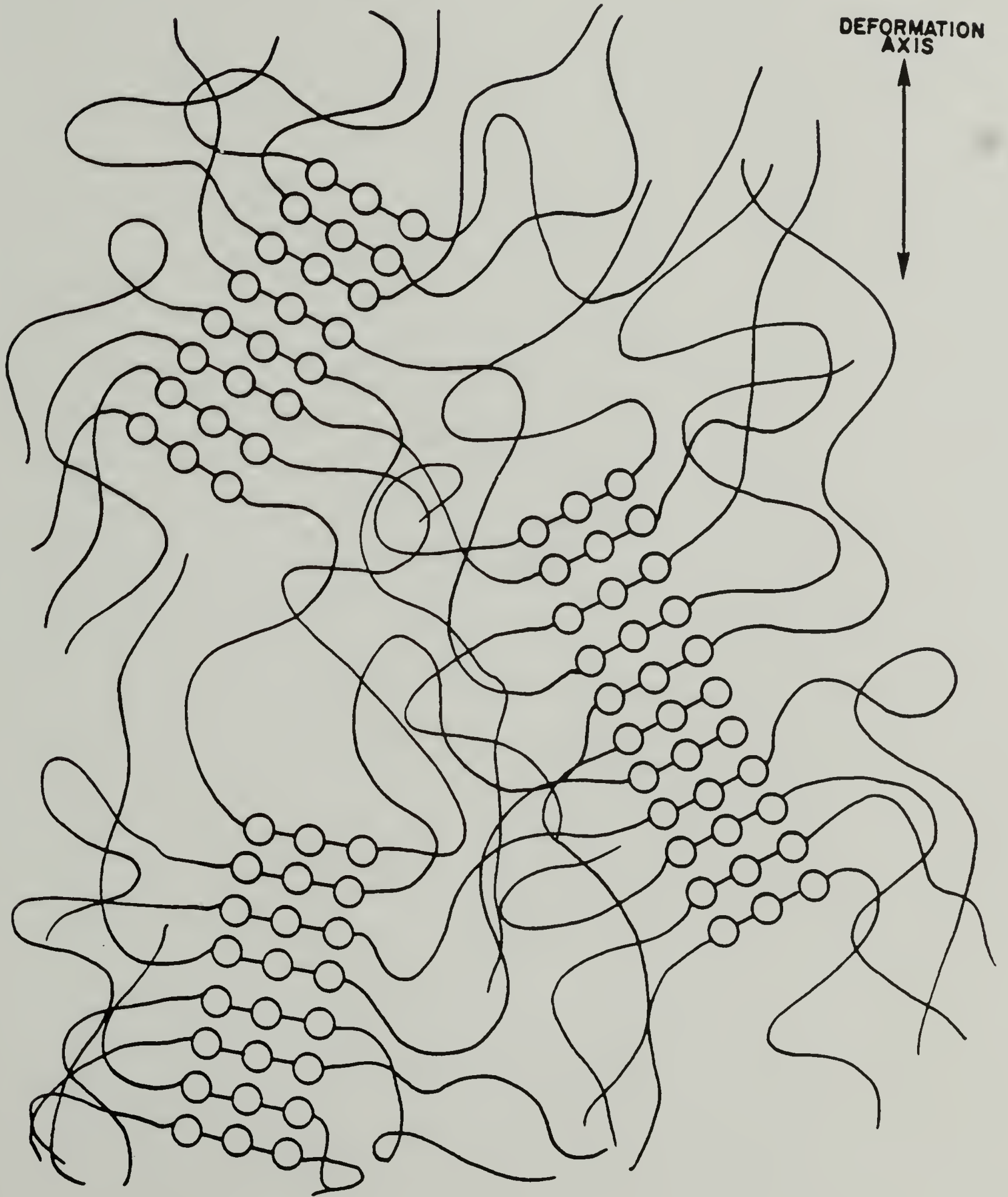


Figure 3.14

urethane model compound discussed in Chapter II, with hydrogen bonding being a strong driving force for crystalline growth. In the deformed polyurethane sample the long axis of the crystallite orients into the stretching direction resulting in the hard segment chain axis being perpendicular to the deformation axis. This is evidence that long range order exists in the ordered fraction of the hard segment for solution cast T3MI.

Hard Segment Length Redistribution by Urethane Interchange Reactions

As discussed previously, when the solution cast polyurethane having an ordered hard segment phase was thermally cycled to 150°C the infrared spectrum indicated that all hard segment order was lost. After treating this sample in THF or toluene vapor the hard segments would again show infrared evidence of reordering. However, when the sample is heat treated at temperatures above 180°C it loses the ability to reform the ordered structure using the solvent vapor treatment method. This indicates that at higher temperatures the chemical structure of the polymer chain is permanently altered to a non-crystallizable structure. It is likely that the hard segments formed during the initial solution polymerization process have crystallizable sequences that result from the unequal reactivity of the isocyanate functional groups of the 2,4 and 2,6 TDI isomers. The isocyanate group at the para position of the 2,4 isomer is reported as having a reactivity which is 12 times that of the isocyanate group in the ortho position. The fraction of unreacted 2,4 isomers is depleted in the

endcapping step of the reaction leaving a higher concentration of 2,6 isomers that may link in crystallizable sequences in the chain extension step. When the sample is heated above a critical temperature, rearrangement occurs, thus disrupting the crystallizable sequences. Several authors have reported this type of rearrangement phenomena occurring when urethane model compounds are heated above 170°C (30,31). This reaction is analogous to the ester-ester interchange reaction which is well known for polyester systems. The model compounds used in these studies were precursors used in the synthesis of polyurethanes with monodispersed hard segments. In general, they are highly crystalline compounds. It has been proposed that when these compounds are heated above a critical temperature the urethane linkages undergo an interchange reaction, which results in a redistribution of the hard segment lengths. This results in the formation of a mixture of hard segment model compound that has a statistical distribution of lengths. Eisenbach has reported the observation of this redistribution for model compounds prepared with p,p'-diphenylmethane diisocyanate (MDI) and butanediol which he has termed "transurethanification". Gel permeation chromatographic analysis of the product mixture shows the presence of a series of peaks that correspond to the distribution. The retention times of each of these peaks is equivalent to retention times of model compounds of specific sequence lengths (30).

To make a more conclusive determination of whether or not thermally induced hard segment rearrangement occurs in the TDI polyurethanes we have investigated the thermal stability of the urethane linkage of a TDI based low molecular weight model compound. This

model compound was prepared by capping 2,4 TDI at each end with butanediol. The sample was heated at 180°C for 8 hours under vacuum. This results in an interchange reaction occurring. As this reaction proceeds, free butanediol is generated and is immediately volatilized in the vacuum. The mole ratio of TDI:BDO gradually changes from 1:2 to 1:1 resulting in the formation of a high molecular weight polymer of TDI linked with butane diol. The infrared spectrum of the resulting compound is compared with that of the solution polymerized TDI/BDO model hard segment homopolymer in Figure 3.15. The similarity of the two spectra indicates that the interchange reaction occurs for this model system. No absorptions may be detected corresponding to side reactions that results in non-urethane degradation products.

In the study of the polyurethane prepared with mixed isomer TDI the fact that the as polymerized structure has the potential to organize to form an ordered phase while redistribution results in sequences which no longer have this ability indicates that the "as polymerized" chain structure has non-random hard segment sequences. In the next chapter a computer simulation of the polyurethane polymerization will be used to determine specific isomer distributions of the system prepared with mixed isomer TDI.

FIGURE 3.15: Comparison of infrared spectra of A) BTB model compound, B) BTB after vacuum heating at 180°C and C) 2,4 TDI/BDO model polymer.

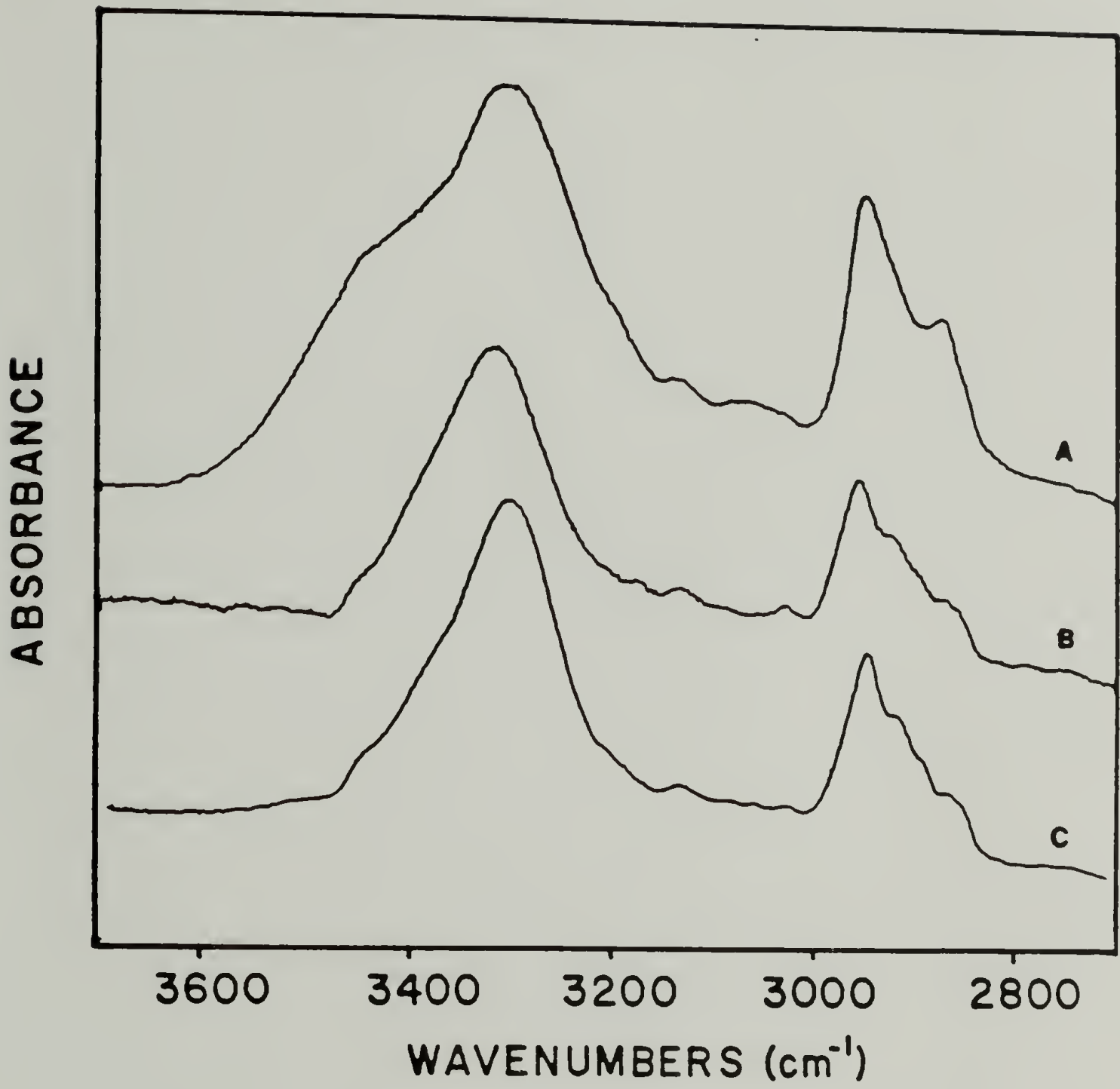


Figure 3.15

References

1. C.S. Paik Sung and N.S. Schneider, "Temperature Dependence of Hydrogen Bonding in Toluene Diisocyanate Based Polyurethanes", *Macromol.*, 10, 452 (1977).
2. N.S. Schneider and C.S. Paik Sung, "Transition Behavior and Phase Separation in TDI Polyurethanes", *Polym. Sci. Eng.*, 17(2), 73 (1977).
3. N.S. Schneider, C.S. Paik Sung, R.W. Matton, and J.L. Illinger, "Thermal Transition Behavior of Polyurethanes Based on Toluene Diisocyanate", *Macromol.*, 8(1), 62 (1975).
4. H. Ishihara, I. Kimura, K. Saito, and H. Ono, "Infrared Studies on Segmented Polyurethane-Urea Elastomers", *J. Macromol. Sci.-Phys.*, B10(4), 591 (1974).
5. T. Tanaka and Y. Yamaguchi, "Quantitative Study of Hydrogen Bonding Between Urethane Compound and Ethers by Infrared Spectroscopy", *J. Polym. Sci.*, A-1, 6, 2137 (1968).
6. R.W. Seymour, A.E. Allegrezza, Jr., and S.L. Cooper, "Segmental Orientation Studies of Block Polymers. I. Hydrogen Bonded Polyurethanes", *Macromol.*, 6, 846 (1973).
7. Y.M. Boyarchuk, L.Y. Rappoport, V.N. Nikitin, and N.P. Apuktina, "A Study of Hydrogen Bonding in Urethane Elastomers By Infrared Spectroscopy", *Polym. Sci.*, USSR, 7, 859 (1965).
8. T. Tanaka, T. Yokayama, and Y. Yamaguchi, "Effects of Methyl Sidegroup on the Extent of Hydrogen Bonding and Modulus of Polyurethane Elastomers", *J. Polym. Sci.*, A-1, 6, 2153 (1968).

9. C.S. Paik Sung, T.W. Smith, and N.H. Sung, "Properties of Segmented Polyether Poly(uurethaneureas) Based on 2,4-Toluene Diisocyanate. 2. Infrared and Mechanical Studies", *Macromol*, 13, 117 (1980).
10. V.W. Srichatrapimunk and S.L. Cooper, "Infrared Thermal Analysis of Polyurethane Block Polymers", *J. Macromol Sci.*, B15(2), 267 (1978).
11. G.A. Senich and W.J. MacKnight, "Fourier Transform Infrared Thermal Analysis of Segmented Polyurethane", *Macromol.*, 13, 106 (1980).
12. S.B. Lin, H.S. Hwang, S.Y. Tsay, and S.L. Cooper, "Segmental Orientation Studies of Polyether Polyurethane Block Copolymers with Different Hard Segment Lengths and Distributions", *Colloid Polym. Sci.*, 263, 128 (1985).
13. B.H. Bengston, "Structure-Property Relationships in Linear Polyurethanes", Ph.D. Dissertation, University of Massachusetts, 1985.
14. M.B. Rossman, "Synthesis and Characterization of Polybutadiene-Containing Polyurethanes", M.S. Thesis, University of Massachusetts, 1981.
15. M. Xu, W.J. MacKnight, C.H.Y. Chen, and E.L. Thomas, "Structure and Morphology of Segmented Polyurethanes I. Influence of Incompatibility on Hard Segment Sequence Length", *Polymer*, 24, 1327 (1983).
16. J.K. Corbett, "A Rapid Attenuated Total Reflectance Infrared Method for Toluene Diisocyanate Isomer Ratio Determination", *J. Appl. Chem. Biotechnol.*, 26, 88 (1976).

17. B. Fu, "Synthesis, Characterization, and Properties of Segmented Polyurethanes Containing Monodisperse Hard Segments", Ph.D. Dissertation, University of Massachusetts, 1984.
18. C.M. Brunette, "Structure-Properties Relationships in Polybutadiene Polyurethanes", Ph.D. Dissertation, University of Massachusetts (1982).
19. G.C. Pimentel and A.L. McClellan, The Hydrogen Bond, W.H. Freeman and Co., San Francisco, 1960.
20. P.C. Painter, private communication.
21. P.C. Painter, M.M. Coleman, and J.L. Koenig, The Theory of Vibrational Spectroscopy and its Application to Polymeric Materials, John Wiley and Sons, New York, 1982.
22. H. Tsubomura, "Nature of the Hydrogen Bond. II. The Effect of Hydrogen Bonding and Other Solute-Solvent Interactions upon the Shape and Intensity of the Infrared OH Band of Phenol", J. Chem. Phys., 23, 2130 (1955).
23. H. Tsubomura, "The Nature of the Hydrogen Bond. III. The Measurement of the Infrared Absorption Intensities of Free and Hydrogen Bonded OH Bands. Theory of the Increase of the Intensity Due to the Hydrogen Bond", J. Chem. Phys., 24, 927 (1956).
24. L. Rebenfeld, P.J. Makarewicz, H.D. Weigmann, and G.L. Wilkes, "Interactions Between Solvents and Polymers in the Solid State", J. Macromol. Sci., Rev. Macromol. Chem., C15, 279 (1976).
25. A.B. Desai and G.L. Wilkes, "Solvent-Induced Crystallization of Polyethylene Terephthalate", J. Polym. Sci., Polym. Symp., 46, 291 (1974).

26. J. Jonza, "Physical Studies of Thermoplastics", Ph.D. Dissertation University of Massachusetts (1985).
27. R.P. Kambour, F.E. Karasz, and J.H. Daane, "Kinetic and Equilibrium Phenomena in the System: Acetone Vapor and Polycarbonate Film", J. Polym. Sci., A-2, 4, 327 (1966).
28. J.P. Mercier, G. Croeninch, and M. Lesne, "Some Aspects of Vapor-Induced Crystallization of Polycarbonate of Bisphenyl A", J. Polym. Sci., Polym. Symp., 16, 2059 (1967).
29. R.S. Porter, private communication.
30. C. Eisenbauch, private communication.
31. Y. Camberlin, J.P. Pascault, M. Letoffe, and P. Claudy, "Synthesis and DSC Study of Model Hard Segments from Diphenyl Methane Diisocyanate and Butane Diol", J. Polym. Sci., Polym. Chem. Ed., 20, 383 (1982).

C H A P T E R I V
MONTE CARLO SIMULATION OF POLYURETHANE
HARD SEGMENT SEQUENCE DISTRIBUTION

Introduction

In the previous chapter the physical properties of a polyurethane elastomer were shown to be dependent on the thermal history of the system. It was proposed that at a critical temperature the initial distribution of hard segment sequence lengths is permanently altered by a urethane interchange reaction termed "transurethanification". This reaction was likened to the ester interchange reaction which is common to polyester copolymers. In this chapter a quantitative approach is taken in the determination of hard segment sequence distributions by modeling this system using a Monte Carlo computer simulation of the polymerization process.

The physical and mechanical properties of a copolymer system have long been known to depend on the distribution of sequences of dissimilar monomer residues. This has led to a great deal of interest in the determination of copolymer sequence distributions, although experimental approaches to this problem have been limited. High resolution NMR has been a valuable technique in determining sequence distributions of some systems (1,2). The number of chain atoms in the monomer units of polyurethane copolymers, however, precludes its usefulness in characterizing polyurethane sequence distributions. One experimental

approach that has been useful is the selective depolymerization of a polyurethane-urea system using perchloric acid (3). Using this method the distribution of hard segment sequences was found to deviate from that of a random system and was attributed to the unequal reactivity of the two isocyanate groups of 4,4'-diphenylmethane diisocyanate (MDI).

The majority of investigations of sequence distributions in segmented copolymers have taken a theoretical approach to this problem by modeling the polymerization process. Deterministic approaches have utilized differential equations of the time rate of change of the various compounds of the reaction mixture (4,5). This method involves the solution of an infinite set of differential equations to determine the molecular weight distribution. A more common statistical approach utilizes probabilistic equations to model the polymerization reaction. This method is more limited than the deterministic approach in that the equations for the distribution of chain lengths or sequence lengths are defined in terms of a specific time or extent of reaction rather than for the general case (6).

Peebles has utilized the probabilistic approach for calculating hard segment sequence lengths of segmented polyurethanes under a variety of starting conditions (7,8). This work took into account the kinetic effect of unequal functional group reactivity and its corresponding effect on hard segment sequence distributions. The reactivity of the first group of an isocyanate is greater than that of the second group due to induction resonance effects (9). In some cases, steric interactions can also result in unequal reactivity ratios (10).

Through these calculations, Peebles found that unequal reactivities of isocyanate functional groups can result in a hard segment sequence distribution which is narrower than for a randomly polymerized system.

These methods have indeed proved useful in developing a better understanding of the effect of reaction kinetics on sequence distributions. However, none have dealt with the more complex situation of reactants involving a diisocyanate that is a mixture of two isomers as corresponds to the polyurethane investigated in this study. Here we are concerned with the effect of functional group reactivity of the 2,4 and 2,6 isomers of toluene diisocyanate (TDI), on the specific isomer sequence distribution for a solution polymerized polyurethane. While a probabilistic approach to the problem is possible, the complexity of the system would result in derivations of the formal mechanisms that are unwieldy and tedious. For this reason a Monte Carlo computer simulation of the two step polyurethane polymerization was chosen. This type of approach to determining sequence distributions in step growth polymers has been reported by several authors (11,12). Recent work by Johnson and O'Driscoll involved a Monte Carlo simulation of polymerization by the process of reaction injection molding (RIM) (12). In this type of polymerization the reactants are blended in one step and injected directly into a mold cavity. The distribution of sequence lengths was determined for the case where the chain extender hydroxyl groups were more reactive than soft segment hydroxyl groups and for the case where the first isocyanate group of the diisocyanate monomer is more reactive than the second

group. In both cases it was found that the sequence distributions were relatively insensitive to functional group reactivities for this one step polymerization simulation.

The complexity of the simulation in the present investigation is extended to account for the fact that the polymer being modeled was prepared by a two step process and that the TDI used was a mixture of two isomers having functional groups of differing reactivities. The para group of 2,4 TDI is taken to be 12 times more reactive than the ortho groups of either isomer (9). Simulation conditions are used to model the sequence distributions in the "as polymerized" state as well as for a random system which corresponds to the polymer after heat treating results in hard segment scrambling (13,14). Of particular interest is the determination of the distributions of sequences having consecutive runs of the 2,6 isomer as they are known to develop order as a crystalline or paracrystalline phase.

Simulation Program

The simulation routine was developed for the determination of hard segment sequence lengths and isomer distributions for segmented copolymers which are prepared by step growth polymerization. While this program is applicable to step growth polymerization in general, it will be discussed in terms of a two step polyurethane polymerization. The program is written in Pascal for use with an IBM CS 9000 laboratory microprocessor. This computer is equipped with two megabytes of random

access memory which is the limiting factor for the number of monomer units assembled in this simulation. Two distinct sections comprise the simulation routine. In the first section, a pseudo-infinite molecular weight polymer is assembled from difunctional monomers and in the second section the sequence and isomer distributions are mapped and tabulated.

Polymerization Simulation

Since the major concern in this simulation is the determination of sequence lengths as well as the ordering of both asymmetric and symmetric monomer residues, pointing arrays are used to keep track of the status of each individual functional group. As the simulation progresses the elements of the arrays are filled with labels so as to define with which one of the complementary functional groups it has been coupled. Each element, "index value", of the array corresponds to a specific functional group. One array points to the index of the functional group at the opposite end of the unreacted monomer and the second array points to the functional group to which it has been coupled. One pair of arrays is used to keep track of hydroxyl groups while the other is used to keep track of the isocyanate groups. Since this program is designed to simulate isomer sequences for TDI which is a mixture of the 2,4 and 2,6 isomers, the NCO arrays must be partitioned so as to distinguish the two monomer types and two NCO group types. The two NCO groups of 2,6 TDI both have ortho substitution relative to the methyl group while the 2,4 TDI has one ortho NCO group

and one para NCO group. An example of the partitioning of the index values in the NCO array is depicted in Figure 4.1a. This array is representative of 20 isocyanate groups (10 TDI molecules) of which 80% are the 2,4 isomer and 20% are the 2,6 isomer. The first 16 elements correspond to the 2,4 isomer with the first half of those corresponding to the functional group with para substitution. The last four elements represent the NCO groups of the 2,6 isomers. In this manner, the para substituted isocyanates are grouped in the beginning of the array and the ortho functional groups at the end. The double-headed arrows designate the pairing of functional groups for each difunctional TDI residue. Since the para and ortho NCO groups are of unequal reactivity, this partitioning facilitates the random selection of isocyanate groups as they react at a rate which is weighted by their reactivity as well as the number of units of each type remaining. The reaction sequence is then determined separately for both the ortho and para groups by using a randomization function to generate arrays with the index values scrambled. This is depicted in Figure 4.1b. As either an ortho or para group is reacted, the appropriate index value is selected at the pointer and the pointer is moved up to the next available index of that type. A weighted randomization function is used to determine whether an ortho or para group is selected. The probability that a para group will react next is determined using equation 4.1

$$P_{\text{para}} = \frac{N_{\text{para}} \cdot R_{\text{para}}}{N_{\text{para}} \cdot R_{\text{para}} + N_{\text{ortho}} \cdot R_{\text{ortho}}} \quad (4.1)$$

where P_{para} is the probability of a para group reacting, N_{para} and

FIGURE 4.1: Indexing array for ortho and para NCO groups of the 2,4 and 2,6 TDI molecules.

- a. Before randomization showing partitioning of NCO types.
- b. After randomization.

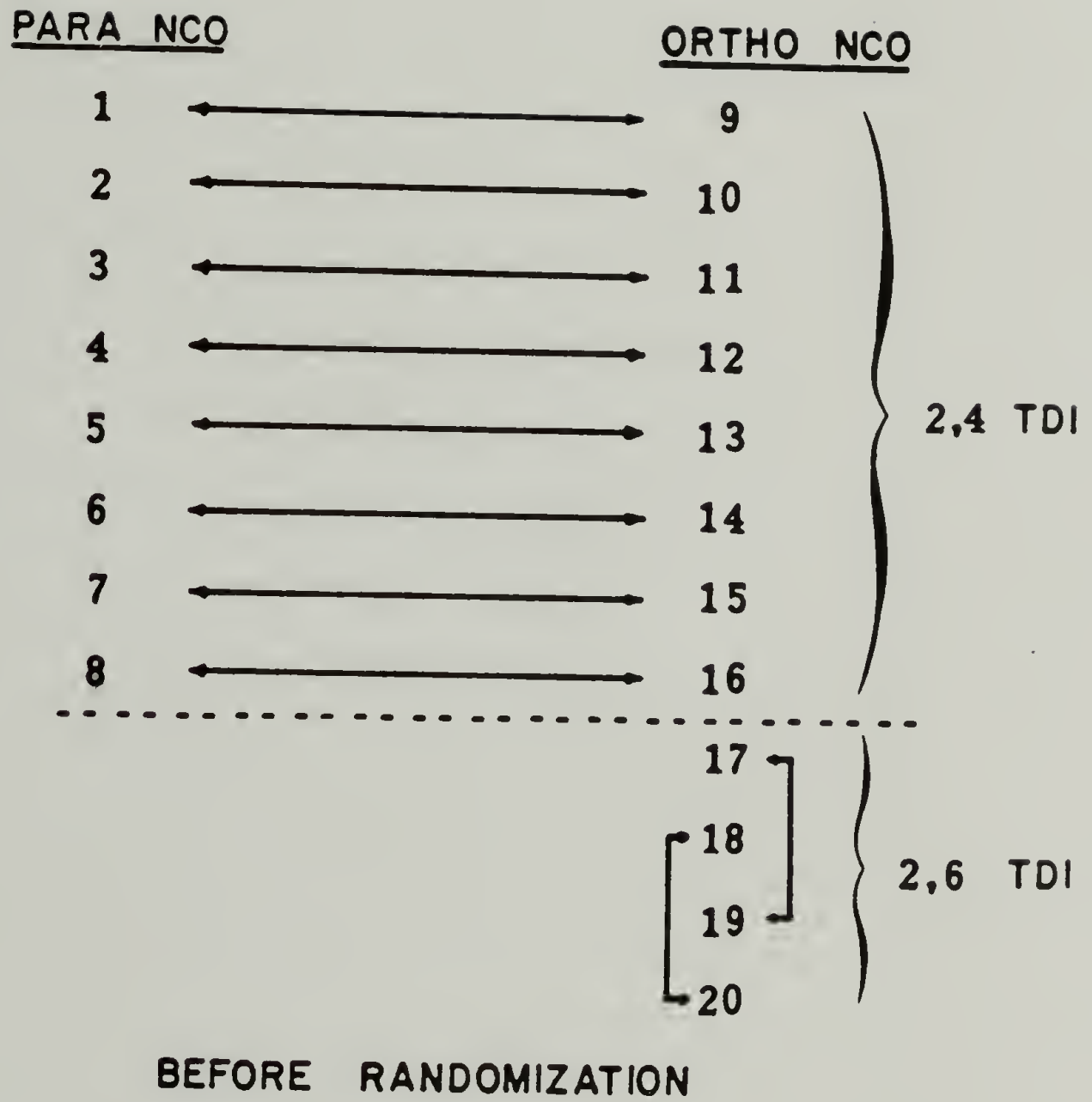


Figure 4.1a

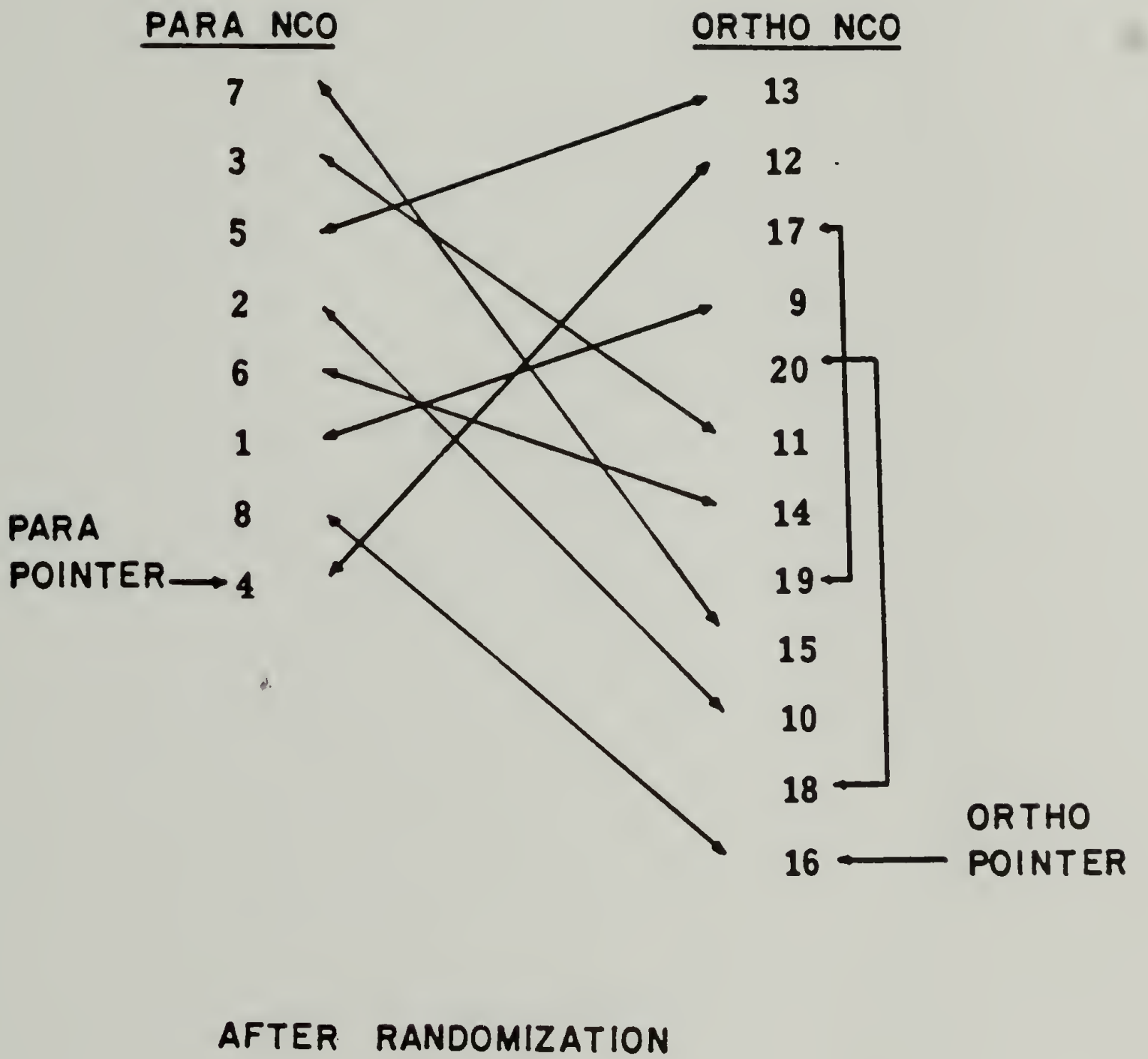


Figure 4.1b

N_{ortho} are the respective numbers of unreacted para and ortho NCO groups, and R_{para} and R_{ortho} are the relative reactivities for the para and ortho functional groups. A random number is then generated having a value between 0 and 1. If the random number is below P_{para} , the next available para NCO group is reacted. Otherwise, the next available ortho NCO group is chosen.

The determination of the sequence of reaction for the hydroxyl groups is less complicated than for the isocyanate groups. Since the reaction being modeled is a two step polymerization, first all of the hydroxyl groups of the soft segments are reacted and then the hydroxyl groups of the chain extender molecules are reacted. The soft segment hydroxyls are reacted sequentially in the order of their index value. Randomization is not necessary as only the sequence distributions of the hard segments are being considered for this reaction simulation. In contrast to the soft segment groups, it is necessary to randomize the order of reaction of the chain extender hydroxyl groups (so that hard segment sequences are statistical in nature). By maintaining exact stoichiometry of functional groups, the finished polymer is made up of several pseudo-infinite molecular weight rings and there are no chain ends.

Determination of Sequence Distributions

The second section of the program tabulates the total hard segment length distribution as well as the distributions of specific isomer sequences. Of particular interest is the determination of weight frac-

tions of sequential runs of the 2,6 TDI isomer. The counting begins at the soft segment end of index value "1". The hard segment sequence that is attached here is mapped by finding the index value of the attached NCO group. The opposite end of this TDI molecule is found using the appropriate pointer array. Next, the first chain extender hydroxyl group is found and its opposite end is pointed to. The hard segment sequence is mapped in this manner to its end, when a soft segment hydroxyl is pointed to. The soft segment hydroxyl is labeled as having is adjacent hard segment checked and the complete isomer sequence of this hard segment is recorded. This procedure is followed for the next unchecked sequence until all sequences have been tabulated. The tabulated distribution is stored on magnetic disc.

Determination of Standard Deviations

A separate computer program was written to determine the average values and standard deviations of sequence distributions for multiple simulations that each use the same starting conditions. A typical determination involved twenty simulations that were each run with the same starting conditions. A primary consideration was the effect of the total number of monomers used in the simulation on the accuracy of the determination.

Results and Discussion

Several probabilistic approaches to the determination of hard

segment sequence distributions have demonstrated that a most probable distribution is followed for systems with functional groups having equal reactivity (7,8,12,15). This is the same distribution as that of Equation 4.2 as derived by Flory for molecular weight distributions of step growth polymers (16)

$$w_x = x(1-p)^2 p^{x-1} \quad (4.2)$$

In this equation, x is the number of units in the hard segment, w_x is the weight fraction of hard segments of length x and P is a probability term related to the mole ratio of TDI to soft segment molecules, r , by

$$P = 1 - \frac{1}{r} \quad (4.3)$$

The derivation of Equation 4.2 can be most easily considered in terms of the mole ratio of chain extender molecules to diisocyanate molecules. This ratio is always less than 1 and has the value of P for stoichiometric conditions. It is the probability that any one isocyanate group in the hard segment is reacted with a chain extender molecule. Soft segments need not be considered as they serve only to separate hard segment sequences. The equation for the distribution of sequence lengths can be developed following the method of Flory (17). The first TDI residue of a hard segment has one urethane linkage attached to a soft segment. The probability that the other urethane group of this residue is attached to a chain extender molecule is P . Due to the monomer ratio, all hard segments are terminated with a TDI residue. Therefore, the chain extender residue is capped by a second

diisocyanate molecule with the probability of P that its second urethane linkage is coupled to a chain extender molecule. This continues on for $X-1$ TDI residues for a sequence of length X . The probability that the last group is coupled to a soft segment is $1-P$. The total probability for the existence of this hard segment is given by:

$$n_x = p^{x-1}(1-p) \quad (4.4)$$

where n_x is the fraction of hard segments having x TDI residues. For a finite system, the total number of hard segments of length x is given by:

$$N_x = N(1 - p)p^{x-1} \quad (4.5)$$

where N is the total number of hard segments in the system. If N_0 is the total number of TDI residues, then:

$$N = N_0(1-p) \quad (4.6)$$

resulting in the following equation

$$N_x = N_0(1-p)^2 p^{x-1} \quad (4.7)$$

The weight fraction of TDI residues in each segment is proportional to x and can be written as

$$w_x = x \frac{N_x}{N_0} \quad (4.8)$$

Substituting this expression into Equation 4.5 completes the derivation of Equation 4.2

$$w_x = x(1-p)^2p^{x-1} \quad (4.2)$$

To check that the new Monte Carlo step growth simulation program followed true random statistics, the generated sequence distributions were compared to values determined using Equation 4.2. The values used for the mole ratio of TDI to soft segment molecules, r , was chosen as 3.3. This is the same hard segment mole ratio as for the sample characterized in Chapter III. The parameters used for this determination are listed in Table 4.1. The continuous function of Equation 4.2 along with weight fraction calculated with the simulation are shown in Figure 4.2. Error bars on the values determined with the simulation represent σ , the standard deviations for the weight fraction of each sequence length when the simulation is repeated twenty times. The standard deviation sets a confidence level for the accuracy of the determination. Simulations with a larger number of monomers will more closely follow a random distribution. The standard deviations of the weight fractions have been determined for several simulations having different magnitudes of the total number, N_0 , of TDI groups assembled. The standard deviation of the weight fraction for a sequence of one TDI residue is plotted as a function of the size of the system in Figure 4.3. In this plot it is found that the standard deviation of the determined weight fraction is inversely proportional to the square root of the number of elements in the system. This straight line relationship is expected for truly random systems. Although the confidence with which weight fractions are predicted improves as the magnitude of the system is increased, computer memory size as well as computation

TABLE 4.1

Polymerization Simulation Parameters

	(Random)	T3MI
Soft segment OH groups	1000	1000
NCO groups	3300	3300
2,4 TDI	80%	80%
2,6 TDI	20%	20%
Para reactivity	12	1
Ortho reactivity	1	1
Extender OH groups	2300	2300

FIGURE 4.2: Most probable distribution of hard segment lengths for TDI/soft segment mole ratio of 3.3 (— : from equation 4.2; *: values generated by the Monte Carlo method).

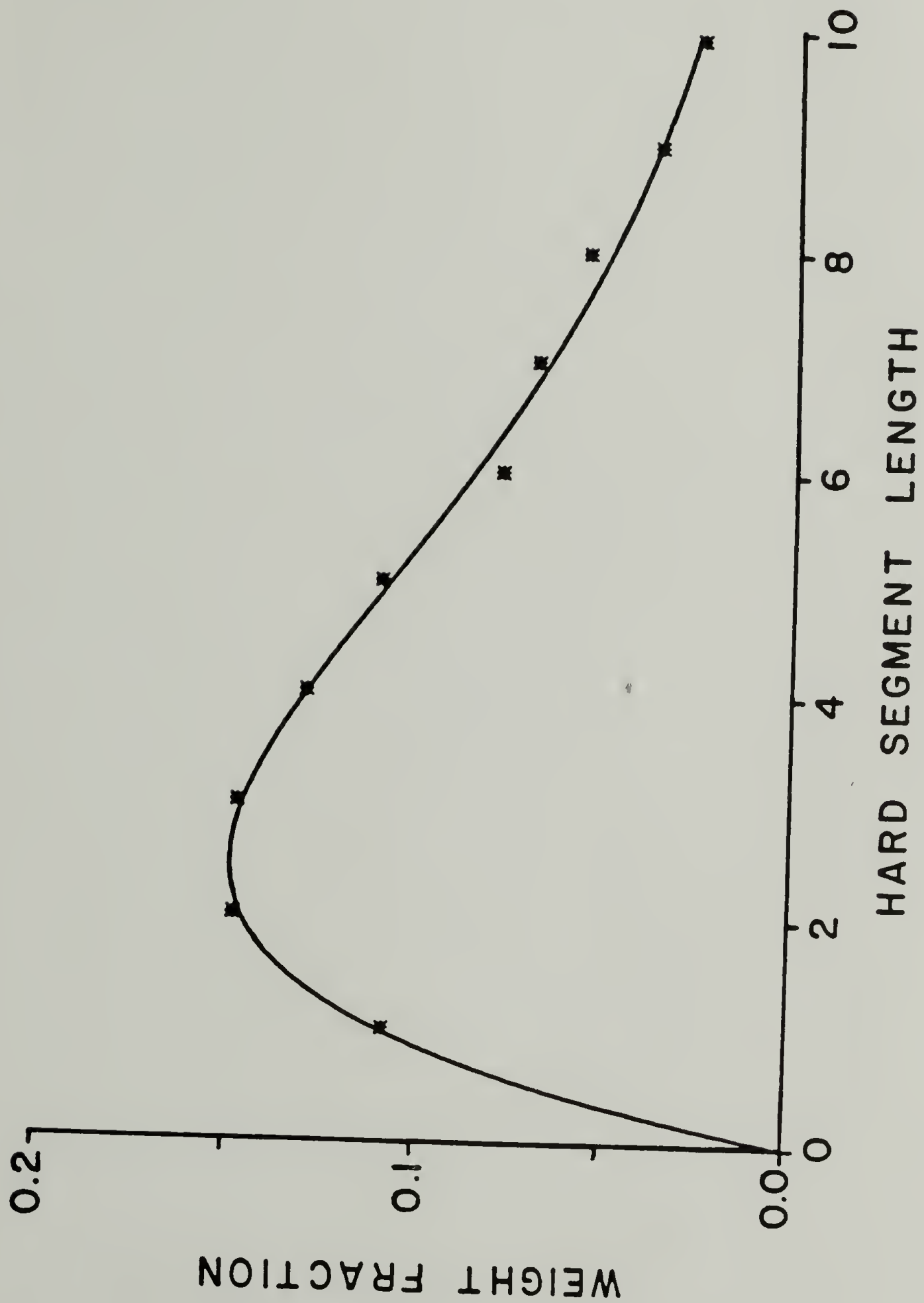


Figure 4.2

FIGURE 4.3: Standard deviation for segment of one TDI unit plotted as a function of the size of the ensemble.

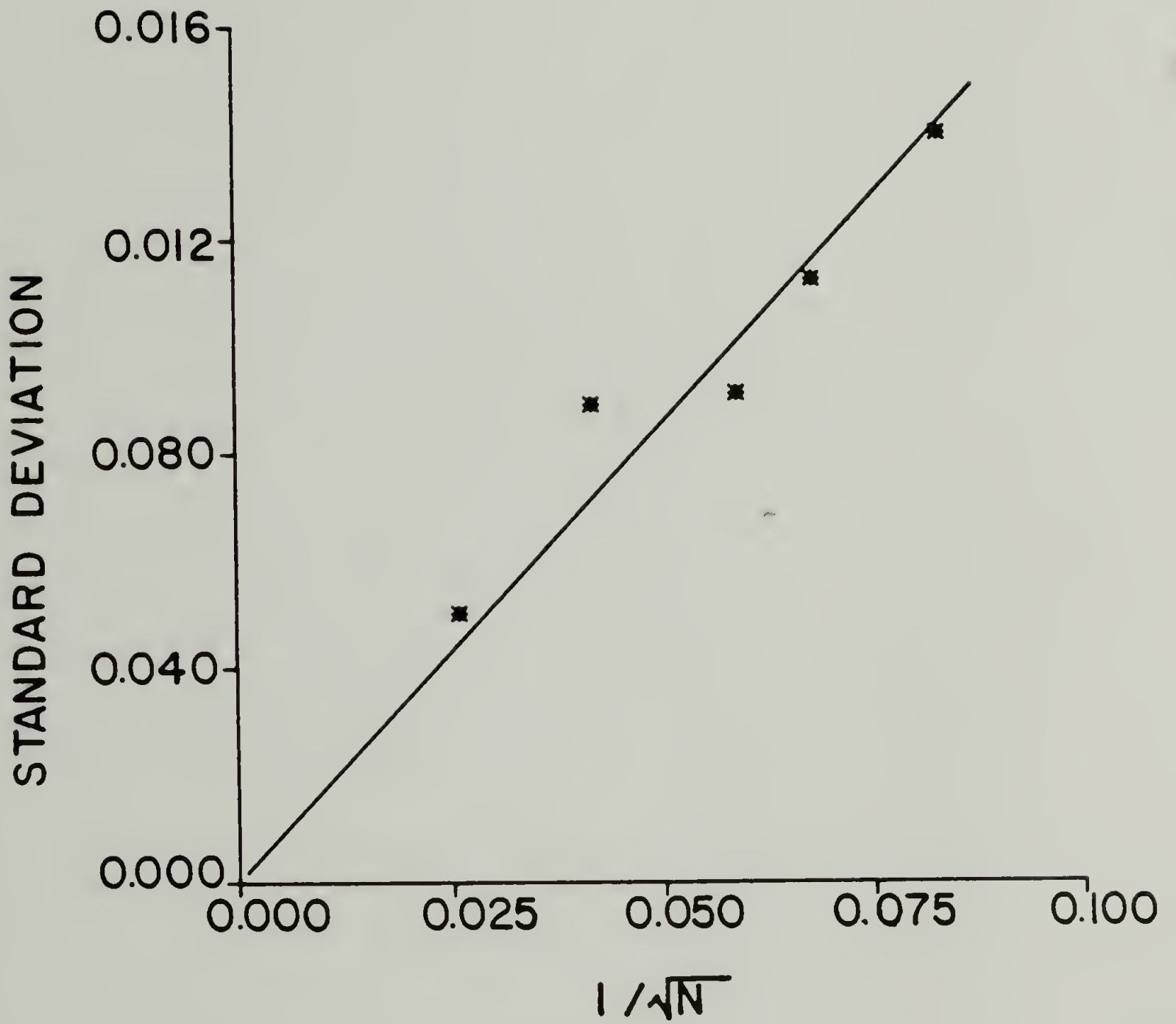


Figure 4.3

time sets an upper limit on the size of these simulations. For this reason, 500 soft segment units was chosen as the optimum number for use in these simulations.

The polyurethane sample (T3MI) characterized in Chapter III has a hard segment sequence distribution that deviates from the most probable distribution due to the unequal reactivities of the isocyanate groups of the 2,4 isomer in the mixed isomer TDI. The parameters that were chosen to simulate the polymerization of this sample are listed in Table 4.1. Since the 2,4 isomer comprises 80% of the diisocyanate mixture and this molecule has an isocyanate in the reactive para position it tends to dominate the first step of the two step polymerization. In this first step the soft segment prepolymers are endcapped with excess diisocyanate. The para isocyanate groups, being more reactive, are consumed more rapidly than the ortho isocyanate groups.

In Figure 4.4 the unreacted fractions of the two functional group types are shown as a function of total isocyanate consumption for three different reactivity ratios. When the reactivity of the ortho and para groups is equal the fraction of groups unreacted will maintain the same ratio throughout the reaction. This results in the two functional group types occurring in random distribution throughout the hard segments. With a reactivity of para:ortho of 12:1, the para isocyanate groups are consumed more rapidly than those in the ortho position despite its lower concentration. As the fraction of para groups becomes exceedingly small the reaction of the ortho groups is more prevalent. The dashed line in Figure 4.4 corresponds to the division

FIGURE 4.4: Unreacted fraction of NCO units as a function of total groups reacted (*: para groups; ■: ortho groups).

- Para/ortho reactivity ratio = 1.
- Para/ortho reactivity ratio = 2.
- Para/ortho reactivity ratio = 4.

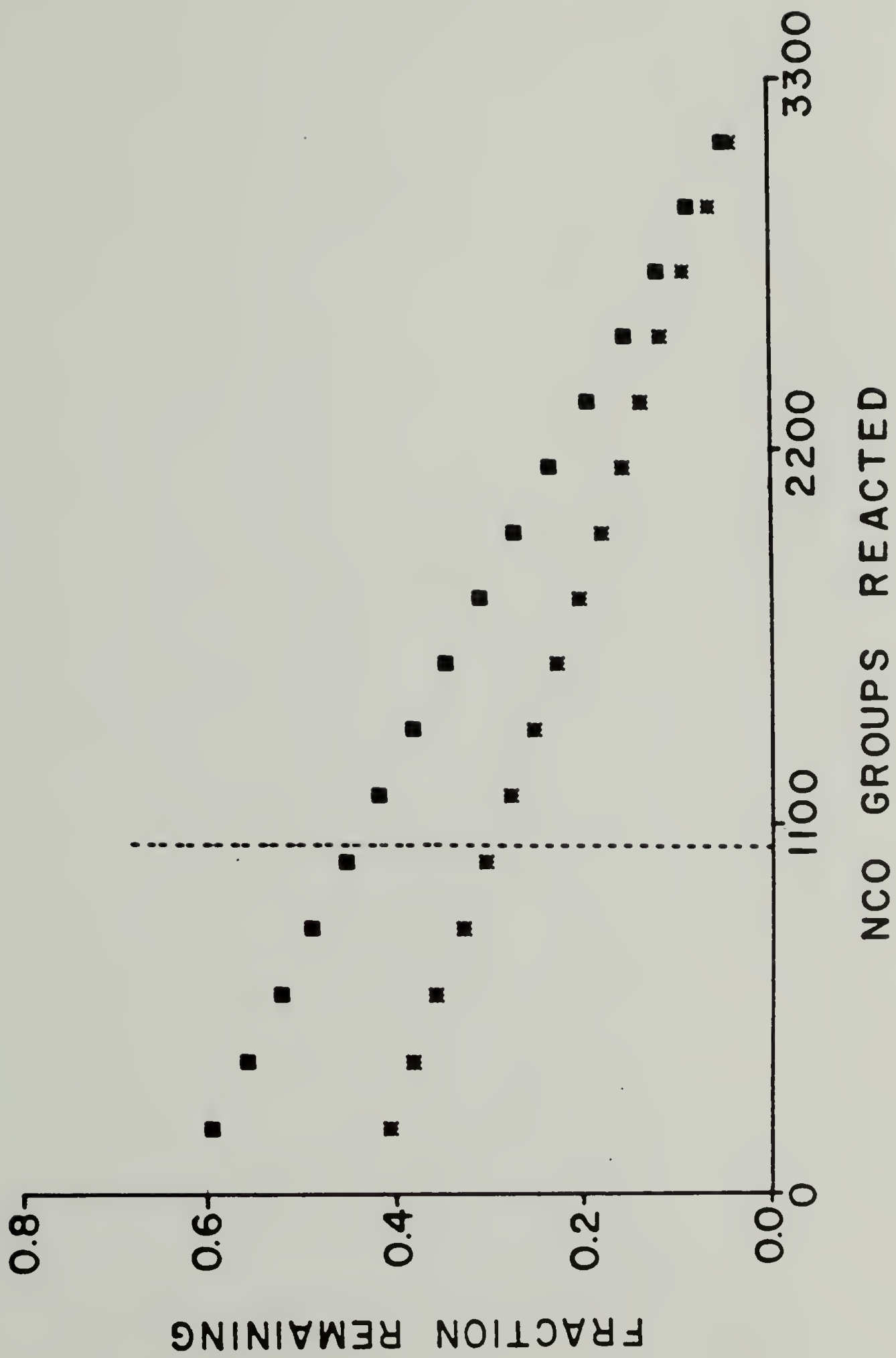


Figure 4.4a

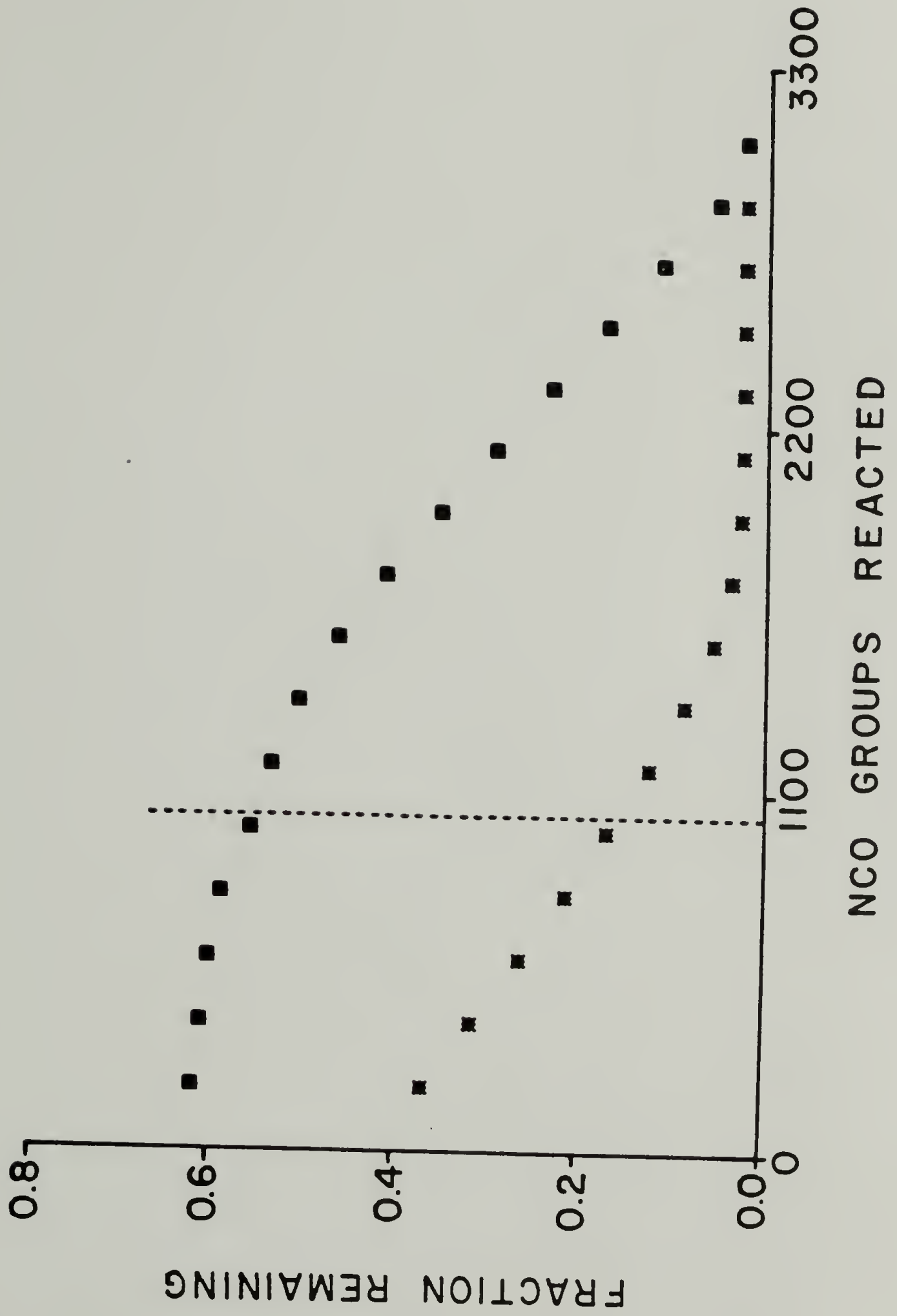


Figure 4.4b

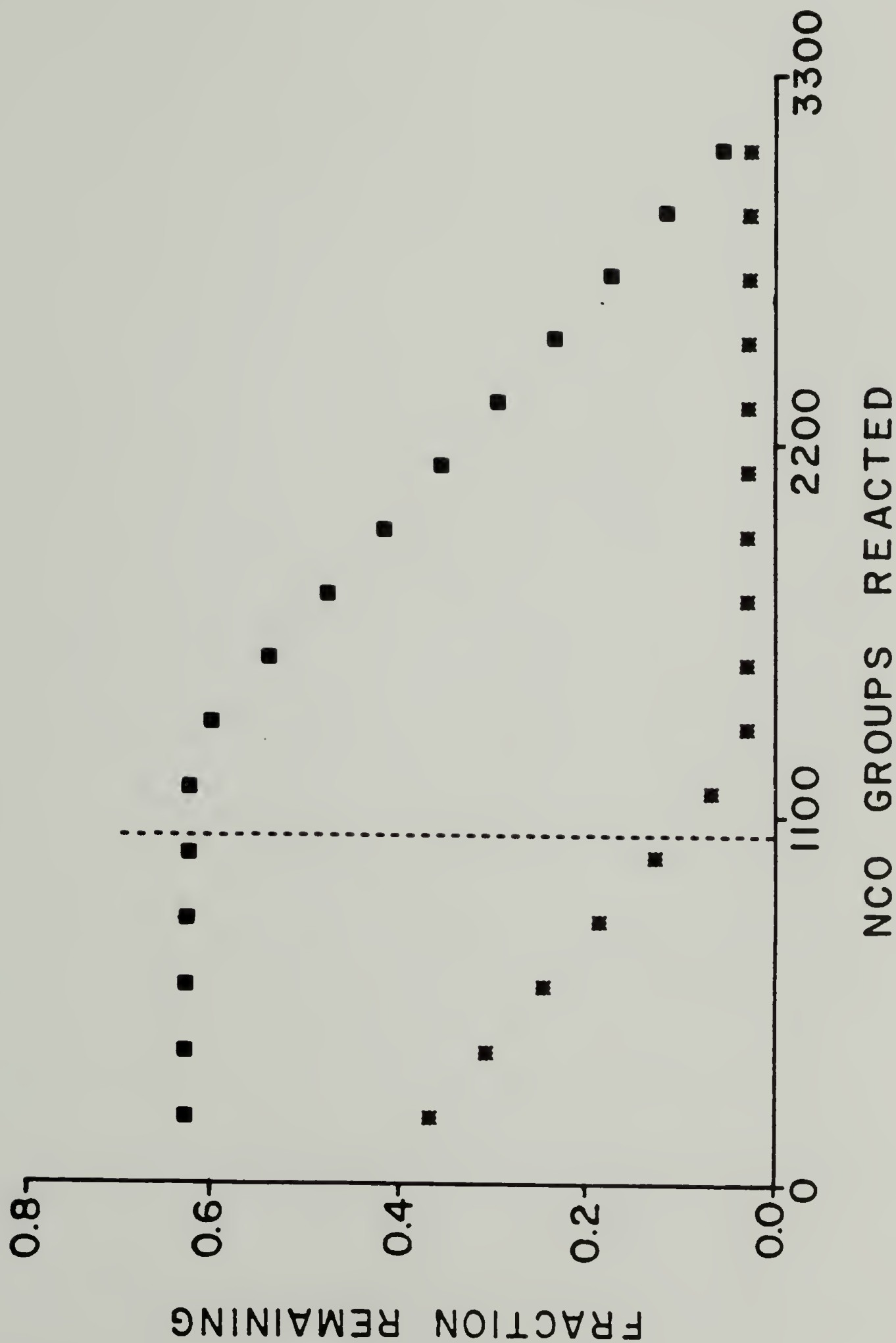


Figure 4.4c

between the endcapping step and chain extending step. It is evident that a major fraction of NCO groups in the para position become reacted with soft segment prepolymers. This results in a high percentage of hard segment sequences being terminated with 2,4 TDI residues with the para position facing away from the hard segment. Another manifestation of the unequal reactivity ratio is to decrease the fraction of isolated TDI residues that couple soft segments. A hypothetical case of the para isocyanate group being 1000 times more reactive than the ortho is shown in Figure 4.4c. Under these conditions, all of the para groups react before any of the ortho groups. Since there are sufficient para isocyanate groups to endcap all soft segments, there would be no sequences containing only one TDI residue.

The simulated hard segment sequence distribution which models our polymer system is shown in Figure 4.5 along with the curve for the most probable distribution. This distribution of sequence lengths is narrower than the most probable distribution due to the unequal reactivities that were assigned to the isocyanate groups. This is in agreement with the previous work of Peebles (8). The weight fraction of TDI residues which are isolated between soft segments is less than one half of that for the most probable case.

Of particular interest in this study is the determination of the distributions of sequences of consecutive 2,6 TDI residues. The sample characterized in the previous chapter had microstructural ordering that was attributed to organization of crystallizable sequences of 2,6 TDI linked by butanediol. Quantitative analysis by infrared spectroscopy indicated that the weight fraction of the ordered phase was 10% of the

FIGURE 4.5: Comparison of the distribution for the most probable case with that generated by Monte Carlo method for para/ortho reactivity ratio of 12/1 (— is for equation 4.2; *: computer simulation with reactivity ratio of 12/1).

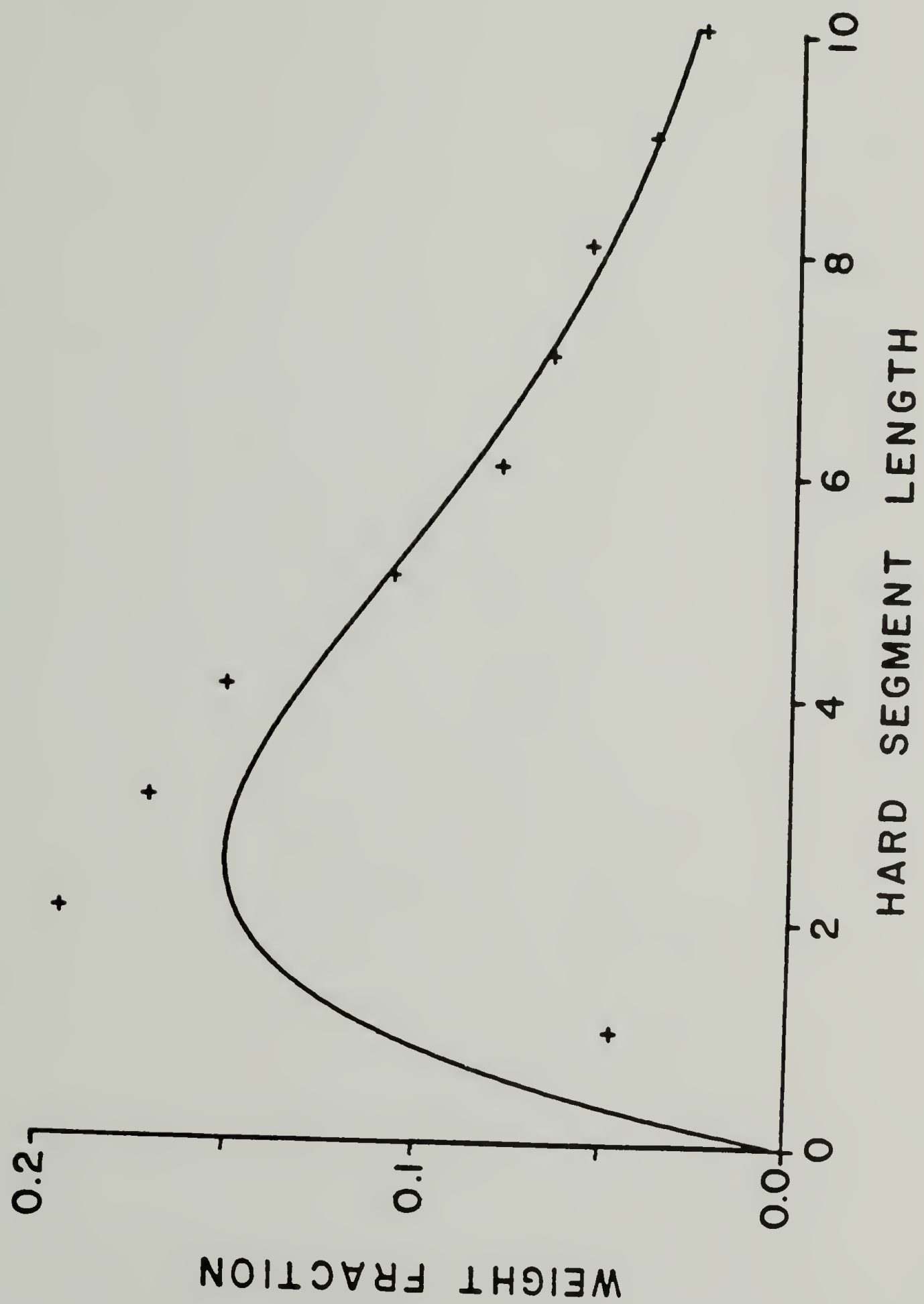


Figure 4.5

total hard segment fraction. The weight fractions as a function of length of the 2,6 isomer sequences as determined by the computer simulation are shown in Figure 4.6. This distribution is shown for the random case as well as for the case corresponding to the as polymerized situation. As can be seen in this figure, randomization results in an increase in the weight fraction of isolated 2,6 TDI residues and a corresponding decrease in the longer sequences. The longer sequences of the 2,6 isomer are of greater interest as they have a greater potential for crystallization. Choosing a value for the sequence length necessary for crystallization is quite arbitrary when considering the information available for this system. However, it is not unreasonable to consider a sequence of two 2,6 isomers as the minimum for crystallization to occur. The weight fraction of 2,6 TDI residues that are in sequences of two or more is 9% of the total. This value is comparable to the weight fraction of the ordered hard segment phase as determined by infrared spectroscopy. The weight fraction of sequences of two or more 2,6 units from a simulation of the random situation is one half that of the as polymerized case or approximately 5%. In the previous chapter virtually no ordered phase was found in the sample that had been randomized by heating at 170°. Even though the simulation for randomization of hard segments suggests that 5% of the 2,6 residues are in consecutive runs of two or more units this may result in an insufficient density of these units for nucleation of ordered growth to occur.

FIGURE 4.6: Distributions of weight fractions of consecutive 2,6 TDI sequences (\square : most probable case; \blacktriangle : para/ortho reactivity of 12/1).

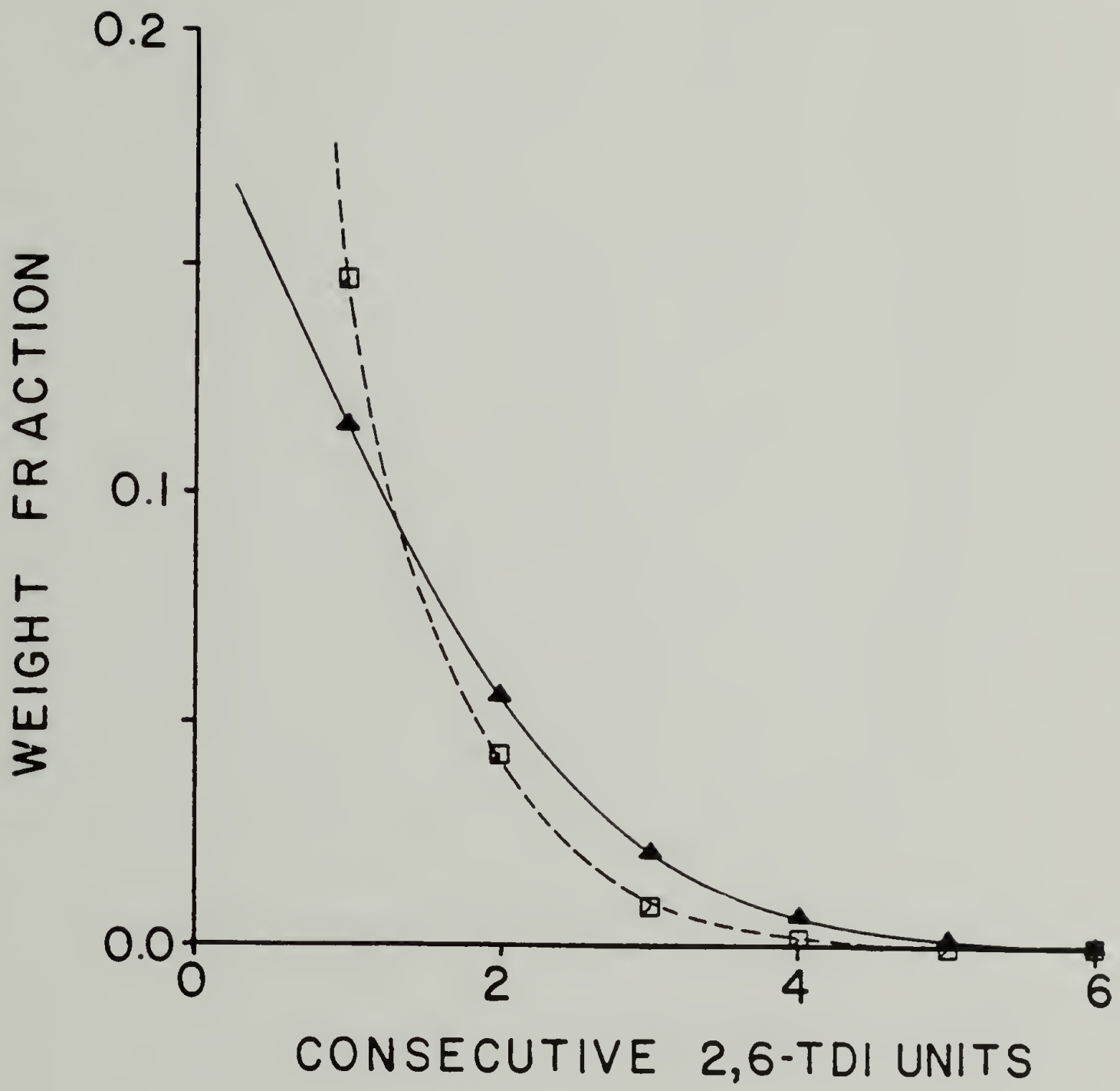


Figure 4.6

References

1. R. Yamadera and M. Murano, "The Determination of Randomness in Copolyesters by High Resolution Nuclear Magnetic Resonance", *J. Polym. Sci.*, A1 5, 2259 (1967).
2. F.A. Bovey, High Resolution NMR of Macromolecules, Academic Press, New York, 1972.
3. H. Suzuki and H. Ono, "Studies of the Structure of Polyurethane Elastomers. I. The Number-Average MW Determination of the Hard-Segments in the Poly(Ether) Urethane Elastomer by Means of Perchloric Acid Depolymerization", *Bull. Chem. Soc. Japan*, 43, 682 (1970).
4. W.H. Ray and R.L. Laurence, Chemical Reactor Theory, Prentice-Hall, Englewood Cliffs, New Jersey, 1977.
5. W.H. Ray, "On the Mathematical Modeling of Polymerization Reactors", *J. Macromol. Sci.*, (Rev. Macromol.Chem), 8, 1 (1972).
6. E. Sorta and A. Melis, "Block Length Distribution in Finite Polycondensation Copolymers", *Polymer*, 19, 1153 (1978).
7. L.H. Peebles, Jr., "Sequence Length Distribution in Segmented Block Copolymers", *Macromol.*, 7, 872 (1974).
8. L.H. Peebles, Jr., "Hard Block Length Distribution in Segmented Block Copolymers", *Macromol.*, 9, 58 (1976).
9. R.W. Lenz, Organic Chemistry of Synthetic High Polymers, Interscience, New York, 1967.
10. J.W. Burkus and C.F. Eckert, "Kinetics of Triethylamine-Catalyzed Reaction of Diisocyanates with 1 Butanol in Toluene", *J. Am. Chem. Soc.*, 80, 5948 (1958).

11. M. Falk and R. Thomas, "Molecular Size Distribution in Random Polyfunctional Condensation with or without Ring Formations Computer Simulation", *Can. J. Chem.*, 52, 3285 (1974).
12. A.F. Johnson and K.F. O'Driscoll, "Monte Carlo Simulation of Sequence Distributions in Step Growth Copolymerization", *Eur. Polym. J.*, 20(10), 979 (1984).
13. Y. Camberlin, J.P. Pascault, M. Letoffe, and P. Claudy, "Synthesis and DSC Study of Model Hard Segments from Diphenyl Methane Diisocyanate and Butane Diol", *J. Polym. Sci., Polym. Chem. Ed.*, 20, 383 (1982).
14. C.D. Eisenbauch, "Synthesis and Properties of Model Urethane Oligomers and Monodisperse Soft Segment for Segmented Polyurethanes", Workshop on the Structure of Polyurethane Elastomers, June 28-29, Boston (1984).
15. F. Lopez-Serrano, J.M. Castro, C.W. Macosko, and M. Tirrell, "Recursive Approach to Copolymerization Statistics", *Polymer*, 21, 263 (1980).
16. P.J. Flory, "Molecular Size Distribution in Linear Condensation Polymers", *J. Am. Chem. Soc.*, 58, 1877 (1936).
17. P.J. Flory, Principles of Polymer Chemistry, Cornell University Press, London, 1953.

C H A P T E R V

TECHNIQUE DEVELOPMENT OF SOFTWARE SYNCHRONIZED TIME RESOLVED INFRARED SPECTROSCOPY

Introduction

The study of the dynamics of microstructural changes occurring with deformation is of great importance in understanding the structure-property relationship of polymers. Previously, the motions of the various structural subunits have been characterized by a combination of dynamic x-ray, light scattering, and birefringence techniques (1-3). Unlike the techniques mentioned above, vibrational spectroscopy possesses high selectivity, i.e. the ability to distinguish chain segments of various conformations and environments. Therefore, if sufficiently high temporal resolution can be achieved, vibrational spectroscopy can be a powerful characterization tool to follow the deformation induced conformation or orientation changes.

The dynamics of structural change occur in times as short as milliseconds. Until very recently, vibrational spectroscopy has generally been used to characterize stationary phenomena or events lasting much longer than the measurement time. The development of the time resolved Fourier transform technique has greatly enhanced the utility of vibrational spectroscopy in following structural changes (4-8). The principles representing several different approaches to this type of time resolved Fourier transform infrared spectroscopy have

been presented in a number of publications (4,6,9,10). Each one of these approaches incorporates some form of ordered sampling technique which generally involves sorting the collected raw data to obtain properly time ordered interferograms. In all cases, spectroscopic data of high temporal resolution is obtained by establishing a definite phase relationship between the temporal variation of the external event, such as deformation, and the interferogram sampling. In our experiments, we employ a commercial fast scanning interferometer, therefore, the phase relationship between the spectrometer and the external event can be established in two ways. We let the external event be controlled by the interferometer sweep signal or alternatively we have correlated the timing of the spectrometer and the external event using an external master clock (11). The first scheme has the advantage that an accurate phase relationship can be maintained with minimal hardware modification. However, this involves stepwise deformation which gives rise to transient effects in polymers. Therefore, it cannot be correlated well with mechanical information obtained from techniques such as rheovibron. The second scheme is a more useful technique which allows the deformation event to run continuously. However, initiation of the external event and the interferogram scan are uncorrelated. Therefore, if experiments demand high time resolution, significant signal averaging is required, resulting in long experimental times.

In this report a new technique is presented whereby the efficiency of data collection is improved. We have incorporated the use of a

separate microprocessor in addition to the one associated with the FTIR for the purpose of controlling the external event. By monitoring a signal which corresponds to the interferometer cycle time, this microprocessor is able to phase-lock the external event to the interferometer scan cycle. Thus the spectroscopic signal corresponding to the same segment of time can be accumulated very efficiently. This newly developed scheme eliminates the need to construct specialized electronic timing circuitry or to write program patches in assembler language for control purposes. All programs for this new method were written in Pascal. Two versions of the synchronization program have been implemented: one for use with a continuous sinusoidal deformation event; and one for use with a periodic programmed event. A detailed description of the newly developed scheme and its applications is reported here.

Technique Development

Because FTIR provides the multiplex and throughput advantage, it achieves a higher speed of spectral acquisition than dispersive instruments. Even so, if one wishes to observe short time phenomena, it is necessary to make a compromise between the signal to noise ratio and spectral resolution of the obtained data. The limit of the conventional FTIR is reached when the time period required for one interferometer scan is longer than the time resolution required to describe the physical phenomenon. This limitation led to the development of time resolved Fourier transform spectroscopy (TRS).

The principles representing several approaches to TRS have been described in detail previously (4,6,9). In all cases an interferogram,

$I(\delta_j)$, covers the sampled data points from $j=1$ to the maximum number, NDP, each taken at equal intervals of retardation (δ_j). TRS observed the time varying sample event (polymer stretching, laser induced chemical events, etc.), by dividing it into discrete time elements, t_j , separated by the equal time width, Δt . For a TRS experiment which takes the interferogram points, $I(\delta_j t_j)$, as a function of both time and retardation, several schemes exist to collect the data for all δ_j and t_j . When the collection is finished, the data points are sorted to reconstruct interferograms at constant time. Each resulting interferogram then contains data points ranging from δ_1 to the maximum retardation, δ_{NDP} , all collected for a particular event time, t_j . In our laboratory, fast scanning interferometers were used and consequently special hardware and software were designed and constructed for the purpose of TRS work (11).

Experimental

Three major components must be incorporated for this time resolved Fourier transform infrared technique: 1) FTIR, 2) microprocessor, and 3) external event. The FTIR used in our study is an International Business Machine model IR-98. The interferometer is housed in a vacuum bench. It is capable of both mid and far infrared analysis. In general, infrared data are obtained with 1 or 2 cm^{-1} spectral resolution. Full or partial spectra are stored on a magnetic disk system for further analysis. The control processor for the IBM has multitasking capability and can be programmed with higher level languages such as

Pascal or FORTRAN. The 8 bit microprocessor, purchased from H-Square, Palo Alto, CA, includes 64K random access memory, two serial ports, two eight line parallel ports, and two 8" floppy disk drives.

Several external event systems have been used with this TRS technique. These include continuous sinusoidal polymer deformation, a squarewave electric field applied to either poly(vinylidene fluoride) film or a thermotropic liquid crystalline compound, and polymer deformation with a squarewave strain function. Due to differences in the timing of electronic pulses necessary to drive these events, one version of the synchronization program was developed for the continuous sinusoidal event and a separate version for control of the squarewave events.

Two mechanical stretching devices were developed in this laboratory for the polymer deformation experiments. For the study discussed in this chapter the stretcher, driven by a Slo-Syn 1/4 horsepower stepping motor, is used to apply a sinusoidal deformation to the sample through a cam which rotates at a constant rate. The stepping motor is microprocessor controlled through a digital stepper driver interface card purchased from Advanced Micro Systems. Four 12 V d.c. power leads supply the current from the stepper driver card to the motor. Internal logic of the driver card switches these power leads in a specific sequence to cause the motor to step either a 200th (full step mode) or 400th (half-step mode) of a full revolution. The half step mode has been used exclusively in our experiments to maintain a smoother deformation cycle. The second type of stretching device is powered by a

d.c. solenoid and results in a square wave strain function. It is controlled using the second version of the synchronization program. In the "on" state the sample is deformed to a constant strain level and in the "off" state it is relaxed to the unstrained state. This device is described in greater detail in the following chapter.

Continuous Sinusoidal Event

The mechanical properties of polymers are most often analyzed by applying a continuous periodic strain function. In our past experiments, we developed highly specialized time circuits to oversee both the interferometer movements and the sample events (11). Furthermore, a considerable amount of software was written to enable the minicomputer of the FTIR system to access information from the external event and incorporate it with the spectroscopic data obtained. Although the TRS package is flexible and can be applied to a large number of experiments with different time resolutions achievable, a substantial effort would be necessary to adapt it to other spectrometer systems. To overcome this disadvantage we have incorporated a microprocessor into the TRS experiment. Its function is to control the external event, subject to the interferometer movements. Using this scheme, the FTIR is essentially decoupled from the external event. Its function is to collect the interferograms and store them on the magnetic disk system. All the interferograms may be coadded using the standard signal averaging technique common to all commercial instruments because the external event is phase-locked to the interferometer cycle. All timing and control functions of the microprocessor are written in higher level

languages such as Pascal.

The experimental parameters which need to be defined are:

NSS = number of scans of the same phase to be coadded.

T = cycle time or event time.

$\Delta T_1 = T/400$ = time interval between each step.

ΔT_2 = time resolution desired.

$N = T/\Delta T_2$ = number of files into which the external event must be divided.

The overall flow diagram of the time resolved experiment is shown schematically in Figures 5.1 to 5.3.

Unlike our previous experiments, the external event is exactly synchronized to the interferometer scan (including the back sweep). This scheme will limit the flexibility of the time resolved experiment since the event time is then determined by the available mirror scan velocities and the number of data points. Practically speaking, this was not a problem since a sufficiently large number of mirror velocities are available, and the resolution needed in our experiments was not critical.

Once the event time period and the time resolution needed to follow the kinetics are determined, all other experimental parameters are calculated by the microprocessor. The experiment is then executed under microprocessor supervision. The Take-Data pulse (TKDA) from the interferometer provides the microprocessor the signal to calculate the period of the sweep time, and in our case the event period, T. The calculated results are stored in computer memory. The computer then

FIGURE 5.1: The schematic diagram of a time resolved experiment.

SCHEMATIC OF TIME RESOLVE COMPONENTS

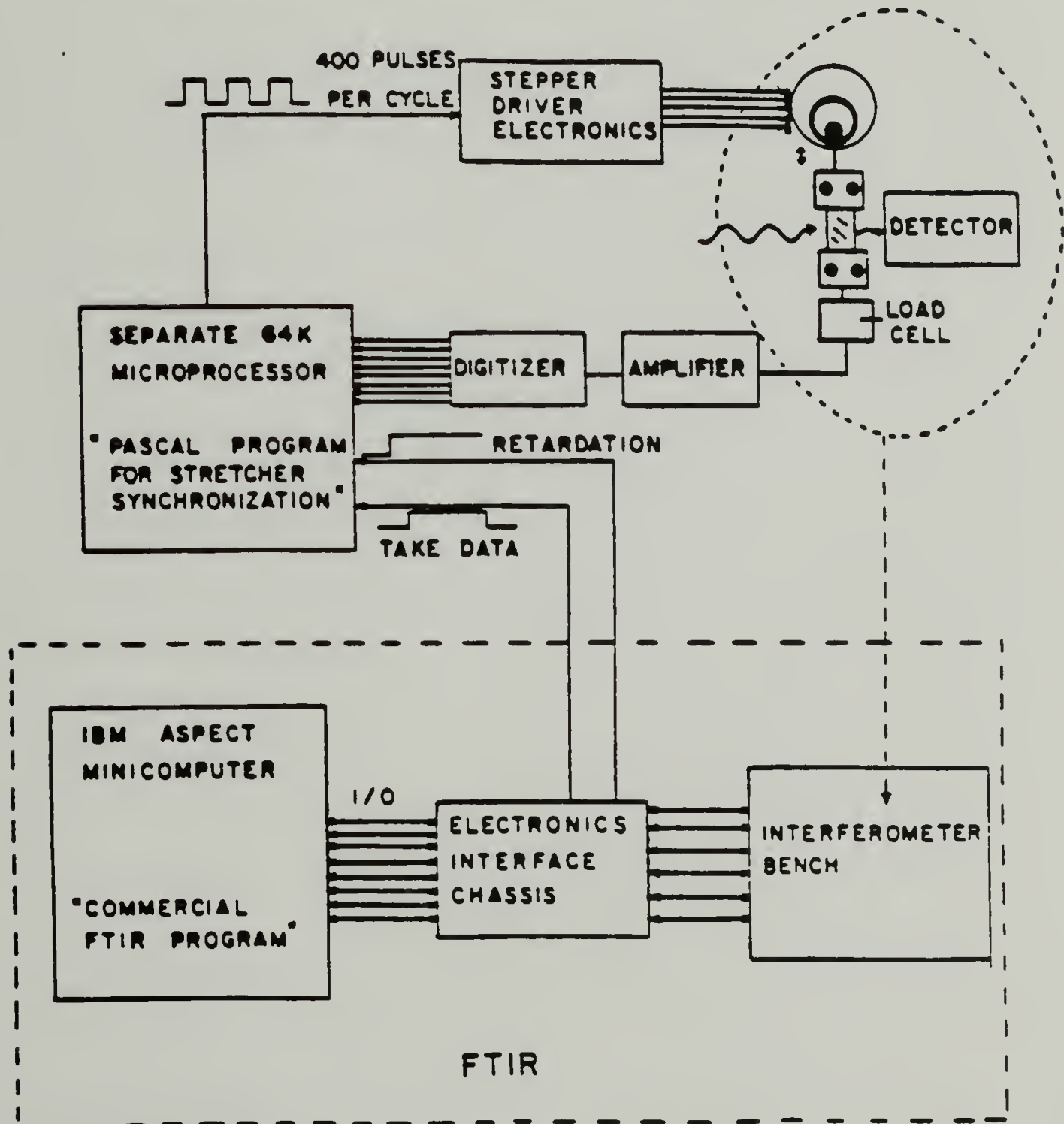


Figure 5.1

FIGURE 5.2: Flow diagram of computer control program for continuous deformation experiment.

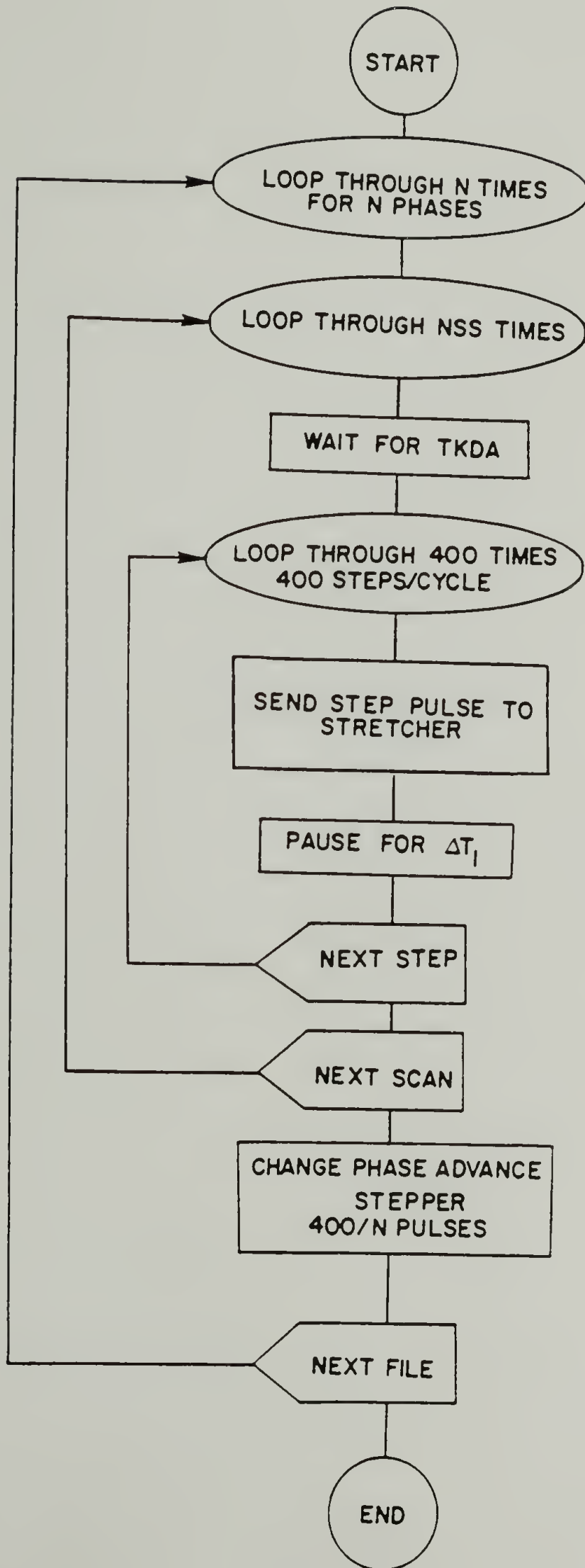


Figure 5.2

FIGURE 5.3: Scheme showing the phase relationship between the interferometer movement and the external event for a continuous deformation cycle. A separate interferogram file is collected for each of n clock values, where $n = \text{event period} / \text{time resolution}$.

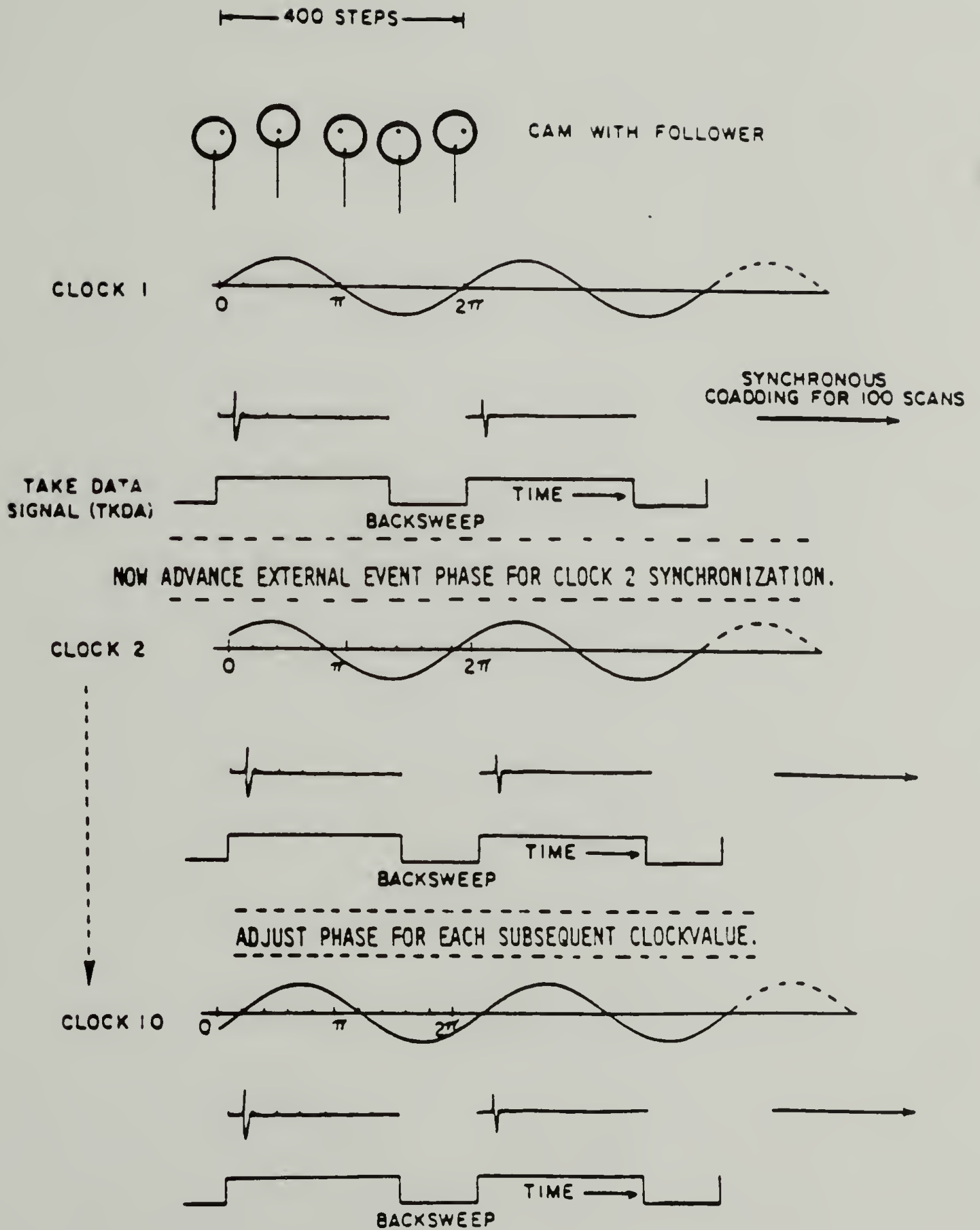


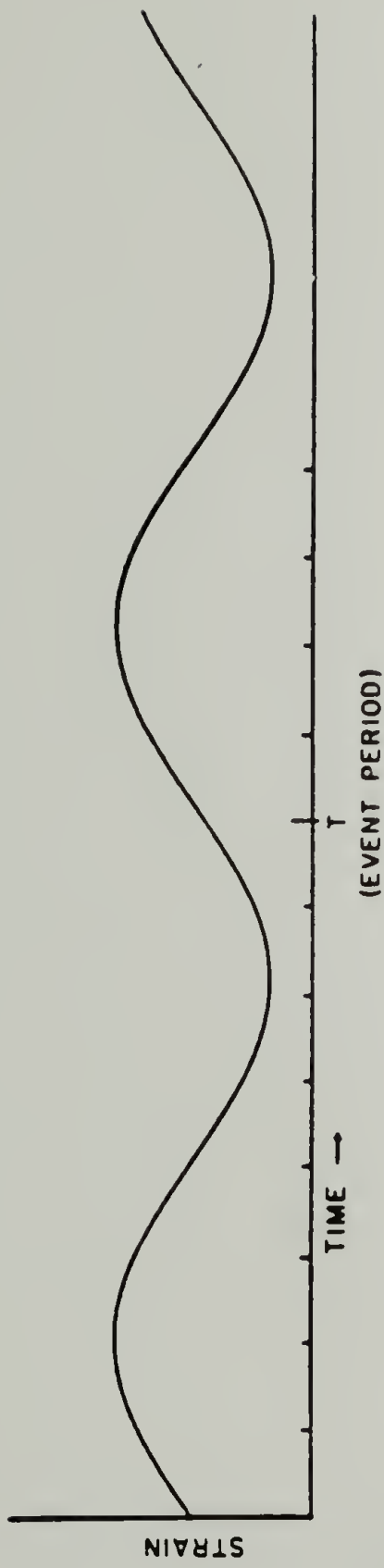
Figure 5.3

calculates ΔT_1 . Since the number of steps to complete a revolution is fixed at 400, it is then a simple matter to send pulses of 10 μsec duration every ΔT_1 to the stretcher driver card. For the first file NSS interferograms are stored in the FTIR processor memory. During the writing operation to the disk, the microprocessor advances the external event by a phase angle $2\pi/N$ to introduce a net time difference, ΔT_2 , between the initiation of the next set of NSS scans and the zero phase point of the external event. This process is repeated until N interferogram files, each containing NSS scans, are collected. Since the time relationship between each file is clearly defined, time resolved interferograms may be constructed for each time element t_j within a time resolution of ΔT_2 of the sample event. In Figures 5.4a and 5.4b the interferograms are shown as being divided into blocks corresponding to ΔT_2 and reconstructed to generate new interferograms corresponding to a particular time in the event with a temporal resolution of ΔT_2 . The program to carry out this process is written in Pascal and listed in Appendix C.

Periodic Squarewave Event

This version of the TRS experiment was developed for external events which are driven by periodic d.c. pulses of specific voltage and duration. This method has been used to characterize the dynamics of electric field induced microstructural changes of a piezoelectric polymer, [poly(vinylidene fluoride) (PVF₂)], and a low molecular weight liquid crystalline compound. The dynamic response of segmental orientation for a polyurethane undergoing periodic squarewave deformation

- FIGURE 5.4:
- a. During the data collection the phase relationship between the interferogram and the external event is varied in a systematic manner. Here the interferogram is shown segmented to depict how it is divided for the sorting procedure.
 - b. After sorting, each interferogram corresponds to a specific segment of time.



UNSORTED
FILENUMBER
"CLOCKVALUE"

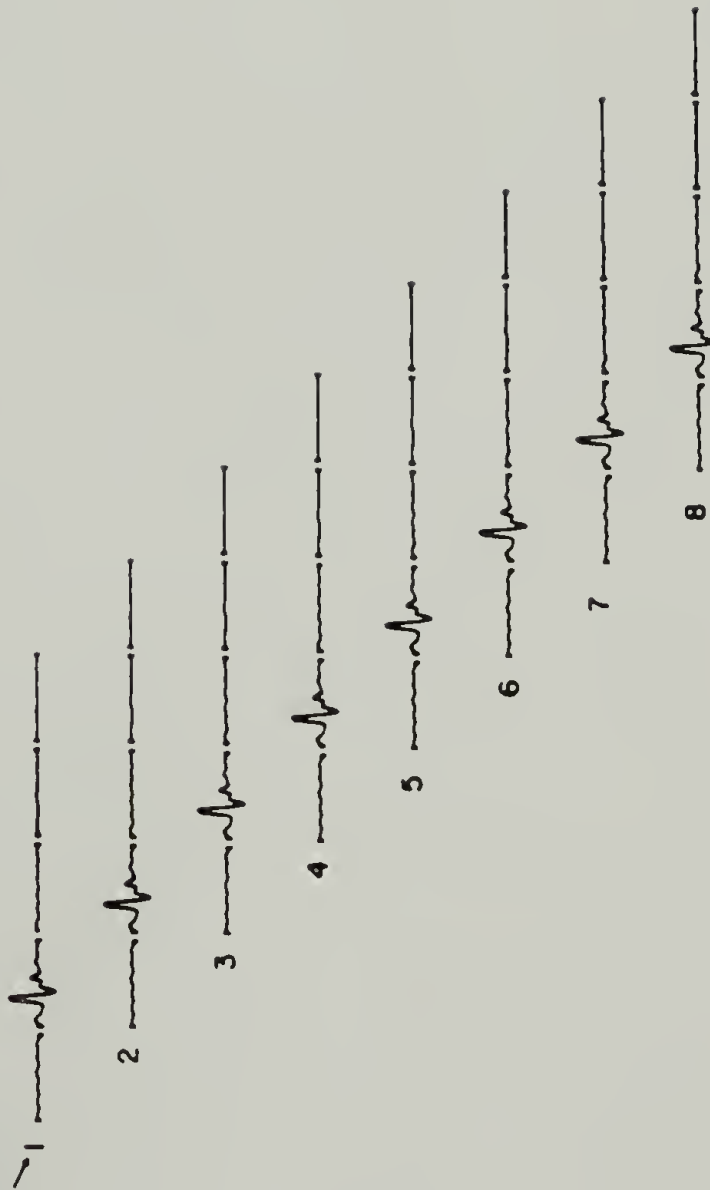


Figure 5.4a

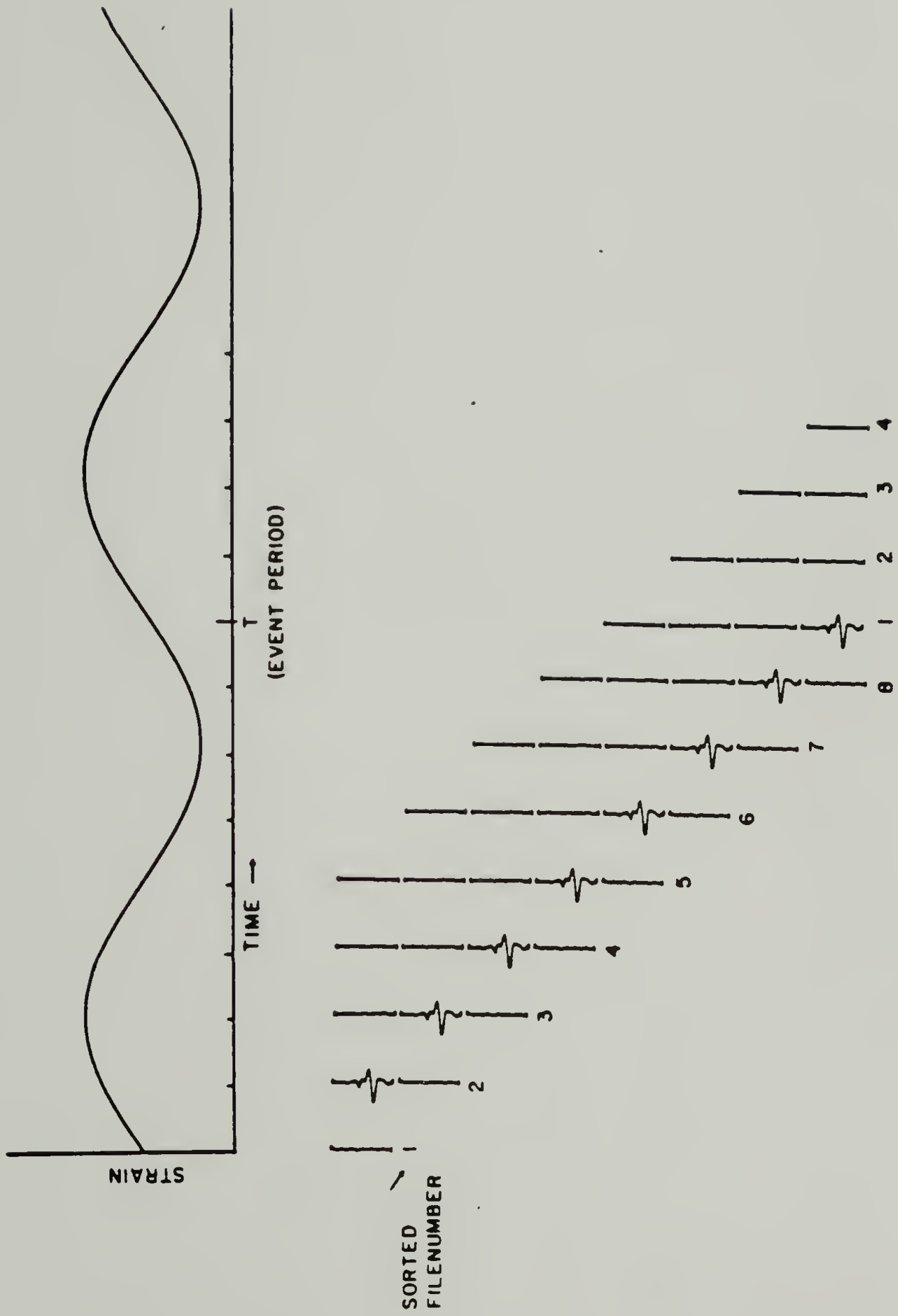


Figure 5.4b

using this method is discussed in the following chapter.

Synchronization of the squarewave event to the interferometer sweep period utilizes a different approach than that of the sinusoidal event. A similarity is that the cycle period, T , is divided into N units each having a temporal span of ΔT_2 , which is the time resolution of the experiment. However, in this case an array of N elements is generated in the software control program and output to the parallel port of the microprocessor to control the state of the external event (Figure 5.5). Successive elements of the array are sent to the port; one at the start of each of the N time segments of the cycle period. The state of the port remains at the value of the array element, A_j for a time ΔT_2 , after which the port is updated with the next output value A_{j+1} . For a simple bi-state event, i.e. on and off, only one bit of the 8 bit port is utilized. The output array consists of ones and zeros corresponding to the on and off states. Since 8 bits are available, it would be possible to generate a more complex external event such as a sinusoidal function. This digital signal could then be converted to an analog sine wave using a digital to analog converter.

The phase relationship between the external event and the interferometer sweep is varied by a permutation of the output array as shown in Figure 5.5. The output of the array values is phase locked to the interferometer cycle so that the output of the first element, A_1 always corresponds to the onset of the interferogram collection. Interferogram files are collected for N permutations of the external event phase and the data is sorted as described previously.

FIGURE 5.5: Scheme showing phase relationship between the interferometer movement and the external event for a squarewave event cycle. The computer output array contains the waveform of the external event.

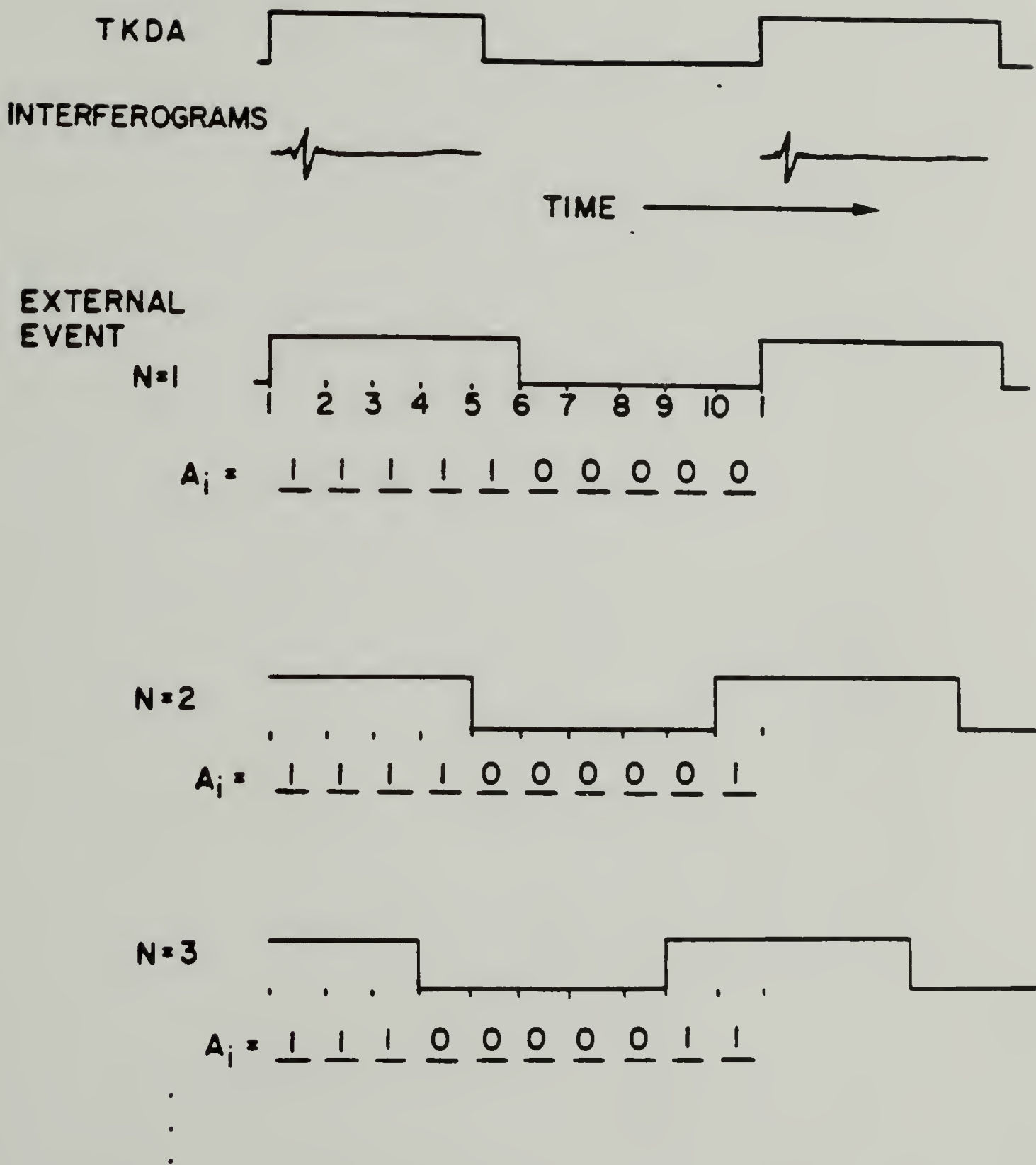


Figure 5.5

Results and Discussion

It is most important to test the accuracy of the phase relationship between the interferogram and the associated external event. We designed an experiment with the event being the continuous rotation of a highly oriented polymer film in front of a stationary silver bromide polarizer. The sample used is an ethylene-vinyl acetate copolymer which has been uniaxially oriented by drawing to a draw ratio of 3.5 at 100°C. It is mounted on a retaining ring rotated by the stepping motor used in the stretcher. The experimental parameters are listed in Table 5.1. Each rotation is synchronized with the cycle time (1.22 seconds) of the interferometer. The difference between the sample period and the interferometer cycle period is no more than 0.75 milliseconds per cycle. This deviation is not cumulative since our timing scheme automatically corrects for any difference every cycle. In this manner, the interferometer and sample rotation remained in phase as each interferogram was coadded to the file. A series of 20 interferogram files was collected with each being an average of 50 scans.

The shape of the unsorted interferograms shows the expected interferometric modulation with a low frequency modulation in the baseline (Figure 5.6), which is the result of large changes in the total absorbance of the sample as a function of angle between the polarizer and the orientation direction. Since the sample is thick (25 μm) and highly polarized, its total absorbance change with respect to the fixed polarizer can be sufficiently large to cause the baseline modulation. The sorted interferograms retain this baseline modulation manifested as

TABLE 5.1

The Experimental Conditions Used to Test the Operation
of the Time-Resolved Infrared Spectroscopic Equipment

Event Period	1.22 sec
Time clocks per event	20
Clock period (time resolution)	61 milliseconds
NDP, points per interferogram	16,384
Spectral resolution	1 cm^{-1}

FIGURE 5.6: The interferogram obtained which shows a low frequency modulation related to absorbance change as a function of the external event.

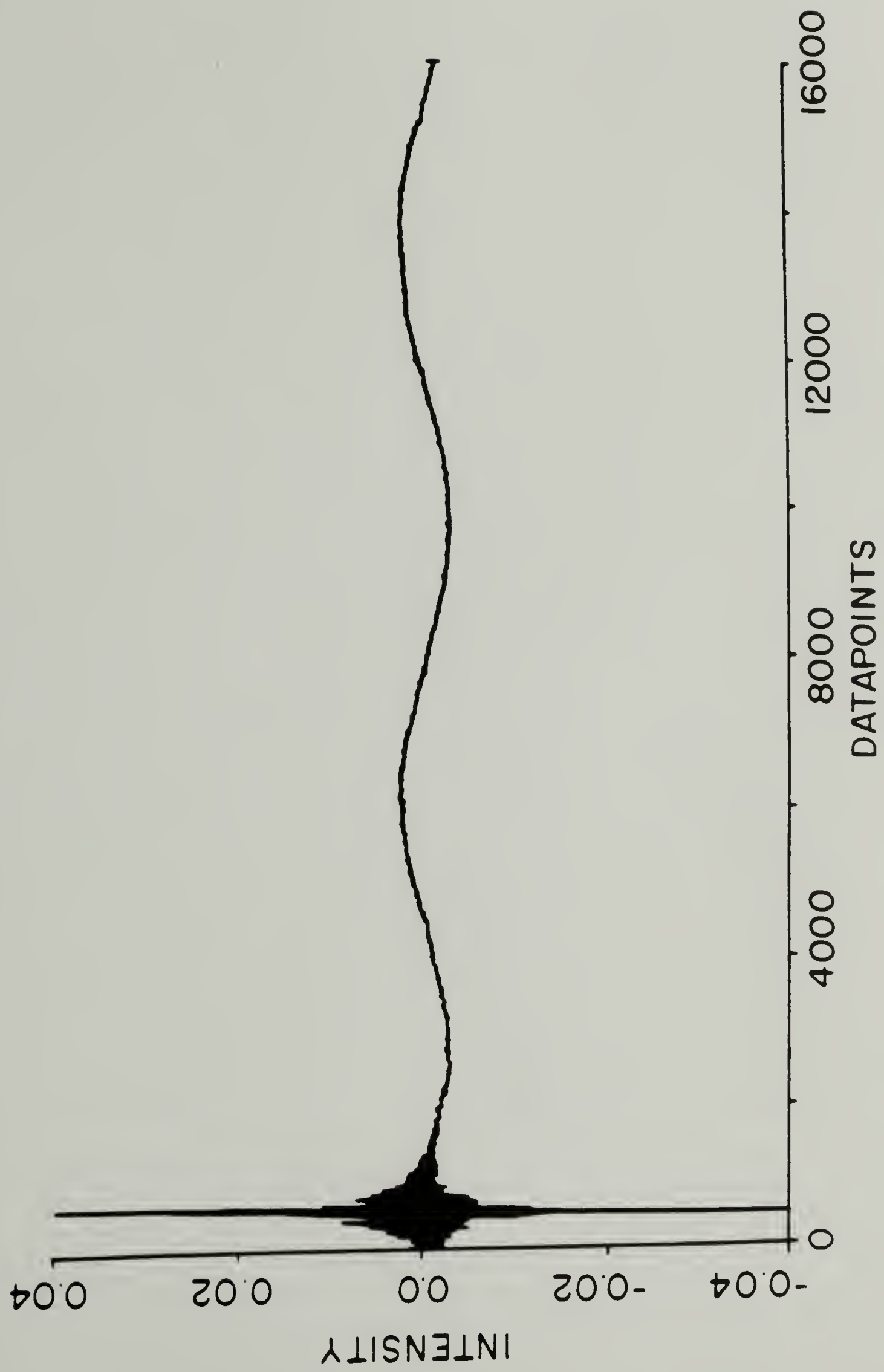


Figure 5.6

a sawtooth function (Figure 5.7). Each segment of the interferogram corresponds to the same phase in the sample rotation. In general a discrete discontinuity occurs at the junction of each segment. When these sorted interferograms were Fourier transformed, the resulting spectra contained period spikes as shown in Figure 5.8. In fact, many of the spectral changes associated with time resolved experiments are small. An evaluation of the spectral artifacts should be interesting, relevant, and important in such cases. In order to simulate such intensity modulation, a periodic sawtooth perturbation was added to a normal background interferogram. The form of this sawtooth function is

$$y_i = y_i^\circ + A[\text{Rem}(\frac{i}{N}) - \frac{N}{2}] \quad (5.1)$$

y_i = resulting interferogram intensity.

y_i° = normal interferogram intensity.

i = data point index of interferogram.

N = number of data points per sawtooth.

A = sawtooth amplitude

Rem = retain the remainder of the quotient.

Figure 5.9 shows the interferogram before and after modification. When the modified interferogram is Fourier transformed the resulting energy curve shows a spectral artifact similar to that observed in the time resolved experiment. The artifact is seen more clearly if one takes the ratio of the perturbed data against the unperturbed (Figure 5.10). The periodicity of this artifact is 10.6 cm^{-1} , which corresponds to

FIGURE 5.7: The modulation manifests itself as a sawtooth pattern in the sorted interferogram.

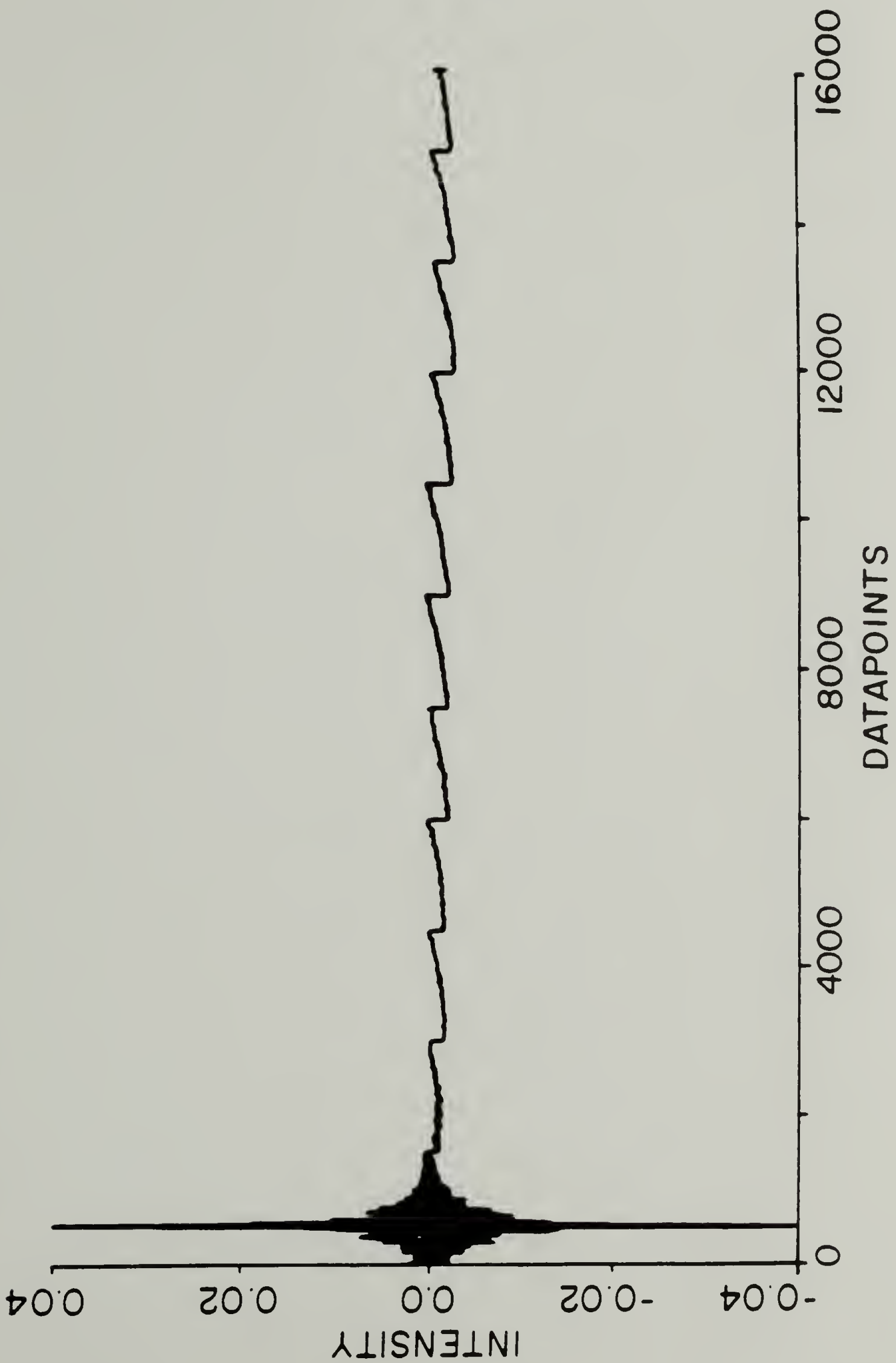


Figure 5.7

FIGURE 5.8: The Fourier transformed spectrum of the interferograms containing low frequency modulation can show an artifact in the form of evenly spaced spikes.

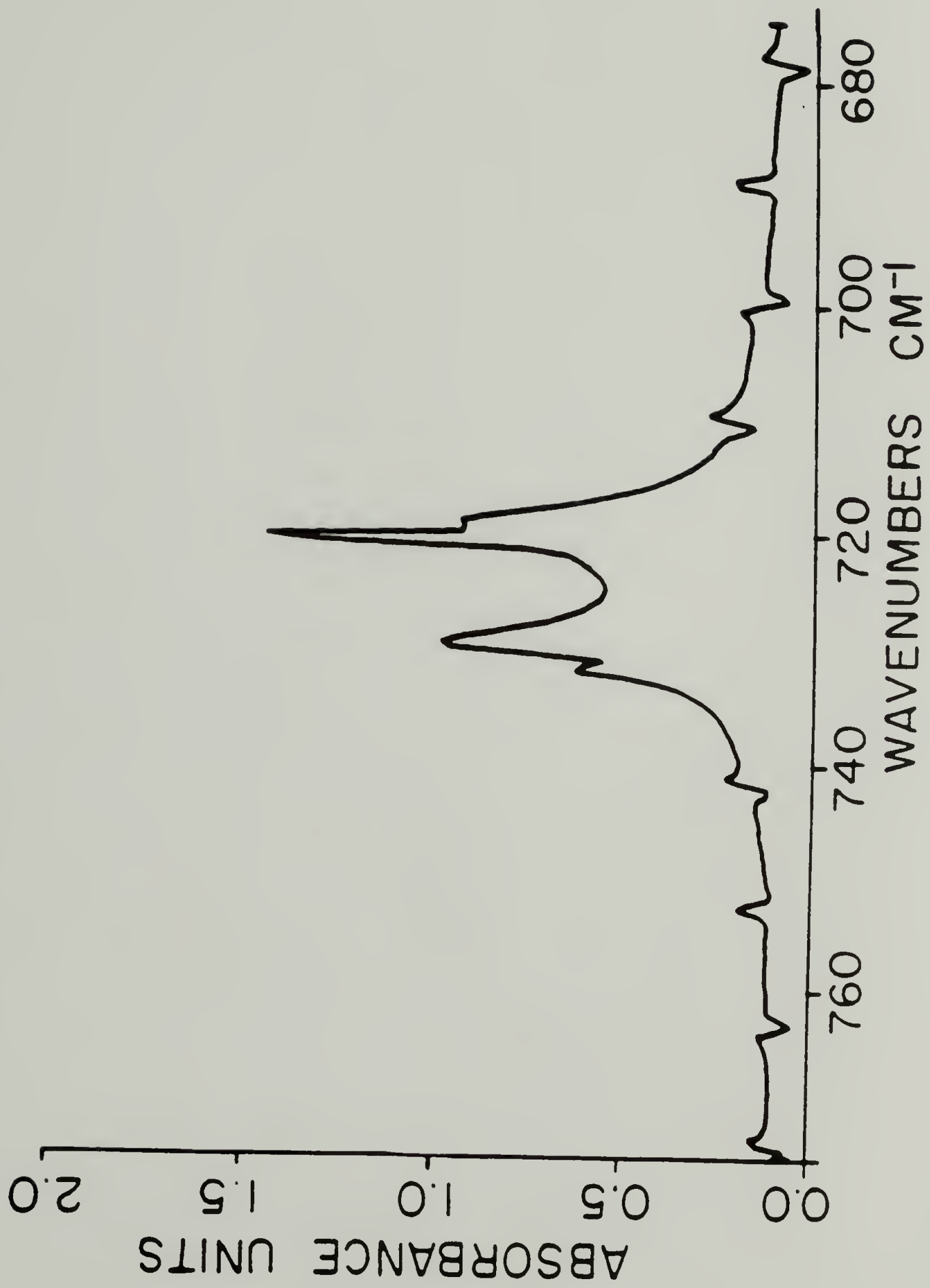


Figure 5.8

FIGURE 5.9: Interferogram containing computer simulated sawtooth function.
a. as collected.
b. after computer modification.

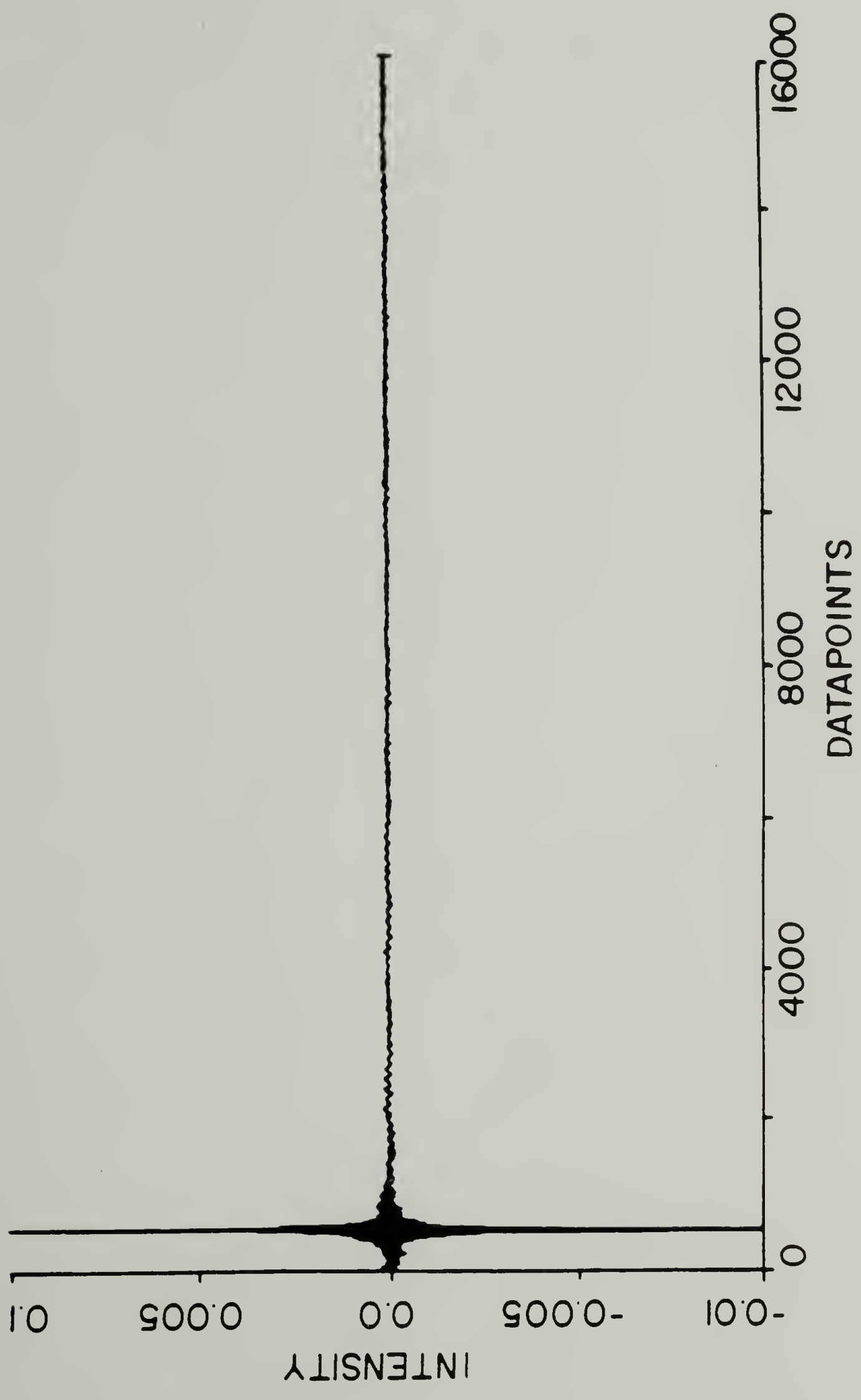


Figure 5.9a

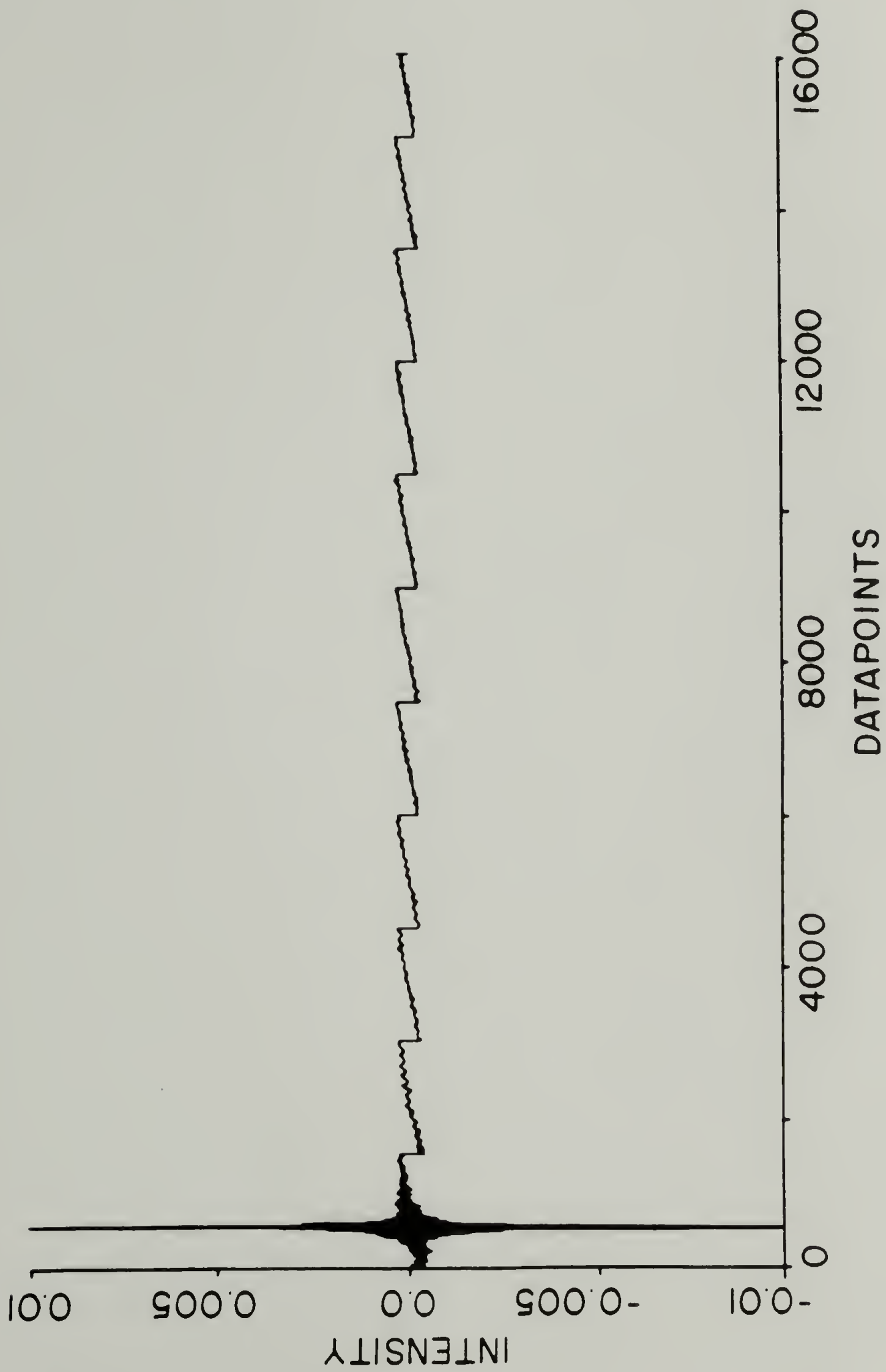


Figure 5.9b

FIGURE 5.10: When the modified interferogram is transformed the resulting ratioed spectrum exhibits a distinct derivative-like artifact.

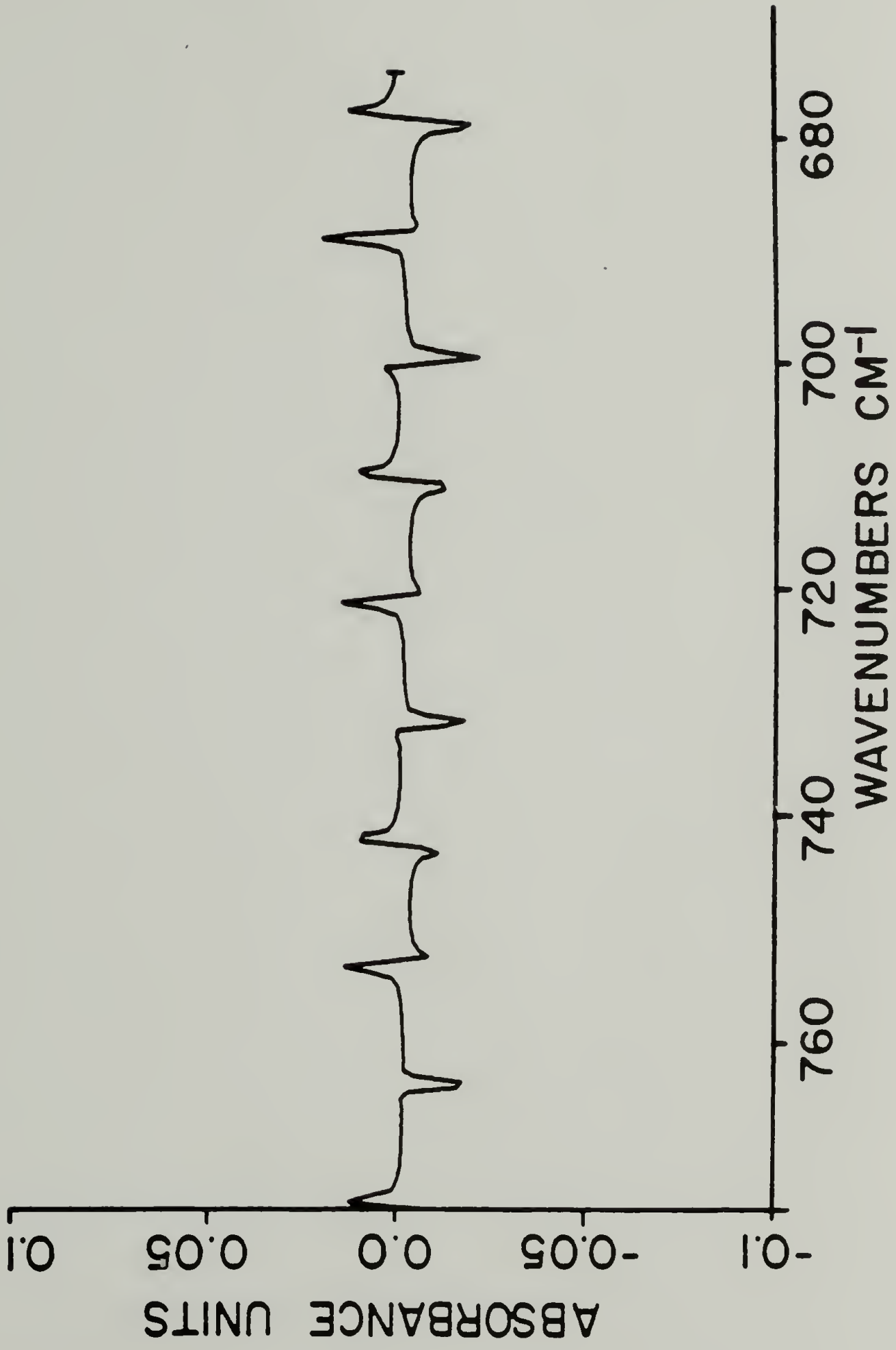


Figure 5.10

$1/[\delta_{\max}(\frac{N}{\text{NDP}})]$, where N is the number of data points per block, NDP is the total number of data points in the interferogram, and δ_{\max} is the spectral retardation of the last data point of the interferogram. We found the intensity of the spikes to be proportional to the magnitude of the discontinuity in the sawtooth. In actual time resolved spectroscopic experiments this would correspond to the change in transmitted energy (for example from sample thickness change) during one clock period, ΔT_2 . In the rotating film test this change in transmission is of sufficiently large magnitude to cause spectral artifacts in the spectra obtained, making interpretation of the time resolved data difficult. For this reason, a method was developed to correct for the discontinuities before the interferogram is transformed. A computer program is used to eliminate the discontinuity by leveling out the slope of each block of the interferogram by applying a function similar to Equation 5.1. This matches the last data point in each block with the first datapoint in the next block. The correction is applied to the time resolved data of the ethylene-vinyl acetate copolymer. This scheme was found to work very well. From the analysis of the simulation data and the ethylene-vinyl acetate copolymer spectra we feel confident that this artifact is generally manageable.

A series of the corrected spectra obtained by the time resolved technique for the CH_2 rocking vibration is shown in Figure 5.11. It is evident that the $720\text{-}730\text{ cm}^{-1}$ doublet due to crystal-field splitting is perpendicularly polarized in this highly oriented film. As expected, the absorption reaches a maximum twice during each cycle. This occurs

FIGURE 5.11: Change in CH rocking intensity as a function of angle between polarizer and film orientation direction.

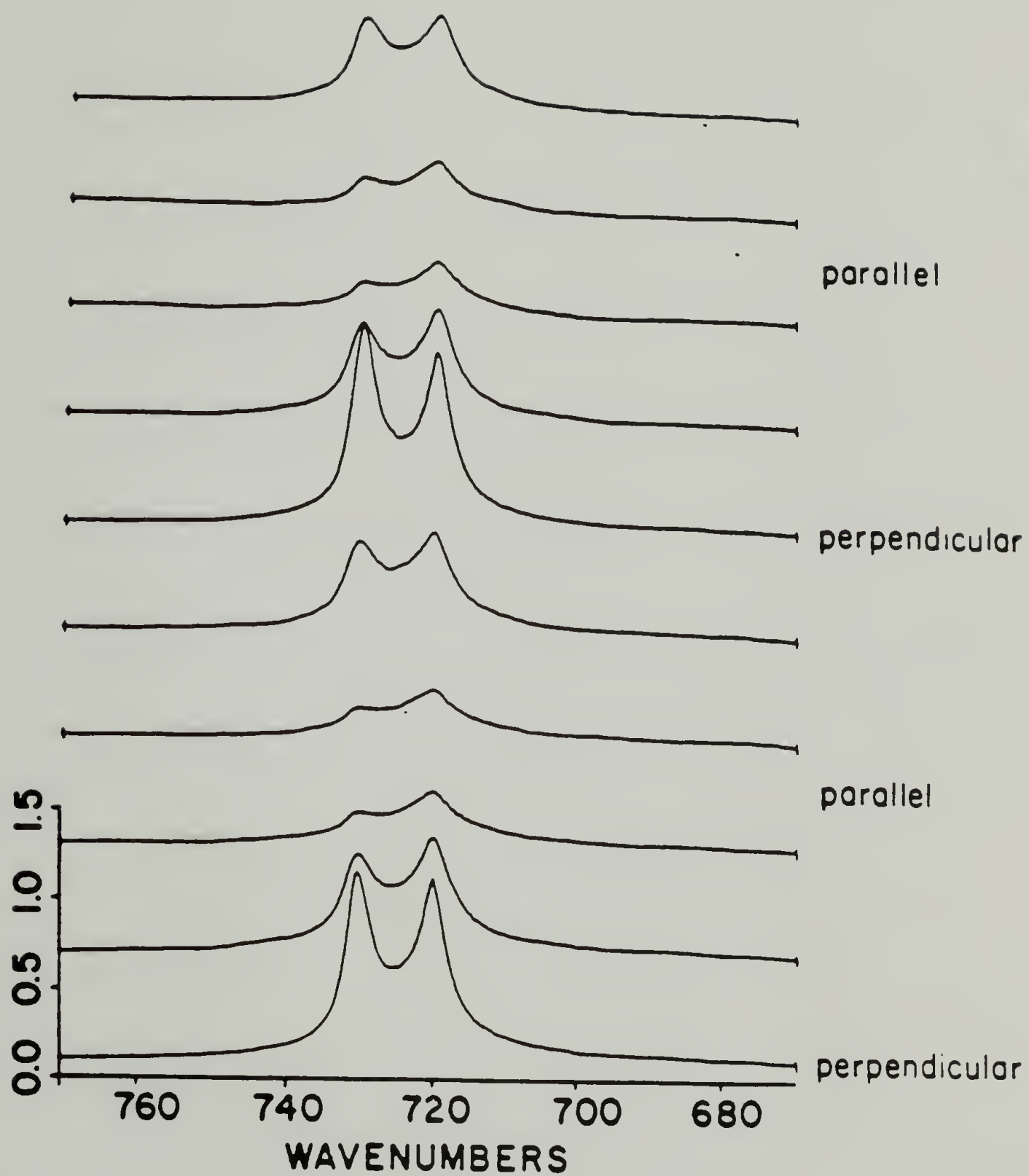


Figure 5.11

when the film orientation is perpendicular to the infrared polarization vector. This series of spectra clearly demonstrates the applicability of our newly modified technique in the collection and computation of time resolved infrared spectral data.

Finally, we want to evaluate and compare the sensitivity of this modified technique in characterizing deformation induced microstructural changes in an actual polymer sample undergoing deformation. The sample chosen for this study is poly(butylene terephthalate) (PBT), which has a first order crystal phase transition (12-14). Since this phase transition is strain dependent and reversible (13,14) it can be suitably followed by the time resolved spectroscopic technique. The vibrational spectra of PBT has been well characterized (15). Several infrared active vibrations are highly sensitive to the conformation of the tetramethylene sequence existing in the various crystalline phases. For example, the 917 cm^{-1} and 960 cm^{-1} are assignable to the CH_2 rocking of the α and β phases respectively (15). The infrared spectrum of this region obtained for PBT is shown in Figure 5.12. For our mechanical-vibrational spectroscopy experiment, the strain amplitude of the deformation used was 4%. Previously a static strain test demonstrated that this was sufficient to observe an increase in the amount of β phase. A complete list of parameters used in this experiment is given in Table 5.2. Ten time resolved spectra corresponding to a time resolution of ~ 122 milliseconds were collected. For such small strain amplitude we found that the total absorbance change due to changing sample thickness during deformation was not sufficient to

FIGURE 5.12: Characteristic CH₂ rocking vibration in PBT associated with the α , β , and amorphous phase.

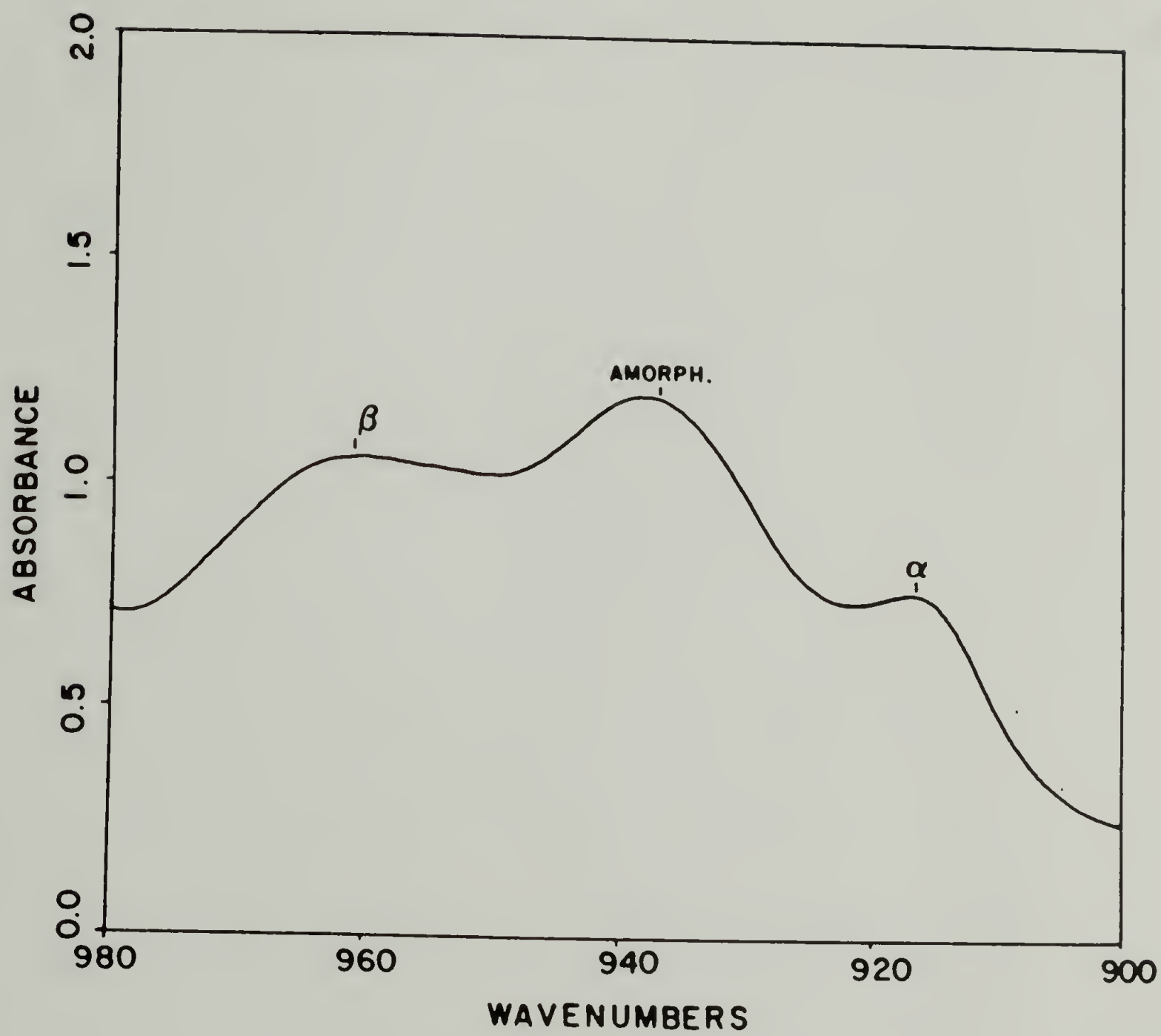


Figure 5.12

TABLE 5.2

The Experimental Conditions Used for the
Poly(butylene terephthalate) Experiment

Event period	1.22 sec
Time clocks per event	10
Clock period (time resolution)	122 milliseconds
NDP, points per interferogram	16,384
Clock periods per interferogram	5.2
Spectral resolution	1 cm^{-1}

cause a baseline modulation in the interferogram. Therefore, no correction in the sorted interferograms was necessary and, in fact, no spectral artifacts were observed. Spectral subtraction has been used to monitor the change in intensity as a function of strain of the vibrations in the 900 cm^{-1} region. The relationship between the integrated absorbance change for these two bands and the applied strain function is shown in Figure 5.13. The maxima of the change for both the 917 cm^{-1} and 970 cm^{-1} bands corresponds to the maximum of the strain value, showing no time lag for the microstructural response, thus indicating that the transition occurs at a rate faster than the temporal resolution of the experiment, which is 122 milliseconds. Even though a great deal of static and dynamic measurements on the order of 30 seconds have suggested that conformation conversion is directly related to strain applied, our study is the first evidence of this type.

In both of the time resolved spectroscopy experiments, infrared data has been obtained for cyclic events with a period of 1.22 seconds. Dynamic events in this time domain have been particularly difficult to characterize in the past. Commercial schemes only apply for much shorter events and the rapid scan method is better suited to longer event periods. This newly developed time resolved method incorporating a microprocessor to control the external event offers high flexibility in studying a variety of cyclic events in polymers with periods of .5 to 5 seconds.

FIGURE 5.13: A measure of the α - β phase transformation in poly(butylene terephthalate). Integrated absorbance change as a function of strain amplitude.

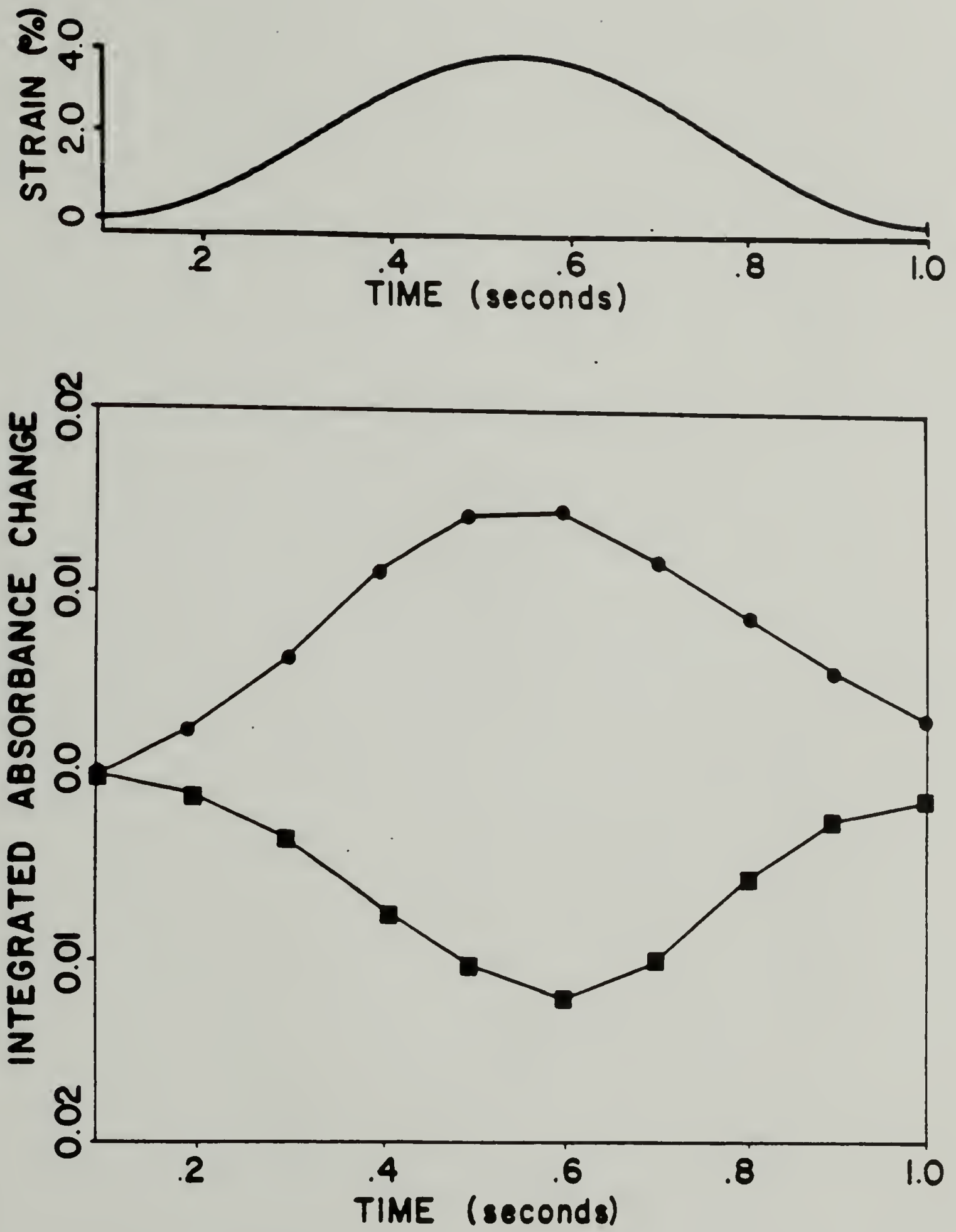


Figure 5.13

References

1. R.S. Stein, S. Onogi, K. Sasaguri, and D.A. Keedy, "Dynamic Birefringence of High Polymers II", *J. Appl. Phys.*, 34, 80 (1963).
2. R.S. Stein, "Rheo-Optical Studies of the Deformation of Crystalline Polymers", *J. Poly. Sci.-Part C.*, 15, 185 (1966).
3. S. Suehiro, Ph.D. Thesis, Kyoto University (1979).
4. R.E. Murphy, F.H. Cook, and H. Sakai, "Time-Resolved Fourier Spectroscopy", *J. Optical Soc. of America*, 65, 600 (1975).
5. H. Sakai and R. Murphy, "Improvements in Time Resolved Fourier Spectroscopy", *Appl. Opt.*, 17, 1342 (1978).
6. A.W. Mantz, "Infrared Multiplexed Studies of Transient Species", *Appl. Spect.*, 30, 459 (1976).
7. A.W. Mantz, "Infrared Spectroscopic Studies of Transients", *Appl. Opt.*, 17, 1347 (1978).
8. A.A. Garrison, R.A. Crocombe, G. Mamantov, and J.A. deHaseth, "Practical Aspects of Rapid Scanning Fourier Transform Time-Resolved Infrared Spectroscopy", *Appl. Spect.*, 34, 399 (1980).
9. W.G. Fately and J.L. Koenig, "Time-Resolved Spectroscopy of Stretched Polypropylene Films", *J. Polym. Sci., Polym. Lett. Ed.*, 20, 445 (1982).
10. D. Burchell, J.E. Lasch, R.J. Farris, and S.L. Hsu, "Deformation Studies of Polymers by Time-Resolved Fourier Transform Infrared Spectroscopy: 1. Development of the Technique", *Polymer*, 23, 965 (1982).

11. J.E. Lasch, D.J. Burchell, T. Masoaka, and S.L. Hsu, "Deformation Studies of Polymers by Time-Resolved Fourier Transform Infrared Spectroscopy III: A New Approach, *Appl. Spectros.*, 38, 351 (1984).
12. G.A. Boye, and J.R. Overton, "A Reversible, Stress-Induced, Solid-Phase Transition in Poly(tetramethylene terephthalate)", *Bull. Am. Phys. Soc.*, 19, 352 (1974).
13. R. Jakeways, I.M. Ward, M.A. Wilding, I.J. Desborough, and M.G. Pass, "Crystal Deformation in Aromatic Polyesters", *J. Polym. Sci., Polym. Phys. Ed.*, 13, 799 (1975).
14. M. Yokouchi, Y. Sakakibara, Y. Chatani, H. Tadokoro, T. Tanaka, and K. Yoda, "Structure of Two Crystalline Forms of Poly(butylene terephthalate) and Reversible Transition Between Them by Mechanical Deformation", *Macromolecules*, 9, 266 (1976).
15. B. Stambaugh, J.L. Koenig, J.B. Lando, "X-Ray Investigation of the Structure of Poly(tetramethylene terephthalate)", *J. Polym. Sci., Polym. Phys. Ed.*, 17, 1053 (1979).

C H A P T E R V I
THE DYNAMICS OF SEGMENTAL RESPONSE
DURING DEFORMATION OF A POLYURETHANE ELASTOMER

Introduction

Much of the emphasis in characterizing polymeric systems has been placed on the development of correlations relating macroscopic properties to the microstructural composition. Their viscoelastic nature is a feature unique to this class of materials, and one which greatly influences the mechanical properties. For this reason there is both commercial and academic interest in developing knowledge of the underlying molecular mechanisms which is the basis of this behavior.

Linear segmented polyurethanes are materials which are well known for their viscoelastic nature. This has led to commercial applications as impact resistant structures and in vibrational dampening systems (1,2). Polyurethanes are particularly useful in these applications as their viscoelastic response occurs with characteristic times of the order of a second or less. While it has been the objective of many rheological studies to describe relationships between stress and strain within this timescale, the origin of these relationships may be best determined by monitoring the dynamics of molecular orientation using optical probing techniques.

Several rheo-optical methods have been developed that allow sampling of microstructural orientation during dynamic deformation.

The most successful of these techniques have been dynamic birefringence (3-5), dynamic light scattering (5-7), and infrared spectroscopy (3,5,8-15). While infrared spectroscopy has not traditionally been known for its rapid sampling rate the advent of Fourier transform infrared (FTIR) instruments and recent developments of time-resolved spectroscopy, TRS, have spurred rapid growth in this field. Infrared spectroscopy is especially suited for investigations of multiphase elastomeric systems such as segmented polyurethane copolymers. Vibrational absorptions are characteristic of specific molecular substituents making it possible to monitor the dynamic response of individual components of the polyurethane microstructure.

The focus of this chapter is the development of a molecular interpretation of the dynamics of the deformation process for a model polyurethane elastomer using time resolved FTIR spectroscopy. This polyurethane is unique in that it has a hard segment component which is monodispersed in length. The sample exhibits no permanent set for deformations up to 75%, making it an excellent candidate for time resolved infrared deformation studies. The relaxation of segmental orientation of the component segments of this polymer is monitored using the method of IR dichroism during dynamic strain at ambient and subambient temperatures.

Experimental

Materials

The model polyurethane characterized in this study is a polybuta-

diene based system with a monodispersed hard segment of five TDI residues, chain extended with butanediol. This is the same polymer as was characterized in the segmental orientation study of Chapter II. The method of film preparation is discussed in the experimental section of that chapter.

A solenoid powered deformation apparatus is utilized for the dynamic deformation and is depicted in Figure 6.1. This stretching device strains the sample with a periodic squarewave deformation function of predetermined strain. The solenoid operates on 24 volts DC. The voltage is turned on and off by means of an electronic circuit which relays the state of a TTL pulse from the California Computer Systems (CCS) microprocessor. The schematic of this circuit is depicted in Figure D. The deformation apparatus may be fitted with a variable temperature chamber for low temperature studies. This chamber is cooled by a nitrogen gas stream which is thermally adjusted as described in the experimental section of Chapter II.

Synchronization of the deformation event with the interferogram data collection is controlled by a Pascal program which is implemented on the CCS microprocessor. This program is specific for the periodic stepwise event mode which is detailed in Chapter V. The source code of the program is listed in Appendix C. The timing relationship between the squarewave strain function and the collected interferograms is depicted in Figure 6.2. The phase relationship before and after sorting follows the same scheme as for the sinusoidal function of Chapter V.

FIGURE 6.1: Solenoid driven polymer deformation apparatus.

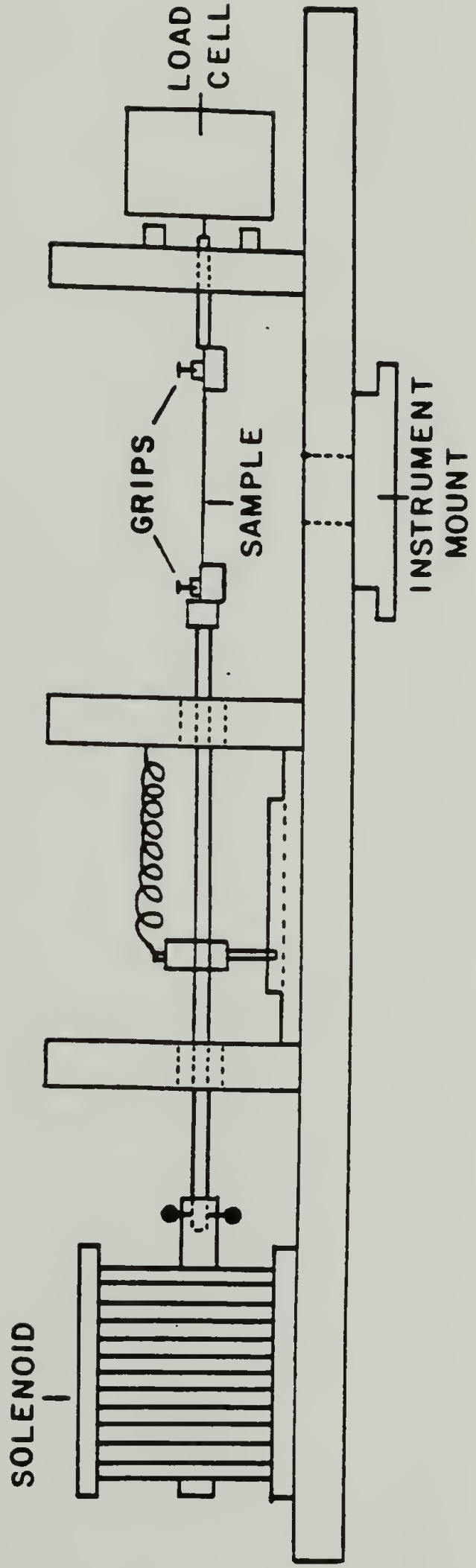
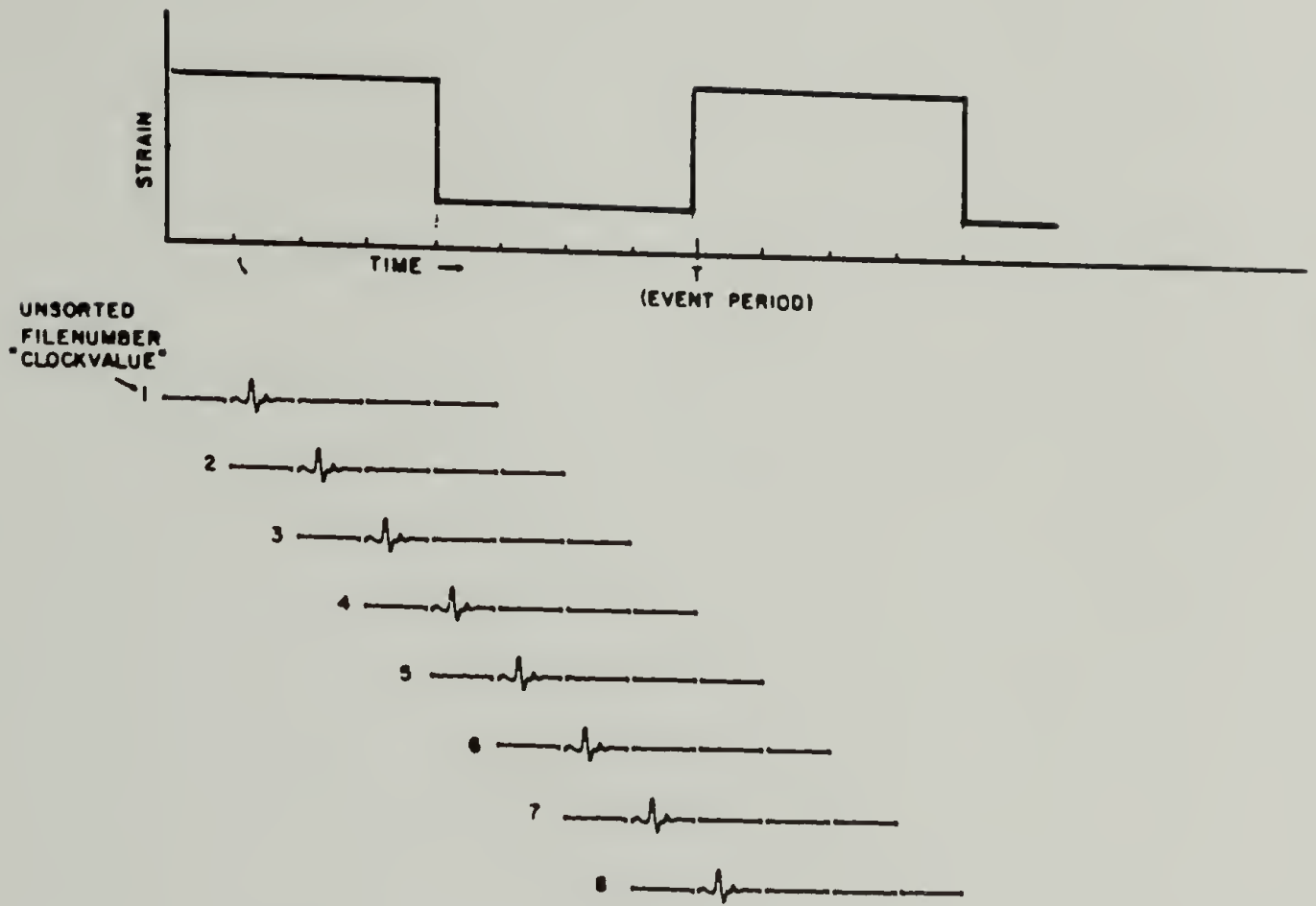


Figure 6.1

FIGURE 6.2: Phase relationship between interferogram files and squarewave strain event.
a. as collected
b. after sorting

A



B

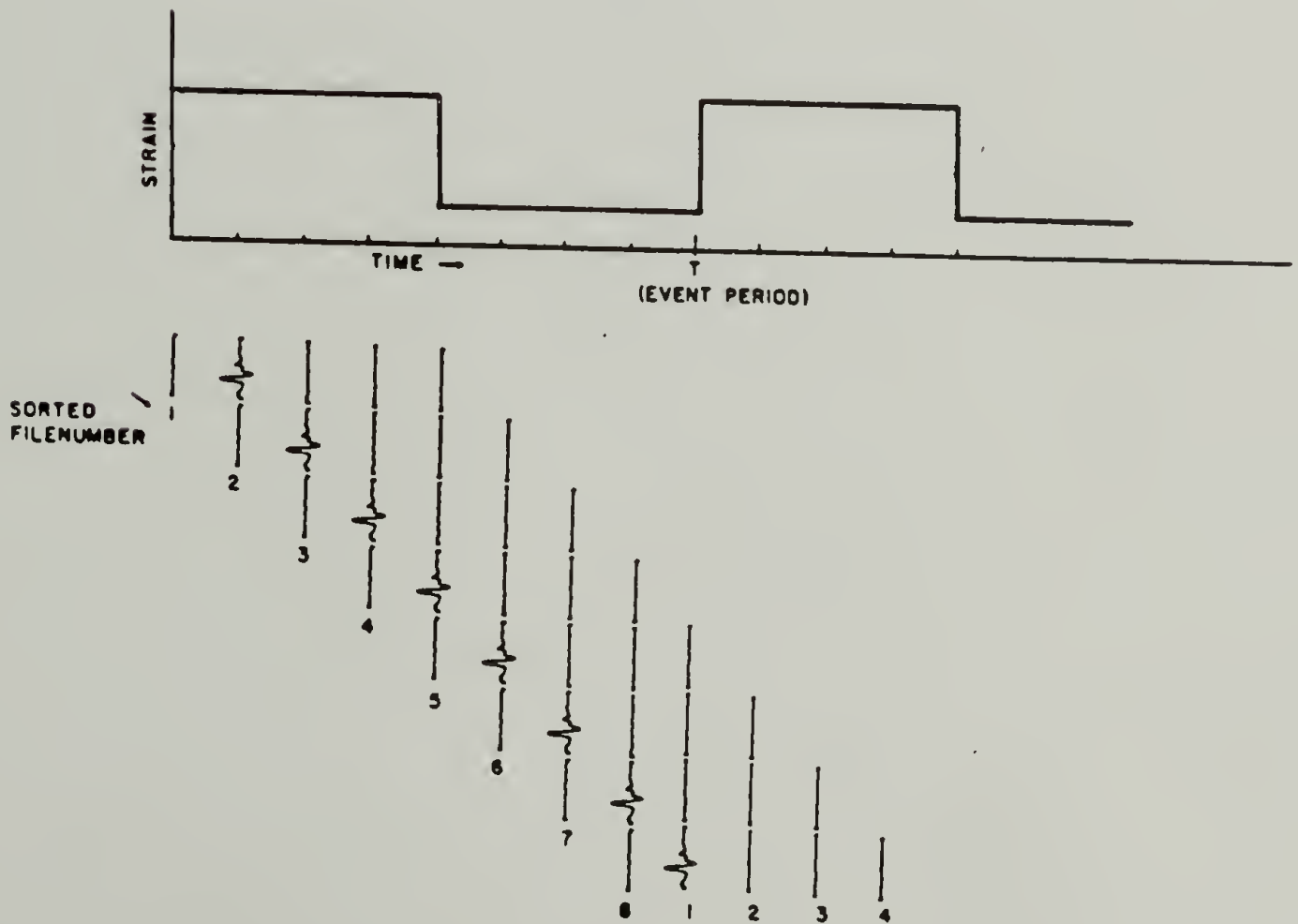


Figure 6.2

Methods

Three deformation experiments were carried out to investigate the dynamics of polyurethane segmental orientation behavior. The first study was for investigating the long term relaxation behavior at constant strain so as to establish the suitability of the sample for TRS characterization. Polarized spectra were collected using the standard collection routines supplied with the IBM FTIR spectrometer. Four sets of parallel and perpendicular spectra were collected for the unstrained sample to determine the noise level of the dichroic ratio under static conditions. Eighteen sets of polarized spectra were collected for a sample strain of 40% over intervals of five minutes each for a total of 1.5 hours. The dichroic ratios for the soft segment 1,2 vinyl vibration are shown as a function of time Figure 6.3. Error bars correspond to the noise level in the dichroic ratio in the undeformed state. The absence of relaxation of segmental orientation during the timescale of this experiment gives confidence that this sample is well suited to time resolved FTIR analysis.

The dynamics of segmental orientation were investigated using the periodic squarewave mode of the software synchronized time resolved infrared technique detailed in Chapter V. The sample was strained at 40% for the first half of the period and relaxed to 15% strain for the second half of the period. The time required for the strain to increase from 15 to 40% was 15 milliseconds, while the time to relax the strain was 25 milliseconds. These rates were a result of the inertia of the moving parts of the deformation apparatus. While the

FIGURE 6.3: Dichroic ratio of 1,2 vinyl absorption as a function of time for 40% static deformation.

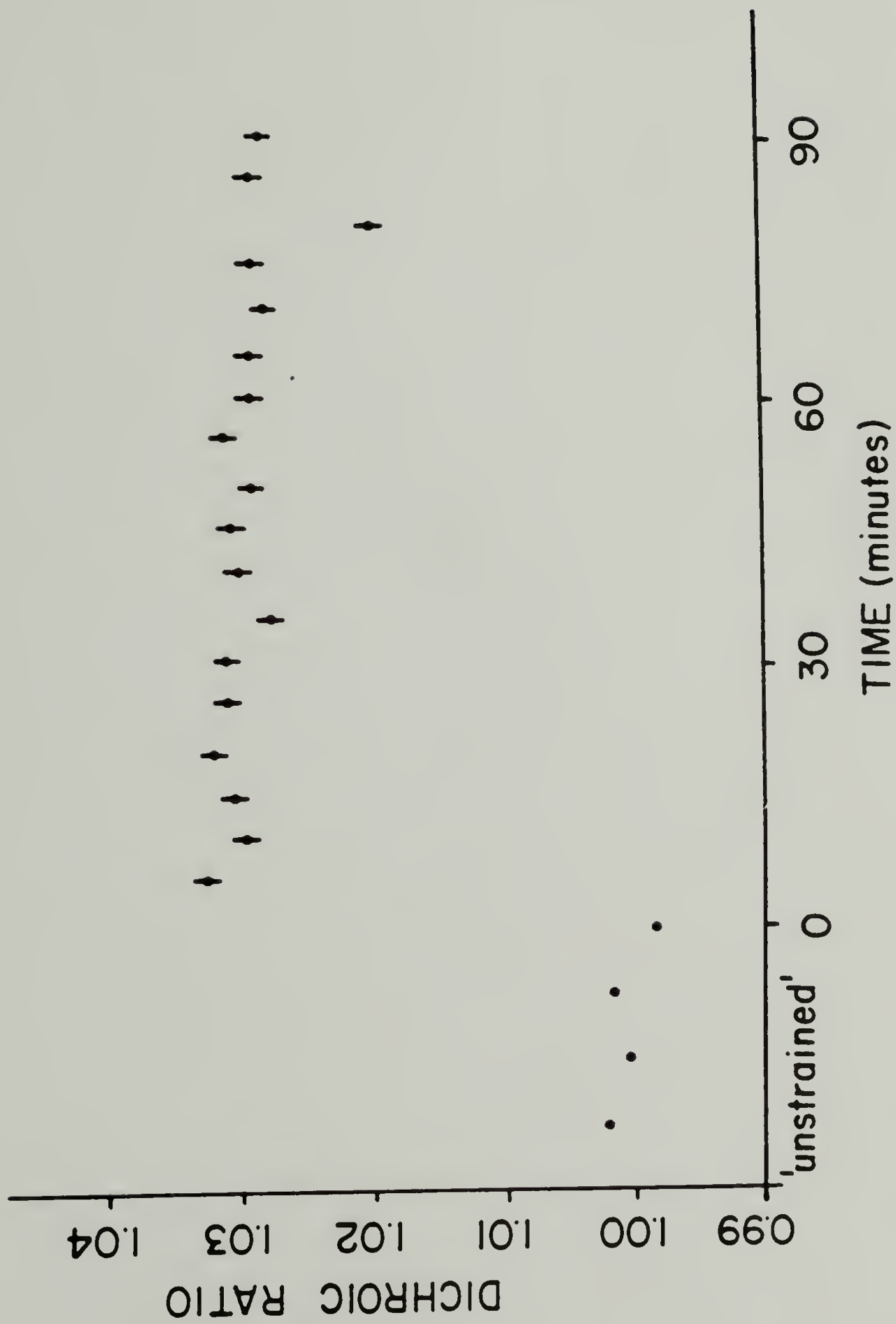


Figure 6.3

sample did become slack for ~20 milliseconds when the strain was released, this was not of concern as the major goal was to investigate the orientation relaxation at the 40% strain level that was attained by rapid deformation. The 15% residual strain was maintained so as to minimize the time period of the slack state. Two time resolved investigations were made; one at 20°C, the other at -20°C. The studies at subambient temperature were facilitated using the nitrogen purged variable temperature chamber. The experimental parameters used for the collection at 20°C are listed in Table 6.1 and those for the collection at -20°C are listed in Table 6.2.

Results and Discussion

Studies described in Chapter II have established that accurate determinations of segmental orientation for a polybutadiene based polyurethane elastomer may be calculated using the method of infrared dichroism. The data collection time for each of these dichroic values was three minutes. To better understand the dynamics of segmental orientation, dichroic ratios of greater temporal resolution must be collected. To accomplish this we have utilized the infrared time resolved method detailed in the previous chapter, using a periodic squarewave deformation as the external event. Sinusoidal deformation studies are more common for polymer characterization as the theory has been well developed. In addition, the continuous deformation process alleviates the problem of transient effects which occur in some defor-

TABLE 6.1

Experimental Conditions Used for the Time-Resolved
Deformation Collection at 20°C

Cycle period	0.75 seconds
Mirror velocity	11
Time clocks per cycle	40
Clock period (time resolution)	19 milliseconds
Spectral resolution	2 cm ⁻¹
Scans per collection	50
Dynamic strain	25%
Prestrain	15%
Deformation waveform	squarewave

TABLE 6.2

Experimental Conditions Used for the Time-Resolved
Deformation Collection at -20°C

Cycle period	1.75 seconds
Mirror velocity	7
Time clocks per cycle	20
Clock period (time resolution)	62 milliseconds
Spectral resolution	2 cm ⁻¹
Scans per collection	40
Dynamic strain	25%
Prestrain	15%
Deformation waveform	squarewave

mation experiments. However, preliminary investigations of this system indicate that when the sample is deformed sinusoidally at a strain which is low enough to eliminate zero stress conditions (i.e., the sample becomes slack), the noise levels of calculated dichroic ratios are as great as any change due to sample deformation. For this reason, the squarewave deformation scheme was chosen for the time resolved studies.

The initial orientation study was the investigation of the long term relaxation behavior of the deformed model polyurethane. The purpose of this was to determine if the system exhibits transient relaxation over extended periods of time, which would complicate the subsequent dynamic relaxation studies using time resolved infrared spectroscopy. As was indicated by the dichroic ratios of the soft segment 1,2 vinyl vibration at 910 cm^{-1} in Figure 6.3, orientation relaxation was negligible over a 1.5 hour time period. Since the time required for the data collection during the time resolved experiment is less than one hour, it was assumed that there was no additional complication due to long term relaxation behavior.

The amplitude of the dichroic ratio of the 910 cm^{-1} vinyl band is 1.03 which corresponds to a sample elongation ratio of 1.68. Using the relationship of Marrinan (16) (Equation 2.10) and the transition moment calculated in Chapter II, the number of Kuhn statistical segments in the butadiene chain was calculated and found to be 23 equivalent links. This is in close agreement with the value of 19 which was calculated in Chapter II and indicates similar sample morphology.

Dynamics of Segmental Relaxation

The stress relaxation response of the polyurethane elastomer subjected to a periodic squarewave deformation at ambient temperature is shown in Figure 6.4. The stress attains a maximum immediately upon deformation and relaxes to an equilibrium value after approximately 25 milliseconds. As the squarewave cycle continues, this same profile is repeated without variation indicating no hysteresis during the deformation cycle. This is a necessary requirement for samples being characterized by the TRS method as they must exhibit no permanent change over the course of the 4000 deformation cycles.

The segmental motion responsible for the stress relaxation occurring after a step deformation of this elastomer can be better understood by analysis of the orientation relaxation of the component segments. The dichroic ratios of the hard and soft segments determined using the time resolved infrared technique during a squarewave deformation at ambient temperature are shown in Figures 6.5 a, b, and c. It is evident that the dichroic ratio of the 1,2 vinyl soft segment vibration follows the strain function and corresponding stress relaxation shown in Figure 6.4. The 1,4 trans vibration (965 cm^{-1}) of the soft segment has a transition moment perpendicular to the chain axis. The changes in the dichroic ratio of this band correspond to orientation relaxation behavior similar to the 1,2 vinyl mode. Although there is considerable noise in these plots, it is clear that soft segment orientation relaxes to an equilibrium value within the first 75 milliseconds. The dichroic ratio of the N-H stretching vibration of the

FIGURE 6.4: Relationship between stress relaxation and squarewave strain function.

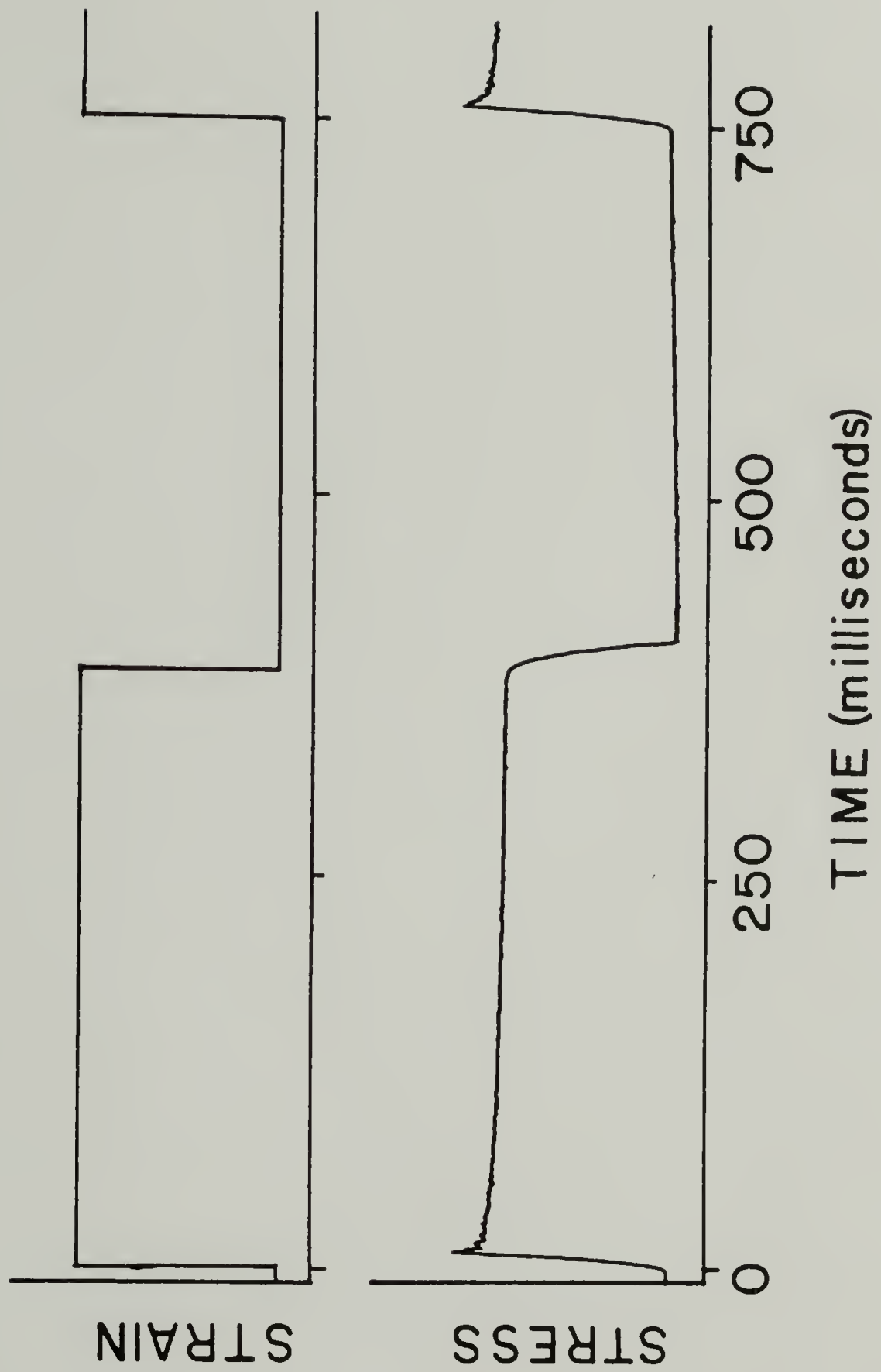


Figure 6.4

FIGURE 6.5: Time resolved dichroic ratios as a function of time at ambient temperature.

- a. 1,2 vinyl C-H deformation
- b. 1,4 trans C-H deformation
- c. N-H stretching vibration

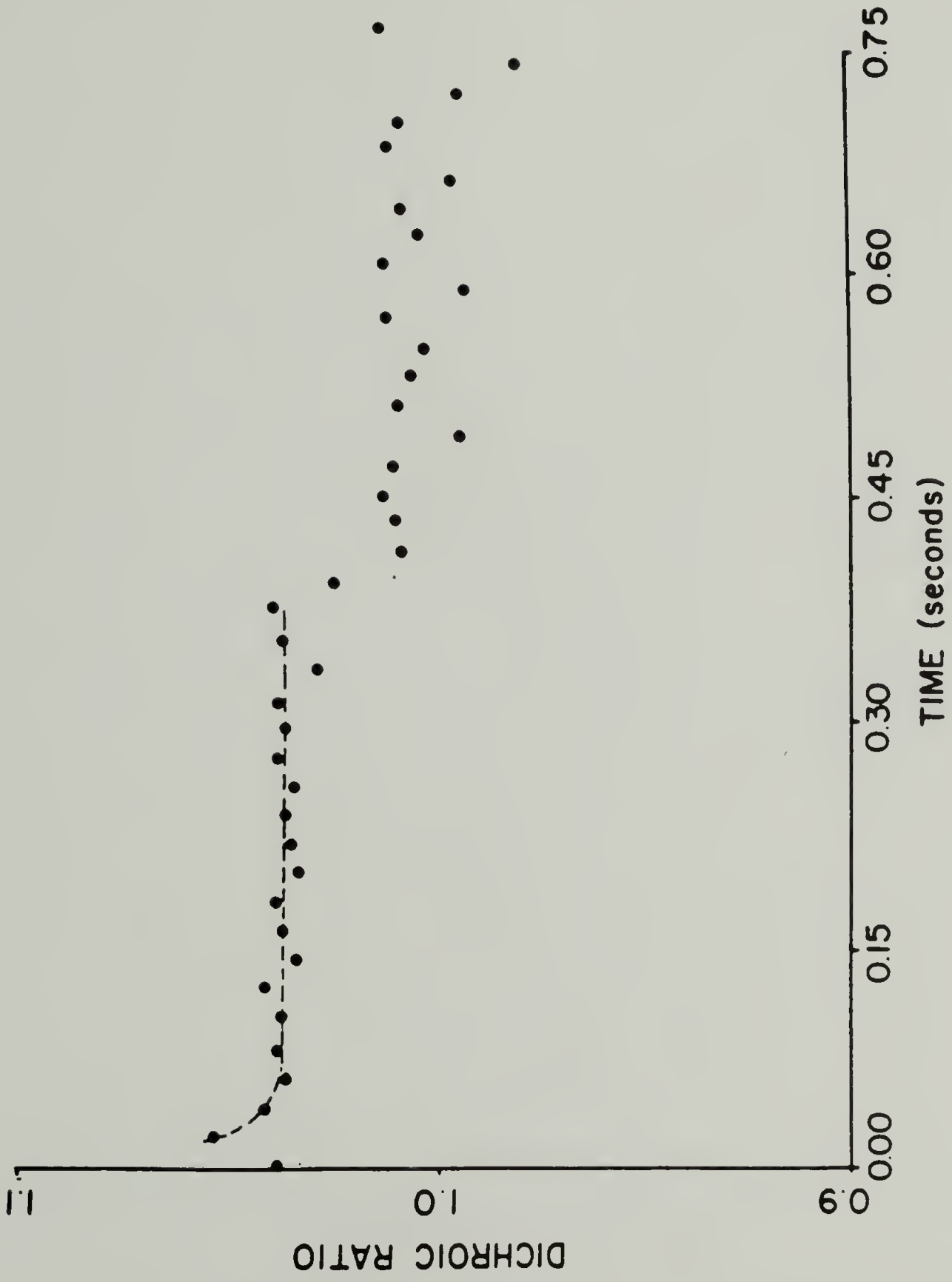


Figure 6.5a

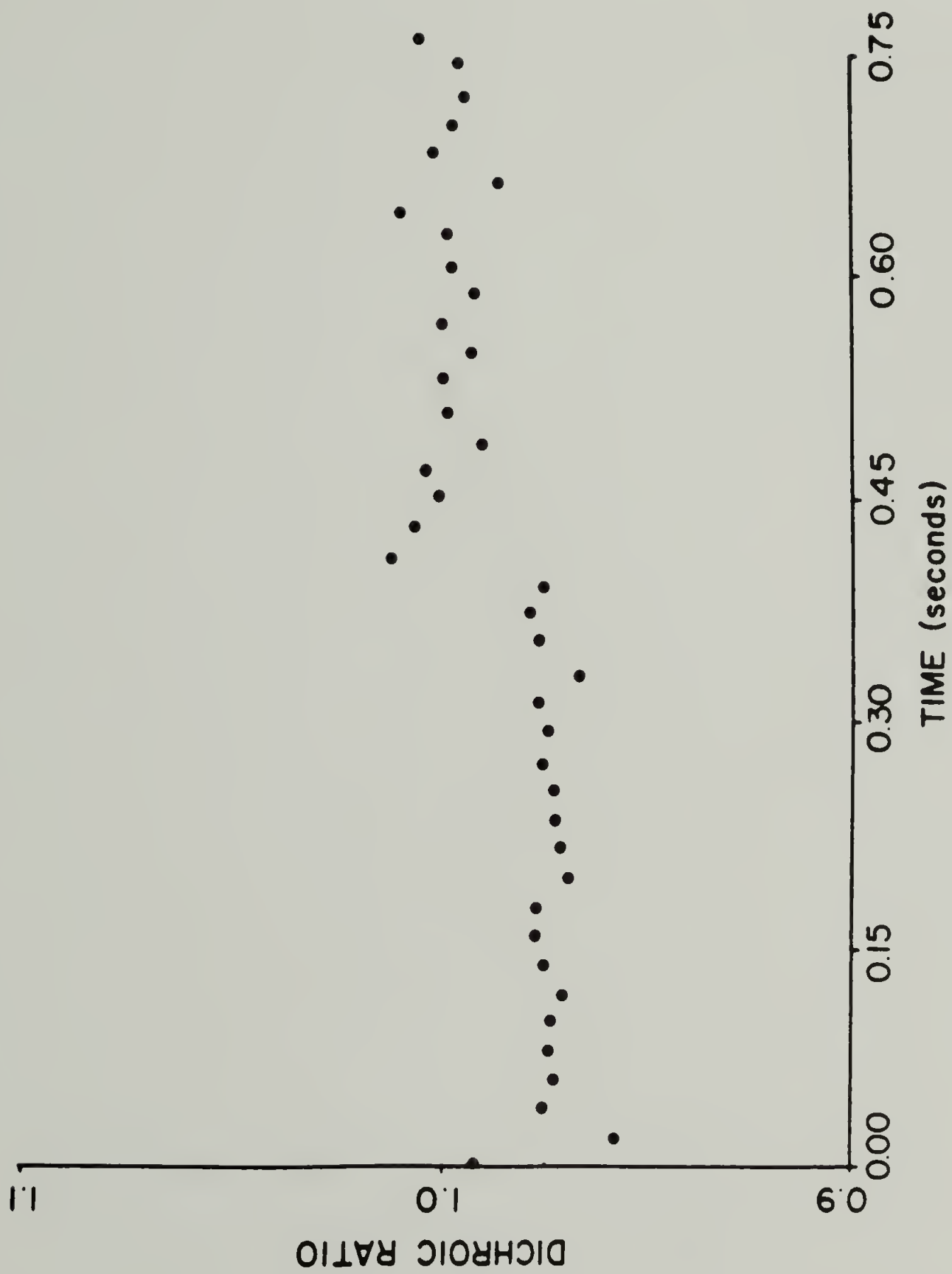


Figure 6.5b

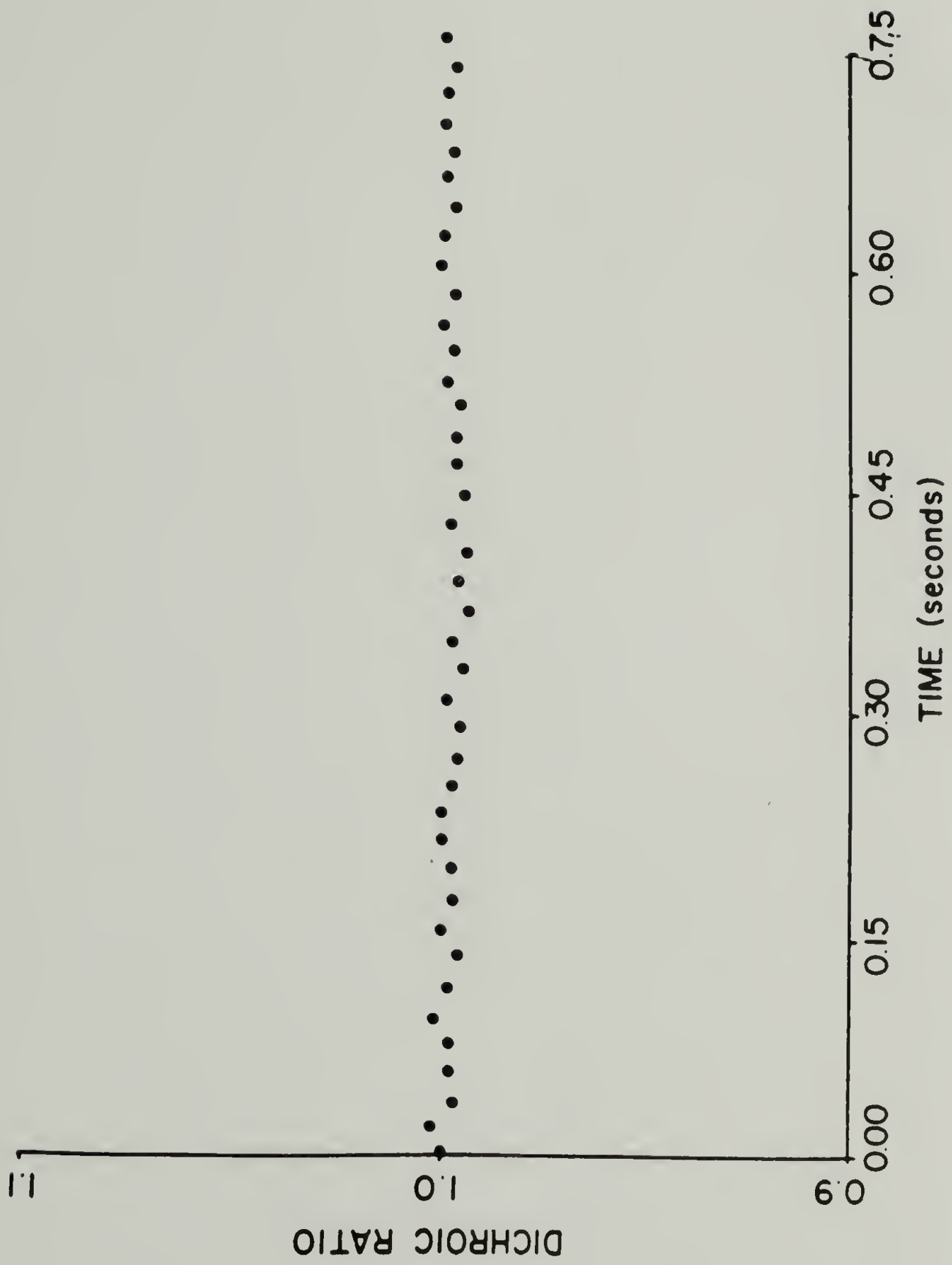


Figure 6.5c

hard segment exhibits no change upon deformation as was observed in Chapter II. The orientation relaxation for this same type of deformation scheme at a temperature of -20°C is shown in Figures 6.6 a, b, and c. Several differences may be noted when comparing soft segment relaxation at -20°C to that occurring at 20°C . While the sample and strain amplitude are the same in both cases, the relaxation rates and equilibrium dichroic ratios exhibit significant change. Although there is significant noise in the data at both temperatures, it is clear that at -20°C the orientation relaxation occurs at a slower rate than at ambient temperature and the equilibrium dichroic ratio is greater. Before discussing these differences in detail, it is first worthwhile to evaluate the degree of uncertainty in the data.

Evaluation of Noise in TRS Spectra

The noise level in absorbance spectra may be evaluated by the subtraction of two spectra collected under identical conditions. The resulting noise spectrum is described by Equation 6.1

$$N_i = (A_{1i} \pm N_{1i}) - (A_{2i} \pm N_{2i}) = (N_{1i}^2 + N_{2i}^2)^{1/2} \quad (6.1)$$

where A is absorbance, N is noise, and the subscript i represents the frequency domain. Noise level spectra for both the TRS collection and static collection are shown in Figure 6.7 along with the absorbance spectrum.

The noise level in these difference spectra is greater in the regions of the absorption bands and has a dependence on absorbance which follows Equation 6.2

FIGURE 6.6: Time resolved dichroic ratios as a function of time at -20°C .

- a. 1,2 vinyl
- b. 1,4 trans
- c. N-H stretch

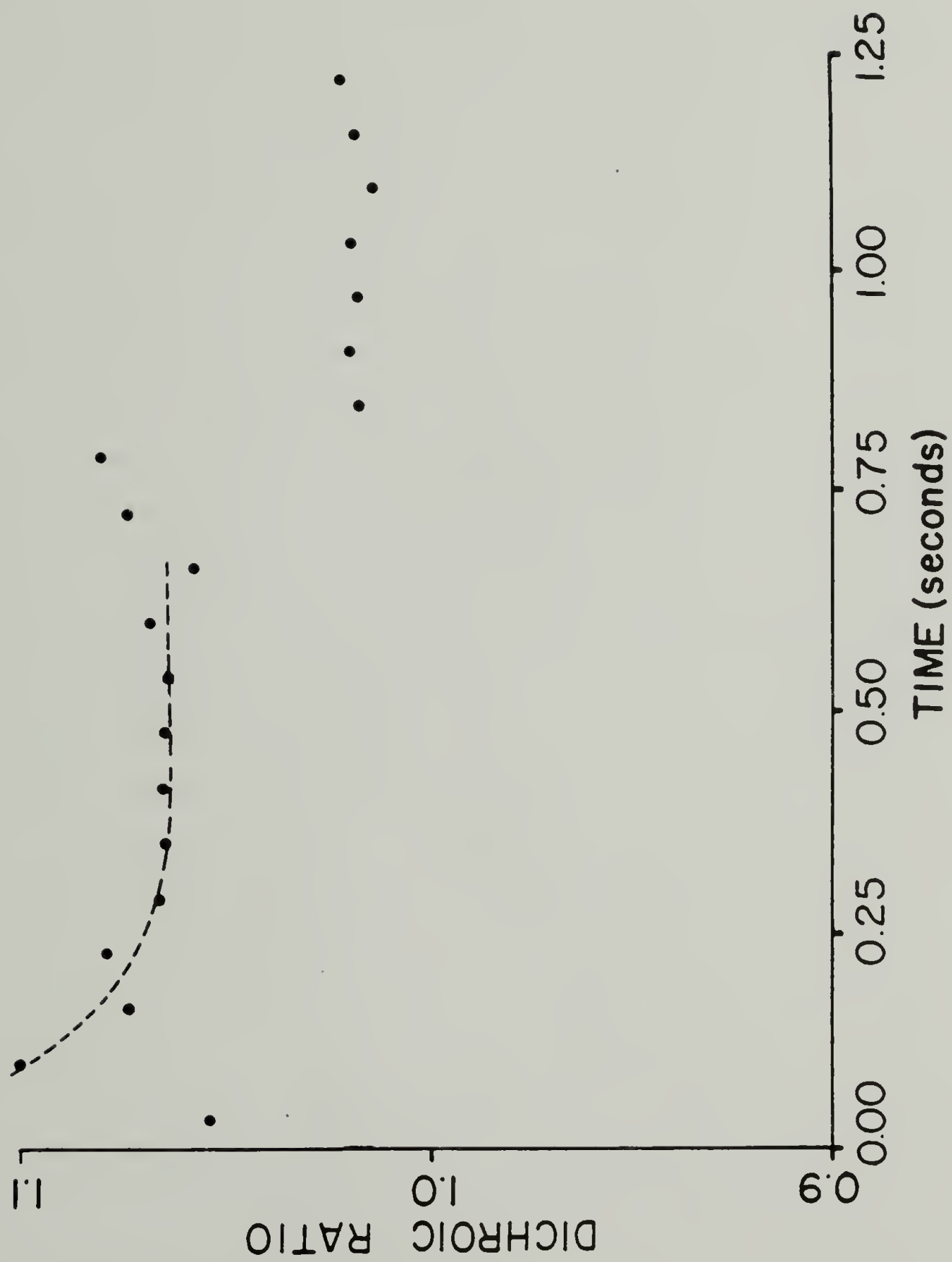


Figure 6.6a

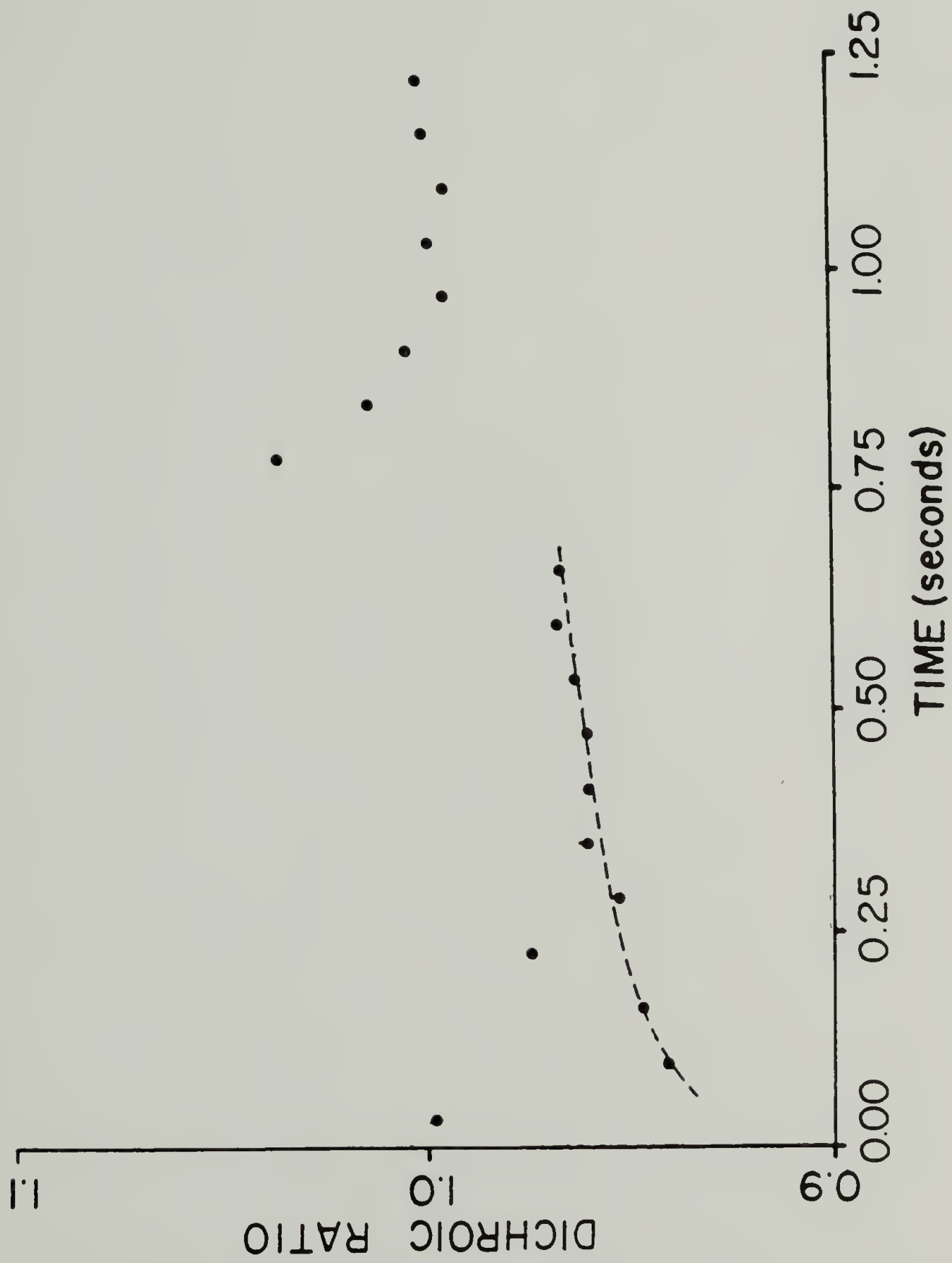


Figure 6.6b

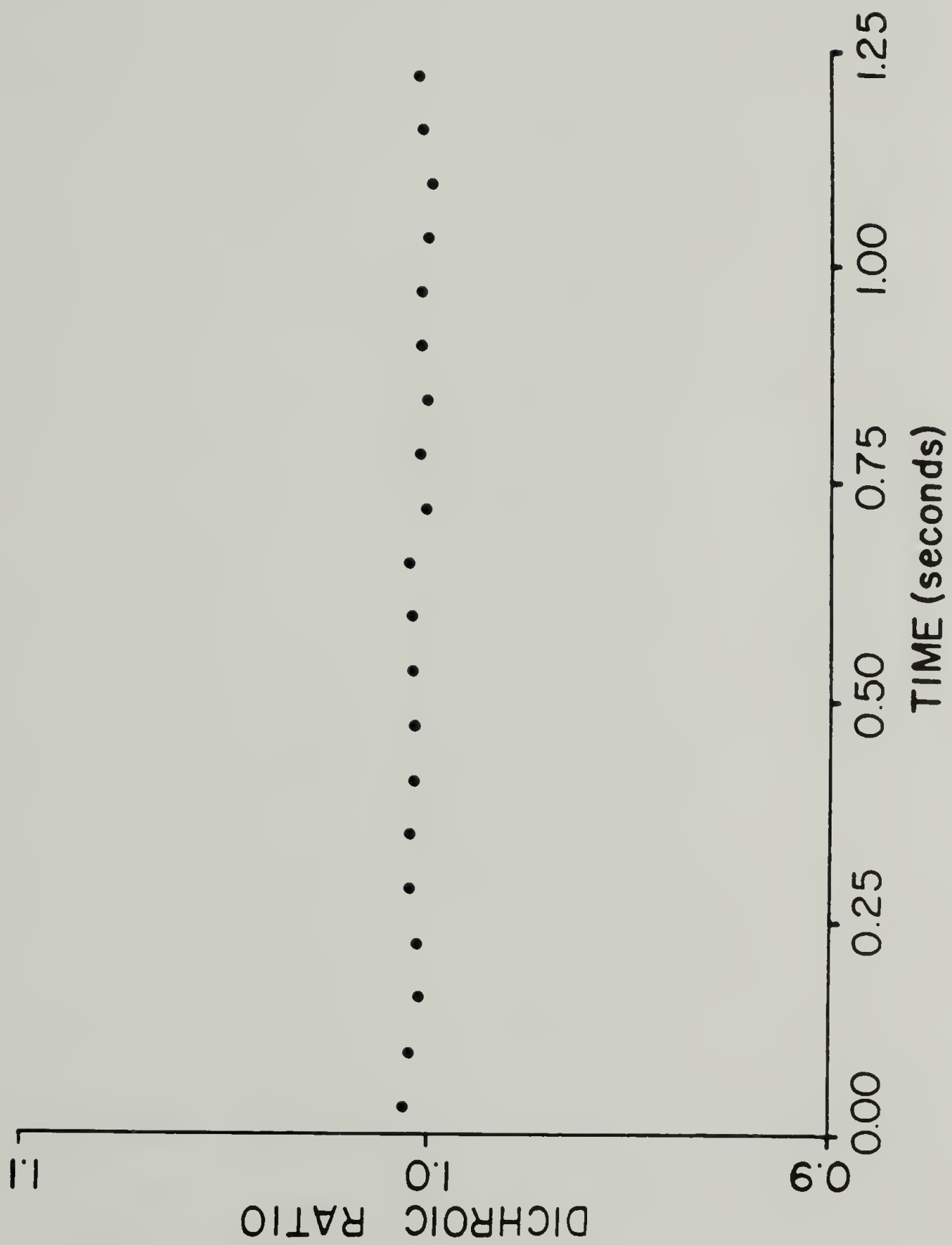


Figure 6.6c

FIGURE 6.7: Noise level spectra and corresponding absorbance spectrum, a. static collection mode, b. time resolved mode, c. absorbance spectrum.

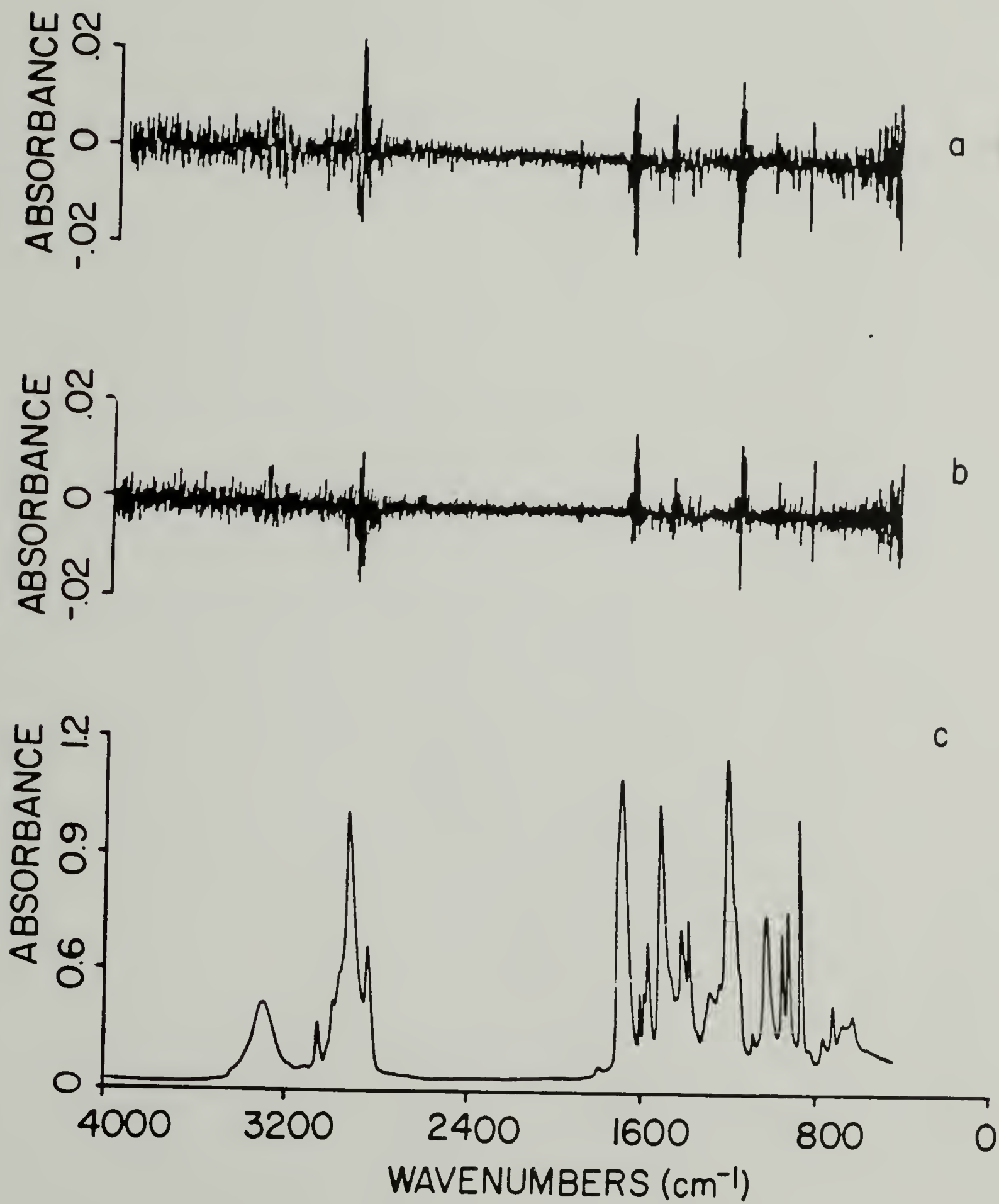


Figure 6.7

$$N_i = - \frac{10^{A_i} N_{S_i}}{I_{0_i} \ln 10} \quad (6.2)$$

where N_S is the noise in the single beam spectrum and I_0 is the intensity of the single beam reference spectrum. The noise in the time resolved spectra using this method is approximately 30% greater than that of the spectra collected under static conditions. This increase in noise in the dynamic absorbance spectra is sufficient to account for the noise of the dichroic ratios corresponding to the strained state of the dynamic case. The absorbance spectra corresponding to the initial 18 milliseconds of the TRS experiment exhibit considerably higher noise levels than the rest of the spectra of the deformation cycle. The step deformation occurred during this time interval, making it likely that mechanical oscillation of the system resulted in an increased noise level. This noise is clearly seen in the lower spectrum of Figure 6.8, which is the absorption corresponding to the 1,2 vinyl C-H deformation mode. The upper plot corresponds to the second time interval. The noise in the spectra of this time interval and all subsequent time intervals is similar to the noise found in spectra collected under static conditions. For both the ambient and subambient TRS experiment the dichroic ratios corresponding to the unstrained state exhibit uncertainty which is greater than in the strained state. This noise is most likely due to the sample becoming slack as the strain is released as well as subsequent acoustic vibrations which occur as it recovers and becomes taut again.

FIGURE 6.8: Time resolved spectra of 1,2 vinyl C-H deformation region. Lower trace: first clock period (0-19 msec), upper trace: second clock period (19-37 msec).

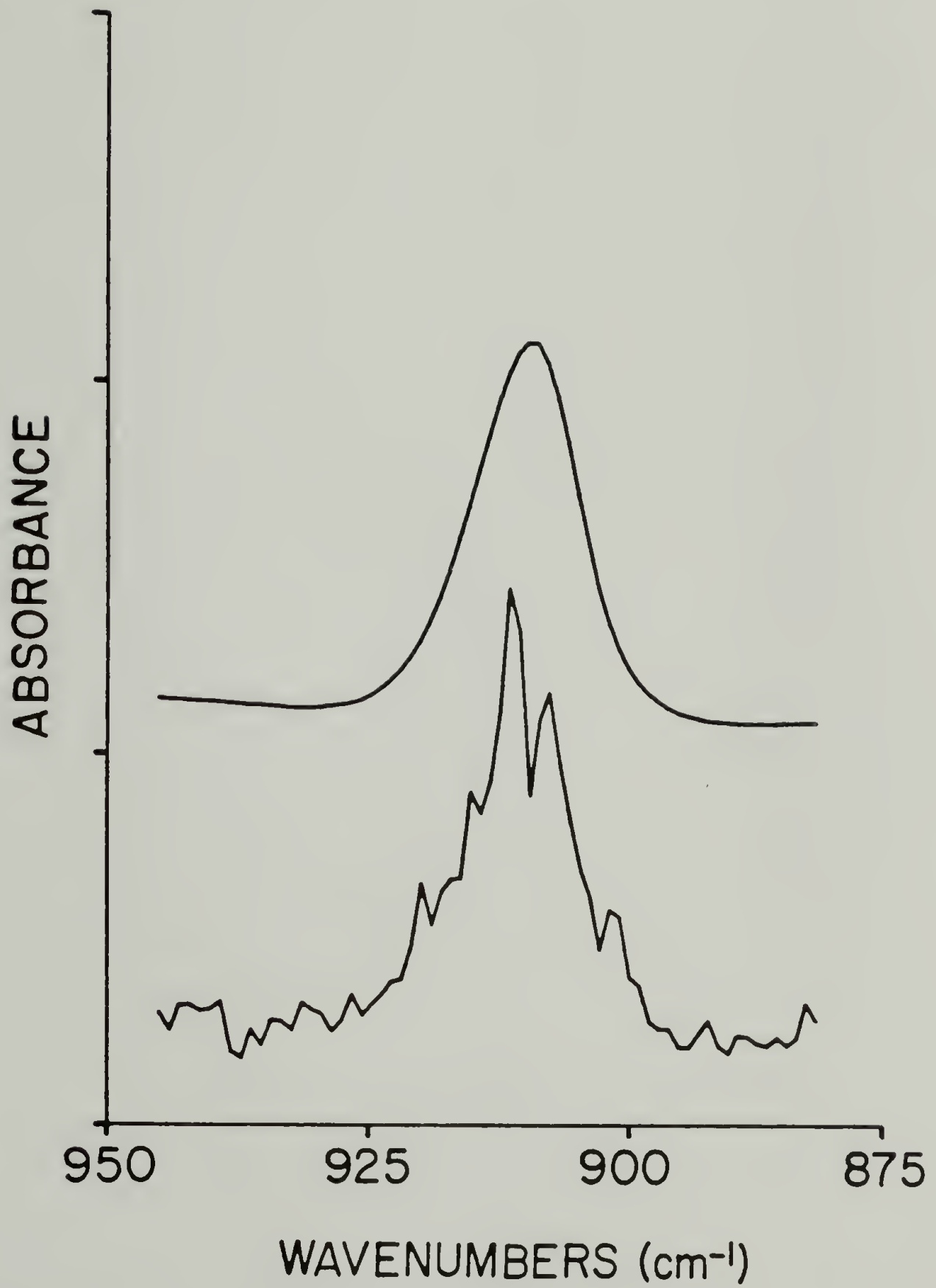


Figure 6.8

Comparison of Ambient and Subambient Orientation Behavior

At ambient temperature the equilibrium dichroic ratio for the 1,2 vinyl vibration in the deformed sample has a value of 1.035 and is in good agreement with the value of 1.03 determined for the static deformation discussed previously. In the low temperature case the dichroic ratio of this band for the deformed sample has an equilibrium value of 1.06. This indicates that the soft segment is oriented to a greater extent at -20°C than at 20°C . The difference in these dichroic ratios for the two different temperatures can also be considered in terms of the number of Kuhn equivalent links between effective crosslinking points. This may be determined using the relationship of Marrinan (Equation 2.10). In the 20°C case the number of Kuhn links is 23, while in the -20°C case the number of Kuhn links is 13. This indicates that the average chain length between equilibrium "physical" crosslinks at -20°C is half that of the ambient temperature case.

A significant difference also exists in the rate of orientation relaxation in the strained state at 20°C compared to that at -20°C . Soft segment orientation has relaxed to an equilibrium value after 75 milliseconds at 20°C while 400 milliseconds is required to reach an equilibrium orientation value at -20°C . The relative relaxation rates for these two cases is discussed in terms of the times required to reach equilibrium values rather than as characterization relaxation times for two reasons. The relaxation of both orientation and stress could not be fitted with a single exponential decay function and thus indicates a distribution of relaxation time is likely. A second

problem in analyzing relaxation after a step deformation is the initial transient in the relaxation due to the fact that a finite time is required to deform the sample. It has been reported by Farris that when the time required to deform a sample is t , the shortest time at which the relaxation process may be evaluated is $10 \cdot t$ (17).

Stress relaxation for the same type of periodic squarewave deformation as is used in the time resolved infrared experiment is plotted for several temperatures in Figure 6.9. The rate of stress relaxation decreases and the equilibrium stress value increases as the temperature of the sample is decreased. This is qualitatively similar to the soft segment orientation behavior plotted in Figures 6.5a and 6.6a.

The lack of hard segment orientation in both the ambient and subambient time resolved data is perplexing considering the differences in equilibrium soft segment orientation for these two cases. Since the lack of permanent set in the deformed sample suggests a series type morphology, it would be expected that as the soft segment orientation decreases the hard segment orientation would increase. Further investigation of hard segment orientation seems necessary to resolve this inconsistency. The time required for the relaxation of sample stress and soft segment orientation can also yield information as to the nature of the deformation and relaxation process. An important consideration which must be resolved is whether the relaxation process is due to soft segment relaxation alone or if there is indeed relaxation of the hard segment domains.

FIGURE 6.9: Temperature dependence of stress relaxation for 40% squarewave deformation.

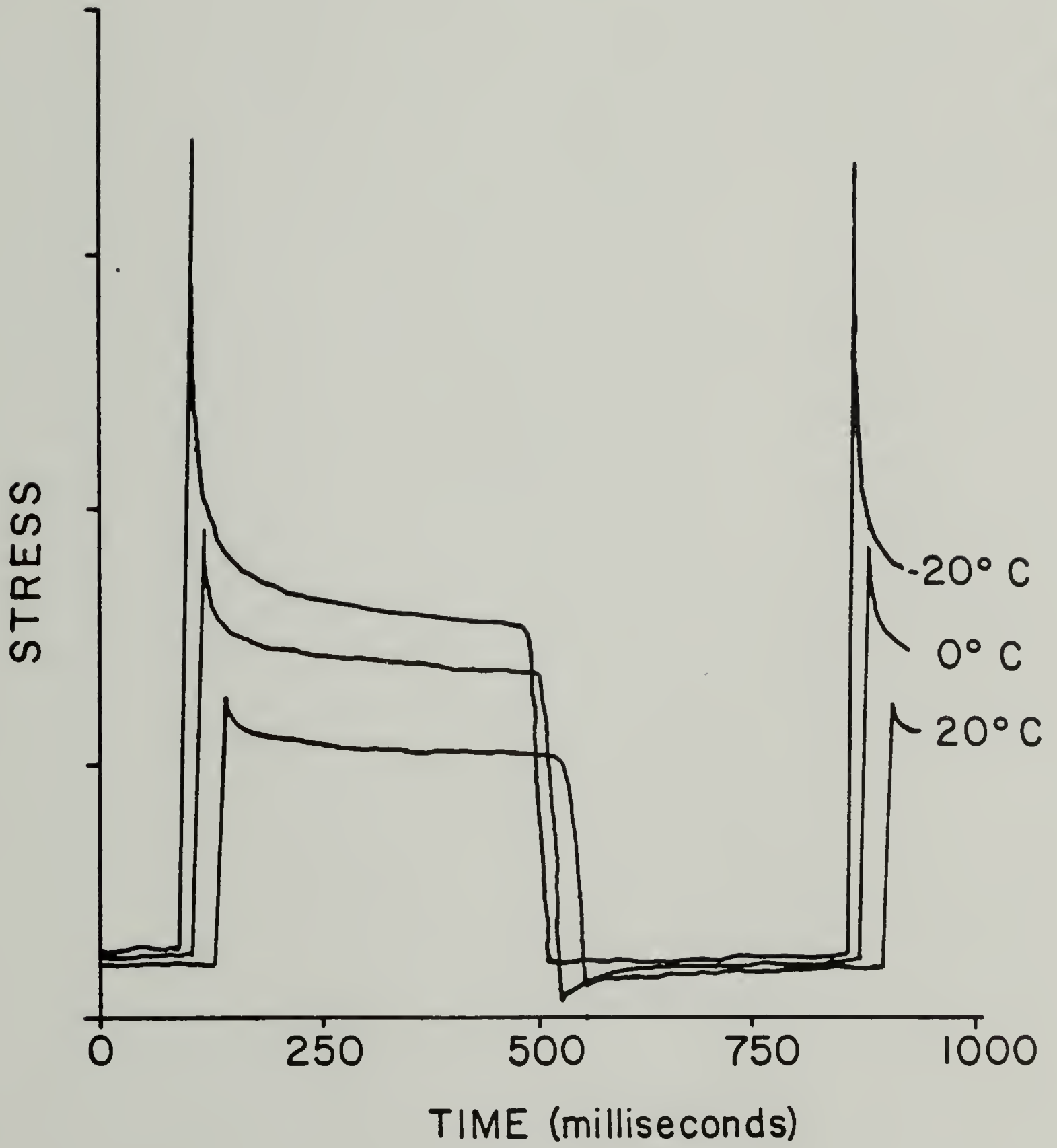


Figure 6.9

The time required for relaxation of pure polybutadiene chains may be estimated from theory based on reports in the literature involving studies of polybutadiene homopolymers. Grassely has developed the following relationship (Equation 6.3) (18) based on the experimental relaxation times determined by Kraus and Rollman for "free" polybutadiene molecules in the polybutadiene phase of butadiene-styrene block copolymers.

$$t_d = 4.3 \times 10^{-16} M^3 \text{ sec} \quad (6.3)$$

In this equation t_d is the disengagement time for reptation of entangled molecules and M is the molecular weight. The disengagement time is the longest characteristic time of a polymer relaxation, and is developed from reptation theory. To consider a polybutadiene chain with a molecular weight of 5000 (which is over twice the molecular weight of our soft segment prepolymer), the value of t_d as calculated from Equation 6.3 is 5×10^{-5} seconds. This relaxation time is more than three orders of magnitude less than that estimated for the soft segment orientation relaxation in this study. This indicates that the relaxation of the segmented polyurethane elastomer does indeed involve a contribution from the hard segment phase. However, since the deformation is completely recoverable and the stress relaxation curve shows no change during repeated deformations, any hard segment contribution must be reversible.

The temperature dependence of both equilibrium soft segment orientation and relaxation can be accounted for using a model where the number of hard segments which are effective as physical crosslinks is

dependent on the temperature of the system.

Morphological investigations of this type of polyurethane system indicate that the hard segments form isolated hard segment domains of elongated spherical geometry which are surrounded by the polybutadiene soft segment matrix (20). While the hard segments are of monodisperse length, it is likely that there would be a distribution of temperatures for the onset of individual hard segment mobility, dependent on the positioning of the hard segment in the domain. Figure 6.10 is a simplified schematic of two types of hard segment positioning. The hard segments which traverse the center of the domains, labeled A, would have severely limited mobility corresponding to the highest glass transition temperature, T_g , of the system. The segment labeled B would have greater mobility due to an increased free volume as it is in contact with the polybutadiene phase. The mobility or yield stress of "B type" hard segments would be a function of temperature and would account for the temperature dependence of the number of effective physical crosslinks.

This same model can also be used to account for the temperature dependence of the orientation and stress relaxation rates. Segmental mobility in the outer layer of the hard segment domain is greater at higher temperatures and would result in more rapid equilibration times. The repeatability of the stress relaxation cycle as can be seen in Figure 6.8 indicates there is rapid recovery of the domain structure in the unstrained state. The entropic force of soft segment chain which couple "A type" hard segments result in the recovery of the original spatial positioning of neighboring hard segment domains. This type of

FIGURE 6.10: Schematic representation of hard segment positioning in hard segment domain; a. traverses domain center, b. on domain surface.

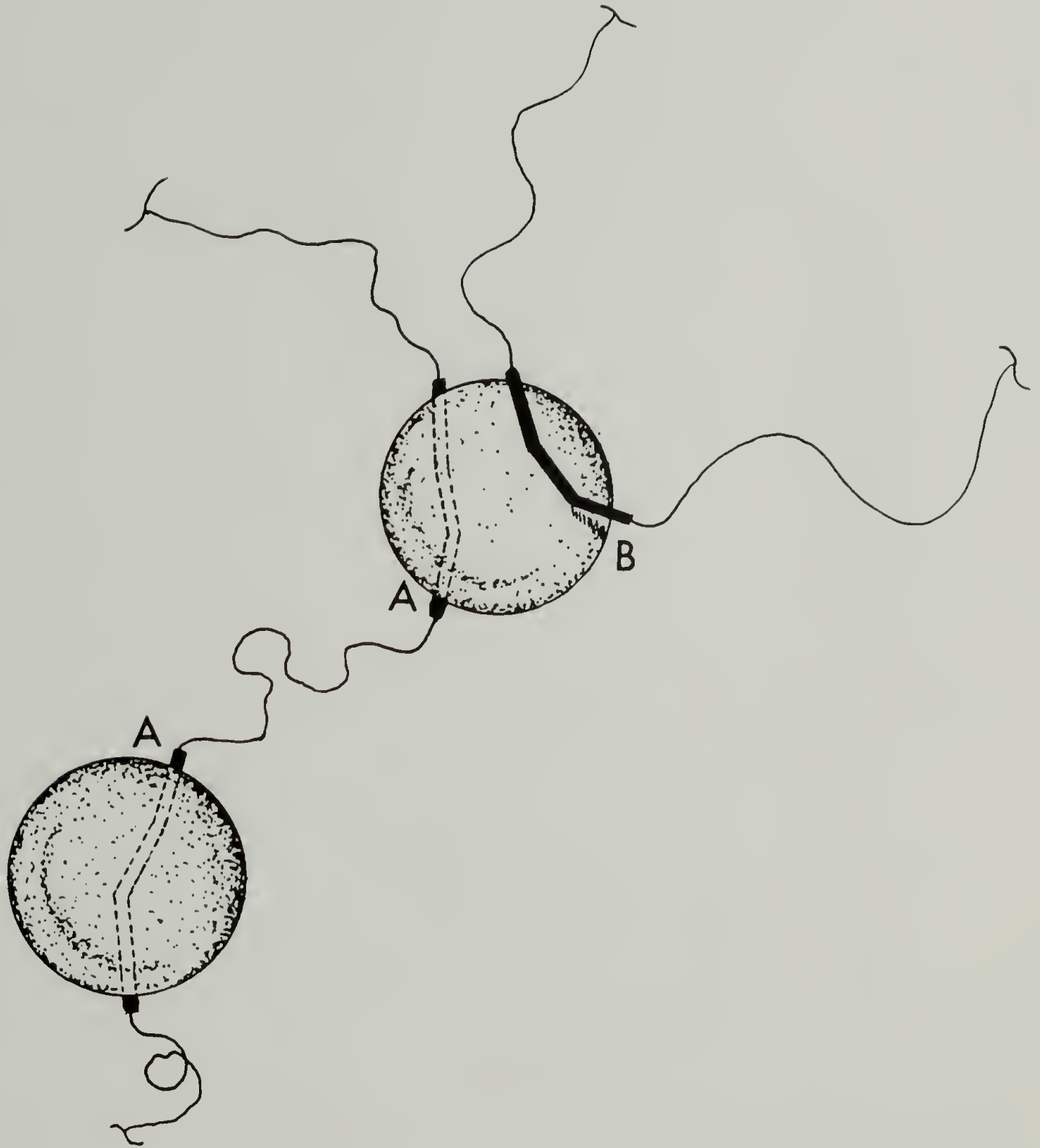


Figure 6.10

behavior has been observed by several authors for Kraton® styrene-butadiene triblock copolymers (21,22).

The fact that no hard segment orientation is observed for this system, even at ambient temperature, is not well understood. It would seem likely that as hard segments are pulled out of the domain structure as the sample is deformed there should be an increase in orientation that could be observed in the dichroic ratio of the N-H or carbonyl vibration. It may be possible that the transition moment angles of the N-H and carbonyl vibrations which are used to interpret hard segment orientation are such that dichroic ratios of these vibrations are insensitive to orientation. This would be the case if the transition moment angles are close to 54.7° ; the angle at which even perfectly oriented chains have a dichroic ratio of one. Further investigations of the dichroism of oriented hard segment model polymers are necessary to better understand this phenomenon. One suggestion for future work would be to incorporate deuterated butane diol chain extender molecules into the modisperse hard segments. This would then allow one to use the C-D stretching vibration as an indication of hard segment orientation, as it would no longer be obscured by the unsaturated C-H stretching vibrations of the soft segment.

REFERENCES

1. R.S. Stein, "Rheo-Optical Studies of the Deformation of Crystalline Polymers, J. Polym. Sci., C15, 185 (1966).
2. G.L. Wilkes and R.S. Stein, "Effect of Morphology on the Mechanical and Rheo-Optical Properties of a Styrene Butadiene-Styrene Block Copolymer, J. Polym. Sci., Polym. Phys. Ed., 7, 1525 (1969).
3. R.S. Stein, "Rheo-Optical Studies of Rubbers", Rubber Chem. Tech., 49(3), 485 (1976).
4. R.S. Stein, "On the Dynamic Light Scattering from Polymer Films:", J. Polym. Sci., 62, S2 (1962).
5. P.F. Erhardt and D.G. LeGrand, J. Appl. Phys., "Rheo-Optical Properties of Polymers. III. Dynamic Polarized Light Scattering", J. Appl. Phys., 34, 68 (1963).
6. S. Onogi and T. Asada, "Rheo-Optical Studies of High Polymers. IX. A Study of Deformation Process of Low Density Polyethylene by Simultaneous Measurements of Stress, Strain, and Infrared Absorption", J. Polym. Sci., C16, 1445 (1967).
7. Y. Fukui, T. Asada, and S. Onogi, "Rheo-Optical Studies of High Polymers XX. Time and Temperature Dependences of Crystalline and Amorphous Orientation in Low Density Polyethylene", Polymer J. 3(1), 100 (1972).
8. G.L. Wilkes, Y. Uemura, and R.S. Stein, "Apparatus for Instantaneously Measuring Ultraviolet, Visible or Infrared Dichroism from Thin Polymers During High Speed Stretching", J. Polym. Sci., Polym. Phys. Ed., 9, 2151 (1971).

9. D.J. Burchell, J.E. Lasch, E. Dobrovolny, N. Page, J. Domian, R.J. Farris, and S.L. Hsu, "Deformation Studies of Polymers by Fourier Transform Infrared Spectroscopy II. Mechanical Stretcher and its Interface to the Spectrometer", *Appl. Spectrosc.*, 38, 343 (1984).
10. J.E. Lasch, D.J. Burchell, T. Masoaka, and S.L. Hsu, "Deformation Studies of Polymers by Time-Resolved Fourier Transform Infrared Spectroscopy III: A New Approach", *Appl. Spectrosc.*, 38, 351 (1984).
11. S.E. Molis, W.J. MacKnight, and S.L. Hsu, "Deformation Studies of Polymers by Time Resolved Infrared Spectroscopy IV: A Modified Approach", *Appl. Spectrosc.*, 38, 529 (1984).
12. I. Noda, A.E. Dowery, and C. Marcott, "Dynamic Infrared Linear Dichroism of Polymer Films under Oscillatory Deformation", *J. Polym. Sci.*, B21, 99 (1983).
13. R.W. Seymour, A.E. Allegrezza, Jr., and S.L. Cooper, "Segmental Orientation Studies of Block Polymers. I. Hydrogen-Bonded Polyurethanes", *Macromol.*, 6, 896 (1973).
14. F.G. Faxe, "Cast Tires", *Plastic Rubber Int.*, 5(3), 105 (1980).
15. M.A. Schulman, W.A. Jackle, and R.V. Ponticiello, "Predicting the Performance of Polyurethanes", *Ind. Res.* 19(8), 54 (1977).
16. H.J. Marrinan, "The Infrared Dichroism of a Stretched Polymer. Part I. The Theoretical Treatment of Rubberlike Polymers", *J. Polym. Sci.*, 39, 461 (1954).
17. R.J. Farris, "Stress-Strain Behavior of Mechanically Degradable Polymers", *Polym. Prepr. Amer. Chem. Soc., Div. Polym. Chem.*, 11(2), 470 (1970).

18. W.W. Grassley, "Some Phenomenological Consequences of the Doi-Edwards Theory of Viscoelasticity", J. Polym. Sci., Polym. Phys. Ed., 18, 27 (1980).
19. G. Kraus and K.W. Rollman, "Dynamic Viscoelastic Behavior of Polybutadiene Networks", J. Polym. Sci., Polym. Symp., 48, 87 (1974).
20. C. Chen-Tsai, "Morphology Studies of Amorphous Segmented Polyurethanes", Ph.D. Dissertation, University of Massachusetts, 1984.
21. J.F. Henderson, K.H. Grundy, and E. Fischer, "Stress-Birefringence Properties of Styrene-Isoprene Block Copolymers", J. Polym. Sci., Polym. Symp., 16, 3121 (1968).
22. E. Fischer and J.F. Henderson, "The Stress-Strain Birefringence Properties of Styrene-Butadiene Block Copolymers", J. Polym. Sci., Polym. Symp., 26, 149 (1969).

C H A P T E R V I I

GENERAL RESULTS AND RECOMMENDATIONS FOR FUTURE WORK

General Results

Several model polyurethane elastomers have been characterized at the molecular level using Fourier transform infrared spectroscopy. These systems were highly phase separated due to the thermodynamic incompatibility of the polybutadiene soft segments and toluene diisocyanate-butenediol hard segments. A system which was well phase separated was desirable so as to eliminate the uncertainty associated with segmental mixing which occurs at the hard-soft domain interface of most commercial polyurethanes. The hard segment microstructure was characterized for a system showing paracrystalline ordering. Segmental orientation was characterized for both semicrystalline and amorphous systems subjected to uniaxial strain. Particular attention was given to the characterization of segmental orientation dynamics.

Microstructural Ordering in Polyurethane Hard Segments

The microstructural ordering of polyurethane hard segments prepared with toluene diisocyanate which is a mixture of the 2,4 and 2,6 isomers has been characterized using Fourier transform infrared spectroscopy. Although semicrystalline hard segment structure has been reported as occurring in polyurethanes with hard segments prepared with pure 2,6 TDI, this is the first report of hard segment ordering for systems with mixed isomer TDI. Detailed analysis of

infrared absorptions characteristic of this phase and its orientation response to uniaxial strain have indicated that the ordered component in the mixed isomer hard segment is of similar origin to that in the system prepared with pure 2,6 TDI. Based on these results it has been proposed that the ordered hard segment phase results from consecutive sequences of the 2,6 isomer in the mixed isomer hard segments. The development of microstructural order (paracrystallinity) occurs only in samples which have been cast from solution or plasticized with solvent vapor. Solvent induced crystallization is well known for polycarbonate systems and it is believed that this is a general phenomenon for polymers in which the crystal melting point and glass transition occur at similar temperatures. The melting temperature of the ordered structure in this system is lower than that of a system prepared with pure 2,6 TDI. It is believed that the 2,4 TDI residues disrupt the crystalline structure. However, the 2,4 TDI hard segment units do add to the hard segment length when adjacent to the 2,6 TDI sequences, thus contributing to an increase in the glass transition temperature. This results in a deviation from the general case where T_g is between $1/2$ and $2/3$ of the value of T_m . Compounds which plasticize the hard segment phase yet are poor solvents for the crystalline component result in increased hard segment mobility, thus allowing crystallization to occur.

Monte Carlo simulation of the kinetics of the polyurethane polymerization process have indicated that the unequal reactivity of the isocyanate groups of the 2,4 TDI isomer results in hard segments with

a greater number of adjacent 2,6 TDI residues than what would be expected for random polymerization kinetics. This results in hard segments which have a greater tendency to undergo microstructural ordering, forming paracrystalline domains.

When this polymer system is heat treated at 180°C, the ordered structure can no longer be reformed, indicating a disruption of the crystallizable hard segment sequences. Infrared thermal analysis of model urethane compounds demonstrates that urethane interchange reactions do indeed occur, supporting the postulation that 2,6 TDI isomer sequences may be disrupted by the incorporation of 2,4 TDI units due to thermal "scrambling".

Characterization of Segmental Orientation

The microstructural response of polymers subjected to uniaxial deformation has been characterized using infrared spectroscopy. The dynamics of segmental orientation of a model polyurethane elastomer have been studied using a new method of time-resolved Fourier transform infrared spectroscopy. Time resolved spectroscopy was used to increase the temporal resolution of the infrared collection beyond that normally associated with commercial FTIR spectrometers. The method utilized in this investigation employed the use of a separate microprocessor to synchronize the deformation event and interferometer movement. The performance of this technique was first tested with a characterization study of the reversible, strain induced crystal phase transition of poly(butylene terephthalate). The resulting data had a higher signal to noise ratio than that of

previous methods and indicated that the phase transition followed the imposed sinusoidal strain function with a response which exceeded the time resolution of the experiment.

Segmental orientation of both the hard and soft segments in a polyurethane elastomer having monodispersed hard segments of 5 units of 2,4 TDI has been characterized using the method of infrared dichroism. Initial characterization was of the static case with polarized spectra being collected at successive increments of strain. The soft segment orientation increased steadily as the sample strain was increased, however, the hard segment component exhibited no orientation. This type of orientation behavior was interpreted as being due to a phase separated morphology where the hard segment domains act as inert spheres which are physical crosslink points for the soft segment matrix. In this same study the transition moment of the 1,2 vinyl CH out of plane deformation mode was found to be independent of sample strain. This is an interesting result as this is a pendant group on the polybutadiene chain. From the relationship between soft segment orientation and macroscopic sample strain it was determined that there were six main chain atoms in a Kuhn type statistical segment for the butadiene soft segment.

The dynamics of segmental orientation of the monodispersed system during uniaxial deformation has been investigated with high temporal resolution using the software controlled time resolved FTIR technique. The extent of orientation of both the hard segments and soft segments has been characterized as a function of temperature for a squarewave

deformation function. The effective soft segment chain length at -20°C was found to be half that for the same sample at ambient temperature. This indicates that there are more hard segments which are active as physical crosslinks at low temperature. The rate of soft segment relaxation is slower at lower temperatures with the time required to attain an equilibrium value being 0.075 seconds at ambient temperature and 0.4 seconds at -20°C . A model has been proposed whereby the major contribution to segmental relaxation is a soft outer layer of the hard segment domains. Since the hard segment chains in the outer layer of the domain have greater mobility due to the higher free volume in the soft segment matrix, they are free to relax, thus decreasing the overall orientation. At lower temperatures the segmental mobility of the hard segments would be less, causing an increase in the time required for relaxation.

Recommendations for Future Work

Characterization studies of the model polyurethanes investigated in this dissertation have led to an increased understanding of the structure and deformation behavior of segmented polyurethanes in general. Due to the complexity of the chemical structure and morphological features of these materials an exacting interpretation of the physics of structural organization and deformation mechanisms has been difficult to achieve. Several questions which still remain, as well as experimental methods which will lead to a more comprehensive

understanding of the physics of polyurethane structure will be discussed in this section. While a number of polyurethane systems have been reported in the chemical literature which are of both commercial and academic importance, the future studies discussed here will be limited to infrared investigations of highly phase separated model systems similar to those utilized throughout this work.

Investigations of Hardsegment Microstructural Ordering

Hard segment microstructural ordering in the polyurethane elastomer prepared with mixed isomer toluene diisocyanate has been found to exist, as evidenced by the orientation behavior and specificity of hydrogen bonding characterized using infrared spectroscopy. The specific hard segment structure required for crystallization to occur is still in question. A determination of this crystallizing component could be facilitated by investigating the crystallization behavior of a series of polyurethane elastomers having monodispersed hard segments prepared with 2,6 TDI. The fundamental question in this investigation would be to determine the minimum number of TDI-butandediol units necessary for crystallization to occur and to characterize the crystallization and melting behavior of these well defined domains. Infrared spectroscopic analysis could be complemented by thermal and wide angle x-ray scattering studies. The preparation of the monodispersed systems using 2,6 TDI would be more difficult than systems prepared with the 2,4 isomer. One approach which would lead to the isolation of monodisperse hard segment units is by a preparative separation using high performance liquid chroma-

tography. This method has been successful in preparing monodisperse hard segments incorporating 4,4'-diphenylmethane diisocyanate (MDI).

Studies of hard segment model polymers, i.e. those without soft segment, prepared with different ratios of 2,4 and 2,6 TDI chain extended with butanediol would be quite useful for developing an understanding of the crystallization of segmented polyurethanes which have mixed isomer hard segments. While previous investigations have utilized both the hard segment homopolymer prepared with 2,4 TDI or 2,6 TDI, none have made a systematic study of hard segment homopolymers incorporating a mixture of the 2,4 and 2,6 isomer in specific ratios.

Further statistical analysis of the isomeric distribution of 2,4 and 2,6 TDI using Monte Carlo calculations would help develop a better understanding of the crystallization behavior of the mixed isomer hard segment. These studies could be particularly helpful in understanding why annealing does not result in an increase in the extent of crystallinity. A computer simulation similar to that described in Chapter IV could be used to determine the distribution of the total hard segment length as a function of the length of consecutive 2,6 TDI units incorporated in these hard segments. This is significant as the glass transition temperature and thus hard segment mobility is a function of the total hard segment length while the temperature at which crystallization by annealing would occur is dependent on the 2,6 TDI sequence length.

Segmental Orientation Investigations

In developing a model of the orientation behavior of the polybutadiene based polyurethanes which are subjected to uniaxial strain, it was found that an understanding of the nature of hard segment orientation was incomplete. While soft segment orientation relaxation was interpreted as being due to reversible deformation of the hard segment domains, infrared analysis showed no evidence of hard segment orientation. That no hard segment orientation was observed may have resulted from an insensitivity of the dichroic ratio of those bands to hard segment orientation. While other hard segment bands are obscured by overlap of other absorptions, it would be possible to incorporate deuterated butanediol as the chain extender molecule, thus bringing the hard segment C-D stretching vibration into a window region of the spectrum.

The characterization of dynamic segmental orientation in the present investigation utilized a periodic squarewave deformation. Although this deformation function produces a dramatic step change in the orientation of a polymer segment, it is not well suited to quantitative studies of polymer viscoelastic behavior. Sinusoidal deformation studies have been found to be most useful for modeling experimental results with existing theory. In the present investigation, a sinusoidal deformation scheme was developed; however, the application of this scheme to polyurethane orientation studies was not successful. It was found that when the deformation was of sufficient amplitude that segmental orientation could be detected the sample

become slack during the component of the sinusoidal function where the strain was relaxed. The utilization of this type of deformation function is desirable for theoretical modeling of dynamic orientation and future work should consider methods for increasing the sensitivity of segmental orientation determinations.

The technique of polarization modulation is one way in which sensitivity to chain orientation can be increased without sacrificing temporal resolution. Further improvement of the software controlled time resolved method can be achieved by increasing the range of frequencies over which dynamic orientation data may be collected. Although the mirror sweep period limits this range of deformation frequencies, modification of the existing TRS software could result in cycle periods ranging from 0.1 to 10 seconds. A range of two decades in the deformation frequency would make this time resolved method a valuable complement to dynamic mechanical investigations.

A P P E N D I X B

PASCAL PROGRAM FOR INTEGRATION OF INFRARED ABSORPTIONS

Integration of the peak area of absorption bands in infrared spectra can be quite useful for quantitative characterization. Since this feature is not a standard implementation on the IBM IR-98, a Pascal Program for this type of determination has been developed in this laboratory. This program is especially useful for the integration of up to 20 peaks in a series of files having the same four letter basename followed by an index value. This is intended for files which are a kinetic series or files which correspond to sequential values of strain as in polymer deformation experiments. The source code listing of the program follows:

```

PROGRAM PEAKARRY;

(* VERSION 9/16/85      *)
(* WRITTEN BY STEVE MOLIS *)
(* FOR USE ON IBM IR-98  *)

(* THIS PROGRAM INTEGRATES THE PEAKAREAS OF ABSORBANCE FILES.      *)
(* THE FILES MUST BEGIN WITH THE HIGHEST FREQUENCY AND END WITH THE *)
(* LOWEST FREQUENCY. IT MAY BE USED FOR MULTIPLE FILES HAVING A    *)
(* COMMON FOUR LETTER BASENAME SUCH AS SAMP1, SAMP2, SAMP3...      *)
(* UP TO 20 PEAKS MAY BE INTEGRATED PER FILE AND THE PEAK MAY BE  *)
(* BASELINED IF NECESSARY.                                          *)

CONST
    SECSIZE=256;      (* FOR CDC DISKS..MAKE IT 296 FOR DIABLOS *)

TYPE
    INDEX1=1..100;
    INDEX2=1..20;
    MATRIX=ARRAY[INDEX1,INDEX2] OF REAL;

VAR
    INFO:CHAR;
    AREA:MATRIX;

```

```

FNAME, MASK: STRING[16];
F1: FILE;
SCALEFAC: REAL;
NDP, BLOCKS, BLOCKNO, I1, I2, IDATA: INTEGER;
FILESTART, FILEEND: INTEGER;
NUMFILES, NUMPEAKS, I, J, ISTART, IEND: INTEGER;
XSP, XEP: ARRAY[1..20] OF INTEGER;
BASELN: ARRAY[1..20] OF CHAR;
STAT: ARRAY[1..SECSIZE] OF INTEGER;
X: ARRAY[1..16384] OF INTEGER;
POINTSPACE: REAL;

(*****
PROCEDURE FILEVALUE(VAR FILENAME: STRING; RANK: INTEGER);
VAR
    DECIVALUE, DECICOUNT: INTEGER;
    COMPLETE: BOOLEAN;
    FORMAT: STRING[16];

BEGIN

COMPLETE:=FALSE;
FORMAT:='          .DATA=D2';
FOR I:=1 TO 4 DO
FORMAT[I]:=FILENAME[I];
FILENAME:=FORMAT;

DECICOUNT:=4;
DECIVALUE:=1000;

REPEAT
IF (RANK >=DECIVALUE)
THEN BEGIN
    FOR I:=1 TO DECICOUNT DO
    BEGIN
FILENAME[4+I]:=CHR(RANK DIV DECIVALUE + 48);
RANK:=RANK-(RANK DIV DECIVALUE)*DECIVALUE;
DECIVALUE:=DECIVALUE DIV 10;
END;
COMPLETE:=TRUE;
END
ELSE BEGIN
    DECIVALUE:=DECIVALUE DIV 10;
    DECICOUNT:=DECICOUNT-1;

END;

UNTIL COMPLETE = TRUE;
END; (*PROCEDURE FILEVALUE*)
(*****

```

```

PROCEDURE INTEGRATE;

VAR
    BASETRAP,AREAL:REAL;

BEGIN
AREAL:=0;

FOR I:=(ISTART+1) TO IEND DO
AREAL:=AREAL + X[I];

IF(BASELN[I2]<>'N')
THEN
    BEGIN
        BASELN[I2]:='Y';
        BASETRAP:=(IEND-ISTART)*(X[ISTART]/1000+X[IEND]/1000)/2;
        AREAL:=AREAL-(BASETRAP*1000);
        END;

AREA[I1,I2]:=(AREAL * SCALEFAC * POINTSPACE);
END; (*PROCEDURE INTEGRATE*)

(*****
)

PROCEDURE INFORM1;

BEGIN    (*INFORM1*)

WRITELN;
WRITELN;
WRITELN('*** IBM FTIR INTEGRATION ROUTINE ***');
WRITELN('*** WRITTEN BY STEVEN MOLIS ***');
WRITELN('*** UNIVERSITY OF MASSACHUSETTS ***');
WRITELN;
WRITELN('THIS PROGRAM INTEGRATES PEAK AREAS IN ABSORBANCE FILES. ');
WRITELN('IT ALLOWS THE INTEGRATION OF A SERIES OF FILES, SUCH AS ');
WRITELN('THOSE WHICH COULD BE CREATED FOR KINETIC DATA. ');
WRITELN('THE FILES MUST ALL HAVE A COMMON 4 LETTER BASENAME GIVEN ');
WRITELN('TO THEM AT THE TIME OF COLLECTION ');
WRITELN('OR USING THE REN# COMMAND. AN EXAMPLE IS TEST1, TEST2.... ');
WRITELN;
WRITELN('SINGLE FILES MAY ALSO BE INTEGRATED BY ENTERING A FILNAME, ');
WRITELN('WHICH IS UP TO 8 LETTERS LONG. IN BOTH CASES THE .DATA=D2 ');
WRITELN('EXTENTION WILL BE ADDED BY THE PROGRAM. ');
WRITELN;
END;    (*PROCEDURE INFORM1*)

(*****
)

```

```

PROCEDURE INFORM2;

BEGIN (*INFORM2*)

WRITELN('THE FORMAT OF THE FILE SHOULD BE SUCH THAT THE FILE BEGINS');
WRITELN('WITH THE HIGH FREQUENCY VALUE AND ENDS WITH THE LOW ');
WRITELN('FREQUENCY VALUE. FOR EXAMPLE XSP > XEP WHEN CREATING A');
WRITELN('FILE WITH THE POP=FILENAME OPTION. ');
WRITELN;
WRITELN('UP TO 20 PEAKS MAY BE INTEGRATED FOR EACH FILE AT ONE TIME. ');
WRITELN('THE PARAMETERS NEEDED ARE STARTING WAVENUMBER, ENDING ');
WRITELN('WAVENUMBER AND WHETHER OR NOT THE PEAK IS BASELINED. THE ');
WRITELN('BASELINE WILL BE DRAWN FROM THE FIRST DATAPOINT OF THE PEAK ');
WRITELN('TO THE LAST DATAPOINT. ');
WRITELN('THE STARTING WAVENUMBER SHOULD BE GREATER THAN THE ENDING ');
WRITELN('WAVENUMBER WITH BOTH VALUES BEING INTEGERS. ');
WRITELN;
WRITELN('THIS ROUTINE HAS BEEN TESTED FOR FILES OF RESOLUTION UP ');
WRITELN('TO 1 CM-1. ');
WRITELN;
WRITELN;
END; (*PRODEDURE INFORM*)

```

```

(*****

```

```

PROCEDURE OUTPUT;

BEGIN (*OUTPUT*)

FOR I1:=1 TO NUMPEAKS DO

BEGIN
WRITELN('      NAME          BSLN          AREA [' ,XSP[I1], '- ',XEP[I1], ' ]');
FOR I2:=1 TO NUMFILES DO
BEGIN

IF (NUMFILES=1)
THEN BEGIN
MASK:='          .DATA=D2';
FOR I:=1 TO LENGTH(FNAME) DO
MASK[I] :=FNAME[I];
FNAME:= MASK;
END
ELSE FILEVALUE(FNAME, I2);

WRITELN(FNAME, '          ',BASELN[I1], '          ',AREA[I2,I1]);
END;

WRITELN;
WRITELN;

```



```
SCALEFAC:=1;
IF (STAT[45] > 0)
THEN BEGIN
    FOR I:= 1 TO STAT[45] DO
        SCALEFAC:=SCALEFAC * 2;
    END

ELSE IF(STAT[45] < 0)
THEN BEGIN
    STAT[45]:=ABS(STAT[45]);
    FOR I:=1 TO STAT[45] DO
        SCALEFAC:=SCALEFAC/2;
    END;

    (* X=Y/SCALEFAC AS IN USERS MANUAL*)
SCALEFAC:=SCALEFAC/((838*10000)+8607);

BLOCKS:=1 + (NDP DIV SECSIZE);

FILESTART:=STAT[46];
FILEEND:=STAT[48];

POINTSPACE:=(FILESTART-FILEEND)/NDP; (*WAVENUMBERS PER POINT*);

BLOCKNO:=0;
IDATA:=1;
J:=BLOCKREAD(F1,X[IDATA],BLOCKS,BLOCKNO);

FOR I2:=1 TO NUMPEAKS DO
BEGIN

    ISTART:=ROUND((FILESTART-XSP[I2])/POINTSPACE);
    IEND:=ROUND((FILESTART-XEP[I2])/POINTSPACE);

    INTEGRATE; (*PROCEDURE TO FIND PEAK AREA*)

END; (*PEAKS*)
END; (*FILES*)

OUTPUT; (*PROCEDURE TO LIST INTEGRATION TABLE*)

END.
```

A P P E N D I X B
PASCAL PROGRAMS FOR A MONTE CARLO SIMULATION OF
HARD SEGMENT LENGTH DISTRIBUTION

Two programs were used in the Monte Carlo simulation of polyurethane hard segment sequence distributions which was reported in Chapter IV. The first program generates the hard segment sequence distributions while the second program compiles these distributions for multiple determinations to calculate the averages and standard deviations. The two programs, written in Pascal, are listed below.

```
PROGRAM REACTN1;

(* version AUGUST 22,1985      *)
(* WRITTEN BY STEVE MOLIS      *)
(* FOR USE ON IBM CS-9000      *)

(* THIS PROGRAM WAS DEVELOPED TO TO SIMULATE A POLYURETHANE SYNTHESIS*)
*)
(* USING A MONTE CARLO APPROACH. THE REACTION WHICH IS SIMULATED IS *)
(* A TWO STEP SOLUTION POLYMERIZATION. THE REACTANT DIISOCYANATE *)
(* IS A MIXTURE OF 2,4 AND 2,6 TDI. THE ORTHO NCO GROUPS MAY HAVE A *)
(* DIFFERENT REACTIVITY THAN THE PARA NCO GROUPS WITH THESE VALUES *)
(* BEING ENTERED INTERACTIVELY. THE DISTRIBUTION OF HARD SEGMENT *)
(* SEQUENCE LENGTHS IS TABULATED AND STORED ON MAGNETIC DISC. *)

(* ANALYSIS PROGRAM IS MULDEVR *)

USES (*$U PASLIB.OBJ*) SYSTEM1/4LIBRARY,
      (*$U SSLDIM.OBJ*) SSLDIM,
      (*$U SSLDCL.OBJ*) SSLDCL;

VAR

(* ARRAYS *)

RANDRAY:RVECT;

COMPOH:ARRAY[1..10000] OF INTEGER;
COMPNCO:ARRAY[1..10000] OF INTEGER;
```

```

EINDEX, OHPOINT, NCOINDEX, NCOPOINT: ARRAY[1..10000] OF INTEGER;
HSLLENGTH, RINGSIZE: ARRAY[0..10000] OF INTEGER;
SIXSTRING, SEQUENCE: ARRAY[0..100] OF INTEGER;
RES: ARRAY[1..20] OF CHAR;
(*RESIDUE: ARRAY[1..15000, 1..50] OF CHAR; *)

```

```

TESTP, TESTN: ARRAY[1..10000] OF BOOLEAN;

```

```

(* SCALARS *)

```

```

RNUM                : REAL;
RFACTO, RFACTP     : REAL;
PROBPARA           : REAL;
PCENT24            : REAL;

TIMES              : INTEGER;
SEQ264             : INTEGER;
SEQ24              : INTEGER;
I2, I3            : INTEGER;
PTOTAL, NTOTAL, ETOTAL : INTEGER;
OHTOTAL, OHMOLEC  : INTEGER;
MOLEC26, N24      : LONGINT;
TOTALPARA, TOTALORTHO : INTEGER;
INDEX, I, J, K    : INTEGER;
NP, NO, OHNUM, NCONUM : INTEGER;
CHECKEDNCO        : INTEGER;
NUMRINGS          : INTEGER;
RANDUSED          : INTEGER;
SIXRUN            : INTEGER;
MAXSEQ            : INTEGER;
MAX6RUN           : INTEGER;

SEEDSAVE, SEED, NRAND : INT;
RESNUM            : CHAR;
HS                : CHAR;
FORM              : CHAR;

ENDHARDSEG        : BOOLEAN;
HARDCOPY          : BOOLEAN;

FNAME2            : STRING[18];
FNAME             : STRING[18];
F1                : TEXT;
F2                : TEXT;

```

```

(*-----*)

```

```

PROCEDURE INITIALIZE;

```

```

BEGIN
HARDCOPY:=FALSE;

```

```

WRITELN;
WRITELN('THIS PROGRAM DETERMINES HARDSEG DISTRIBUTIONS FOR');
WRITELN('POLYURETHANES PREPARED WITH MIXED ISOMER TDI. ');
WRITELN;
WRITE('ENTER THE TOTAL PREPOLYMER OH GROUPS. ');
READLN(PTOTAL);
WRITE('ENTER THE TOTAL ISOCYANATE GROUPS. ');
READLN(NTOTAL);
WRITELN;
WRITE('WHAT IS THE PERCENT OF 2,4-TDI IN THE ISOMER MIXTURE? ');
READLN(PCENT24);
WRITELN;
WRITE('WHAT IS THE REACTIVITY OF THE PARA GROUP? ');
READLN(RFACTP);
WRITE('WHAT IS THE REACTIVITY OF THE ORTHO GROUP? ');
READLN(RFACTO);
WRITELN;
WRITE('WHAT IS THE TOTAL NUMBER OF EXTENDER OH GROUPS? ');
READLN(ETOTAL);
WRITE('ENTER THE SEED VALUE FOR RANDOMIZER. 0..2147483647 ');
READLN(SEED);
SEEDSAVE:=SEED;
WRITE('ENTER THE OUTPUT FILENAME. ');
READLN(FNAME);
WRITE('HARDCOPY ? ');
READLN(HS);
IF (HS='Y') THEN HARDCOPY:=TRUE;
WRITE('ENTER THE NUMBER OF RUNS. ');
READLN(TIMES);
WRITE('ENTER THE FILENAME FOR MATRIX. ');
READLN(FNAME2);

END; (*OF PROCEDURE INITIALIZE*)

(*-----*)

PROCEDURE SETUP;

VAR
I:INTEGER;

BEGIN
writeln('set up ');
writeln;
OHTOTAL:=ETOTAL +PTOTAL;
OHMOLEC:=OHTOTAL DIV 2;

FOR I:= 1 TO OHMOLEC DO
BEGIN
COMPOH[2*I]:=2*I - 1;
COMPOH[2*I -1]:=2*I;
END;

```

```

(* NOW DO THE NCO COMPLEMENTS *)
writeln('pcent24 = ',pcent24);
N24:=ROUND(NTOTAL * PCENT24);
writeln('n24 = ',n24);
IF ODD(N24) THEN
N24:=N24 + 1;

MOLEC26:=(NTOTAL-N24) DIV 2;
writeln('molec26 = ',molec26);
writeln('n24 = ',n24);
writeln('ntotal = ',ntotal);
TOTALPARA :=N24 DIV 2;
TOTALORTHO := NTOTAL - TOTALPARA;

FOR I:= 1 TO TOTALPARA DO
BEGIN
    COMPNCO[I]:=TOTALPARA+I;
    COMPNCO[TOTALPARA+I]:=I;
END;

FOR I:= N24+1 TO N24+MOLEC26 DO
BEGIN
    COMPNCO[I]:=I+MOLEC26;
    COMPNCO[I+MOLEC26]:=I;
END;

END; (*PROCEDURE SETUP*)

(*-----*)

PROCEDURE RANDOMIZE;

BEGIN
SEEDSAVE:=SEED;
NRAND:=100;

IF RANDUSED>=99 THEN
BEGIN
UNIRN(SEED,RANDRAY,NRAND);
RANDUSED:=0;
END;

RANDUSED:=RANDUSED+1;
RNUM:=RANDRAY[RANDUSED];

END;

(*-----*)

```

```

PROCEDURE MIXNCO; (* THIS GENERATES A RANDOM ARRAY *)
                  (* OF THE NCO INDEX VALUES. *)
                  (* PARA GROUPS ALL COME BEFORE *)
                  (* THE ORTHO GROUPS IN THE NCO *)
                  (* ARRAY. *)

```

```

VAR
I,J:INTEGER;

```

```

BEGIN
writeln('mixnco');
writeln;
FOR I:= 1 TO TOTALPARA DO
BEGIN

```

```

RANDOMIZE;
INDEX:=1+TRUNC(I*RNUM);

```

```

IF INDEX < I THEN
BEGIN
    FOR J:= I DOWNT0 INDEX+1 DO
        NCOINDEX[J]:=NCOINDEX[J-1];

```

```

END;

```

```

NCOINDEX[INDEX]:=I;

```

```

END;

```

```

writeln;
FOR I:= TOTALPARA+1 TO NTOTAL DO
BEGIN
RANDOMIZE;
INDEX:=1+TOTALPARA + TRUNC((I-TOTALPARA)*RNUM);

```

```

IF INDEX < I THEN
BEGIN
    FOR J:=I DOWNT0 INDEX+1 DO
        NCOINDEX[J]:=NCOINDEX[J-1];

```

```

END;
NCOINDEX[INDEX]:=I;
END;

```

```

writeln;
END; (* PROCEDURE MIXNCO *)

```

```

(*-----*)

```

```

PROCEDURE ENDCAP;

(* THIS PROCEDURE REACTS THE OH GROUPS OF THE
   SOFTSEGMENT WITH THE NCO GROUPS
   OF THE ISOCYANATE IN A RANDOM MANNOR.. *)

VAR
I:INTEGER;

BEGIN
WRITELN('ENDCAP');
WRITELN;
NP:=TOTALPARA;
NO:=TOTALORTHO;
WRITELN(NP,' ',NO);
FOR I:= 1 TO PTOTAL DO
BEGIN
    PROBPARA:=NP * RFACTP/(NP*RFACTP + NO*RFACTO);

    RANDOMIZE;
    IF(RNUM < PROBPARA) THEN

(*REACTION IS AT PARA POSITION *)
    BEGIN
        NCOPOINT[NCOINDEX[NP]]:=I;

            (*INDEX OF OH GROUP *)

        OHPOINT[I]:=NCOINDEX[NP];
        (*??NCOLINK*)

if np=0 then writeln('np=0');
        NP:=NP-1;

    END

    ELSE (*REACTION IS AT PARA POSITION *)
    BEGIN
        NCOPOINT[NCOINDEX[TOTALPARA+NO]]:=I;
            (*INDEX OF OH GROUPS *)

        OHPOINT[I]:=NCOINDEX[NO+TOTALPARA];
        NO:=NO-1;

    END;

END;
END; (*PROCEDURE ENDCAP*)

(*-----*)

```

```

PROCEDURE MIXEX;
VAR
I,J: INTEGER;
BEGIN
WRITELN('MIX EXTENDER');
FOR I:=1 TO ETOTAL DO
BEGIN
RANDOMIZE;
INDEX:=1 + TRUNC(I*RNUM);
IF INDEX < I THEN
BEGIN
FOR J:=I DOWNTO INDEX+1 DO
EINDEX[I]:=EINDEX[J-1];
END;
EINDEX[INDEX]:=I;
END;
END; (*PROCEDURE MIXEX*)
(*-----*)
PROCEDURE EXTEND;
VAR
I: INTEGER;
BEGIN
writeLn('extend');
writeLn;
FOR I:= 1 TO ETOTAL DO
BEGIN
PROBPARA:=NP * RFACTP/(NP*RFACTP + NO*RFACTO);
RANDOMIZE;
IF(RNUM < PROBPARA) THEN
BEGIN
NCOPOINT[NCOINDEX[NP]]:=EINDEX[I]+PTOTAL;
(*INDEX OF OH GROUP*)

```

```

        OHPOINT[EINDEX[I]+PTOTAL]:=NCOINDEX[NP];
        NP:=NP-1;
    END

    ELSE
    BEGIN
        NCOPOINT[NCOINDEX[TOTALPARA+NO]]:=EINDEX[I]+PTOTAL;
        (*OH INDEX*)

        OHPOINT[EINDEX[I]+PTOTAL]:=NCOINDEX[NO+TOTALPARA];
        NO:=NO-1;
    END;

END;

END; (*PROCEDURE EXTEND*)

(*-----*)

PROCEDURE MAPSEG;
    VAR
    I:INTEGER;
    I2:INTEGER;

    BEGIN
    writeln('map');
    writeln(np,' ',no);
    writeln;

    REWRITE(F1,FNAME);

    K:=1;
    J:=1;

    CHECKEDNCO:=0;
    ENDHARDSEG:=FALSE;

    FOR I:=1 TO NTOTAL DO
    BEGIN
    TESTP[I]:=FALSE;
    TESTN[I]:=FALSE;
    END;

    FOR I:= 1 TO 100 DO
    BEGIN
    SEQUENCE[I]:=0;
    SIXSTRING[I]:=0;
    END;

```

```

SEQ24:=0;
SEQ264:=0;
FOR I:=1 TO 20 DO
RES[I]:='0';
MAX6RUN:=0;
SIXRUN :=0;
MAXSEQ :=0;

FOR I:= 1 TO PTOTAL DO

BEGIN
OHNUM:=I;
IF NOT TESTP[I] THEN
BEGIN
write(f1,i);
TESTP[I]:= TRUE;      (*WE ARE TESTING THIS PREPOL GROUP*)

WHILE NOT ENDHARDSEG DO
BEGIN
NCONUM :=OHPOINT[OHNUM];

TESTN[NCONUM]:=TRUE;

IF NCONUM<=TOTALPARA THEN
BEGIN
WRITE(F1,'<');
RESNUM:='2';
END;

IF (NCONUM<=N24) AND (NCONUM>TOTALPARA) THEN
BEGIN
WRITE(F1,'>');
RESNUM:='4';
END;

IF NCONUM>N24 THEN
BEGIN
WRITE(F1,'1/2');
RESNUM:='6';
END;

                (*EACH WORD WILL CORRESPOND TO A HARDSEGMENT*)
                (* SEQUENCE                               *)
(*CHECK 6 RUNS *)

FOR I2:= 20 DOWNT0 2 DO
RES[I2]:=RES[I2-1];
RES[1]:=RESNUM;

```

```

IF      (RES[1] = '4') AND
        (RES[2] = '6') AND
        (RES[3] = '2')      THEN

        SEQ264:=SEQ264+3;

IF      (RES[1] = '4') AND
        (RES[2] = '2')      THEN
begin
        SEQ24:=SEQ24+2;
end;
IF RESNUM='6' THEN
SIXRUN:=SIXRUN+1

ELSE
BEGIN
SIXSTRING[SIXRUN]:=SIXSTRING[SIXRUN] + SIXRUN;
IF SIXRUN>MAX6RUN THEN
MAX6RUN:=SIXRUN;
SIXRUN:=0;
END;

OHNUM:=NCOPOINT[COMPNCO[NCONUM]];

IF(OHNUM <= PTOTAL) THEN
    BEGIN
        write(f1,ohnum);
        ENDHARDSEG:= TRUE;
        TESTP[OHNUM]:=TRUE;
        HSLength[J]:=K;      (*STORE LENGTH OF SEQUENCE*)
        CHECKEDNCO:=CHECKEDNCO+K;
        WRITELN(F1, ' ');
        SEQUENCE[K]:=SEQUENCE[K]+K;
        IF K > MAXSEQ THEN
            MAXSEQ:=K;
        SIXSTRING[SIXRUN]:=SIXSTRING[SIXRUN]+SIXRUN;
        IF SIXRUN > MAX6RUN THEN
            MAX6RUN :=SIXRUN;
        SIXRUN:=0;
        FOR I2:=1 TO 20 DO
            RES[I2]:='0';

        END

ELSE
    BEGIN
        K:=K+1;
        OHNUM:=COMPOH[OHNUM];
        END;

END;      (* END OF THIS HARDSEG *)

```

```

K:=1;
J:=J+1;
ENDHARDSEG:=FALSE;

END;      (*END OF TESTING CURRENT SEGMENT *)
END;      (*ALL PREPOLYMERS TESTED          *)

IF CHECKEDNCO < NTOTAL THEN
BEGIN
      (*SOME NCO GROUPS ARE IN HS LOOPS *)
NUMRINGS:=0;

FOR I:=1 TO NTOTAL DO
BEGIN
IF TESTN[I]=FALSE THEN
      BEGIN
NUMRINGS:=NUMRINGS+1;
NCONUM:=I;

      REPEAT
NCONUM:=OHPOINT[COMPOH[NCOPOINT[COMPNCO[NCONUM]]]];
RINGSIZE[NUMRINGS]:=RINGSIZE[NUMRINGS]+1;

      (*CHECK RUNS OF 2,6 TDI *)

TESTN[NCONUM]:=TRUE;
TESTN[COMPNCO[NCONUM]]:=TRUE;

      UNTIL NCONUM=I;

      END;

END;

END;      (*ALL NCO GROUPS TESTED *)

CLOSE(F1,LOCK);
Writeln(F2,'RUN # ',I3);
Writeln(F2,MAXSEQ);
FOR I:= 1 TO MAXSEQ DO
Writeln(F2,SEQUENCE[I]);
Writeln(F2,MAX6RUN);
FOR I:= 1 TO MAX6RUN DO
Writeln(F2,SIXSTRING[I]);
Writeln(F2,2);
writeln(f2,'seq462');
Writeln(F2,SEQ264);
Writeln(F2,SEQ24);

END;      (*PROCEDURE MAPSEG*)

(*-----*)

```

PROCEDURE OUTPUT;

VAR

I,J : INTEGER;

TDITOTAL: INTEGER;

BEGIN

TDITOTAL := NTOTAL DIV 2;

FORM:=CHR(12);

WRITELN(F1,FORM);

WRITELN(F1,'TDI MOLECULES = ',TDITOTAL);

WRITELN(F1,'PERCENT 2,4TDI IS ',PCENT24);

WRITELN(F1,'2,6 TDI MOLECULES = ',MOLEC26);

WRITELN(F1,'PARA REACTIVITY = ',RFACTP);

WRITELN(F1,'ORTHO REACTIVITY = ',RFACTO);

WRITELN(F1,'SEED VALUE IS ',SEEDSAVE);

WRITELN(F1,' ');

WRITELN(F1,'HARDSEG SEQUENCE DISTRIBUTION');

WRITELN(F1,' ');

FOR I:=1 TO MAXSEQ DO

WRITELN(F1,I,' RESIDUES = ',SEQUENCE[I]);

WRITELN(F1,' ');

WRITELN(F1,'DISTRIBUTION OF 2,6 TDI RUNS');

WRITELN(F1,' ');

FOR I :=1 TO MAX6RUN DO

WRITELN(F1,I,' 2,6 RUN = ',SIXSTRING[I]);

WRITELN(F1,'RESIDUES COUNTED = ',CHECKEDNCO);

WRITELN(F1,' ');

WRITELN(F1,' ');

END;

(*-----*)

BEGIN (*MAIN*)

INITIALIZE;

REWRITE(F2,FNAME2);

WRITELN(F2,'TIMES');

WRITELN(F2,TIMES);

WRITELN(F2,NTOTAL);

WRITELN(F2,PCENT24);

WRITELN(F2,PTOTAL);

WRITELN(F2,ETOTAL);

WRITELN(F2,SEEDSAVE);

WRITELN(F2,RFACTP);

WRITELN(F2,RFACTO);

```

FOR I3:= 1 TO TIMES DO
BEGIN

SETUP;

RANDUSED:=100;

WRITELN;
WRITELN('CYCLE # ',I3);
WRITELN;
MIXNCO;

ENDCAP;

MIXEX;

EXTEND;

MAPSEG;

REWRITE(F1,'#SCRNO');
OUTPUT;
CLOSE(F1,LOCK);

IF HARDCOPY THEN
BEGIN
REWRITE(F1,'#PR');
OUTPUT;
CLOSE(F1,LOCK);
END;

END;
CLOSE(F2,LOCK);

END.

```

Second program:

```
PROGRAM MULDEV;
```

```
(* VERSION 9/16/85      *)
(* WRITTEN BY STEVE MOLIS *)
```

```
(* THIS PROGRAM IS DESIGNED FOR USE IN CONJUNCTION WITH THE *)
(* MONTE CARLO SIMULATION "REACTNCO". IT TAKES AS INPUT *)
(* THE FILE GENERATED BY REACTNCO FOR STORING THE MATRIX *)
(* OF SEQUENCE DISTRIBUTIONS FOR MULTIPLE SIMULATIONS. *)
(* THE AVERAGES AND STANDARD DEVIATIONS ARE CALCULATED FOR *)
(* THE WEIGHT FRACTIONS OF EACH SEQUENCE LENGTH. *)
```

VAR

XVAL,
YVAL,
I, I2,
DUMB,
TIMES,
TOTNCO,
PCENT24,
PTOTAL,
ETOTAL,
MAXSEQ,
MAXSIX,
SUM462,
SUM42

:LONGINT;

SEQ462,
SEQ42,
SQR462,
SQR42

:ARRAY[1..50] OF LONGINT;

SEQUENCE,
SEQSQUAR,
SIXSTRING,
SIXSQUAR

:ARRAY[1..50,1..50] OF LONGINT;

XREAL,
YREAL,
RFACTP,
RFACTO,
DIF462,
DIF42,
MEAN462,
MEAN42,
DEV462,
DEV42

:REAL;

SEQSUM,
SIXSUM,
SEQDEV,
SIXDEV,
SEQMEAN,
SIXMEAN,
SEQDIF,
SIXDIF

:ARRAY[1..50] OF REAL;

DUMBS,
FNAME

:STRING[18];

```
FORM          :CHAR;

F1            :TEXT;
F2            :TEXT;

BEGIN  (* MAIN *)

WRITE('ENTER THE FILENAME. ');
READLN(FNAME);

FOR I:= 1 TO 50 DO
BEGIN
FOR I2:= 1 TO 50 DO
BEGIN
SEQUENCE[I,I2]:=0;
SEQSQUAR[I,I2]:=0;
SIXSTRING[I,I2]:=0;
SIXSQUAR[I,I2]:=0;
END;

SEQSUM[I]:=0;
SIXSUM[I]:=0;
SEQDEV[I]:=0;
SIXDEV[I]:=0;
SEQMEAN[I]:=0;
SIXMEAN[I]:=0;
SEQDIF[I]:=0;
SIXDIF[I]:=0;
SEQ462[I]:=0;
SEQ42[I]:=0;
SQR462[I]:=0;
SQR42[I]:=0;

END;

SUM462:=0;
SUM42:=0;
DIF462:=0;
DIF42:=0;

(* END OF INITIALIZATION *)

RESET(F1,FNAME);

READLN(F1,DUMBS);
READLN(F1,TIMES);
READLN(F1,TOTNCO);
READLN(F1,PCENT24);
READLN(F1,PTOTAL);
READLN(F1,ETOTAL);
```

```
READLN(F1,DUMB);
READLN(F1,RFACTP);
READLN(F1,RFACTO);

FOR I2:= 1 TO TIMES DO
BEGIN

READLN(F1,DUMBS);

READLN(F1,MAXSEQ);

FOR I:= 1 TO MAXSEQ DO
BEGIN
READLN(F1,XVAL);
SEQUENCE[I,I2]:=XVAL;
SEQSQUAR[I,I2]:=SQR(XVAL);
SEQSUM[I]:=SEQSUM[I] + XVAL;
END;

READLN(F1,MAXSIX);

FOR I:= 1 TO MAXSIX DO
BEGIN
READLN(F1,XVAL);
SIXSTRING[I,I2]:=XVAL;
SIXSQUAR[I,I2]:=SQR(XVAL);
SIXSUM[I]:=SIXSUM[I] + XVAL;
END;

READLN(F1,DUMB);
READLN(F1,DUMBS);

READLN(F1,XVAL);
SEQ462[I2]:=XVAL;
SQR462[I2]:=SQR(XVAL);
SUM462:= SUM462 + XVAL;

READLN(F1,XVAL);
SEQ42[I2]:=XVAL;
SQR42[I2]:=SQR(XVAL);
SUM42:=SUM42 + XVAL;

END;      (* INPUT LOOP *)

FOR I:= 1 TO 20 DO
BEGIN
SEQMEAN[I]:=SEQSUM[I]/TIMES;
SIXMEAN[I]:=SIXSUM[I]/TIMES;
END;
```

```

MEAN462:=SUM462/TIMES;
MEAN42:=SUM42/TIMES;

FOR I:= 1 TO 20 DO
BEGIN

FOR I2:= 1 TO TIMES DO
BEGIN
SEQDIF[I]:=SEQDIF[I] + (SEQSQUAR[I,I2] - SQR(SEQMEAN[I]));
SIXDIF[I]:=SIXDIF[I] + (SIXSQUAR[I,I2] - SQR(SIXMEAN[I]));
END;

SEQDEV[I]:=SQRT(SEQDIF[I]/(TIMES-1));
SIXDEV[I]:=SQRT(SIXDIF[I]/(TIMES-1));

END;

FOR I:= 1 TO TIMES DO
BEGIN
DIF462:=DIF462 + (SQR462[I] - SQR(MEAN462));
DIF42:=DIF42 + (SQR42[I] - SQR(MEAN42));
END;

DEV462:=SQRT(DIF462/(TIMES-1));
DEV42:=SQRT(DIF42/(TIMES-1));

(* OUTPUT *) REWRITE(F2,'#SCRNO');
FOR I2:= 1 TO 2 DO
BEGIN
IF I2 = 2 THEN REWRITE(F2,'#PR');
FORM:=CHR(12);
WRITELN(F2,FORM);
WRITELN(F2,'FILENAME IS ',FNAME);
WRITELN(F2);
WRITELN(F2,'LISTING OF CALCULATED MEANS AND DEVIATIONS.');
```

```

WRITELN(F2);

FOR I:= 1 TO 20 DO
BEGIN
XREAL:=SEQMEAN[I]/TOTNCO*2;
YREAL:=SEQDEV[I]/TOTNCO*2;
WRITELN(F2,I:2,' RESIDUES: MEAN = ',XREAL:7:5,' STND DEV =
',YREAL:7:5);
END;

WRITELN(F2);

FOR I:= 1 TO 10 DO
BEGIN
```

```
XREAL:=SIXMEAN[I]/TOTNCO*2;  
YREAL:=SIXDEV[I]/TOTNCO*2;  
WRITELN(F2,I:2,' SIXRUN : MEAN = ',XREAL:7:5,' STND DEV = ',YREAL:7:5);  
END;  
  
WRITELN(F2);  
  
XREAL:=MEAN462/TOTNCO*2;  
YREAL:=DEV462/TOTNCO*2;  
WRITELN(F2,' MEAN OF 462 SEQ IS ',XREAL:7:5,' STND DEV = ',YREAL:7:5);  
  
WRITELN(F2);  
  
XREAL:=MEAN42/TOTNCO;  
YREAL:=DEV42/TOTNCO;  
WRITELN(F2,' MEAN OF 42 SEQ IS ',XREAL:7:5,' STND DEV = ',YREAL:7:5);  
  
CLOSE(F2,LOCK);  
END;  
  
END.
```

A P P E N D I X C
SYNCHRONIZATION AND SORTING PROGRAM FOR
TIME RESOLVED INFRARED SPECTROSCOPY

Two programs were specifically developed for software controlled TRS. The first listing is of the source code for the driver program which synchronizes the external event to the interferogram collection. This program was developed for use on a California Computer systems S-100 microprocessor, however, only the port access commands are specific to this unit. This program is specific for a pulsed type on-off external event. The second program necessary for the time resolved experiment is the interferogram sorting routine. This program runs on the Aspect 2000 processor of the IBM 1R-98 Fourier transform infrared spectrometer. It uses as input the series of interferograms which are collected during the time-resolved experiment. The data of these interferograms is a function of both time and optical retardation. The output files of the sort are interferograms which each correspond to a specific phase of the event. The standard FTIR routines supplied with the instrument are then used to Fourier transform these interferograms. The source code for both of these programs is written in Pascal and listed below.

PROGRAM TRS1IP;

(* VERSION 9/16/85 *)
(* WRITTEN BY STEVE MOLIS *)

(* TIME RESOLVE PROGRAM FOR STEPWISE EVENT *)
(* THIS PROGRAM IS INTENDED FOR USE WITH AN *)
(* IBM MODEL IR-98 FT-IR SPECTROMETER *)

VAR

```

NSCN,N2,N1,NSS,NCLKS           : INTEGER;
DELAY,I1,I2,I3,J,STEPCLK       : INTEGER;
K,Y,CLKON,CLKOFF,ON,OFF,EVENT  : INTEGER;
TYMEVNT,TYMON,TYMREPEAT,ICLOCKS,
EVENT2                          : REAL;
A                               : ARRAY[1..500] OF INTEGER;
J1                              : ARRAY[1..500] OF INTEGER;
KEY,OK                          : CHAR;
FACTOR                          : REAL;
POL                             : INTEGER;
DELAYCHK                        : INTEGER;

```

(*****)

FUNCTION DONE :BOOLEAN;

CONST

KBRDY=\$25;

KBMASK=01;

VAR

CHRRDY :BOOLEAN;

CH :CHAR;

BEGIN

CH:=' ';

DONE:=FALSE;

CHRRDY:=((ORD(INPUT[KBRDY]) & KBMASK) <> 0);

IF CHRRDY THEN

BEGIN

READ(CH);

IF ORD(CH) =24 THEN DONE:=TRUE;

END;

END; (*FUNCTION DONE*)

BEGIN

OUTPUT[\$5A]:=\$38; (* INITIALIZE PARALLEL PORT *)

OUTPUT[\$58]:=\$0;

OUTPUT[\$5A]:=\$3C;

OUTPUT[\$5B]:=\$38;

OUTPUT[\$59]:=\$1;

OUTPUT[\$5B]:=\$3C;

```
WRITELN('START CLX# FOR SCANNER CALIBRATION, THEN TYPE RETURN.');
```

```
READLN;
```

```
TYMREPEAT:=77.66E-6;          (* CONVERTS TO SECONDS *)
```

```
OUTPUT[$59]:=0;
```

```
REPEAT
```

```
FOR I1:=1 TO 10 DO
```

```
BEGIN
```

```
ON:=0;
```

```
OFF:=0;
```

```
REPEAT
```

```
UNTIL ORD(INPUT[$58] & $1)=0;
```

```
REPEAT
```

```
UNTIL ORD(INPUT[$58] & $1)=1;
```

```
REPEAT
```

```
ON:=ON + 1;
```

```
UNTIL ORD(INPUT[$58] & $1)=0;
```

```
REPEAT
```

```
OFF:=OFF + 1;
```

```
UNTIL ORD(INPUT[$58] & $1)=1;
```

```
WRITELN('ON= ',ON,' OFF= ',OFF);
```

```
BEND;
```

```
WRITELN('LAST TIMING VALUES OK?');
```

```
READLN(OK);
```

```
IF OK='Q' THEN EXIT;
```

```
UNTIL OK='Y';
```

```
IF OK = 'N' THEN
```

```
BEGIN
```

```
WRITE('ENTER TIME ON...');
```

```
READLN(ON);
```

```
WRITE('ENTER TIME OFF...');
```

```
READLN(OFF);
```

```
END;
```

```
WRITELN ('INPUT THE NUMBER OF CLOCKS PER CYCLE.');
```

```
READLN(NCLKS);
```

```

WRITELN ('
READLN(NSS);
NSCN:=NSS + 1;
WRITE('INPUT THE STARTING CLOCK OF THE PULSE....');
READLN(CLKON );
WRITE('INPUT THE END CLOCK OF THE PULSE....');
READLN(CLKOFF);
.....NUMBER OF SCANS.');
```

```

FACTOR:=3.33; (*THIS IS A CALIBRATION VARIABLE. *)
(*IT RELATES THE SPEED OF THE FOR-TO DELAY LOOP *)
(*TO THE SPEED OF THE REPEAT-UNTIL INPUT[] LOOP *)
```

```

EVENT:=ON + OFF;
EVENT2:=EVENT * FACTOR;
```

```

DELAY:= TRUNC(EVENT2 / NCLKS);
```

```

WRITELN;
WRITELN('COARSE DELAY VALUE = ',DELAY);
WRITELN;
```

```

ICLOCKS:=ON/EVENT * NCLKS; (*REAL NUMBER*)
```

```

TYMEVNT:=EVENT* TYMREPEAT;
```

```

TYMON:=ON * TYMREPEAT;
```

```

WRITELN('** RECORD THESE VALUES ***');
WRITELN;
WRITELN('CLOCKS PER INTEFEROGRAM = ',ICLOCKS);
WRITELN;
WRITELN('PERIOD OF EVENT = ',TYMEVNT,' SECONDS.');
```

```

WRITELN;
WRITELN('TIME OF INTERFEROGRAM COLLECTION = ',TYMON,' SECONDS.');
```

```

(*****)
```

```

IF (CLKON<CLKOFF) THEN
BEGIN
```

```

FOR J:=1 TO NCLKS DO (*INITIALIZE CODE ARRAY*)
```

```

BEGIN
```

```

IF(J>=CLKON)&(J<CLKOFF) THEN A[J]:=1
```

```

ELSE A[J]:=0;
```

```

END;
```

```

END
```

```

ELSE FOR J:=1 TO NCLKS DO
BEGIN
IF(J<CLKOFF)OR (J>=CLKON) THEN A[J]:=1
ELSE A[J]:=0;
END;

(*****
)

IF DONE THEN EXIT;

(*NOW DO THE FINE TUNING*)

WRITELN;
WRITELN('FOR FINE TUNING THE EVENT PERIOD START CLS#, THEN RETURN. ');
READLN;

REPEAT
UNTIL ORD(INPUT[$58] & $1)=0;

REPEAT
UNTIL ORD(INPUT[$58] & $1)=1;

FOR I2:=1 TO 20 DO
J1[I2]:=0;
J1[1]:=-1;

FOR I2:= 1 TO 20 DO

BEGIN

REPEAT
J1[I2]:=J1[I2] + 1;
UNTIL ORD(INPUT[$58] & $1) =1;
IF J1[I2] > 10 THEN DELAY:=DELAY +J1[I2] * 3 DIV NCLKS;
IF J1[I2] = 1 THEN DELAY:=DELAY - 1-DELAY DIV 750;

FOR I3:=1 TO NCLKS DO

BEGIN
OUTPUT[$59] :=A[I3]; (*THIS ARRAY CONTAINS THE EVENT SEQUENCE CODE*)
FOR J:= 1 TO DELAY DO; (*THIS IS THE ACTUAL TIMING LOOP*)
END;

END; (*EXIT LOOP AFTER 10 SCANS.*)

WRITELN;
WRITE('WAIT COUNTS ARE... ');

```

```

FOR J:=1 TO 20 DO
BEGIN
WRITE(J1[J], ' ');
END;

FOR J:=1 TO NSCN DO
J1[J]:=0;
J1[1]:=2;
WRITELN;
WRITELN(DELAY);
DELAYCHK:=DELAY;

WRITELN;

WRITELN('FINE TUNING IS COMPLETE. ');
WRITELN('DO SBS# IF NECESSARY THEN TYPE RETURN. ');
READLN;
WRITELN;
WRITELN('START TIME RESOLVE MACRO TR1# ON IR 98. ');
WRITELN;

FOR I1:=1 TO NCLKS DO
BEGIN
FOR POL:=1 TO 2 DO (*PARALLEL AND PERPENDICULAR*)
BEGIN
DELAY:=DELAYCHK;
REPEAT

IF DONE THEN EXIT;

UNTIL ORD(INPUT[$58] & $E)=$0; (*THIS WILL BE COLLECTION SIG*)
REPEAT
UNTIL ORD(INPUT[$58] & $1)=$1;
REPEAT
UNTIL ORD(INPUT[$58] & $1)=$0;
REPEAT
UNTIL ORD(INPUT[$58] & $1)=$1;

FOR I2:= 1 TO NSCN DO
BEGIN
REPEAT
J1[I2]:=J1[I2] + 1;
UNTIL ORD(INPUT[$58] & $1) =1;
IF J1[I2] > 10 THEN DELAY:=DELAY +J1[I2] * 3 DIV NCLKS;
IF J1[I2] = 1 THEN DELAY:=DELAY - 1 - DELAY DIV 750;

```

```

IF J1[I2] > 75 THEN DELAY:=DELAYCHK;
FOR I3:=1 TO NCLKS DO
BEGIN
OUTPUT[$59] :=A[I3];    (*THIS ARRAY CONTAINS THE EVENT SEQUENCE CODE*)
FOR J:= 1 TO DELAY DO;  (*THIS IS THE ACTUAL TIMING LOOP*)
END;

END; (*EXIT LOOP AFTER NSCN*)

OUTPUT[$59]:=0;    (*TURN OFF PULSE*)

WRITELN('CLOCKVALUE= ',I1);
WRITE('WAITING COUNTS...');

FOR J:=1 TO NSCN DO
BEGIN
WRITE(J1[J], ' ');
J1[J]:=0;
END;
J1[1]:=1;
WRITELN;
WRITE('DELAY = ',DELAY);
WRITELN;
WRITELN;

REPEAT
UNTIL ORD(INPUT[$58] & $E)<>0;

END; (*FOR EACH POLARIZATION*)

(* NOW CHANGE EVENT CODE ARRAY. *)
(* THIS CHANGES THE ARRAY WITH AN EVEN PERMUTATION OF ONE *)
(* INDEX VALUE. IT ADVANCES THE STARTING PULSE BY ONE CLOCK VALUE. *)

Y:=CLKON -I1;
IF Y <=0 THEN Y:=Y+NCLKS;
A[Y]:=1;

Y:=CLKOFF-I1;
IF Y <= 0 THEN Y:=Y + NCLKS;
A[Y]:= 0; (*THIS IS THE CRITICAL CHANGE*)

END;    (* OF EACH CLOCK VALUE *)

END.

```

Second Program:

PROGRAM SORT;

(* VERSION 9/16/85 *)
 (* WRITTEN BY STEVE MOLIS *)

(* THIS PROGRAM SORTS THE INTERFEROGRAM FILES GENERATED DURING *)
 (* A TIME RESOLVED COLLECTION. IT IS MODIFIED SO AS TO REMOVE *)
 (* ANY DISCONTINUITIES CREATED DURING THE SORT DUE TO *)
 (* UNSTABLE INTEFEROGRAM BASELINES. *)

VAR

Y:ARRAY[1..16384] OF INTEGER;
 SORTFILE,ORIGFILE:STRING[16];
 SORTNO,ORIGNO,BLOCKNO:INTEGER;
 IDATA,ICLOCKS,I1,I2,I3:INTEGER;
 NCLKS,NDP,BLOCKS,POINTSCLK:INTEGER;
 STARTPOINT,ENDPOINT,J:INTEGER;
 STAT:ARRAY[1..256] OF INTEGER;
 P:INTEGER;
 F1:FILE;
 REALCLKS:REAL;

ORIG1,ORIG2,SORT1,SORT2:STRING[16];
 RATIO:REAL;
 LASTPOINT,FIRSTPOINT,BIAS:INTEGER;

PROCEDURE SWAPBLOCK;

(*THIS PROCEDURE SORTS THE ORIGIN FILES INTO THE SORTED FILE
 ONE BLOCK AT A TIME FOR ALL THE POINTS IN ONE CLOCK*)

VAR

STARTBLOCK,ENDBLOCK:INTEGER;
 FIRST,LAST,BLOCKPOINT:INTEGER;
 SORTPOINT:INTEGER;
 X:ARRAY[1..256] OF INTEGER;

BEGIN (*PROCEDURE SWAPBLOCK*)

STARTBLOCK:=(STARTPOINT-1) DIV 256;
 ENDBLOCK:=(ENDPOINT-1) DIV 256;
 BLOCKNO:=STARTBLOCK;

REPEAT

IF (BLOCKNO=STARTBLOCK)
 THEN FIRST:=STARTPOINT MOD 256
 ELSE FIRST:= 1;

```

IF (BLOCKNO = ENDBLOCK)
THEN LAST:=ENDPOINT MOD 256
ELSE LAST:=256;
IF LAST=0 THEN LAST:= 256;
SORTPOINT:=(BLOCKNO)*256+FIRST;

J:=BLOCKREAD(F1,X[1],1,BLOCKNO);

FOR BLOCKPOINT:=FIRST TO LAST DO
  BEGIN
    Y[SORTPOINT]:=X[BLOCKPOINT];
    SORTPOINT:=SORTPOINT + 1;
  END;
BLOCKNO:=BLOCKNO + 1;

UNTIL BLOCKNO > ENDBLOCK;

END; (*PROCEDURE SWAPBLOCK*)

(*****
PROCEDURE FILEVALUE(VAR FILENAME:STRING;RANK:INTEGER);
VAR
  DECIVALUE,I,DECICOUNT:INTEGER;
  COMPLETE:BOOLEAN;
  FORMAT:STRING[16];

BEGIN

COMPLETE:=FALSE;
FORMAT:='          .DATA=D2';
FOR I:=1 TO 4 DO
FORMAT[I]:=FILENAME[I];
FILENAME:=FORMAT;

DECICOUNT:=4;
DECIVALUE:=1000;

REPEAT
IF (RANK >=DECIVALUE)
THEN BEGIN
  FOR I:=1 TO DECICOUNT DO
  BEGIN
    FILENAME[4+I]:=CHR(RANK DIV DECIVALUE + 48);
    RANK:=RANK-(RANK DIV DECIVALUE)*DECIVALUE;
    DECIVALUE:=DECIVALUE DIV 10;
  END;
  COMPLETE:=TRUE;
END

```

```

ELSE BEGIN
    DECIVALUE:=DECIVALUE DIV 10;
    DECICOUNT:=DECICOUNT-1;
    END;

UNTIL COMPLETE = TRUE;
END; (*PROCEDURE FILEVALUE*)
(*****
)

PROCEDURE UNSAW;

BEGIN

J:=1;
FIRSTPOINT:=POINTSCLK +1;
LASTPOINT:=FIRSTPOINT-1;

FOR I2:= 1 TO ICLOCKS-1 DO
BEGIN

BIAS:=Y[FIRSTPOINT]-Y[LASTPOINT];
FOR I3:= 1 TO POINTSCLK DO

BEGIN

RATIO:=(I3-1)/(POINTSCLK-1);
Y[J]:=Y[J]+ROUND(BIAS*RATIO);

J:=J+1;
END;

LASTPOINT:=LASTPOINT+POINTSCLK;
FIRSTPOINT:=FIRSTPOINT+POINTSCLK;
END;
END;

(*****
)

BEGIN (*MAIN*)

WRITE('ENTER ORIG1 BASENAME. ');
READLN(ORIG1);
WRITE('ENTER ORIG2 BASENAME. ');
READLN(ORIG2);
WRITE('ENTER SORT1 BASENAME. ');
READLN(SORT1);
WRITE('ENTER SORT2 BASENAME. ');
READLN(SORT2);
WRITE('ENTER THE NUMBER OF CLOCKS PER EVENT. ');

```

```

READLN(NCLKS);
WRITE('ENTER THE NUMBER OF CLOCKS PER INTERFEROGRAM REAL. ');
READLN(ICLOCKS);

FOR P:= 1 TO 2 DO
BEGIN

IF (P=1) THEN
BEGIN
ORIGFILE:=ORIG1;
SORTFILE:=SORT1;
END

ELSE
BEGIN
ORIGFILE:=ORIG2;
SORTFILE:=SORT2;
END;
(*INITIALIZE FILENAMES*)
FILEVALUE(SORTFILE,1);
FILEVALUE(ORIGFILE,1);

WRITELN(ORIGFILE);
(*FIND # OF DATAPPOINTS IN THE INTERFEROGRAMS*)
RESET(F1,ORIGFILE);
IDATA:=1;
BLOCKNO:=-1;
J:=BLOCKREAD(F1,STAT[IDATA],1,BLOCKNO);
NDP:=STAT[42];
WRITELN(NDP);

(*FIND THE # OF POINTS IN ONE CLOCK*)
POINTSCLK:=NDP DIV ICLOCKS +1;

(*FIND THE # OF BLOCKS IN A DATAFILE*)
BLOCKS:=NDP DIV 256;

(*START THE SORT*)

SORTNO:=1;
FOR I1:=1 TO NCLKS DO
BEGIN
WRITE(I1, ' ');

STARTPOINT:=1;
ENDPOINT:=POINTSCLK;
ORIGNO:=I1;
FILEVALUE(ORIGFILE,ORIGNO);

FOR I2:=1 TO ICLOCKS DO

```

```

      BEGIN
      RESET(F1,ORIGFILE);

      SWAPBLOCK;    (*PROCEDURE TO DO THE SWAP
                    ONE BLOCK AT A TIME*)

      STARTPOINT:=STARTPOINT+POINTSCLK;
      ENDPOINT:=ENDPOINT+POINTSCLK;
      IF ENDPOINT > NDP THEN ENDPOINT:=NDP;

      ORIGNO:=ORIGNO-1;
      IF ORIGNO = 0 THEN ORIGNO:=NCLKS;
      FILEVALUE(ORIGFILE,ORIGNO);
      END;

UNSAW;
      IDATA:=1;
      BLOCKNO:=-1;
      REWRITE(F1, SORTFILE);
      J:=BLOCKWRITE(F1,STAT[IDATA],1,BLOCKNO);
      IDATA:=1;
      BLOCKNO:=0;
      J:=BLOCKWRITE(F1,Y[IDATA],BLOCKS+1,BLOCKNO);

      CLOSE(F1,LOCK);

      SORTNO:=SORTNO+1;
      FILEVALUE(SORTFILE,SORTNO);
      END;
END;    (*EACH POLARIZATION*)

END.

```

A P P E N D I X D
INTERFACE AND DRIVER ELECTRONICS FOR TIME RESOLVED METHOD

The time resolved FTIR experiment utilizes a separate microprocessor interfaced with the FTIR interferometer electronics and the external event driver board. This interface is depicted schematically in Figure D.1. A 34 conductor ribbon cable connects the microprocessor parallel port to the interface junction on the spectrometer chassis. At the parallel port, pin 3 corresponds to bit 0 of the output and is used to drive the external event. Pins 22, 24, 26, and 28 correspond to the low order bits of the input and receive status signals from the interferometer electronics. The Take Data signal (TKDA) is high during actual interferogram collection and the retardation bits (RTD) all go low for the duration of a multiple scan collection.

The stretcher driver circuit is depicted in Figure D.2. This circuit receives as inputs the control pulse (CLK) from the microprocessor along with a signal ground. It is powered by a separate 5 volt supply which drives the transistors and relay. The stretcher solenoid is interfaced to the driver circuit and is powered by a separate 3 amp, 24 volt d.c. supply. The stretcher is activated by applying a signal of 2 volts or greater at the CLK input.

FIGURE D.1: Wiring diagram for interface of CCS micro-processor, infrared digital driver board, and stretcher solenoid driver board.

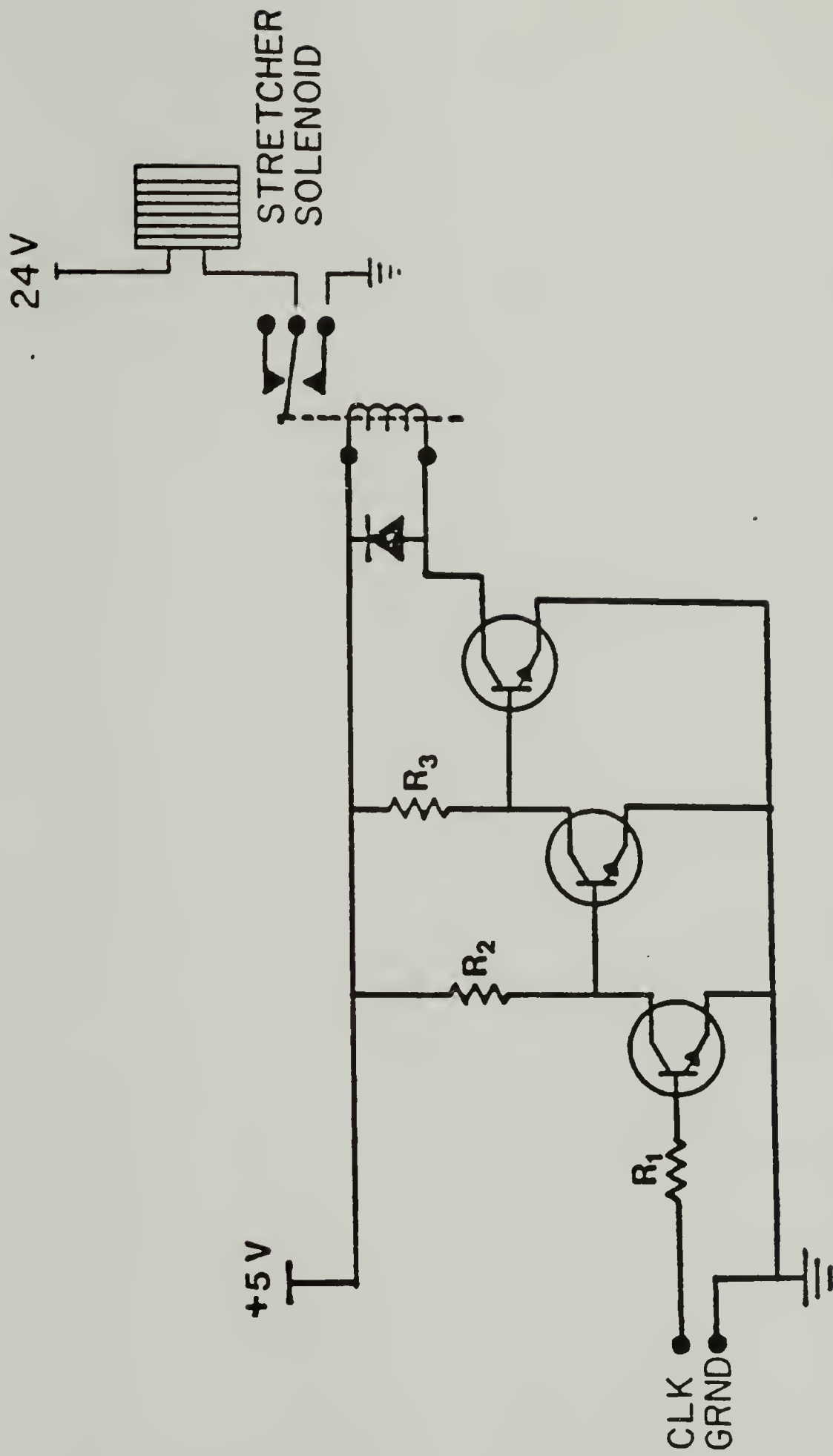


Figure D.1

FIGURE D.2: Circuit diagram of stretcher solenoid driver

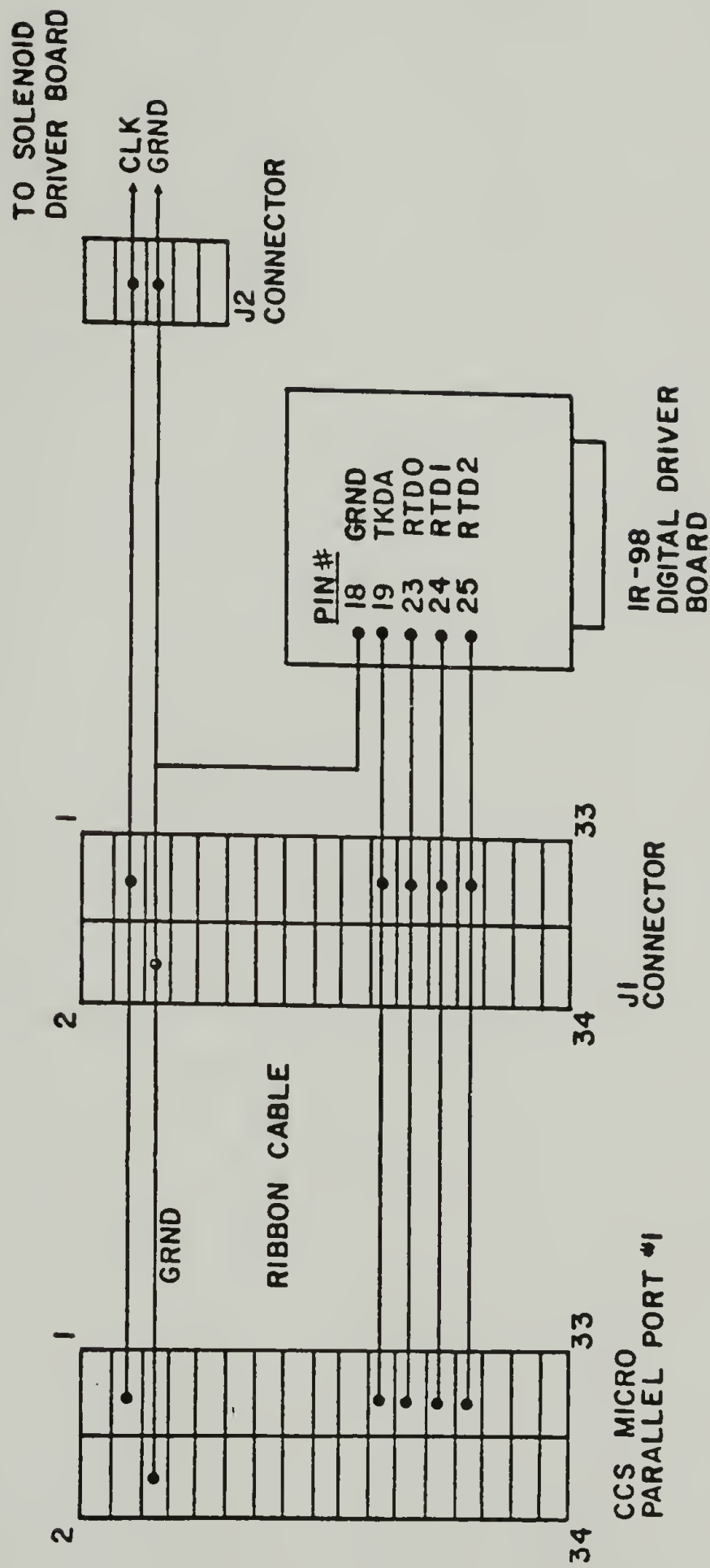


Figure D.2

